ARC Centre of Excellence for Coral Reef Studies
and
The College of Public Health, Medical and Veterinary Sciences
James Cook University
Townsville, Australia

A comparison of the molecular bases of regeneration and bleaching in *Heliofungia*

By

Beatriz Diaz-Guijarro

April 2024

A thesis submitted in partial fulfilment of the requirements for the degree of

DOCTOR OF PHILOSOPHY

(Natural and Physical Sciences)

Statement of sources

I, Beatriz Diaz-Guijarro certify that the presented thesis:

A comparison of the molecular bases of regeneration and bleaching in Heliofungia

fulfils the requirements for the degree of ***Doctor of Philosophy*** at James Cook University.

The thesis presented is, to the best of my knowledge and belief, original and my own work and has not been submitted in any form for another degree or diploma at any university or other institution of tertiary education. Information derived from the published or unpublished work of others has been acknowledged in the text and a list of references is given.

Every reasonable effort has been made to gain permission and acknowledge the owners of copyright material. Therefore, this work in no way infringes or violates another person's copyright, trademark, or patent. However, I would be pleased to hear from any copyright owner who has been omitted or incorrectly acknowledged.

_____

Beatriz Diaz-Guijarro

Acknowledgements

First, I would like to thank my family, in particular my parents. Their support, patience and guidance saw me through every stage of my candidature. I am blessed to have parents that have always pushed me to strive for greatness and to love learning.

I would also like to thank my fellow PhD students who provided me with guidance and helped me navigate the ins and outs of being a PhD candidate within the Miller lab: Chloe Boote, Ramona Brunner, Casey Whalen, Mila Grinblat, Legana Fingerhut, Felicity Kuek, Bruna Pereira Luz, and Jia Zhang. Also, I would like to thank my supervisors Prof. David Miller, Dr. Ira Cooke, and Dr. Aurelie Moya for taking me on as a PhD candidate and allowing me to embark on this adventure.

I would like to acknowledge the funding support provided to me by James Cook University and the Australian Government through the James Cook University Research Training Program (RTP) Scholarship. I would also like to thank the Australian Research Council (ARC) for funding this research through grants awarded to myself and my supervisors.

I would like to thank many staff members at James Cook University for their technical assistance, guidance, and advice, in particular Christine Blight for making sure the Miller lab always ran efficiently and everything needed was acquired as quickly as possible. Also, Simon Wever and Ben Lawes at MARFU for setting up the equipment for my experiments, for helping with equipment issues and maintenance of aquaria.

I would like to thank the staff members at the Australian Institute of Marine Sciences, in particular Craig Humphrey for allowing me to do my pilot experiments at SeaSim and providing the corals for them. Also, Andrea Severati and Lonidas Koukoumaftsis for all their help with any technical aquaria questions or issues. I would also like to thank the staff at the Orpheus Island Research Station for their technical assistance, guidance, and advice during sample collection.

Finally, I would like to dedicate this thesis to my husband Graham, you have been a never-ending source of support throughout this entire experience. There is no way I would have accomplished this without your sacrifices and constant love and understanding. You have been there to celebrate the ups and to lean on for strength during the downs. I truly do not know where I would be without you, but one thing is for sure, taking on this journey would not have been possible. I love you with all my heart and profoundly appreciate everything you have done for me.

Statement of Contribution of Others

Nature of Assistance	Contribution	Names, Titles, and Affiliations of Co-Contributors
Intellectual Support	Proposal writing	Prof. David Miller
		Dr. Ira Cooke
		Dr. Chloe Boote
	Data analysis	Dr. Ira Cooke
		Dr. Jia Zhang
	Statistical support	Dr. Ira Cooke
	Editorial assistance	Prof. David Miller
		Dr. Ira Cooke
		Dr. Zoe Pettifer
Financial support	Fee offset/waiver and stipend	JCUPRS
	Research costs	James Cook University, Townsville, AU
		Australian Research Council - Centre of Excellence
	Travel award	ACRS travel award
Data collection	Sample collection	Dr. Mila Grinblat
		Volunteers
	Sample processing	Dr. Mila Grinblat
		Dr. Bruna Pereira Luz

Contribution of authors to each chapter

Chapter 2:

Project conceptualization: Beatriz Diaz-Guijarro, David J Miller, Ira Cooke, and Aurelie Moya

Data collection: Beatriz Diaz-Guijarro

Analysis: Beatriz Diaz-Guijarro

Writing: Beatriz Diaz-Guijarro

Editing: David J Miller and Ira Cooke

Chapter 3:

Project conceptualization: Beatriz Diaz-Guijarro, David J Miller, Ira Cooke, and Aurelie Moya

Data collection: Beatriz Diaz-Guijarro

Analysis: Beatriz Diaz-Guijarro

Writing: Beatriz Diaz-Guijarro

Editing: David J Miller and Ira Cooke

Chapter 4:

Project conceptualization: Beatriz Diaz-Guijarro, David J Miller, Ira Cooke

Data collection: Beatriz Diaz-Guijarro

Analysis: Beatriz Diaz-Guijarro

Writing: Beatriz Diaz-Guijarro

Editing: David J Miller and Ira Cooke

Thesis abstract

Climate change-associated anthropogenic stressors have put corals on the global threatened list. Mass coral bleaching threatens reefs worldwide predominantly due to ocean warming, ocean acidification, and altering salinity levels and light intensity. Other anthropogenic stressors that threaten the existence of corals are damage, overfishing, pollution, collection of live corals for aquarium markets, and mining coral for building materials. All these can also have detrimental effects on both the health and mortality rate of the epifauna that inhabit our oceans. Due to the critical threats posed to corals, recent research has focused on the molecular and cellular mechanisms of the coral response to damage and anthropogenic stressors. Over the past 15 years, numerous transcriptomic studies have examined gene expression responses to anthropogenic stressors and regeneration. However, despite this considerable effort, our knowledge on the biological dynamics of the stress response or regeneration from wounding are incomplete. Therefore, the main objective of this project was to examine the molecular bases of regeneration and heat-stress bleaching on the Fungiid coral *Heliofungia actiniformis*. It focused on the gene expression changes during tentacle regeneration and heat stress associated with bleaching on the host coral and the inhabiting symbionts. It hoped to create a clearer understanding of the processes involved in coral survival and aimed to fill current gaps in coral regeneration for possible future implementation of reef conservation.

There were five main morphological stages present in the regeneration process: wound closure; “pinched” like closure; smooth appearance; start of acrosome formation; and acrosome fully regenerated. The focal five indistinguishable morphological stages were observed across all *Heliofungia* corals from the pilot and main experiments. Transcriptional analysis (PCA) showed that genotype accounted for most of the variation in all three studies. It required inclusion in the model and made it possible to identify and analyse differentially expressed genes across the timepoints with the adjusted p-value < 0.05. The results from all three studies that made up this project supported past research. For instance: the regeneration study supported the theorised cnidarian regeneration stages, early regeneration (composed of wound healing and cell mobilisation) and late regeneration (comprised of tissue morphogenesis); the host heat-stress bleaching study supported the core cnidarian heat-stress response system theorised by Cziesielski in 2018; and the symbiont heat-stress results supported the activation of genes observed in other symbiont studies.

Furthermore, the results of the three studies also supported each other as several activated genes during tentacle regeneration were also activated during the heat-stress timepoints. There was also novelty in the results observed. For example, the ATP-binding family was the primary function activated throughout regeneration which has only been previously recorded as activated in mammal

regeneration, which could imply that some of the processes involved in cnidarian regeneration has connections to mammals. At the same time, in the bleaching studies, endoplasmic reticulum BiP was the primary function activated before bleaching, which has not been previously recorded in coral bleaching implying that there is gene folding and quality control occurring during bleaching in the endoplasmic reticulum lumen.

This project developed new methods and identified molecular processes involved in *Heliofungia* bleaching and regeneration for the first time. The heat-stress bleaching methodology was the first recorded study on bleaching that began at acclimation temperature, continued through heat-stress, and ended once the corals were considered entirely bleached. Overall, the project supported the hypotheses outlined and disclosed findings potentially novel to *Heliofungia*. Coral reefs are vital marine ecosystems, and given the current pace of global climate change, efforts to understand and protect them are more urgent than ever. The knowledge derived from this project adds to the valuable information that researchers and conservationists can utilize to mitigate the effects of climate change and damage on these invaluable marine ecosystems.

Table of contents

List of tables

List of figures

Chapter 1: Regeneration and heat-stress bleaching

Coral reefs are prime global economic assets and, as one of the world's seven natural wonders, Australia's Great Barrier Reef (GBR) constitutes 10% of the global coral reef ecosystems (White et al., 2000). Within the 2015-2016 financial year, the GBR contributed an estimated A$56 billion in total economy, social, and icon asset value, an estimated A$6.4 billion in the national economy, and 64,000 jobs. Providing Australia with more capital than12 Sydney Opera Houses and more jobs than those provided by central banks and corporates, such as Qantas (Authority, 2019; Day, 2019). The GBR is considered the most complex natural system on Earth as it extends over 14 degrees of latitude and has a unique variety of ecological communities, species, and habitats (Authority, 2019; Day, 2019).

Threats from anthropogenic climate change (e.g., mass bleaching due to ocean warming) and natural disasters (such as cyclones) are negatively impacting global coral reefs and their associated biodiversities (Emanuel et al., 2008; Emanuel, 2013). The rise in atmospheric greenhouse gases contributes to increasing ocean temperature resulting in mass coral bleaching, which has put corals on the global threatened list. Therefore, understanding regeneration and heat stress at the molecular level contributes vital knowledge on gene functions for improved coral reef management efforts. Studying regeneration provides a good comparative framework within which the molecular processes in different species can be understood. Ultimately, insight into the mechanism of regeneration in simple organisms can lead to a better understanding on the limited regeneration in mammals and other "higher" animals, which can aid in the adoption of improved therapeutic approaches on human injuries. Heat stress and regeneration studies at the molecular level can provide insights that may lead to improved conservation approaches of corals reefs. Also, employing damage and recuperation rates could be a vital tool for anticipating demographic adaptations in coral populations (Bak & Meesters, 1999; Fisher et al., 2007).

The molecular mechanisms involved in heat-stress bleaching in robust corals and regeneration in symbiotic corals remain largely unexplored. The hope is that research into regeneration of non-model organisms, such as *Heliofungia*, might provide new general perspectives on regeneration processes. Heat stress studies into robust corals, such as *Heliofungia*, provide new information to a knowledge base that is largely built on studies in complex corals. Therefore, in Chapters 2, 3 and, 4, gene expression patterns during heat-stress bleaching and regeneration in the Fungiid coral *Heliofungia actiniformis* and its inhabiting symbionts were studied. The present chapter provides an overview of regeneration across the animal kingdom.

1.1. *Heliofungia* as a model for research

Heliofungia actiniformis (Scleractinia: Fungiidae) is ranked as one of the top five species exploited for the live coral market (Knittweis, 2008). Their large size, free-living nature, the ease with which they can be maintained in aquaria, anemone-like appearance, and ease of collection and transport make them highly prized in the international aquarium trade industry. *Heliofungia* individuals are capable of rapid regeneration and can exploit two modes of nutrition as they are both zooxanthellate, and therefore can fulfil most of their energy needs via photosynthesis and can also feed heterotrophically to a greater extent than many colonial corals by using their long tentacles. These features make them ideal candidates for research and developing genomic models to study the process of regeneration.

Heliofungia and its relatives (the Fungiidae corals; also known as mushroom corals) are distinctive from other cnidarians as they are large solitary polyps, considered the largest of all corals, with two named species, *actiniformis* and *fralinae* (Knittweis, 2008). They have a striped oral disk and are pale brown/grey or dark blue/green tentacles with white or pink tips (Dai & Horng, 2009). These corals are circular or oval with a diameter of up to 20 centimetres and a height of around seven centimetres (Dai & Horng, 2009). They have a single mouth slit in the centre of their thick and fleshy polyp surrounded by hundreds of tentacles ending in white acrosomal tips (Figure 1.1 A and B). Their corallum is thick and solid, and an attachment scar is in the centre of their underside (Dai & Horng, 2009). These corals are easily identified via their long colourful tentacles and large single polyp characteristic (Knittweis, 2008). They are commonly located on flat soft or rubble substrates, particularly in shallow turbid environments or reef lagoons. Limited research has been conducted on *Heliofungia actiniformis* despite their many advantages.

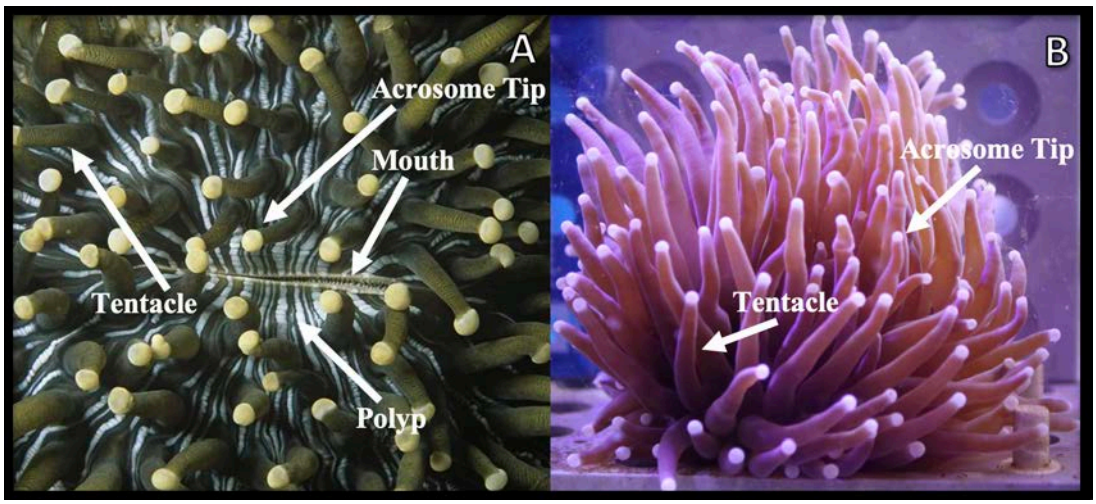

Figure 1.1A-B. Morphology of *Heliofungia actiniformis*. (A) Aerial view of *H. actiniformis* coral showing the mouth, polyp, tentacles, and acrosomes. (B) Profile view of *H. actiniformis* coral, with tentacles and acrosome tips.

1.2. Regeneration

Regeneration is a well-documented phenomenon reported in various types of fauna. The 14 most studied genera with regenerative abilities are metazoans, including humans. Simpler animals such as cnidarians (*Heliofungia*, *Hydra*), platyhelminthes (planarians), and chordata (amphibians) can regenerate more significant body parts such as their heads and hearts. Ongoing research into the regeneration abilities of these types of animals may ultimately assist in regenerating human limbs and organs as the connection between simpler and more complex animals has been shown at cellular and molecular levels. For example, chordates (flatworms, salamanders), and cnidarians (*Hydra)* have significantly different morphologies but share fundamental molecular mechanisms within their regeneration systems (Nagelkerken & Bak, 1998; Stewart et al., 2017). Molecular processes active during regeneration include generating bioelectrical currents via the nervous system, creating injury epithelium at the site of injury, inflammation, and the immune system (Brockes & Kumar, 2008; Stewart et al., 2017).

There are three different kinds of regeneration, and the type used is determined by the animal. Epimorphosis is considered the first main type of regeneration, and it comprises the dedifferentiation of adult configurations to form an accumulation of cells that then become respecified. Epimorphic regeneration involves two main changes as a response to injury which are the transformation of mature tissue into a blastema followed by the transformation of the blastema into a regenerated organ (Gilbert, 2000). Blastema regeneration (the second type) has seven key components: wound epidermis establishment that attracts blastemal cells and preserves cell proliferation; an innervation and exposure to nerve or Schwann cell secreted factors; extracellular matrix creation; developmental signalling pathways are deployed; physical interaction of cells; level-specific (new vs old tissue) replacement of tissue for the generation of a complete organ; and a requirement of macrophages to instigate regeneration (Seifert & Muneoka, 2018). Therefore, the blastema and epimorphic regeneration are closely linked during limb, vertebrate, and organ regeneration in vertebrates such as fish, amphibians, rodents, and mammals (Seifert & Muneoka, 2018). Morphallaxis is considered the second main form of regeneration (but third overall), and it involves slight new growth as it repatterns existing tissues and it is mostly seen in cnidarians, such as *Hydra* (Reddy et al., 2019). This third type of regeneration is generally associated with mammalian liver regeneration (Gilbert, 2000).

The extent of regenerative capacity is not directly correlated with phylogeny, although in general “lower” animals (such as cnidarians and platyhelminthes) have greater capacity for regeneration than do “higher” animals such as vertebrates. However, in vertebrates, extensive regeneration during adulthood is only possible amongst Actinopterygians and Urodeles (Tawk et al., 2002), whereas others including mammals, can only heal wounds due to their limited regenerative abilities.

Nevertheless, research into the regeneration of limbs in animals such as the (Urodele) salamander is employed in medicine to understand stem-cell recruitment, proliferation, and differentiation (Tawk et al., 2002). Therefore, understanding the molecular mechanisms underlying regeneration in "simple" organisms (such as cnidarians and planarians) could help in identifying critical factors involved in regeneration present in "higher" organisms (Alvarado & Tsonis, 2006).

Despite significant progress, little is known about how cnidarians translate amputation stress into a regeneration-inducing signal. The molecular signals involved in communication between cell populations during regeneration are also mainly unknown (Amiel et al., 2015). However, some of the genes and activities involved in regeneration are also active during development, therefore, functional data from developmental studies may be used to help interpret those on regeneration and vice-versa. (Burton & Finnerty, 2009; Röttinger, 2021; Warner et al., 2020; Warner et al., 2021). In this study, transcriptomic data were used to investigate the molecular bases of regeneration in the mushroom coral *Heliofungia,* and comparisons are made with regeneration in other animals. This work is intended to address a significant knowledge gap in coral biology concerning their regenerative capacity, as details of involved mechanisms are largely unknown (L. Knittweis et al., 2009; Leyla Knittweis et al., 2009). The aim is to observe morphological and temporal differences in the corals that cannot be observed in colonial corals.

Heliofungia should be a model organism for regeneration studies. Unlike most coral polyps, which are relatively small and have very little fleshy tissue making the retrieval of molecular information challenging, *Heliofungia* has large tentacles and is a large polyp that allows for a section of an individual polyp to be analysed instead of a collection of polyps. As tentacles do not a have skeleton, they regenerate at a faster rate than when dealing with skeleton and their large size make them more accessible. However, currently there are no studies that have been implemented on robust corals such as *Heliofungia* leaving a gap in the understanding of robust coral regeneration (Pollock et al., 2011).

1.2.1 Regeneration in different animals

Primarily studied fauna with regenerative abilities include cnidarians, planarians, annelids, echinoderms, teleost fish, amphibians, and reptiles. However, many other animals can regenerate specific body parts, including arachnids and arthropods (which can regrow legs), and mammals such as deer (able to "shed" and regenerate antlers), bats (can regrow parts of their wings when injured), and rabbits (which can regenerate parts of their ear lobes). Representative organisms discussed here (e.g. cnidarians, planarians, amphibians, and teleost fish) were chosen due to their impact on understanding the molecular mechanisms underlying regeneration. By performing preliminary research on the regeneration of other taxa we develop a baseline understanding of the possible

mechanisms that may arise in our study, which also allows the discovery of processes that are unique to our target organism. The focus will be on corals as they have extensive regenerative abilities; however, the molecular mechanisms involved in these processes remain largely unknown.

1.2.1.1 Cnidarians

The phylum Cnidaria comprises over 11,000 species, including Hydra, corals, sea anemones and jellyfish. Despite differences in appearance and behaviour, they share several attributes, such as having microscopic stinging capsules called cnidae or nematocysts, and they have some regenerative steps and pathways in common. For example, the regeneration process of cnidarians involves three stages as in other Metazoans: wound healing, tissue rearranging through cell mobilisation, and restoration or differentiation of lost tissue through cell proliferation, axial patterning, and morphogenesis (Cary et al., 2019; Luz, 2020). Many of the genes expressed immediately after amputation either participate in cellular stress responses (e.g., heat shock genes), are associated with cell signalling pathways (e.g., MAPK cascade) or are transcription factors (Cary et al., 2019; Stewart et al., 2017). Regeneration in sea stars, corals, and Hydra feature some genes and pathways in common with other animals (Figure 1.2), such as regulatory genes and Wnt signalling components. Like other Metazoans, cnidarians use pathways such as MAPK, JNK, and ERK, during regeneration. Components affecting the regeneration process are studied to understand what impairs the regeneration ability of animals (Cameron & Edmunds, 2014; Forsman et al., 2020; Lirman, 2000; Luz et al., 2018). For example, the regeneration rate of mouth fragments in *Tubastraea* is increased in the presence of abundant food (Luz et al., 2018). *Porites asteroides* can completely regenerate within 140 days from 64% tissue damage or 48% tissue and skeleton damage if the area of damage is less than $5cm^2$ (Bak & Steward-Van Es, 1980).

In corals, regeneration rates differ among species (Bak, 1977; Fisher et al., 2007; Kawaguti, 1937; Nagelkerken & Bak, 1998), and are determined by the characteristics of the contusion such as the type of laceration, the contusion's initial shape, size, and perimeter (Fisher et al., 2007; Lirman, 2000; Oren et al., 1997). Size and other characteristics can also influence regeneration rates of individual coral colonies (Fisher et al., 2007; Kramarsky-Winter & Loya, 2000; Oren et al., 1997).

Molecular and cellular processes underlying the regenerative abilities of corals, especially robust corals are not yet understood, however, research on Hydra (a model cnidarian) has been extensive as it is capable of regenerating its entire body due to its highly proliferative stem cells (Fatima et al., 2024; Holstein, 2023; Steichele et al., 2024; Vogg et al., 2019). Hydra is considered a model organism partially due to its three distinct somatic stem cell lineages containing 50,000 to 100,000 cells (Fatima et al., 2024; Tomczyk et al., 2015) and is considered a valuable research model because of its high

regenerative capacity and swift reproduction. Hydra also shares over 6,071 genes with humans and it has 36 metazoan genomes making it one of the most basally divergent cnidarian genome (Gehrke et al., 2019; Holstein, 2022; Holstein, 2023; Kalafatić et al., 2001; Wenger & Galliot, 2013). The regeneration process is inhibited through the repression of genes associated with Wnt signalling (Duffy, 2011; Duffy et al., 2010), which has also been encountered in coral development (Cameron & Edmunds, 2014; Forsman et al., 2020; Lirman, 2000; Luz et al., 2018).

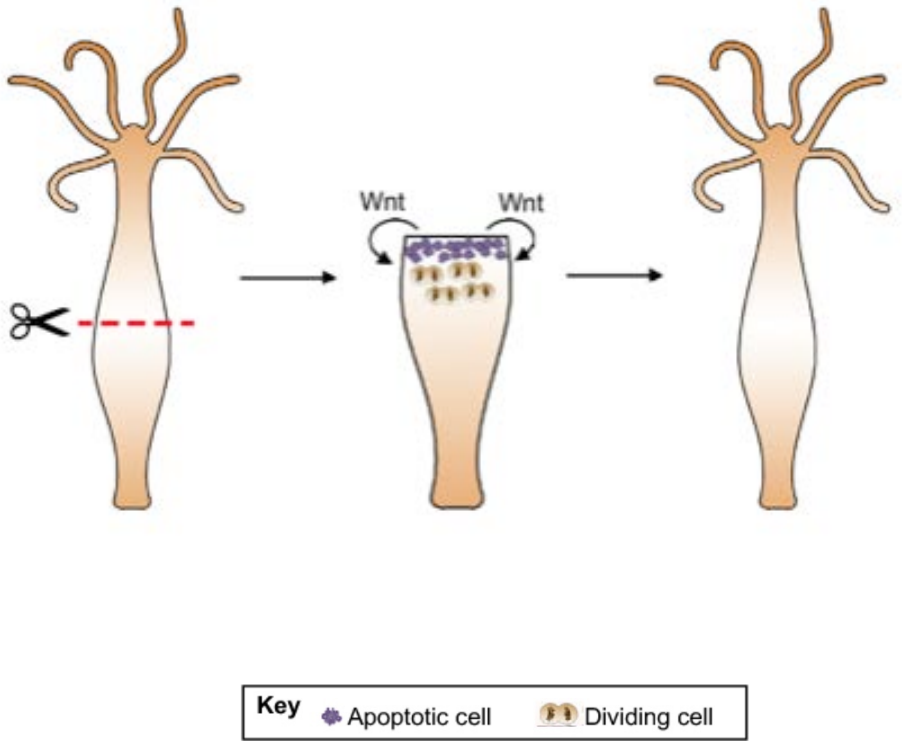

Figure 1.2. Regeneration in cnidarian. Illustration of where the Wnt genes are located during half-body regeneration in the cnidarian *Hydra*.

A specific chain of events is required to initiate regeneration in cnidarians and many other Metazoans. Commonly, ROS production is the initiating event followed closely by apoptosis, eventually resulting in cell proliferation via Wnt molecules (Bideau et al., 2021). Wnt/B-catenin signalling pathways and Wnt pathways are vital to regeneration as their primary role is to establish longitudinal axis polarity, drive tentacle regeneration, and participate in later stages of regeneration (Bideau et al., 2021; Cary et al., 2019; van der Burg et al., 2020; van der Burg & Prentis, 2021). It is considered likely that the Wnt, MAPK/ERK, and FGF pathways serve conserved roles during regeneration across the Cnidaria as their expression primarily occurs during the first stage of the regeneration process, as found in studies on Hydra, anemones, and corals (Cary et al., 2019; DuBuc et al., 2014; Fumagalli et al., 2018; Kawakami et al., 2006; Levin et al., 2016; Maddaluno et al., 2017; Minowada et al., 1999; Plotnikov

et al., 2011; van der Burg & Prentis, 2021; Xu, 2022). At later stages of regeneration, Wnt signalling is vital to specify the axis before the occurrence of a significant cell proliferation event associated with the expression of different genes (Amiel et al., 2015; Bideau et al., 2021; Fumagalli et al., 2018; Passamaneck & Martindale, 2012; Röttinger, 2021).

1.2.1.2 Amphibians

Different types of amphibians have differing levels of regenerative ability. For example, Urodela amphibians possess the most extensive regenerative ability of all tetrapods, known as epimorphic regeneration, which allows them to completely regenerate their retinas, tails, jaws, and limbs (Brockes & Kumar, 2002; Brockes et al., 2001)

Blastema regeneration occurs in amphibians. Blastemal cells immediately generate all the cells for the new body part after amputation, during which cells around the wound dedifferentiate into progenitor cells (Brockes et al., 2001; Endo et al., 2004; Iten & Bryant, 1973). After amputation, damaged cartilage is removed by the gene products associated with Mmp-9 genes which can be downregulated by retinoids (Yang et al., 1999). Next, epidermal cells form a wound epithelium over the remnants of the amputated fragment (Figure 1.3) (Christensen & Tassava, 2000). The blastema is generated over the next few days, followed by the activation of genes such as HoxD and HoxA (Figure 1.3) (Bryant, 2002). The whole process builds the autopod (most distal part of the limb which serves as a model system of pattern formation during limb development) of the limb through the blastema, followed by intercalation of motor neurons, blood vessels and muscle (Bryant, 2002). The time taken for complete regeneration depends on the age of the animal but can be up to three months in an adult (Bryant, 2002).

Axolotls are the first amphibian model organisms whose whole genome sequence has been developed due to advances in somatic cell transgenesis, bioinformatics and genomics (Han et al., 2001). The Fgf-8 gene is expressed during the development of the forelimb region at two different bud-developing phases and in limb regeneration, during the creation of the blastema and in the basal layer of the apical epithelial cap (Han et al., 2001). Some of the genes involved in amphibian development and limb regeneration are also expressed during cnidarian regeneration. For example, some of the homeobox (Hox) genes are thought to provide positional information in axial patterning during development and regeneration in both cnidarians (Chiori et al., 2009; Galliot, 2000; Galliot & Schmid, 2002) and amphibians.

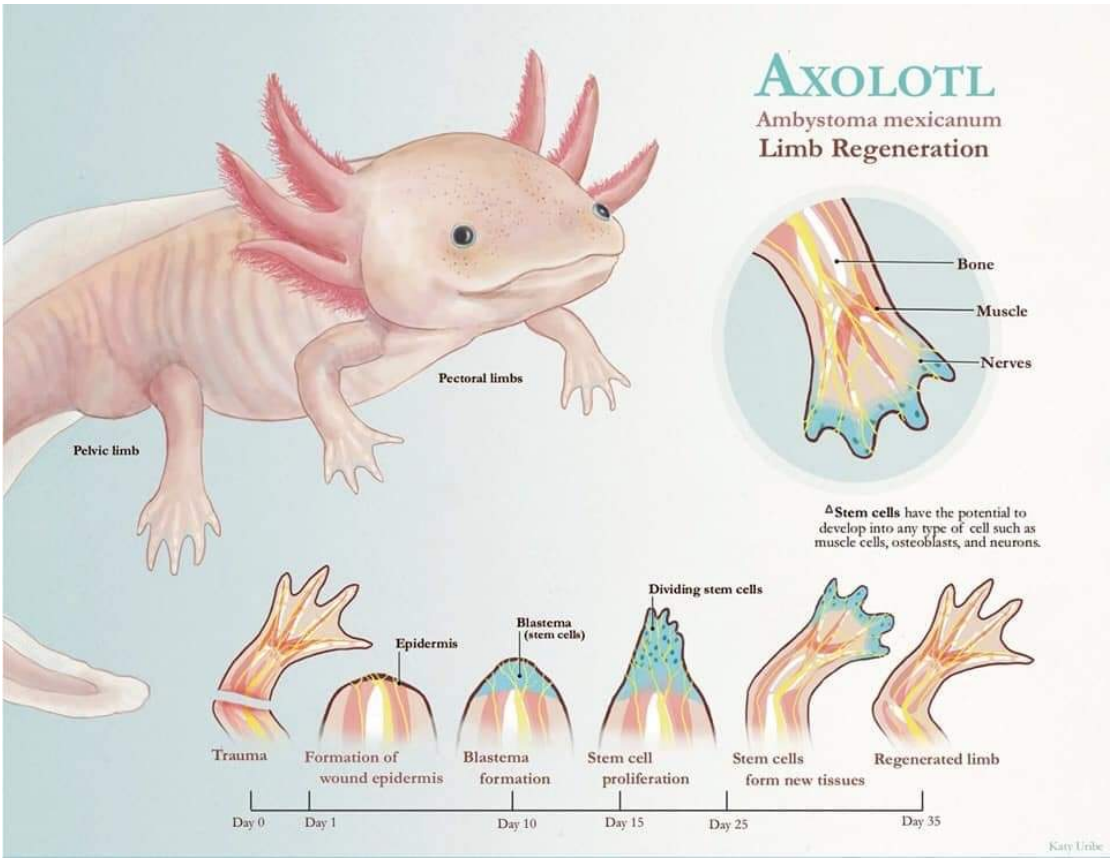

Figure 1.3. Limb regeneration in axolotl. Pictorial explanation of the process of limb regeneration in the axolotl. From Uribe. K (2019) UQ Herpetological Society.

1.2.1.3 Chondrichthyes

Chondrichthyes can regenerate teeth, skin, scales, cells, and organs with the use of micro-RNAs (Lu et al., 2013; Reif, 1978; Sun & Ripps, 1992; Tucker & Fraser, 2014; Vorontsova & Liosner, 1960). Micro-RNAs (miRNAs) participate in many functions such as, in the regulation of cell proliferation, cell cycle, developmental timing, maintenance of cell reprogramming, cell differentiation and fate, regulation of gene expression networks, and fine tuning of gene expression (Ribeiro et al., 2022). MiRNAs mostly bind to certain areas in the 3'-unstranslated region section of the target mRNA and down-regulate or inhibit gene expression (Ribeiro et al., 2022). MiRNAs are considered to control tissue repair and regeneration, and their many functions allow them to be utilised as predictive biomarkers of adaptive responses in mammals (Sen & Ghatak, 2015; Spakova et al., 2020). The miRNAs and genes present during shark tooth regeneration have been associated with liver regeneration in other animals (Diaz-Rodriguez et al., 2019; García-González et al., 2020). Tail regeneration in a second species of Chondrichthyes, the finned ray, *Polypterus*, has also been extensively studied. This property is not shared by paired fin sharks, and is initiated by the creation of a blastema expressing the Sonic hedgehog genes (Shh) in the caudal region, a process resembling fin, scale, and organ development in zebrafish (Akimenko & Ekker, 1995; Cuervo et al., 2012; Sire, 2004;

Sun & Ripps, 1992). Shh expression has also been associated with cnidarian epithelial signalling during gut and germline development (Matus et al., 2008).

1.2.1.4 Teleost fish

Teleost fish are established as genetic models for the study of brain regeneration and lost cells in the central nervous system as their ability to regenerate missing cells, organs, and appendages has contributed to the foundational knowledge on regeneration (Eguchi et al., 2011; Lust & Tanaka, 2019; Poss et al., 2002; Singh et al., 2012). For example, teleosts possess a primary function of neurogenesis to maintain the ratio of the number of central neuronal elements within motor and sensory pathways, which is hypothesised to be critical to brain regeneration that is no longer active in mammals (Koumans & Akster, 1995; Rowe & Goldspink, 1969; Rowlerson & Veggetti, 2001; Zimmerman & Lowery, 1999). Amongst teleosts, zebrafish are the preferred model for regeneration research as they provide a genetically tractable model mechanism making them an exceptional model for research into the roles of vertebrate genes (Akimenko et al., 1995; Jaźwińska & Blanchoud, 2020; Nakatani et al., 2007; Reimschuessel et al., 1993; Reimschuessel & Biggs, 1996; Tawk et al., 2002). Predominantly zebrafish are the leading genetic model organism in heart and liver regeneration as the procedures resemble that of more complex animals; for example, the mechanisms in teleost and mammal liver regeneration are accomplished by cell replication and migration in a distal and proximal direction around the injury (Reimschuessel, 2001).

1.2.2 Molecular mechanisms in regeneration

Homeobox genes are a family of developmental regulatory genes that direct cell patterning activities during embryogenesis and have also been associated with limb regeneration in different types of organisms (Hu et al., 2001). Msx genes are essential for normal limb and ectodermal organ morphogenesis in corals, mice, and mammals (Alappat et al., 2003; Shumaker et al., 2019). Wnt genes are seen in every organism in the animal kingdom, are highly conserved throughout species (Zheng et al., 2010) and function in three pathways; canonical Wnt pathway, noncanonical planar cell polarity (PCP) pathway, and canonical Wnt/calcium pathway (Zheng et al., 2010). These mechanisms are related to one another as Msx genes are members of the homeobox gene family and Wnt signalling genes activate Msx genes (Figure 1.4) (Liu et al., 2021; Nallasamy et al., 2019).

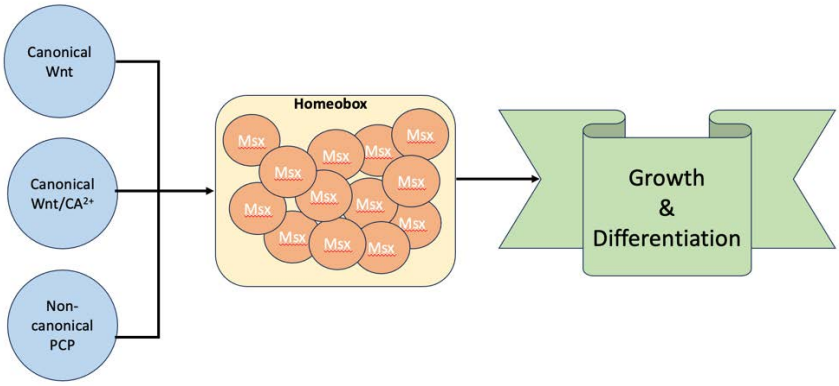

Figure 1.4. Model for Wnt pathways. An outline of interactions between Wnt genes and homeobox genes.

Genes homologous to those involved in axis formation, tissue patterning and neural development in bilaterians are present in morphologically simple animals, such as cnidarians and other non-bilaterian animals (Bideau et al., 2021). Expression of some of these genes is critical to initiate regeneration by reiterating tissue development and the start of tissue growth post-injury (Chen et al., 2022; Shao et al., 2020; van der Burg et al., 2020). Genes associated with regeneration are typically enriched in the KEGG categories of signal transduction, transcription, translation, cellular proliferation, differentiation and programmed cell death (e.g. FOS and HUNB) (Shao et al., 2020). FOS is a vital component of the cell signalling system that is activated instantly after cell damage, and it contributes to neoblast maintenance and wound response programs across bilaterians (Shao et al., 2020; Xu, 2022). The genes that are most highly expressed during the earliest stages of regeneration are transcription factor c-Fos response genes (implicated in injury and stress response in multiple model systems) and genes encoding components of the JNK cascade (regulates c-Fos across bilaterians) (Shao et al., 2020; Xu, 2022). Genes involved in cell interaction, cell movement, and matrix metallogeneases (including Adam22, CTRB1, and Casd1) are among the most highly expressed genes during regeneration in anemones and are expressed across all time points of regeneration (Bideau et al., 2021; van der Burg et al., 2020). Inhibiting Notch and MEK/ERK signalling block regeneration or regeneration and wound healing, so these processes are considered essential (Röttinger, 2021; van der Burg et al., 2020). Early growth response gene (EGR1) is a family member of the early response gene transcription factor and is associated with the alteration of various cellular processes (e.g. development, cell growth and stress responses) in numerous tissues and can control the propagation and localisation of stem cells (Boros et al., 2011). It is also a core regulator of wound healing that encodes an epidermal growth factor receptor (EGFR). This transmembrane receptor tyrosine kinase that can regulate cell propagation and variation (Fraguas et al., 2011) and is upregulated along with an immediate early response gene, IER5L, throughout the regeneration process in annelids (Shao et al., 2020).

1.3 Bleaching

Climate change is considered one of the most critical threats to coral reefs in the next 100 years (Howells et al., 2020). The most obvious consequence of climate change is the rise of ocean temperatures, which will increase the frequency of global coral bleaching (Sato et al., 2020; Sully et al., 2019). Bleaching is commonly observed as the decolourisation of corals. It is the condition where environmental stressors cause either expulsion or a reduction of symbiotic algae, leaving the coral host white (Roach et al., 2021). The possible triggers for coral bleaching include photosynthesis-produced ROS, activation of endogenous viruses by a rise in temperature, bacterial infection, and excessive rise in turbidity and sedimentation. These triggers associate the leading cause of bleaching with the loss of symbionts due to thermal stress.

Coral biologists hope to make more informed decisions about conservation actions when the mechanisms underlying in coral bleaching or dysbiosis are better understood through research. Multiple studies have attempted to document the cellular complexity of bleaching, host cell detachment, mechanisms of host cell apoptosis, exocytosis, necrosis, and *in situ* degradation (Oakley & Davy, 2018; Roberty & Plumier, 2022; Suggett & Smith, 2020). However, two main types of systems associated with bleaching have been recognised: the loss of pigments by symbionts *in situ* and the loss of symbionts, either by being ejected or choosing to exit the host (Weis, 2022).

1.3.1 Heat-stress bleaching

On exposure to heat-stress, corals show variations in their response based on the region and species (Dixon et al., 2020; McClanahan & Maina, 2003; McClanahan et al., 2007; Safaie et al., 2018; Van Woesik et al., 2012). Modelling of real world data implies that rates of change of sea-surface temperature (SST) are effective predictors of bleaching as increased levels of change correlated with increased levels of bleaching (Sully et al., 2019). The hypothesis of a core cnidarian heat-stress response system was suggested in 2018 and supported in 2019 (Cziesielski et al., 2018; Cziesielski et al., 2019). The comparison of cnidarian response towards heat stress highlighted the involvement of several common pathways, including regulation of gene folding, oxidative stress response, and calcium homeostasis. These response pathways have been supported in research involving adult, larvae, and larval development as similar cellular responses have been witnessed (Negri et al., 2007; Polato et al., 2010; Portune et al., 2010; Voolstra et al., 2009).

1.4 Symbiont

Some of the metabolic interactions between a coral and its symbionts seem to be particularly significant in determining whether bleaching occurs. (Dixon et al., 2020; Lawson et al., 2019; Stuhr, Blank-Landeshammer, et al., 2018; Stuhr, Meyer, et al., 2018). Therefore, understanding how heat stress affects symbionts in-hospite and how molecular products of symbionts under stress affect the host is central to understanding the bleaching process. Furthermore, symbionts have evolved in various ways in response to increased thermal stress, such as DNA damage repair systems and expression of heat-shock genes, to increase the adaptive potential of subsequent generations (Klosin et al., 2017; Richter et al., 2010; Tedeschi et al., 2016). Therefore, understanding how these evolutionary changes affect both the host and symbiont are crucial in the production of conservation plans.

1.4.1 Relationship between *Symbiodiniaceae* and host corals

Algal endosymbionts enable corals to thrive in nutrient-poor waters by providing photosynthetically derived energy and metabolic building blocks. In 2018, the taxonomy of the genus previously known as *Symbiodinium* was comprehensively revised, resulting in *Symbiodinium* clades being elevated to genus level within the newly recognised family *Symbiodiniaceae* (LaJeunesse et al., 2018). There are 15 genus equivalent lineages of *Symbiodiniaceae* amongst them are*; Symbiodinium, Breviolum, Cladocopium, Durusdinium, Effrenium, Freudenthalidium, Fugacium, Gerakladium, Halluxium,* and *Miliolidium* which are the ten main genera erected from the divergence of the clades (LaJeunesse et al., 2018; LaJeunesse et al., 2021; Nitschke et al., 2020a; Nitschke et al., 2020b). The last five have not currently been formally describes as they lack type material for species designation (LaJeunesse et al., 2018). The genus from the ten formal *Symbiodiniaceae* identities hosted by a coral species is considered to be a critical factor in determining the ability of their host to tolerate environmental stress, as different *Symbiodiniaceae* have varying degrees of thermal tolerance and photosynthetic responses (LaJeunesse et al., 2018; Robison & Warner, 2006).

However, understanding changes in thermal tolerance based upon genera of symbionts is challenging as different types of hosts are inhabited by different genera. Cnidarian hosts can simultaneously harbour multiple symbiont species, creating complex and dynamic communities (Ferrari & Vavre, 2011). The system comprising the eukaryotic (the *Symbiodiniaceae* and others) and prokaryotic symbionts, and their cnidarian host is known as the holobiont. The many and various components of the microbiome include protists, endolithic algae, and viruses, as well as both eubacteria and archaebacteria. Although the metabolic roles of these symbionts are unknown, some are thought to participate in antibiotic synthesis, carbon fixation and sulphur cycling (Allemand & Furla, 2018; Bourne et al., 2016).

The host-symbiont relationship can be thought of as going through three phases: the establishment of symbiosis, the dynamic preservation of the relationship, and finally, dysbiosis – the breakdown of the relationship (Figure 1.5) (Davy et al., 2012). This host-symbiont relationship theory has previously been supported; for example, the expression of immunity-related homologs (TGFbeta - TGFb) has been observed during bleaching in *Aiptasia* (Kitchen et al., 2017; Kitchen & Weis, 2017), *Orbicella faveolate* (Fuess, 2018), and *Fungia scutaria* (Detournay et al., 2012).

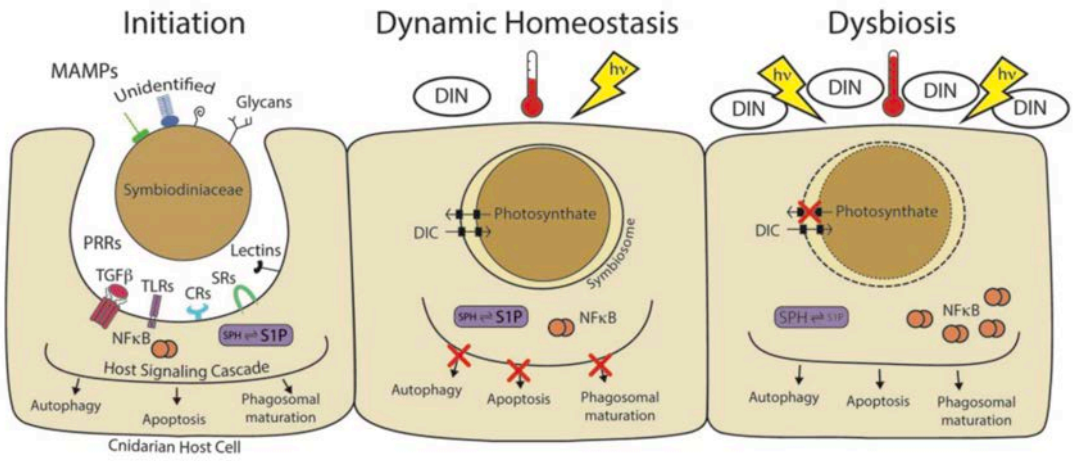

Figure 1.5. Schematic diagram of cnidarian host pathways interacting with *Symbiodiniaceae* during symbiosis. Three phases of symbiosis are depicted: **Initiation phase (left)**: *Symbiodiniaceae* are grouped with other symbionts from the cell surface, such as MAMPs, which encounter PRRs (such as TGFb, TLRs, CRs SRs, and lectins) during phagocytosis. An appropriate *Symbiodiniacea* connection will adapt the immune response and maintain inhabitation of the host. **Dynamic homeostasis phase (middle):** During a stable symbiosis, symbiont and host engage in a dynamic exchange of nutrients whereby the host passes dissolved inorganic carbon (DIC) to the symbionts, which in turn fix the carbon by photosynthesis and pass it back to the host as photosynthate. **Dysbiosis phase (right):** Certain environmental stressors, such as elevated temperature, increased light, and excess dissolved inorganic nitrogen (DIN), result in photosynthate transport interruption to the host and a re-engagement of the innate immune system. The sphingosine rheostat is pushed toward pro-apoptotic Sph, NF-jB is upregulated, and the host mounts an immune response to eliminate the stressed symbiont. This dysregulation results in dysbiosis and bleaching. From: (Davies et al., 2023).

1.5 Thesis aims and objectives.

The goals of this thesis are:

(i) to identify the critical stages of tentacle regeneration and heat-stress-associated bleaching in the Fungiid coral *Heliofungia actiniformis* and its inhabiting symbionts,

(ii) to investigate the molecular mechanisms during regeneration and throughout heat-stress and bleaching,

(iii) to identify the gene expression patterns and changes occurring during tentacle regeneration and heat-stress bleaching.

The following objectives will be performed to accomplish these goals.

1. **Identify regeneration stages.** Previously no research has been conducted on tentacle regeneration in *Heliofungia* corals. Therefore, background research on the regeneration of other cnidarians will be conducted and followed with a pilot experiment to determine whether *Heliofungia* corals follow the same morphological stages of regeneration as observed in other cnidarians. This pilot experiment will also allow the determination of a tentacle regeneration timeline that will be utilised to identify the timepoints appropriate for the main regeneration experiment.

2. **Identify heat-stress bleaching stages.** Long term (from acclimatation temperature to past bleaching) bleaching studies at higher (than 31ºC) temperatures have not been conducted on corals and, despite their hardiness, no experimental work has been conducted on *Heliofungia.* Therefore, a small pilot experiment will be conducted on *Heliofungia* corals to identify appropriate sample collection timepoints, an appropriate experimental timeline and the size of individual corals that should be utilised for the main experiment.

3. **Gene expression analyses.** Transcriptome assembles will be created for the samples from the three studies, and transcriptomic analysis will be conducted. This type of bioinformatic analysis will allow the investigation of gene expression changes during the different timepoints of the studies. It will also help to understand the molecular pathways activated at various stages of regeneration and bleaching in both the host coral and symbiont

Chapter 2: Molecular mechanisms involved in the regeneration of *Heliofungia actiniformis* tentacles.

2.1. Abstract

Regeneration is a natural process exhibited in various plants and animals that involves the replacement or restoration of damaged or missing tissue, organs, cells, or entire body parts to full function. This process has been in intriguing scientists for centuries as understanding the mechanisms involved in regeneration could aid the creation of improved therapeutic approaches to human injury. The ability to regenerate differs from one organism to another, so identifying shared and distinct genes and pathways involved in regeneration in different taxa can help to understand its molecular underpinnings. In this chapter I examine the molecular process of regeneration in the robust coral, *Heliofungia actiniformis.* This organism was selected because its large tentacles regenerate rapidly allowing observation of changes in morphology and sampling for gene expression analyses. The "wounding" protocol consisted of amputating the distal half of several tentacles from individual corals and subsequently removing and collecting the corresponding proximal region at nine timepoints over ten days. The morphological changes and the timescale of tentacle regeneration in *H. actiniformis* resembled those observed in other cnidarians. The gene expression activity showed different regeneration stages compared to other species, and most of the modulated genetic pathways were consistent with other organisms. The analyses of differentially expressed genes (DEGs) and gene ontology (GO) enrichment identified molecular processes and genes involved in both the early and late stages of regeneration. The involvement of conserved genes and processes such as TNF receptors, Wnt receptors, and ATP-binding cassette transporters demonstrates the intricate interplay between immunity, development, and regeneration in *H. actiniformis*. Notably, the ATP-binding cassette transporter family members were highly expressed throughout the regeneration timepoints, a gene family previously reported only in mammalian regeneration. This chapter revealed novel pathways and gene families in a coral species that has the potential to become a model organism for research purposes. It increased the understanding of regeneration in the phylum Cnidaria and revealed a molecular mechanism previously only reported in mammal regeneration

2.2. Introduction

The process of partial body regeneration in any taxon is often described in three sequential steps: wound healing, cell population mobilisation, and tissue morphogenesis (Figure 2.1) (Alvarado & Tsonis, 2006; Brockes & Kumar, 2008; Gurtner et al., 2008; Poss, 2010; Tanaka & Reddien, 2011; van der Burg & Prentis, 2021). This process is applied to taxa ranging from single-celled eukaryotes (such as protists) to complex metazoans (such as mammals) (Alvarado & Tsonis, 2006; Brockes & Kumar, 2008; Gurtner et al., 2008; Poss, 2010; Tanaka & Reddien, 2011; Tiozzo & Copley, 2015; van der Burg & Prentis, 2021). However, processes occurring during and between these stages vary among taxa because their ability to regenerate depends on histogenesis and morphogenesis, which further depends on the plasticity of each taxon (Candia Carnevali & Bonasoro, 2001). For example, wound closure may proceed with or without cell proliferation, and new tissue may be formed either via the differentiation of stem cells or through the trans- or dedifferentiation of somatic cells (Tanaka & Reddien, 2011; van der Burg et al., 2020). The sequence of these processes is similar among organisms regardless of variations in the processes.

There are three morphological stages that are often classified into two temporal phases (Figure 2.1). The first temporal phase, early regeneration, involves the first two morphological stages, wound healing, and cell mobilisation. The second temporal phase, late regeneration, engages the last morphological stage, tissue morphogenesis (Figure 2.1) (Cary et al., 2019; Luz, 2020; Stewart et al., 2017).

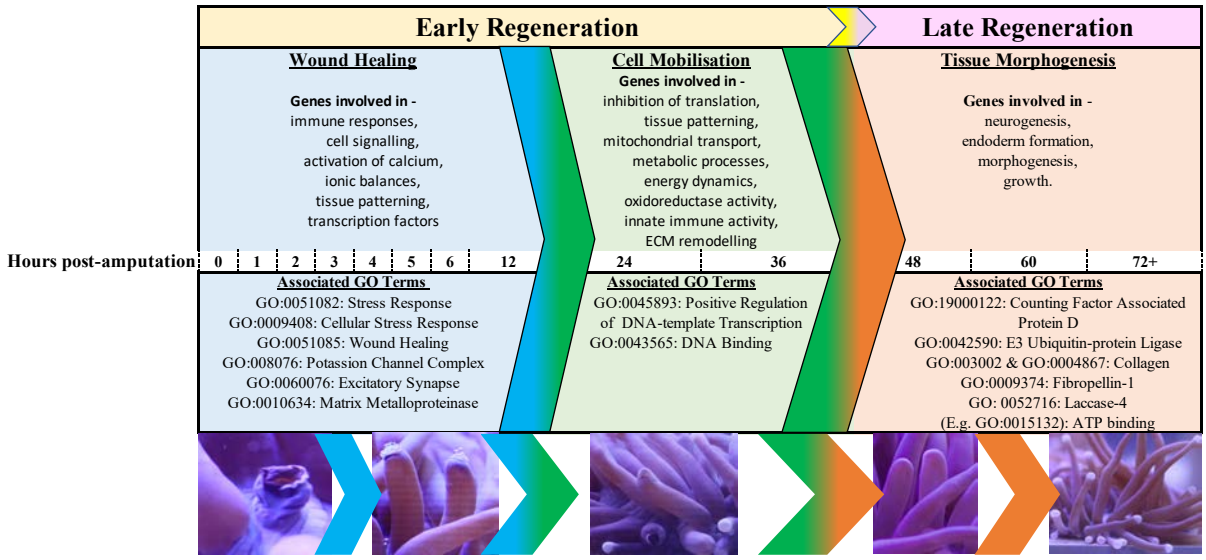

Figure 2.1. Morphology of tentacle regeneration in *Heliofungia actiniformis*. Schematic representation of three main stages of tentacle regeneration in *H. actiniformis* and the active genes and GO terms expected (from previous pilot experiment and as observed in other cnidarian regeneration) in each stage within cnidarian regeneration.

Cell migration to a wound site is considered an initial stimulus for regenerative cells in some organisms, including many cnidarians and zebrafish (Bideau et al., 2021; Boehm & Bosch, 2012; Bradshaw et al., 2015). The migration process tends to occur quickly, during which interstitial stem cells move to the site of injury to restore the stem cells and lost tissues (Bideau et al., 2021; Boehm & Bosch, 2012; Bradshaw et al., 2015). Also, regeneration, development, and immunity share cellular and genetic mechanisms as an organism's immune- and regeneration-related genes respond simultaneously upon experiencing an injury. For example, genes related to the immune system of several metazoan lineages differentially express within the first ten hours post-injury (Eming et al., 2009; Godwin & Brockes, 2006; Peiris et al., 2014; van der Burg et al., 2020).

Cnidaria is an early diverging phylum within the Metazoa, consisting of over 11,000 aquatic species, including corals, sea anemones, jellyfish, and *Hydras* (Steele et al., 2011). cnidarians are considered ecologically important components of the ocean ecosystem due to their diverse roles, such as reef structure builders, food, predators, or refuge for many organisms. Their distinctive characteristic is cnidocytes, specialised cells used primarily to capture prey (Mariscal et al., 1977).

Cnidarians have the capacity for regeneration, a key for the survival of many epifauna, which must cope with wounding predators, damage from exposure at low tide, and natural disasters (Poss, 2010; Tiozzo & Copley, 2015; van der Burg & Prentis, 2021). Regeneration in cnidarians has been studied extensively in hydrozoans (Cary et al., 2019; Erofeeva et al., 2022). However, the small stature of individual hydrozoans means that gathering regeneration post amputation data is virtually impossible. Therefore, the procedure involved in translating amputation stress into a signal that ignites the regeneration process in cnidarians remain primarily unknown (Amiel et al., 2015) and it is essential to understand the patterns of gene expression during the regeneration process to allow for the development of new strategies for the long-term preservation of organisms (Röttinger, 2021; van der Burg & Prentis, 2021; Warner et al., 2020).

This research seeks to help fill several gaps in current knowledge on coral regeneration as studying regeneration-related genes could provide insight into possible ways to improve organisms' development and survival factors (Burton & Finnerty, 2009; Röttinger, 2021; Warner et al., 2020; Warner et al., 2021). The broad study of regeneration in various animal models might reveal primitive regeneration mechanisms, which could be beneficial to find an evolutionary link among various organisms. For example, the lack of regeneration in several tissues of humans can be examined by studying the mechanistic process of regeneration in various other animal models.

This chapter aims to describe the changes in gene expression and morphology that occur during the regeneration of tentacles in *Heliofungia actiniformis*. This study will provide insights into tissue

regeneration processes in corals that are difficult to observe in colonial species with small polyps due to the large polyp size of *H. actiniformis*. It was observed that *H. actiniformis* undergoes morphological regeneration stages and patterns of gene expression like other cnidarians (such as *Hydra*) during tentacle regeneration. This chapter provides some insights into how *H. actiniformis* corals recuperate from damage and the molecular mechanisms that may be involved in response to other types of stress. It also provides an enhanced understanding of the regeneration in the Scleractinia stony coral, *Heliofungia*, a coral species with the potential to become a model organism by documenting the presence of the ATP-binding function during most of the regeneration morphology experienced by *H. actiniformis*.

This chapter uses transcriptomic data to investigate the molecular bases of tentacle regeneration in the mushroom coral *H. actiniformis* and compare it to other regenerating genera. Corals have a considerable regenerative capacity; however, their mechanisms are unknown (L. Knittweis et al., 2009; Leyla Knittweis et al., 2009). Therefore, this study intends to examine the morphological and temporal differences in coral regeneration that defy observations in colonial corals.

2.3. Materials & Methods

A pilot experiment was performed to determine the morphology of tentacle regeneration after amputation in *H. actiniformis* (Appendix A).

2.3.1 Coral collection and aquaria conditions

Twelve *Heliofungia actiniformis* individuals were collected, via SCUBA diving, from several sites at Orpheus Island Research Station (OIRS) in Queensland, Australia. The individuals were collected by me via a field trip that was comprised of a three-person team. I was the team leader, Mila Grinblat was the guide, and she took turns with our volunteer to be a dive buddy and assist me when collecting samples or in charge of the boat. The corals collected (using the Marine Parks permit: G21/44879.1) were identified via their colouring (striped oral disk and pale brown/grey tentacles with white tips), their shape (circular/oval with a single mouth slit in the centre surrounded by hundreds of tentacles) and were chosen if healthy and with a diameter of >20cm. Three of the sites were searched at various depths to find appropriately sized and genetically unrelated (speculated) *H. actiniformis* corals (Table 2.1). The collected corals were enclosed into labelled plastic containers and transported to the Marine and Aquaculture Research Facilities Unit (MARFU) at James Cook University (JCU), Townsville, Queensland, Australia. The transported *H. actiniformis* were put into labelled individual tanks and acclimated to 26ºC (the midrange water temperature at the collection sites) for 14 days with limited

husbandry. There were neither further interactions nor other collections of samples during the acclimation period. The aquaria system encompassed twelve tanks attached to two semi-closed sump systems (six tanks per sump system). Each tank had artificial daylight for 12 hours (6:00 am to 6:00 pm). Temperature, salinity, and nutrients of individual tanks and two sump systems were tested every 24 hours during acclimation and before sampling.

Table 2.1. Coral individual and collection site information. Explanation of specimen collection sites around the Orpheus Island Research Station of each individual *Heliofungia actiniformis* collected for the main experiments. Depth of each site (metres), date of specimen collection, and size of each individual coral (centimetres) is also recorded.

Coral Number	Collection Site	GPS Coordinates		Depth (meters)	Collection Date	Size of Specimen (cm)
1	Pelorus – Northwest	-18.548349,	146.495678	5 – 6m	26/06/2020	20
2	Pelorus – Northwest	-18.548349,	146.495678	7 – 8m	27/06/2020	22
3	Pelorus – Northwest	-18.548349,	146.495678	7 – 8m	27/06/2020	27
4	Pelorus – Northwest	-18.548349,	146.495678	7 – 8m	27/06/2020	32
5	Pelorus – Northwest	-18.548349,	146.495678	7 – 8m	27/06/2020	20
6	Resort – South	-18.63239	146.49946	2 – 4m	27/06/2020	25
7	Resort – South	-18.63239	146.49946	2 – 4m	27/06/2020	23
8	Resort – North	-18.6177	146.4895	4 – 5m	27/06/2020	22
9	Resort – North	-18.6177	146.4895	4 – 5m	27/06/2020	23
10	Cattle Bay	-18.5865	146.4814	8 – 10m	28/06/2020	25
11	Cattle Bay	-18.5865	146.4814	8 – 10m	28/06/2020	20
12	Cattle Bay	-18.5865	146.4814	8 – 10m	28/06/2020	25

The initial "wounding" was performed by removing the distal half of a predetermined number of tentacles from each acclimated coral. The subsequent sampling involved removing the remaining tentacle nubbins of the pre-cut tentacles at one of the nine-time points. The timepoints were derived from a pilot regeneration experiment (Table 2.2, Appendix A). Sampling was done between six morphological timepoints found during the pilot experiment (Appendix A) to see the changes in gene expression patterns during regeneration. Large changes in gene expression have been observed in some corals within the first 24 hours post-amputation; hence, three more timepoints were included during the first 24 hours post-amputation in our study (Luz et al., 2018; Stewart et al., 2017; Xu, 2022).

Subsets of samples were made to facilitate the analysis. The subsets comprised four (1, 2, 4, and 5) of the 12 corals collected from the same site (Table 2.1). Therefore, all had the greatest likelihood of

having experienced similar environments (depths and water quality) throughout their life stages. Additionally, six (T0, T1, T4, T6, T7, and T9) of the nine timepoints (Table 2.2) were chosen based on the best representations of the morphological stages of regeneration in *H. actiniformis*.

Table 2.2. Experimental timepoints and their associated descriptions. Timepoints of regeneration experiment showing time post-amputation and morphological descriptions.

Timepoint	Time post-amputation (hours/days)	Description
T0	0	First amputations of the distal half of tentacles
T1	1	Wound partially "scabbed."
T2	2	Closing of the wound, "scab" formation
T3	8	Between "scab" and "pinched."
T4	24 (1 day)	Nubbin ending – "pinched" like closing
T5	48 (2 days)	Nubbin ending (smooth covering) continues
T6	72 (3 days)	Nubbin ending (smooth covering) completed
T7	96 (4 days)	Tip starts to form
T8	168 (7 days)	Tip formation continues
T9	240 (10 days)	Tip formation completed

2.3.2 Preparation of RNA for transcriptome sequencing

Total RNA was extracted from subsets using the Qiagen RNeasy Plus Mini Kit, following manufacturer instructions, and suspended in RNase-free water. The purity of isolated RNA was determined using the Nanodrop ND-1000 spectrophotometer and concentration using the Invitrogen Qubit 4 Fluorometer with RNA HS (High Sensitivity) Assay kits. The integrity and concentration of RNA were further confirmed by using the Agilent 2200 Tapestation with the High Sensitivity RNA ScreenTape System. The sequencing generated was Sanger/Illumina 1.9 NovaSeq S1 200 lane for 100bp paired end run configuration, which resulted in 27-33M reads/sample. To prepare the samples for sequencing, in compliance with AGRF requirements, the amount of RNA in the samples was calculated, then their concentrations were adjusted to 20ng/µl by using the RNase-free water (2-12µl) and 500ng RNA was delivered to Australian Genome Research Facility (AGRF) for library preparation.

2.3.3 Bioinformatic analysis

FastQC (https://www.bioinformatics.babraham.ac.uk/projects/fastqc/) assessed the quality of raw sequences with further consolidation by MultiQC (Ewels et al., 2016) for multiple sequence quality management. A *Heliofungia actiniformis* genome, and associated gene models, obtained from

https://coral.genome.edu.au, were used as reference for mapping the read sequences from each regeneration phase by using Bowtie2 and paired-end to construct Bowtie 2 transcriptome indices (Supplementary Table S2.1). Gene expression levels from RNA-seq data were quantified using the Expectation Maximization (RSEM) package (Li & Dewey, 2011).

Analysis with RSEM generated a table of counts from the reads of all isoforms of an associated gene. The R BiocManager (Robinson et al., 2009) package, tximport (Love et al., 2018), was used to import and summarise the transcript abundance from the table counts. The R Bioconductor package, DESeq2 (Love, 2014), was used to measure differential gene expression between different stages of regeneration by comparing timepoint to genotype to visualisation. Counts were normalised depending on the dispersion and size factors, followed by a variance stabilising transformation (VST). Data quality control and overall characterisation of gene expression throughout the regeneration timepoints were derived by principal component analysis (PCA).

A pairwise-contrast test was used to analyse the Differentially Expressed Genes (DEGs) by grouping two sequential timepoints (e.g., T0 vs. T1, T1 vs. T4). The genes with an adjusted p-value lower than 0.05 were considered as significantly differentially expressed to control false discovery rate (FDR). The GO enrichment analysis was then performed, using the R Bioconductor package TopGO, on the gene sets to identify over-represented (or under-represented) GO terms. A p-value less than 0.005 was considered significantly enriched for the GO terms.

The R Bioconductor package, WGCNA (Langfield & Horvath, 2008), was used to identify the correlation patterns among genes across the six regeneration timepoints. The co-regulated groups of genes were correlated into WGCNA modules, and outliers were removed. The soft-threshold power was set as 6 for network topology analysis, and the gene network was constructed using TOM. Modules and module eigengenes were identified, and TopGO (Alexa et al., 2006) was utilised to identify the significantly enriched GO terms. The resulting modules with significantly enriched GO terms were correlated between eigengenes and regeneration stages. Gene functionality of DEGs and co-expressed genes in each module were examined, and functional profiles were created through statistical visualisation.

2.4. Results

2.4.1. Morphological stages of tentacle regeneration

Morphological stages and timing of regeneration in *H. actiniformis* were similar across all individuals in the pilot experiment (four individuals) and main experiment (12 individuals) and are recorded in Table 2.3 and Figure 2.2. Tentacles appeared to shrink and deflate immediately after amputation (Timepoint 0 = T0), resulting in a primary amputation morphology (T0; Table 2.3) with the appearance of an open tube (Figure 2.2A). One of the first morphologically discernible steps was the formation of the wound epithelium, which was a "scab"-like structure that was formed 1-hour post-amputation (Timepoint 1 = T1; Table 2.3) that effectively closed the wound with a new epithelium (Figure 2.2B). The site of amputation showed a "pinched" appearance at 24 hours post-amputation (Timepoint 4 = T4; Table 2.3; Table 2.3), which was the earliest indication of a transition from wound healing to tentacle regeneration (Figure 2.2C). The regenerating stump ends became smooth after 72 hours of amputation (Timepoints 6 = T6; Table 2.3). The acrosome formation started with the first appearance of white tentacle tips after 96 hours post-amputation (Timepoint 7 = T7; Figure 2.2E). After ten days of amputation (Timepoint 9 = T9), the appearance of acrosomes indicated the completion of regeneration (Figure 2.2F).

Table 2.3. Analysis timepoints of *H. actiniformis* tentacle regeneration. Timepoints that were chosen for further analysis and their corresponding visual morphological stages.

Timepoint	Time Post-amputation (PA)	Morphological Stage
T0	Primary Amputation	N/A
T1	1 hour PA	Wound closed by a "scab."
T4	24 hours (1 day) PA	Nubbin ending – "pinched" like closing
T6	72 hours (3 days) PA	Nubbin ending – smooth appearance
T7	96 hours (4 days) PA	First visual indication of acrosome formation
T9	240 hours (10 days) PA	Acrosome fully regenerated

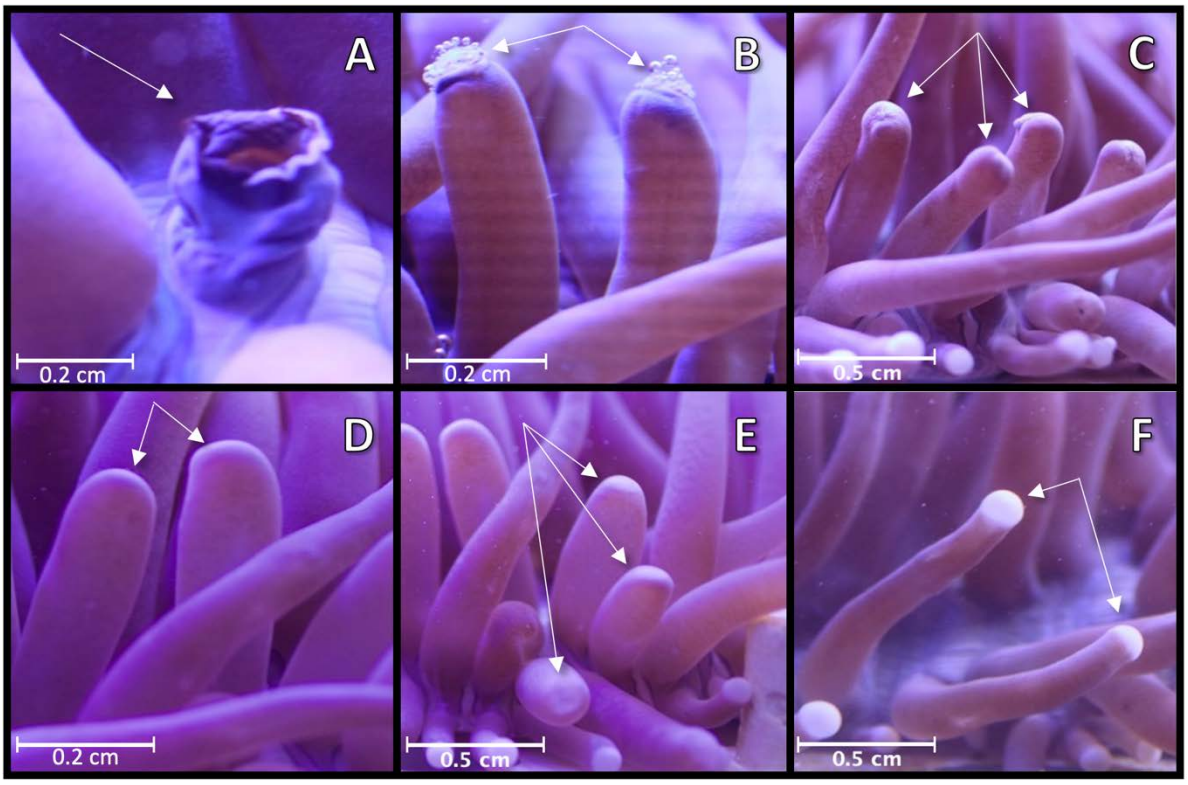

Figure 2.2 A-F. Morphological stages of tentacle regeneration in *H. actiniformis*. The regeneration process is illustrated in temporal order. (A) The appearance of an open tube (indicated by arrow) at timepoint 0 = T0. (B) Formation of a "scab" like structure (indicated by arrows) showing the accumulation of bubbles toward the end of scab formation at timepoint 1 = T1). (C) Formation of pinched ends of nubbins (indicated by arrows) by 24 hours (Timepoint 4 = T4). (D) The formation of smooth regenerating stump ends (indicated by arrows) was smooth. (E) The formation of acrosome with the appearance of white tentacle tips (indicated by arrows; Timepoint 6 = T6) at 96 hours post-amputation (Timepoint 7 = T7). (F) At 10 days post-amputation (Timepoints 9; T9), acrosomes (indicated by arrows) appear to be fully regenerated.

2.4.2. Principal Component Analysis (PCA) of transcriptomic data

As indicated above, transcriptome data were obtained (Chapter 2; Section 2.2) for four individuals at six-time points during the regeneration process. The filtered individual reads were mapped against an assembled transcriptome and were subjected to principal component analyses (PCA) to analyse gene expression throughout the regeneration timepoints. Genotype effects dominated sample clustering in principal components 1 and 2, accounting for 32% and 23% of the variance, respectively (Figure 2.3A, B). PC3 accounted for 19% of the variance and displayed a mixture of variation due to genotype and timepoint (Figure 2.3C). By principal component 4, explaining 9% variance, there was a clear separation by timepoint (Figure 2.3D, E). Figure 2.3D illustrates the lack of clustering by genotype in PC4, while Figure 2.3E uses coloured convex hulls to highlight the clear separation of samples by timepoint. Our findings that genotype was the dominant factor determining gene expression agree with earlier findings in soft corals (Al-Shaer et al., 2023; Farag et al., 2016) and *Hydra* (Murad et al., 2021). Such changes in the expression of genes were also observed during the

bleaching of corals (see Chapter 3). The results of the PCA confirm that individuals with the most variations in the samples must be included in the model, which aids in identifying and analysing differentially expressed genes (DEGs) across six timepoints with the adjusted p-value < 0.05. Note here that in Fig 2.3A, there is uncertainty around whether individuals 1 and 4 have been mislabelled, and this issue could not be resolved by checking records.

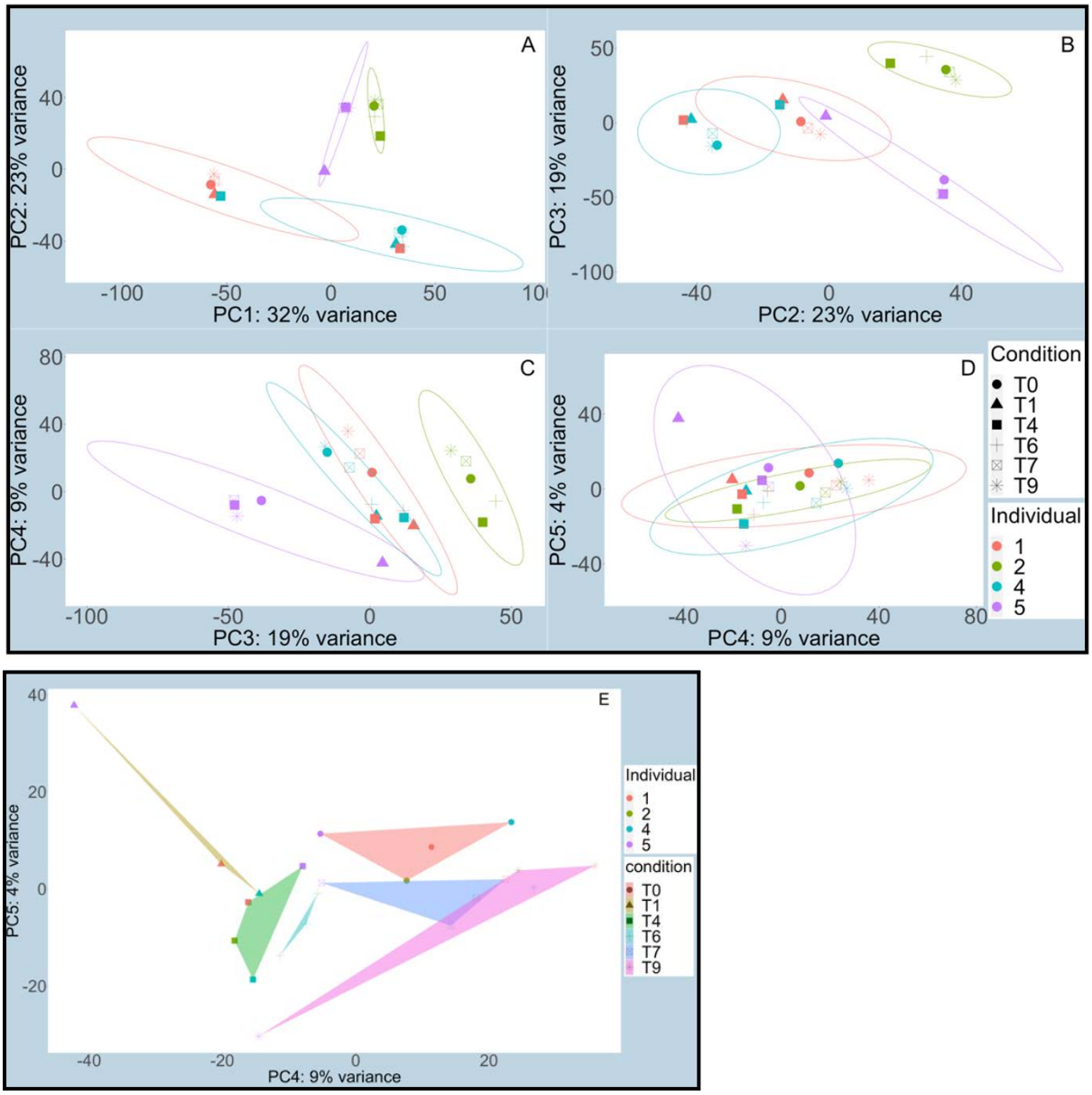

Figure 2.3A-E. Principal Component Analysis (PCA) of regenerating individuals at different timepoints. PCA plot of samples from *H. actiniformis* individuals (identified by colour) at different regeneration time points (identifiable by symbol). (A) A comparison of the highest principal component levels (32% vs 23%; PC1). (B) A comparison of component levels 23% vs 19% (PC2). (C) Compares component levels 19% vs 9% (PC3). (D, E) Comparison of the lowest principal component levels (9% vs 4%; PC4) and (E) Polygons around points are convex hulls coloured by a particular condition. Note: there is uncertainty in the labelling of individuals 1 and 4 in part A od this figure as genotype effects are strong except for red and blue mis-matched samples. This issue could not be resolved by checking records. The axis titles represent the principal component and their respective variation percentage. The ellipses represent the orientation and spread of points according to the method of stat_ellipse().

2.4.3. Differential gene expression through regeneration

Analysis of gene expression differences between timepoints revealed 1,752 genes that were differentially expressed across all successive pairs of timepoints. Changes during early regeneration involved far more differentially expressed genes (T0-T1: 966 genes, T1-T4: 543 genes) than did transitions between later timepoints (T4-T6: 5 genes, T6-T7: 213 genes, T7-T9: 25 genes) (Figure 2.4). A considerable variation in gene expression was observed between successive timepoints with very little change from T4-T6 (a time between pinching and smooth appearance of nubbin endings) compared to T6-T7. Based on variation in numbers of genes undergoing changes in expression the regeneration process can be classified into three stages: early stage affecting the maximum number of genes, middle stage affecting the minimum number of genes, and late stage with a renewed burst of genes undergoing differential expression.

2.4.4. Gene Ontology (GO) enrichment of DEGs

Analysis of GO terms associated with DEGs supported the enrichment of 103 terms (BP = 50, MF = 37, CC = 16) across all pairs of consecutive timepoints (Figure 2.5). The quantity of significantly enriched GO terms followed the same pattern as DEGs which supports the distinction between three morphological stages during the regeneration process. These results also implied that DEGs at each successive pair comprised distinctly different functional groupings as evidenced by the little overlap between developmental transitions shown by the enriched GO terms.

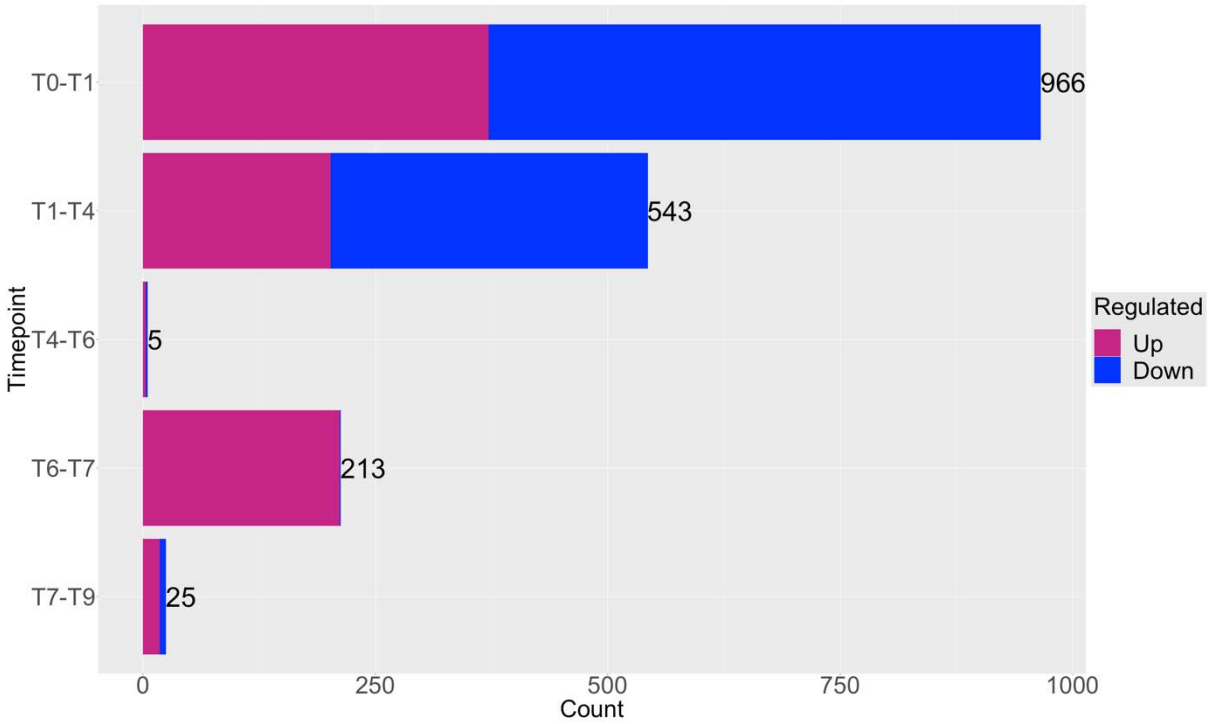

Figure 2.4. Differentially Expressed Genes (DEGs) during regeneration. The number of upregulated and downregulated genes is shown through the sequential pairing of regeneration timepoints in *H. actiniformis* (p-value<0.05). T0 = primary amputation; T1 = 1-hour post-amputation ("scab" formation); T4 = 24 hours post-amputation ("pinched" appearance); T6 = 72 hours post-amputation (smooth stump ending); T7 = 96 hours post-amputation (beginning of tip formation); and T9 = 10 days post-amputation (fully regenerated acrosome, end of regeneration).

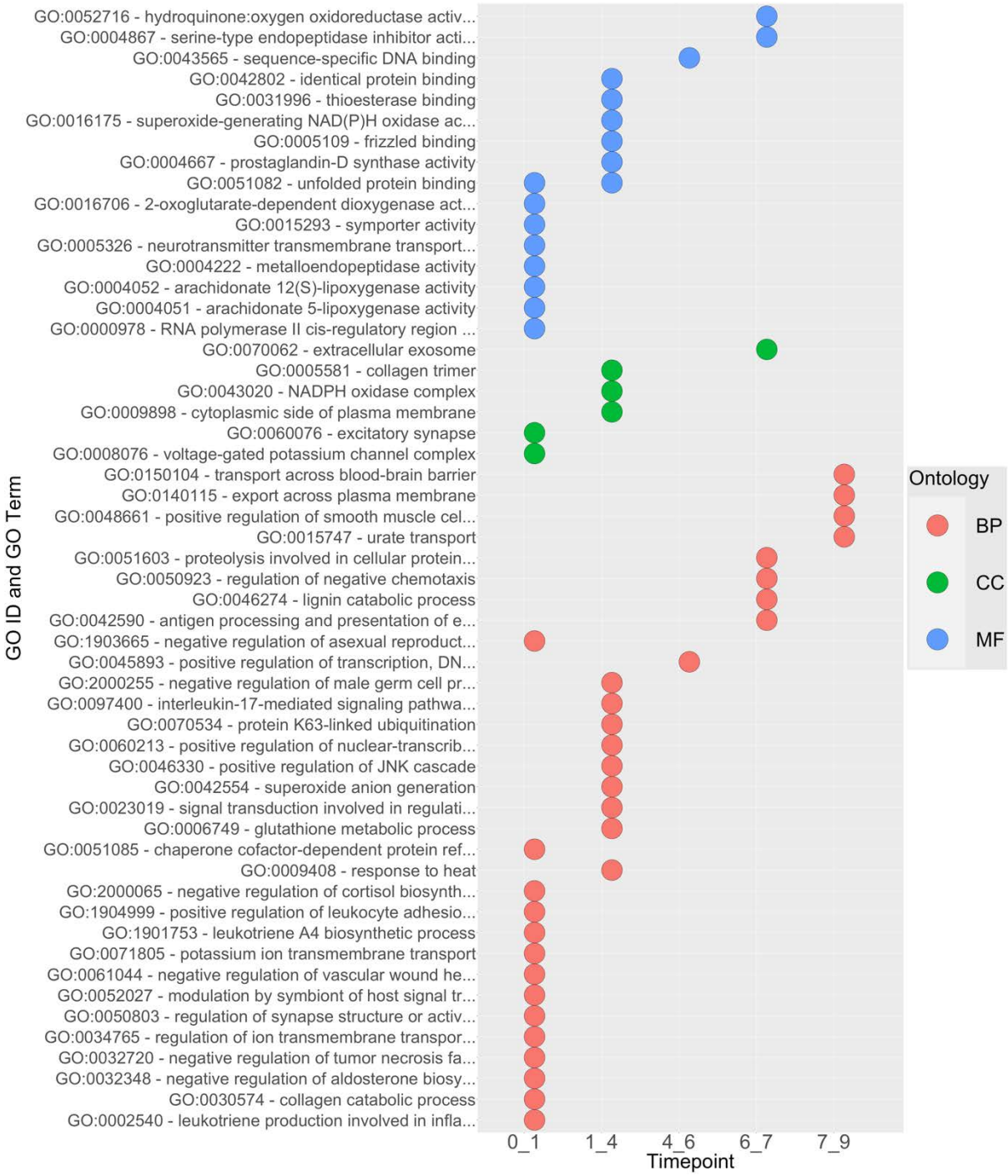

Figure 2.5. Gene Ontology (GO) Enrichment. The significant (p-value < 0.005) GO IDs along with their corresponding GO terms are arranged in the order of their decreasing p-values (from top to bottom) and are separated by ontology per timepoint pair. Timepoint pair 0_1 represents comparison of timepoints T0 (primary amputation) to T1 (1-hour post-amputation, "scab" formation). Timepoint pairs T1 to T4 (24 hours post-amputation, "pinched" formation) are represented by 1_4. 4_6 represents timepoint pair T4 to T6 (72 hours post-amputation, smooth covering). Timepoint pair T6 to T7 (96 hours post-amputation, the beginning of tip formation) are represented by 6_7. 7_9 represents timepoint pair T7 to T9 (10 days post-amputation, fully regenerated acrosome, end of regeneration).

2.4.4.1. Gene activity – Early regeneration stage

During the timepoints of new amputation and 1-hour post-amputation "scab" formation (timepoints T0-T1), 33 GO terms enclosed 232 genes across all ontologies. The CC ontology contained three GO terms (Supplementary Table S2.2) with 42 genes: (1) voltage-gated potassium channel complex (GO:0008076) that is comprised of genes associated with potassium channels. These account for the most prominent ion family and have many physiological functions, such as regulating cell migration and proliferation (Arias-Mejias et al., 2020). (2) The excitatory synapse (GO:0060076) is mainly associated with vesicular glutamate transporters. (3) Postsynaptic membrane GO (GO:0045211) which is a mixture of genes primarily associated with Ankyrin, Gamma-aminobutyric acid receptors, Glutamate, Glycine receptors, Metabotropic glutamate receptors, and neuronal acetylcholine receptors.

The 11 GO terms (Supplementary Table S2.2) enriched within MF ontology covered the most significant proportion of genes of all the ontologies (109 genes in total), as well as most of the genes associated with the first stage of regeneration (timepoints T0-T1). Four of the enriched terms in the MF ontology have been associated with the wound healing phase of other studies (Luz, 2020; Röttinger, 2021; van der Burg et al., 2020; van der Burg & Prentis, 2021; Xu, 2022). The enriched terms were supported by differential expression in: Homeobox genes (GO:0000978, GO:0000981); zinc finger genes (GO:0000978, GO:0000981, GO:0004222); forkhead box genes (GO:0000978, GO:0000981); and matrix metallogenease (GO:0004222).

Enriched terms in the BP ontology included those related to tissue patterning and regeneration in other cnidarians and were supported by the differential expression in polyunsaturated fatty acids (GO:1904999, GO:1901753, GO:0061044, GO:0002540) and fibroblast growth factors. Both, polyunsaturated fatty acids, and fibroblast growth factor genes have been associated with morphogenesis and growth (Luz, 2020; Stewart et al., 2017; Xu, 2022). Furthermore, the BP ontology contained enriched terms that are associated with MAPK cascade and tissue patterning (Bideau et al., 2021; Luz, 2020; van der Burg & Prentis, 2021) and have been observed during the initial stages of regeneration in other taxa (Luz, 2020; van der Burg et al., 2020; van der Burg & Prentis, 2021; Xu, 2022). Such as matrix metallogenease (GO:0010634, GO:0030574, GO:0034765, GO:0060022), potassium voltage-gated channel (GO:0034765 and GO:0071805), polyunsaturated fatty acid (GO:0002540, GO:0061044, GO:1901753, GO:1904999), and fibroblast growth factor receptors (FGFR3) (GO:0070374).

Only three significant enriched terms between timepoints T0 and T1 and T1 and T4 were found, of which response to heat (GO:0009408) and chaperone cofactor-dependent genes (GO:0051082) were from BP. The unfolded gene binding (GO:0051085) was from MF (Supplementary Table S2.2). The

genes associated with these GO terms (especially heat shock genes and DnaJ homologs) play an essential role in stress response and wound healing across the animal kingdom. The expression level of these genes is increased in response to stress-causing factors in cnidarians (Alvarado & Tsonis, 2006; Brockes & Kumar, 2008; Poss, 2010; Sehring & Weidinger, 2020; Su et al., 2022). The upregulation of genes associated with DnaJ and heat shock genes has been reported at 4 hours post-amputation in other cnidarians (Chera et al., 2006; DuBuc et al., 2014; Holstein et al., 2003; Luz, 2020; Stewart et al., 2017). These are among the earliest genes which respond after tentacle amputation in sea anemone Calliactic polypus (Stewart et al., 2017; van der Burg et al., 2020; van der Burg & Prentis, 2021).

There were eighteen significantly enriched GO terms across all ontologies during the T1-T4 timepoint pair (Supplementary Table S2.3). TNF receptor-associated factors genes was included in 32% of the eighteen enriched terms (within the GO terms GO:0023019, GO:0031996, GO0035631, GO:0042802, GO:0046330, GO:0070534, GO:0097400, GO:0009898). The nine enriched terms in the BP ontology (Supplementary Table S2.2) contained genes associated with JNK cascade (GO:0046330), interleukin-17 (GO:0097400), homeobox genes (GO:0023019), Glutathione S-transferase (GO:0006749), and TNF receptors (GO:0023019, GO:0046330, GO:0070534, GO:0097400).

The CC ontology includes cytoplasmic side of plasma membrane (GO:0009898), NADPH oxidase (GO:0043020), and neutrophil cytosolic factor (GO:0043020). The cytosolic neutrophil factor activates NADPH oxidase, whose function is to produce reactive oxygen species (ROS) and modulate tissue repair and regeneration in multicellular organisms such as mice and zebrafish (Chan et al., 2014; Leisegang et al., 2016; Rieger & Sagasti, 2011). These activities were associated with TNF receptor-associated factors, which are a gene family that regulates inflammation, apoptosis, and antiviral responses and is found in the early stages of regeneration in cnidarians (Luz, 2020; van der Burg et al., 2020).

Six other enriched terms were found within the MF ontology, such as frizzled binding (GO:0005109) and identical gene binding (GO:0042802) (Supplementary Table S2.2). The frizzled binding enriched term involves genes associated with Wnt signalling, collagen and tyrosine-gene kinase. All these genes are found in the early regeneration stage of other taxa such as *Tubastraea*, sea anemones, and sea stars (Bideau et al., 2021; Cary et al., 2019; Luz, 2020; van der Burg & Prentis, 2021). Genes associated with frizzled binding are found to be involved in adapting cell and tissue polarity, embryonic development, and related processes in developing and mature organisms (Huang et al., 2017). Identical gene binding has genes associated with transcription factors, TNF receptor-associated factors, zinc, heat shock factors (HSF), and collagen. Other genes constituted NADPH oxidase (GO:0016175) and glutathione transferase (GO:0004364), which are known to affect the activity of

transcription factors and gene kinases involved in stress response, differentiation, or apoptosis. They can also interact with other genes (such as JNK) to control the activation of signalling pathways and cell cycle during regeneration in multicellular organisms such as mice (Pajaud et al., 2012; Pajaud et al., 2015).

There was no significant activity between 24- and 72-hours post-amputation (Timepoints T4-T6), a stage at which "pinched" like formation becomes completely smooth. Only two significantly enriched terms were found during the T4 and T6 timepoints (Supplementary Table S2.2). The first term, positive regulation of DNA-template transcription (GO:0045893), belongs to the BP ontology and participates in the regulation of transcription. The second enriched term, sequence-specific DNA binding (GO:0043565), was in the MF ontology and involves binding to specific regions of DNA (e.g., GC-rich), types of DNA, or motifs (e.g., rDNA or promotor region). Other studies have investigated sequence-specific DNA binding in jellyfish, *Hydra* (Sun et al., 1997), and cnidarians (de Jong, 2005); however, none reported finding this enriched term.

2.4.4.2. Gene activity – Late regeneration stage

During the late stage of tentacle regeneration in *H. actiniformis*, the expression of different genes changed compared to those in the early regeneration stage. During the timepoint pair T6-T7, 15 differentially expressed GO terms contained 130 genes across all ontologies (Supplementary Table S2.2). Eight of the enriched terms were expressed during the BP ontology, and 75% of these terms (GO:1900122, GO:1903665, GO:0030435, GO:0031288, GO:0050923, GO:0051603) contained the counting factor-associated gene D. They also contained E3 ubiquitin-gene ligase which is essential for gene modification (Luz, 2020; van der Burg et al., 2020); cysteine genease 2, which is also found in early regeneration (Stewart et al., 2017); macrophage, which swiftly populates the wound region post-amputation (Bideau et al., 2021); and Laccase-4 (GO:0042590, GO:0046274, GO:0051603) which is generally associated with plants, fungi, and bacteria (Berthet et al., 2011).

In the MF ontology, 50% of the genes were associated with collagen (GO:0004867 and GO:0030020), 25% with Fibropellin-1 (GO:0009374) and the remaining 25% with Laccase-4 (GO:0052716). Laccase-4 is also associated with detoxification, morphogenesis, cell pigmentation, and defence against hostile organisms in sponges; hence, it can be used as an antimicrobial agent and to detoxify xenobiotics (Janusz et al., 2020; Li et al., 2015). There were five enriched terms within the CC ontology containing a wide variety of genes (>90). These enriched terms included those involved in collagen, endoplasmic reticulum, ATP binding, endoplasmic reticulum, fibropellin, gene disulphide-isomerase, and laccase-4 (Supplementary Table S2.2) and all have essential functions in cnidarian regeneration. For example, collagen is present during early regeneration in various cnidarians and it is a vital part of the mesoglea as it enables the transportation of epithelial cells through ECM

reconstruction (Luz, 2020; Shao et al., 2020; Stewart et al., 2017; van der Burg et al., 2020; van der Burg & Prentis, 2021).

The timepoint pair T6-T7 contained three enriched terms in common with two other sets of timepoints, T0-T1 and T6-T7. Two of the enriched terms containing counting factors associated with Gene D (GO:1900122 and GO:1903665) were within the BP ontology and the extracellular space (GO:0005615) enriched term was in the CC ontology. The extracellular space enriched term contained 24 genes, 25% of which were associated with collagen and the remainder 75% constitute a vast array of genes, including matrix metallogenease, fibropellin, polyunsaturated fatty acids, and endoplasmic reticulum.

ATP-binding cassette transporter is critical for signal transduction and is enriched at 48- and 72-hours post-amputation during regeneration in earthworms. It is also associated with tissue defence and organ regeneration in rats (Chang et al., 2021; Shao et al., 2020). Furthermore, ATP-binding cassette transporter was the primary function occurring four days post-amputation (Timepoint T7). Across all three ontologies (BP, CC, and MF), there were 28 differentially expressed enriched terms containing 34 genes in the T7-T9 timepoints (4 days post-amputation; commencement of acrosome formation and ten days post-amputation; acrosome completion and regeneration end). Eighty-six percent of these enriched terms were associated with ATP-binding cassette sub-family C member 4 (BP = GO:0002576, GO:0015721, GO:0015747, GO:0032310, GO:0038183, GO:0048661, GO:0070730, GO:0071716, GO:0140115, and GO:0150104; CC = GO:0016323, GO:0031088, and GO:0098591; MF = GO:0001409, GO:0008559, GO:0015132, GO:0015143, GO:0015431, GO:0015432, GO:0015562, GO:0015662, GO:0016404, GO:0034634, and GO:0043225; Supplementary Table S2.2). The remaining 14% of enriched terms contained genes associated with mycocerosic acid synthase (BP = GO:0006633; MF = GO:0004315, GO:0031177, and GO:0050111), multidrug resistance-associated gene 1 (CC = GO:0016323; MF = GO:0008559), and phenolphthiocerol/phthiocerol polyketide synthase subunit C (BP = GO:0006633; MF = GO:0004315 and GO:0031177). These genes are not reported to be differentially expressed or enriched in previous regeneration studies.

2.4.5. Weighted Gene Co-expression Network Analysis through regeneration

Weighted gene co-expression network analysis (WGCNA) was performed to investigate the relationship between co-expression modules by identifying the genes with related expression configurations among all DEGs and their relationship with the various stages of regeneration in the *H. actiniformis* coral.

The results indicated 48 co-expression modules (clusters) with corresponding colours covering 33,050 genes (Figure 2.6). Filtering the modules by enriched significant GO terms reduced the number of modules to 30, with 282 GO terms that covered 13,556 genes (Supplementary Table S2.2). The size of individual modules was highly variable ranging from two (lightcyan1) to 6,648 (turquoise) genes.

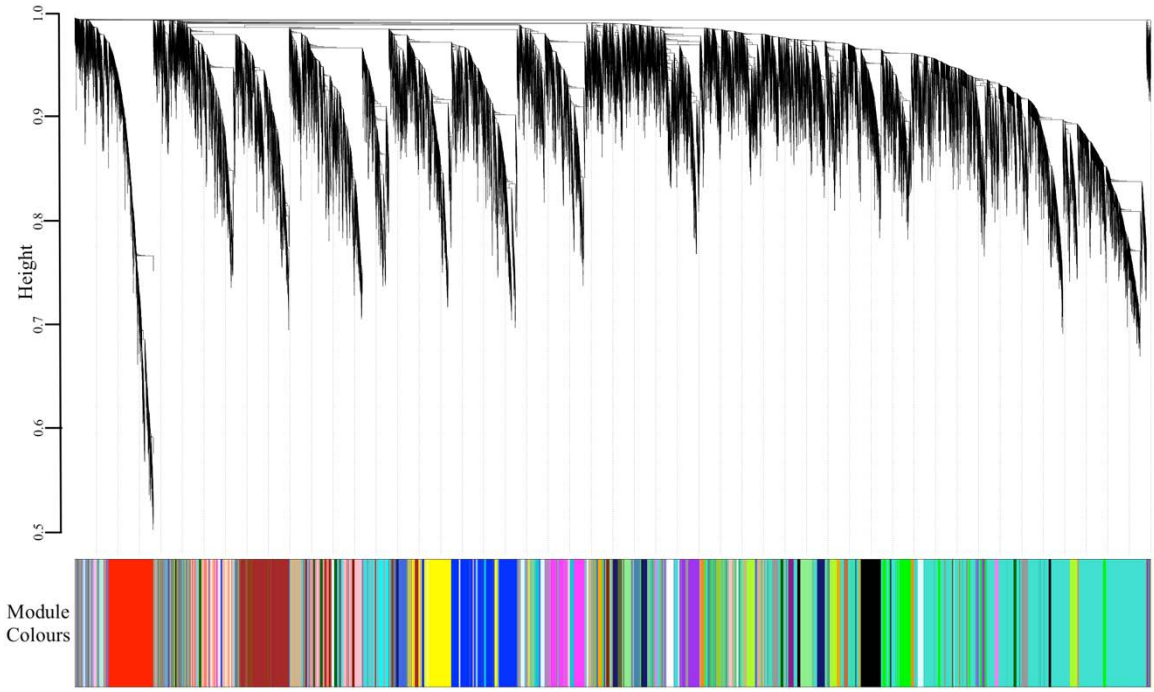

Figure 2.6. Dendrogram of all the WGCNA cluster modules present in tentacle regeneration of *H. actiniformis*. A hierarchical gene clustering tree was constructed by grouping adjacency-based divergence to identify 48 co-expression modules with their corresponding colour assignments, where module size determines the colour assignment. For example, turquoise represents the most extensive module; therefore, it holds the most significant number of genes (8,352), while dark slate blue represents the smallest module with the fewest genes (35).

2.4.5.1. Representative expression profiles for each WGCNA cluster module.

A vector of expression values (module eigengene) was used to represent the gene expression for all genes within a module. The change in expression over time (expression profile) for the module eigengene was utilised to examine the relationship between the 48 modules by comparing their eigengenes (Supplementary Figure S2.1). The modules in the colours of pale turquoise, floral white, ivory, grey60, white, green-yellow, dark olive green, dark orange 2, violet, dark orange, and yellow-green demonstrate a contrasting pattern of high levels of activity during the early stages of regeneration (Timepoints T0 and T1), followed by a decrease through the late regeneration stages until the end of tentacle regeneration (Timepoint T9; Figure 2.7). In contrast, the pattern illustrated with module colours of green, turquoise, saddle brown, tan, dark magenta, black, light green, grey, plum 1, medium purple 3, and red indicates a low expression through the early stage (Timepoints T0 and T1) of regeneration that gradually increases through the late stages of regeneration (timepoints T4

to T9). The middle two timepoints (T4 and T6) appeared to be a neutral section of regeneration during which a pause in the rate of change of gene expression was observed as evidenced by the small amount of activity present (Figure 2.7). As evidenced by the small amount of activity present.

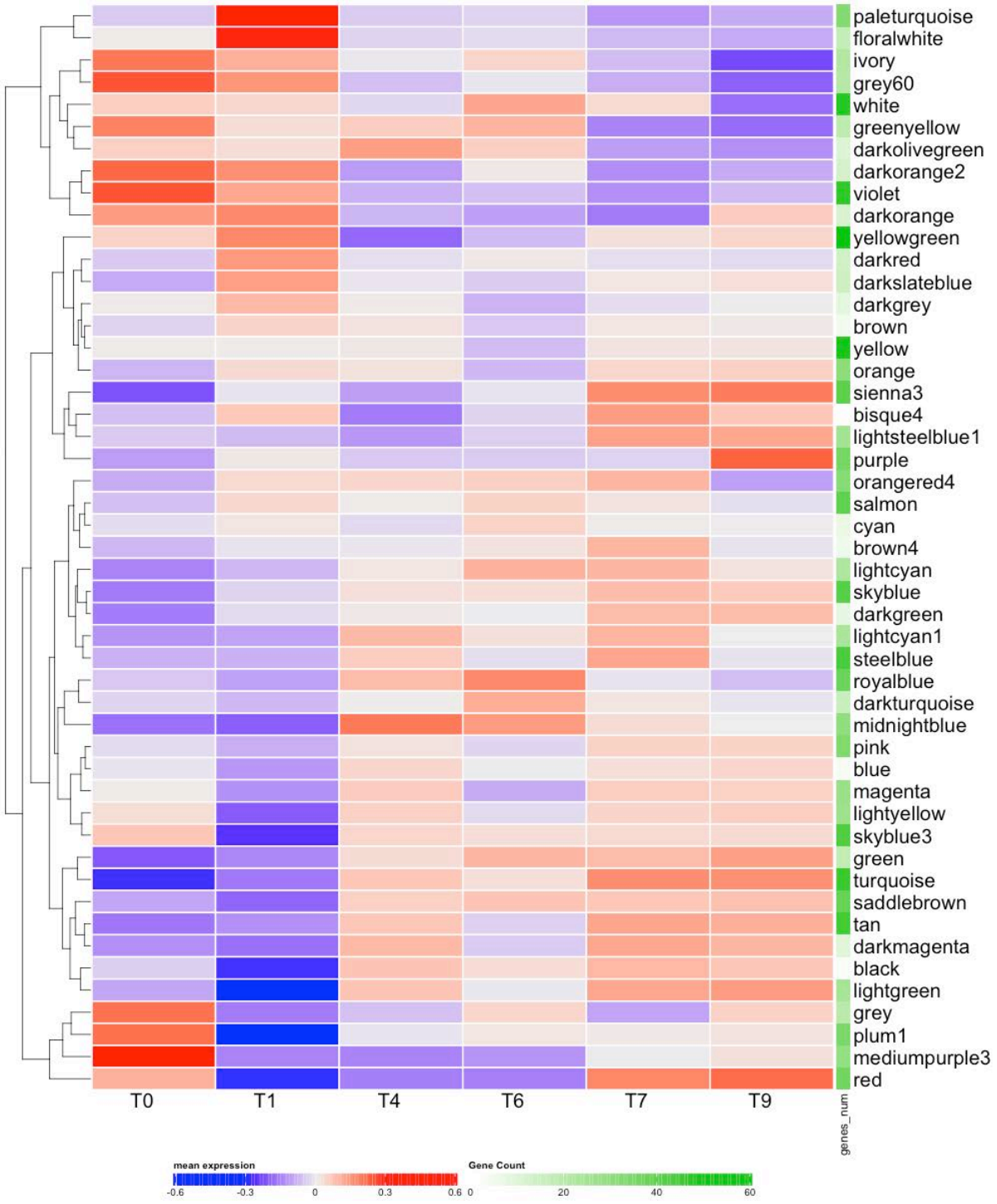

Figure 2.7. Heatmap of Module-Timepoint Connection. Heatmap of the relationship between module eigengenes and regeneration stages with an annotation symbolising the number of genes in each module where coloured cells represent eigengene quantities. T0 = primary amputation; T1 = 1-hour post-amputation ("scab" formation); T4 = 24 hours post-amputation ("pinched" appearance); T6 = 72 hours post-amputation (smooth stump ending); T7 = 96 hours post-amputation (beginning of tip formation); T9 = 10 days post-amputation (fully regenerated acrosome, end of regeneration).

2.4.5.2. Patterns within individual cluster modules.

Patterns within the individual modules revealed that some modules capture genes with divergent gene expression patterns between individual corals. This highlights the variability in molecular activity between individuals during regeneration and allows for the identification of specific groups of genes with highly divergent expression patterns. For example, light yellow and salmon modules showed that individuals 2 and 5 were in the higher expression section of light yellow while individuals 1 and 4 remained in the lower expression area (Figure 2.8). The salmon module showed the same connection but in the opposite order, i.e., individuals 1 and 4 remained in the higher expression region and individuals 2 and 5 in the lower expression region (Figure 2.8). The same pattern can be seen between magenta and dark turquoise but with different individuals. The magenta module only has four individuals at the higher expression and the other three at the lower expression levels. The dark turquoise module showed the same pattern in reverse, i.e., individual four remained in the lower expression range, and the other four were in the higher expression range (Figure 2.8).

The most interesting thing in the modules is that some of them capture divergent expression patterns between corals. Therefore, some of the enrichment terms and genes associated with those modules are interesting because they potentially represent sources of variation in response between individuals. For instance, the "mirroring" modules salmon and light yellow contain the functional genes TNF receptor-associated factors 2, 3, 5, and 6 within different enriched terms. Enriched terms were not observed within the dark turquoise module; however, the magenta module had 13 enriched GO terms (Supplementary Table S2.3). Three GO terms were associated with Wnt signalling (GO:0017147, GO:0060071, GO:0090090) and constituted 40 functional genes. Among them, 36 genes were collagen triple helix repeat-containing gene 1, and the other four were Nephrocystin-3 or Tyrosine-gene kinase transmembrane receptors. Another GO term of interest located within the magenta module was frizzled binding (GO:0005109) that contained 13 genes, 12 of which were also collagen triple helix repeat-containing gene 1, and the last one was Tyrosine-gene kinase transmembrane receptors.

The 13 GO terms of the magenta module contained 163 functional genes. Eighty-eight per cent were collagen triple helix repeat-containing gene 1, and 3% were Histidine ammonia-lyase (Histidase). Tyrosine-gene kinase transmembrane receptors and Ficolin (a type of collagen) constituted 2%. Collagen alpha-1(XII) chain (Fibrochimerin), Short-chain collagen C4 (Fragment), Chloride intracellular channel gene 1, Discoidin domain-containing receptor 2, and Nephrocystin-3 constituted 1% each. Wnt signalling and binding and frizzled binding were seen in the regeneration of sea stars, corals, and *Hydra* (Cary et al., 2019; Liu et al., 2013; Sikes & Newmark, 2013; Umesono et al., 2013).

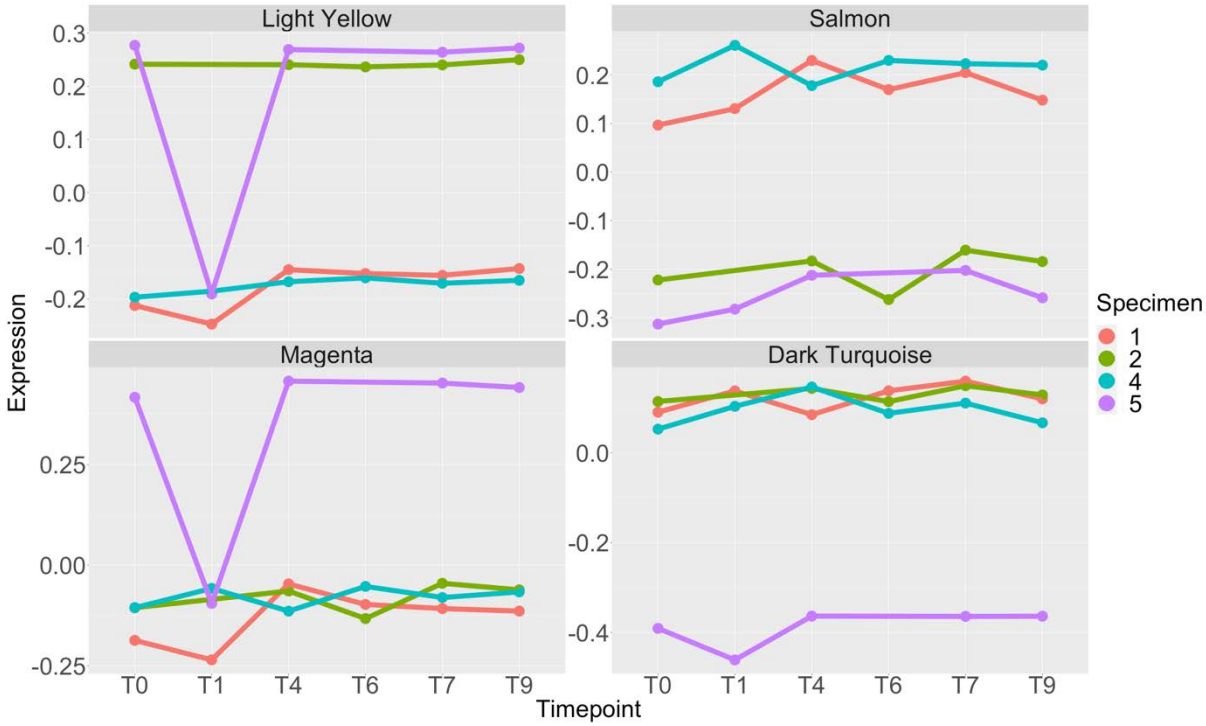

Figure 2.8. WGCNA plot of four individual module eigengenes. Comparison of eigengene patterns in four individual modules by timepoints. T0 = primary amputation; T1 = 1-hour post-amputation ("scab" formation); T4 = 24 hours post-amputation ("pinched" appearance); T6 = 72 hours post-amputation (smooth stump ending); T7 = 96 hours post-amputation (beginning of tip formation); and T9 = 10 days post-amputation (fully regenerated acrosome, end of regeneration).

2.4.5.3. Patterns within the red cluster module

The red module contained many genes that predominantly possessed the same configuration throughout the regeneration process. When comparing the GO terms within the modules to those observed in the GO term enrichment analysis the observation that more than 25% of the GO terms within the red module were associated with timepoints T0-T1 (new amputation and 1-hour PA ("scab" formation) became apparent. These 17 GO terms were mainly associated with regulation and transport through transmembrane. It was observed that three out of the four individuals moved in the same pattern throughout the regeneration timepoints in the red module (Figure 2.9). There was a decrease in expression from T0 (new amputation) to T4 (24 hours PA; "pinched" nubbin), followed by an increase in expression until it reached T7 (96 hours PA; tip starts forming), where it plateaus (Figure 2.9). Little variations were observed between the T1 and T6 timepoints on securing the enclosed wound. The examination also confirms intensive activity at the beginning of the tip formation (Figure 2.9). The red module has 60 GO terms containing 323 genes of different functions, while the total genes were 2,466 (Supplementary Table S2.2). The five most prevalent genes were potassium voltage-gated channel gene (7.18%), gamma-aminobutyric acid receptor (6.33%), neuronal acetylcholine receptor (5.6%), glutamate receptor (4.22%), and Golgi-associated plant pathogenesis-related gene (4%).

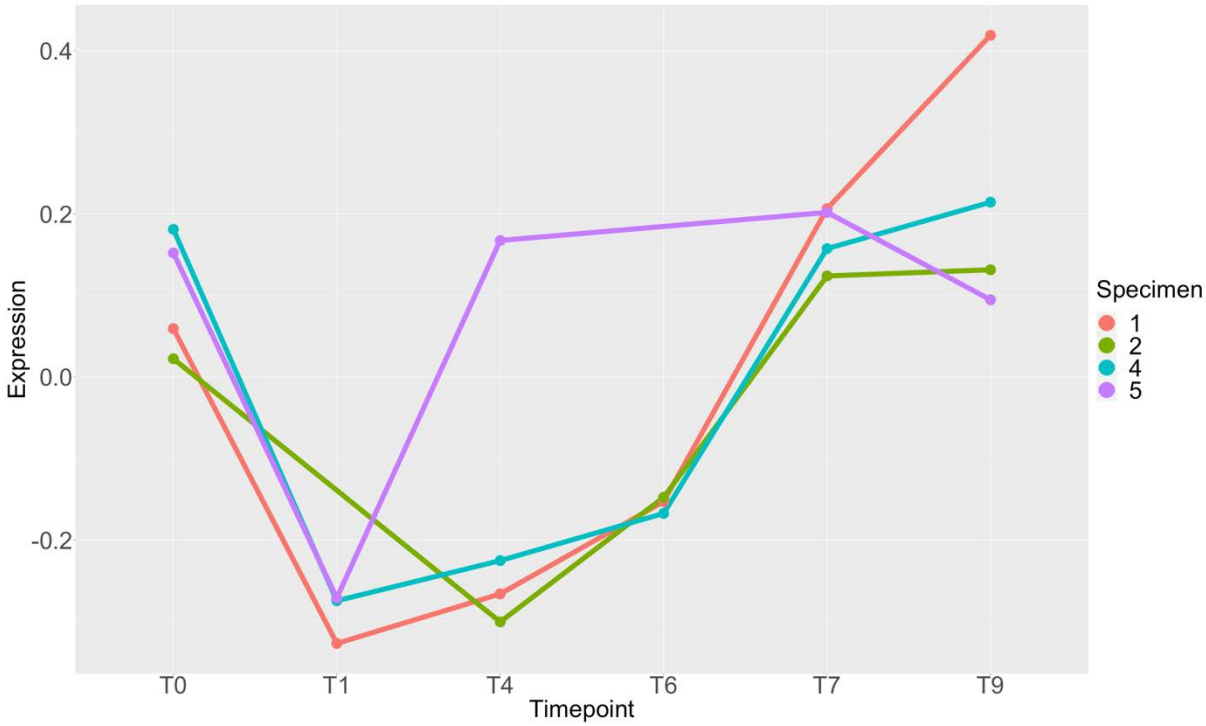

Figure 2.9. WGCNA plot of the red module. A comparison of patterns in the red module eigengenes across all six timepoints is shown. T0 = primary amputation; T1 = 1-hour post-amputation ("scab" formation); T4 = 24 hours post-amputation ("pinched" appearance); T6 = 72 hours post-amputation (smooth stump ending); T7 = 96 hours post-amputation (beginning of tip formation); T9 = 10 days post-amputation (fully regenerated acrosome, end of regeneration).

2.5. Discussion

Heliofungia actiniformis (Cnidaria, Hexacorallia, Scleractinia, Fungiidae) is a unique organism with high potential for research in the field of regeneration due to its impressive capacity for regrowth, life cycle plasticity, and unique taxonomic position as a model coral. Furthermore, the high regeneration potential of this organism and its complex phylogenetic structure make it a valuable model organism with the potential to shed light on the molecular mechanisms behind regeneration in other organisms.

This study is an essential first step in understanding the molecular mechanisms behind tentacle regeneration in *H. actiniformis*, which could help develop regenerative medicine techniques in the future. By analysing changes in gene expression and network functioning during different stages of regeneration, both expected and unexpected patterns were revealed. Interestingly, this study also reports the distinct morphological changes observed during tentacle regeneration in *H. actiniformis* for the first time, with the regeneration timeframe being consistent with other cnidarians (Luz, 2020; Xu, 2022).

2.5.1. Stages of tentacle regeneration in *H. actiniformis*: Morphological changes

The consistent morphological stages of tentacle regeneration observed in this study align with previous research on cnidarian regeneration (Luz, 2020; Xu, 2022), suggesting a well-conserved process among cnidarians. The results of this study offer additional insights into the established concept of the three stages of regeneration, contributing to the growing body of evidence related to regeneration timelines (Amiel et al., 2015; Brockes & Kumar, 2008; DuBuc et al., 2014; Galliot & Chera, 2010; Galliot & Ghila, 2010; Gufler et al., 2018; Kawakami et al., 2006; Luz, 2020; Marques et al., 2019; Minowada et al., 1999; Pellettieri et al., 2010; Petersen et al., 2015; Stewart et al., 2017; Xu, 2022).

The wound healing and closed "scab" like structure observed within the first-hour post-amputation implies a rapid response to injury, which is crucial for survival and avoiding infection. Cell migration and proliferation characterise this initial regeneration stage, forming a blastema-like structure from which the new tentacle will emerge. The formation of the nubbin-like structure during the intermediate phase represents a transition from the early regenerative stages to the late stages, where tentacle elongation and tissue differentiation occur. The subsequent stages of regeneration involve differentiation and morphogenesis of the regenerating tentacle, exhibiting a distinct progression of events that ultimately lead to the complete restoration of the tentacle's function and structure.

The completion of regeneration within ten days post-amputation is consistent with the fast regenerative abilities observed in other cnidarian species, further demonstrating the resilience and adaptability of these organisms. This rapid regeneration process can be attributed to the activation of various molecular pathways and the expression of genes related to cell proliferation, differentiation, and tissue remodelling. Moreover, stem cell-like populations, such as interstitial cells, might contribute to the efficient regenerative response observed in cnidarians.

2.5.2. Transcriptomic insights into *H. actiniformis* regeneration

The use of transcriptomic data for investigating the molecular mechanisms underlying regeneration has become increasingly common in recent years. However, the complexity of gene expression patterns and the individual variability within populations challenge data interpretation. This study performed a principal component analysis (PCA) on transcriptomic data to gain insight into the molecular mechanisms of regeneration in the mushroom coral *H. actiniformis*. The analysis revealed the impact of genotype on gene expression variation, the gradual shift towards a stronger connection between regeneration conditions, and the identification of critical genes and pathways involved in regeneration.

The variation due to genotype that accounted for at least 74% of transcriptomic variability showed that genotype significantly impacted gene expression variation, particularly in the first two principal components. This finding is consistent with previous studies in soft corals (Al-Shaer et al., 2023; Farag et al., 2016), emphasising the importance of considering individual variability in transcriptomic studies. Despite the genotype-driven variation, our analysis also identified a gradual shift towards a stronger connection between the conditions in subsequent principal components, indicating consistent gene expression changes associated with tentacle regeneration. This observation suggests that, although individual genotypic differences may influence overall gene expression patterns, the core molecular mechanisms driving regeneration are conserved across individuals. This observation led to the identification and analysis of differentially expressed genes (DEGs) across the six regeneration timepoints, ultimately revealing critical genes and pathways involved in the regeneration process.

The observed pattern of DEGs across the regeneration timepoints aligns with the proposed three sequential stages of regeneration: wound healing, early regeneration, and late regeneration, as previously described in other cnidarian species (Luz, 2020; Xu, 2022). The high number of DEGs and associated gene ontology (GO) terms during the wound healing stage and early regeneration stage suggest the activation of numerous genes and biological processes to initiate regeneration and tissue repair and highlight the complexity of these processes, consistent with the findings of previous studies on coral and cnidarian regeneration (Al-Shaer et al., 2023; Cary et al., 2019; Farag et al., 2016; Luz, 2020; Sikes & Newmark, 2013; Umesono et al., 2013). They also

The low number of DEGs during the cell mobilisation phase may indicate a transitional period marked by reduced gene activity as the organism prepares for the final regeneration stage. This observation is in line with the findings of previous research on regeneration in other cnidarians and model organisms (Bely, 2014; Liu et al., 2013), suggesting that a temporary decrease in gene activity or in the rate of change activity may be a common feature of regenerative processes across species. It also suggests that this stage is marked by more specialised gene activity, focusing on specific functions like sequence-specific DNA binding and positive regulation of transcription.

2.5.3. H. actiniformis regeneration: Gene activity and related processes

Regeneration is a complex biological process that involves various molecular and cellular mechanisms. Some organisms have emerged as excellent models to study regeneration due to their remarkable ability to regrow body parts. Transcriptomic studies have been instrumental in unravelling the molecular underpinnings of regeneration in these organisms.

The early regeneration stage (the first 48 hours post-amputation) was significantly enriched for genes involved in calcium transport/activation, cell signalling pathways (e.g. MAPK cascade), JNK cascade, apoptosis, mitochondrial transport, metabolic processes, inhibition of translation, tissue patterning (e.g. FGF and metallogenease), transcription factors (e.g. Sox E1), Notch and ERK. Some of these genes are cnidaria-specific, while others are common across various organisms (Cary et al., 2019; Röttinger, 2021; Shao et al., 2020; van der Burg et al., 2020; Xu, 2022). Interestingly, certain previously identified cnidarian-specific gene classifications, such as those involved with an immune response (e.g. autophagy-related genes and alpha-2 macroglobulin), cell signalling (e.g. small GTPases), and ionic balances, were not observed during the first two days of the regeneration process. Also not viewed were genes classified as involved in cilium/cilia (e.g. Ccdc11, Rsph 3, 1qcd, Iqub), signalling, ncRNA processing, ribosome, de novo gene synthesis, inhibition of translation, nor ECM remodelling, all of which have been observed in the regeneration of other species as well as in cnidarians (Brockes & Kumar, 2008; Kawakami et al., 2006; Marques et al., 2019; Minowada et al., 1999; Pellettieri et al., 2010).

At five days post-amputation, gene classifications involved in immune response, translation inhibition factors, and axis formation were observed. Neural development, however, was not observed at this stage. It could be suggested that regeneration initiates after day two in *H. actiniformis*, and the early tentacle nubbin changes may fall under the category of wound healing. Also, the actual regeneration begins with the acrosome formation (Galliot & Chera, 2010; Galliot & Ghila, 2010; Petersen et al., 2015; Stewart et al., 2017). The lack in expression of genes involved in neural development is not surprising, as tentacles are unlikely to have genes involved in neural development. This observation also supports the suggestion that genes not required for regeneration remain silent to conserve energy given regeneration's vast energy demand (Matus, Pang, et al., 2007; Matus, Thomsen, et al., 2007). Cell proliferation, morphogenesis and stem cell differentiation were observed during the wound healing stage of early regeneration and three- and four-days post-amputation. Enriched genes in the KEGG categories of signal transduction, transcription, translation, cellular proliferation, differentiation, and programmed cell death were also observed throughout regeneration timepoints. Notably, genes involved in matrix metallogenease and FGF-18 were expressed only during specific timepoints rather than throughout the entire regeneration process.

In the late stage of tentacle regeneration in *H. actiniformis*, a distinct set of genes was active compared to the early regeneration stage. At the T6-T7 timepoint pair (72- and 96-hours post-amputation), 15 differentially expressed GO terms containing 130 genes across all ontologies were observed. Most of the GO terms expressed in the biological processes (BP) ontology were related to counting factors associated with gene D, with the remainder being E3 ubiquitin-gene ligase, cysteine genease 2, macrophages, and Laccase-4. Laccase-4, primarily found in plants, fungi, and bacteria, is

known for its roles in detoxification, morphogenesis, and defence against hostile organisms. Several GO terms in the T6-T7 timepoint pair were also shared with T0-T1 and T1-T4 timepoint pairs, indicating a conserved set of genes and pathways involved in regeneration. The primary function observed from four days post-amputation onwards is ATP binding, crucial for signal transduction, tissue defence, and organ regeneration in other organisms.

Twenty-eight differentially expressed GO terms containing 34 genes in the T7-T9 timepoints were found, with 86% associated with ATP-binding cassette sub-family C member 4. The remaining 14% of GO terms were related to Mycocerosic acid synthase, multidrug resistance-associated gene 1, and Phenolphthiocerol/phthiocerol polyketide synthase subunit C. Besides Phthiocerol synthesis and polyketide synthase type I PpsC, these genes were not found in previous regeneration studies, suggesting novel molecular mechanisms in *H. actiniformis* tentacle regeneration.

The study provides valuable insights into the molecular mechanisms underlying regeneration in *H. actiniformis*. By analysing the gene activity and related processes during various regeneration stages, we identified essential genes and pathways involved in wound healing, inflammation, apoptosis, antiviral responses, cell and tissue polarity regulation, and neural development. These findings contribute to our understanding of the complex tissue repair and regeneration process and have potential applications in biomedicine and biotechnology. In conclusion, the regeneration process in *H. actiniformis* involves a dynamic interplay of gene expression patterns and cellular processes across different stages. This study highlights the importance of understanding the molecular mechanisms underlying regeneration to inform future applications in regenerative medicine, tissue engineering, and biotechnology. Further research is needed to fully elucidate the complex interactions between these genes and pathways and their implications for wound healing and tissue regeneration in cnidarians and other organisms.

2.5.4. Interconnected genetic and cellular processes in regeneration.

Genes associated with development and immunity were present during regeneration in *H. actiniformis*. During the early stages of tentacle regeneration (within the first 24 hours post-amputation), TNF receptor factors and frizzled binding were expressed, exhibiting connections between immunity and regeneration and between development and regeneration. The connection between immunity and regeneration is that TNF receptor factors regulate inflammation, apoptosis, and antiviral responses and affect the immune system (Chera et al., 2009; Galliot & Chera, 2010). The connection between development and regeneration is that Frizzled bindings involve genes associated with Wnt, collagen and Tyrosine-gene kinase. They play a vital role in adapting cell and tissue polarity and are critical in embryonic development and in a variety of other procedures both in mature

and developing organisms (Chera et al., 2009; Galliot & Chera, 2010; Huang et al., 2017; Röttinger, 2021; van der Burg & Prentis, 2021; Warner et al., 2020).

Another connection between development, immunity, and regeneration was apoptosis expression during the first-hour post-amputation, when the immune system must remove cells during development. These genes contribute significantly to regeneration as fundamental suppliers of Wnt signalling during the first 24 hours post-amputation. They are also vital to initiating cell proliferation between four days and ten days post-amputation during acrosome formation (Chera et al., 2009; Galliot & Chera, 2010; Huang et al., 2017; Röttinger, 2021; van der Burg & Prentis, 2021; Warner et al., 2020).

In summary, the regeneration process in *H. actiniformis* involves shared genetic and cellular mechanisms related to development and immunity. The expression of TNF receptor factors, Frizzled binding, and apoptosis-associated genes highlights the complex interplay between immunity, development, and regeneration. Understanding these connections provides valuable insights into the molecular underpinnings of regeneration and can inform future research and applications in regenerative medicine, tissue engineering, and biotechnology. Further investigation is needed to fully elucidate the complex interactions between these genes and pathways and their implications for wound healing and tissue regeneration in cnidarians and other organisms.

2.5.5. The original: ATP binding and its implications in regeneration

Adenosine triphosphate (ATP) binding is the primary function observed from four days post-amputation until the end of the regeneration experiment in *H. actiniformis*. The ATP-binding cassette (ABC) family plays a crucial role in signal transduction and tissue defence. It was significantly enriched at 48- and 72-hours post-amputation in earthworms and organ regeneration in mammals (Huls et al., 2009; Kimura et al., 2012; Shao et al., 2020). It is not observed in coral regeneration, however, Kochman et al. (2021) have observed ATP-binding during thermally bleached symbiotic cnidarians (Kochman-Gino et al., 2021). Generally, ATP-binding cassettes are present across all living organisms, such as gene secretion and signal transduction. Its importance is often more notable when defective, leading to inheritable human diseases such as cystic fibrosis and Stargardt's disease (Schneider & Hunke, 1998). ATP-binding cassette genes are also involved in drug and antibiotic resistance.

The presence of ATP binding in *H. actiniformis* regeneration suggests that the acrosome formation of the tentacles might involve some level of toxin resistance to protect the coral tips from predatory toxins. Another possibility may be that the drug-resistant genes are necessary to protect the rest of the

H. actiniformis from the poisons or drugs within the cnidae/nematocysts (microscopic intracellular stinging capsules) present in the tips. This observation highlights the potential role of ATP-binding cassette genes in regeneration and warrants further investigation into their function and implications in coral regeneration and other organisms.

2.6. Conclusion

The complex process of tentacle regeneration in the mushroom coral *H. actiniformis* was explored, focusing on the molecular mechanisms and cellular processes involved. We have discussed various stages of regeneration, highlighting the essential genes and pathways associated with wound healing, inflammation, apoptosis, antiviral responses, and cell and tissue polarity regulation. The involvement of conserved genes and processes such as TNF receptor factors, Frizzled binding, and ATP-binding cassettes demonstrate the intricate interplay between immunity, development, and regeneration in *H. actiniformis.*

By analysing differentially expressed genes (DEGs) and Gene Ontology (GO) enrichment, we identified the essential molecular processes and genes involved in both the early and late stages of regeneration. In the early stages, wound healing, tissue patterning, stress response, and potassium channel regulation were crucial. In contrast, the late stages showed distinct active genes related to inflammation, apoptosis, antiviral responses, and cell and tissue polarity regulation. The DESeq analysis allowed us to understand better the dynamic changes in gene expression throughout the regeneration process. We also identified a novel method of data collection and novel genes and pathways that have not been reported in other coral regeneration studies, suggesting unique molecular mechanisms in *H. actiniformis* tentacle regeneration. We discussed the potential implications of ATP binding in the context of regeneration, including drug resistance and protection against predatory poisons.

The study provides valuable insights into the molecular underpinnings of regeneration in *H. actiniformis* and enhances our understanding of the complex process of tissue repair and regeneration. These findings contribute to the growing knowledge of regeneration in cnidarians and have potential applications in biomedicine, tissue engineering, and biotechnology. Further research is needed to fully elucidate the interactions between these genes and pathways and their implications for wound healing and tissue regeneration in *H. actiniformis* and other organisms. This chapter sets the stage for future investigations to uncover the intricate mechanisms governing regeneration and harness its potential for various application

Chapter 3: Molecular mechanisms involved during thermal induced bleaching in *Heliofungia actiniformis.*

3.1. Abstract

Mass coral bleaching, a process in which symbiotic algae are expelled, causing their host to become white, is a severe threat to reefs. This phenomenon can be fatal to marine symbiotic organisms and is mainly correlated to increasing climate change-associated anthropogenic stressors. Therefore, it is vital to understand the process of bleaching under heat stress. This study aimed to detect changes in the expression of genes associated with heat stress bleaching in corals to increase the limited knowledge on the molecular changes that occur during coral bleaching. The experiment involved increasing the temperature of *Heliofungia actiniformis* coral individuals from acclimation until bleaching occurred and samples were collected every 24 hours. Gene expression activity decreased after three days at the heat stress temperature as basal cellular functions ceased and gene activity shifted towards survival. Calcium ion transport and the progranulin were the most highly expressed throughout the heat stress time points, and the bleaching time points were associated with translation, innate immunity, and self-regulation. The novelties of this experiment include that it is the first study of coral bleaching on a robust coral and the length of the experiment as it allowed the detection of functions throughout the heating process and not just at the point of bleaching, therefore it should be adopted by future studies on symbiont organisms for improved future comparisons to other species. Adopting the increased experimental length will enhance the understanding of gene expression changes during heat stress and bleaching as it will allow for investigation into the modifications that occur during heating and not just at the bleaching point when it may be too late to stop it. This kind of longer experiment could guide progressive coral conservation efforts as by knowing the changes corals go through in the process to bleaching may allow for coral health to be assessed in a broader scale.

3.2. Introduction

The coral reefs are considered some of the world's most diverse marine ecosystems and they are responsible for billions of dollars in the economy through food, coastal protection, pharmaceutics, and tourism (Costanza et al., 2014). However, these corals undergo a phenomenon called "bleaching" when facing stressors (for instance, increased temperature), during which corals lose their symbiotic algae (*Symbiodiaceae* spp.) and turn white (Baumgarten et al., 2015; Burriesci et al., 2012; Phillip A. Cleves et al., 2020; Phillip A Cleves et al., 2020; Hoegh-Guldberg et al., 2017; LaJeunesse et al., 2018; Xiang et al., 2015). Bleaching can result in increased coral mortality rates and decreased growth rates, coral cover, species diversity and disease resistance (Phillip A. Cleves et al., 2020; Phillip A Cleves et al., 2020; Cui et al., 2019; Dani et al., 2017; Hambleton et al., 2019; Hughes, Anderson, et al., 2018; Ishii et al., 2019; McDermott, 2020). Coral reefs are among Earth's most productive and biodiverse ecosystems; hence, taking measures for their protection, mitigation, adaptation, and repair is essential. To design conservation measures it is vital to understand the mechanisms underlying bleaching as the duration and magnitude of stress influence the severity and subsequent mortality of corals (Allemand & Osborn, 2019; Hughes et al., 2020; Szabó et al., 2020).

Different types of stressors can cause corals to bleach. These stressors include ocean warming (Núñez-Pons et al., 2017; Pryor et al., 2020; Steinberg et al., 2021), ocean acidification (Patel et al., 2022), osmolarity (Barros et al., 2021; Chavanich et al., 2009; Gegner et al., 2019; Kerswell & Jones, 2003) and light intensity (Higuchi et al., 2015; Kabil et al., 2019; Reynolds et al., 2008; Xiang et al., 2015). Two main types of systems have been associated with bleaching in corals, the first constitutes the loss of pigments by symbionts *in situ* degradation (Ishii et al., 2019), and the second involves the loss of symbionts – either by being ejected or choosing to exit the host (Cziesielski et al., 2019). Algae fulfil most of the energy requirements of specific coral hosts, enabling them to calcify effectively and become the foundation of coral reefs. Hence, the loss of *Symbiodiniaceae* can result in an energy deficit that can lead to the death of the corals (Phillip A. Cleves et al., 2020; Phillip A Cleves et al., 2020; Cziesielski et al., 2019).

The mechanism of coral bleaching is still a topic of debate among experts. However, several theories have been proposed to explain the triggers of coral bleaching, such as the production of reactive oxygen species (ROS) via photosynthesis, the activation of endogenous viruses due to rising temperature (Davy et al., 2006; Levin et al., 2017; Szabó et al., 2020), and presence of bacteria (Szabó et al., 2020; Zaragoza et al., 2014). One of the main reasons for coral bleaching is debated to be due to the increased production of H_2O_2 and NO by algal endosymbionts during heat stress (Altieri et al., 2017; Baird et al., 2017; DeSalvo et al., 2012; Hadaidi et al., 2017; Hawkins & Davy, 2012; Hughes

et al., 2020; Suggett et al., 2008). Hence, thermal stress-related bleaching poses a significant threat to coral reefs globally, emphasising further research to ensure their survival.

Recent advancements in technology, genomics, proteomics, and transcriptomics have shifted research focus towards cellular and molecular mechanisms of bleaching. For example, the increase in temperature has been reported to increase the expression of molecular chaperons, i.e., heat shock genes (HSPs) in symbiotic cnidarians such as *Fungiids*, *Porites* spp., *Acropora* spp., and the anemone *Aiptasia* (Kenkel et al., 2011; Kenkel et al., 2014; B. Meyer et al., 2011; E. Meyer et al., 2011; Richier et al., 2008; Traylor-Knowles et al., 2017). In both eukaryotic and prokaryotic organisms a response to high temperatures is the increase in the expression of HSPs which are associated with the occurrence of two inter-related phenomena in corals (Shende et al., 2019; Sottile & Nadin, 2018). These phenomena are heat stressed, which occurs in all organisms and is often associated with the production of HSPs; and bleaching, which involves loss of symbionts and is therefore specific to symbiotic organisms. Even an environmental temperature that is a few degrees higher than the average body temperature of an organism can cause heat shock; hence, corals undergo thermal stress at 32°C which is higher than their optimal temperature of the mid to late 20s (Sottile & Nadin, 2018; Tomanek, 2010). Several genes and genes are associated with the phenomenon of bleaching. For example, in symbiotic anemones, the de novo serine biosynthesis genes are active during healthy symbiosis. However, their activity is reduced during heterotrophic feeding for energy, suggesting that bleaching might be characterised by the decrease in some enzymes involved in serine metabolism (Cui et al., 2019; Moya et al., 2015).

Studies on bleaching have primarily focused on the model organism *Aiptasia* (Cui et al., 2019) or a limited number of *Acropora* (Howells et al., 2011; Moya et al., 2015; Petrou et al., 2021; Seveso et al., 2014; Strader, 2022) or *Pocillopora* species (Thummasan et al., 2021; Zhang et al., 2018). Also, analytical methods have been advanced from microarrays and quantitative RT-PCR to RNAseq with more information and features, affecting the comparison of previous studies (Phillip A. Cleves et al., 2020; Phillip A Cleves et al., 2020; McLachlan et al., 2020). Moreover, sampling procedures are also significantly different, i.e., few studies involved the collection of samples right after the set temperature of thermal stress (usually within 48 hours) (Avila-Magaña et al., 2021; Barshis et al., 2013; Bieri et al., 2016; Cziesielski et al., 2018) while others involved collection during ramping up to thermal stress levels and stopping on set point (Ainsworth et al., 2008).

According to reviewed literature, only two studies have examined the effects of heat stress on gene expression comprehensively, including acclimation temperatures, heat stress, and complete bleaching. One of them focused on *Aiptasia* (Phillip A. Cleves et al., 2020; Phillip A Cleves et al., 2020), while the other study focused on aposymbiotic larvae (B. Meyer et al., 2011; E. Meyer et al., 2011).

Therefore, there is limited information about the role of symbiotic algae during thermal stress reactions; hence, increasing this knowledge is of vital importance as thermally stressed symbionts release reactive oxygen species (ROS), which leads to bleaching and results in coral mortality (Lesser, 2010; Weis, 2008). There is also a requirement to understand transcriptional changes in response to heat stress and specific responses involved in bleaching among symbiotic cnidarians.

This research is among the initial studies to detect changes in the expression of genes associated with heat stress by analysing the RNAseq data from samples collected from optimal body temperature to heat-stress temperatures and maintaining them up to the point of bleaching in cnidarian corals. RNAseq analysis is vital to identify the genes that play a crucial role in thermal tolerance, which can participate in the development of genetic engineering techniques to enhance heat tolerance in corals (McDermott, 2020).

This chapter aims to document changes in gene expression during the thermal-induced bleaching process in *Heliofungia actiniformis* to understand the molecular mechanisms employed by symbiotic corals in response to thermal stress. RNAseq analysis will be utilised to analyse *H. actiniformis* samples obtained over a full-time progression initiated shortly before the imposition of heat stress and continued until corals were white, signalling complete bleaching. This chapter observes that gene expressions change when *H. actiniformis* corals are exposed to high temperatures and when they bleach. Also, some of these changes will mirror gene expression pathways observed in other symbiotic-dependent animals. The contribution of this chapter to the overall project is to provide an understanding of the molecular processes present during *H. actiniformis* heat stress associated with bleaching. These molecular processes will then be compared with those involved in the ejection of symbionts in the symbiont chapter (Chapter 4). This chapter's original contribution to knowledge is to achieve a clearer picture of gene expression during heat stress-related bleaching in robust corals.

3.3. Materials & Methods

3.3.1. Aquaria conditions

H. actiniformis corals (12 individuals) of >25cm in diameter were collected from the Orpheus Island research station (OIRS) (exact locations and collection information can be found in Chapter two; Section 2.1; Table 1.). The corals were then packed into individually labelled plastic containers and transported back to the Marine and Aquaculture Research Facilities Unit (MARFU) at James Cook University (JCU), Townsville, Queensland, Australia. The corals were then kept in twelve separately labelled 60-litre tanks attached to two sump systems (six tanks per sump system) in two semi-closed

systems. Each tank-maintained daylight hours (on at 6:00 am and off at 5:30 pm), and the individual tanks' temperature, salinity, nutrients, and the two sump systems were tested every 24 hours before sampling. The corals were acclimated at 26ºC (the midrange water temperature at the collection sites) for fourteen days with basic husbandry and no other interactions or collection of samples. The basic husbandry involved keeping corals on a diet of live brine shrimp offered twice per week without any other source of nutrition or animal association.

3.3.2. Thermal regime & sampling

The water temperature was increased by one degree Celsius from the acclimation temperature (26ºC) to 27ºC. Every 24 hours after the initial increase, the temperature was further increased by one degree Celsius per day until it reached 34ºC, which took eight days. The corals were maintained at 34ºC until bleached (more than 75% of the tentacles turned white), followed by a further three days (post bleaching). As individual corals bleach at different times (see the pilot experiment in Appendix A), each coral's bleaching time and date were recorded. A full description of the minimum timepoints and the number of samples collected can be found in Table 3.1, as the individual number of timepoints depended on the time required by a particular coral to be bleached.

The experimental samples constituted three tentacles collected from each coral simultaneously (8:00-9:00 am) every morning. The samples were either snap-frozen in liquid nitrogen, stored at -80ºC, or fixed in formaldehyde for future analysis. Before sampling, photographs of each coral were taken next to a Chemwatch Coral Health Chart to record colour change (aka bleaching level). Samples were collected just before subsequent temperature increases, ensuring a minimum of 24 hours of exposure to a particular temperature.

Table 3.1. Timepoints of heat-stress experiment of *Heliofungia actiniformis*. Description of the different heat-stress and bleaching conditions during the heat-stress experiment and their associated timepoints.

Description	Timepoint
Last 24 hrs @ 26ºC	T0
24 hrs (1 day) @ 34ºC	T1
48 hrs (2 days) @ 34ºC	T2
72 hrs (3 days) @ 34ºC	T3
96 hrs (4 days) @ 34ºC	T4
120 hrs (5 days) @ 34ºC	T5
144 hrs (6 days) @ 34ºC	T6
168 hrs (7 days) @ 34ºC	T7
192 hrs (8 days) @ 34ºC	T8
216 hrs (9 days) @ 34ºC	T9
240 hrs (10 days) @ 34ºC	T10
264 hrs (11 days) @ 34ºC	T11
292 hrs (12 days) @ 34ºC	T12
First time bleached	B1
24 hrs (1 day) bleached	B2
48 hrs (2 days) bleached	B3
72 hrs (3 days) bleached	B4

3.3.3. Aquaria issues

Sump system one contained coral individuals one to six, while system two contained individuals seven to twelve—some technical issues were experienced during the experiment. Firstly, due to miscommunication, sump system one was not fitted with automated heating, which delayed the experiment for individuals 1-6 by three days, creating a 3-day offset between the two sump systems; no other issues were incurred with system one. Secondly, technical issues with the automated heating equipment in system two required a few days of troubleshooting. The troubleshooting resulted in the individuals in sump system two experiencing an environment of 32ºC for three days (instead of 24 hours) before the temperature was increased by the last two degrees in the following 48 hours. Finally, 48 hours after sump two reached 34ºC, the water in the tanks and sump became cloudy as the ammonia level increased in the tanks and sump due to technical difficulties with the gene skimmer. Once this was rectified, 60% of the water was replaced with newly heated water, which took several days to heat to the right temperature, which led to the corals being at 34ºC in cloudy ammonia-filled

tanks for over four days. Samples were collected from all twelve individuals throughout the experiment; however, analysis was only performed on individuals from sump system one.

All corals were supposed to bleach around similar timepoints within each sump system, but issues in sump two (as discussed above) affected the bleaching rate and corals' health (Table 3.2). These issues affected the sampling process as bleaching samples could not be collected for two of the individuals due to their rapid death caused by the presence of ammonia in the system. The individuals in sump one bleached within 11 days (on average). In sump two, surviving corals took two days (on average) to bleach.

Table 3.2. Timeframe that *H. actiniformis* coral individuals bleached. Description of the timepoint that each individual coral bleached and the associated sump system of the corals.

Individual Number	Timepoint prior to bleaching	Time @ 34ºC prior to bleaching (hours/days)	Sump System
1	T12	192 / 8 days	1
2	T12	192 / 8 days	
3	T7	72 / 3 days	
4	T11	168 / 7 days	
5	T10	144 / 6 days	
6	T12	192 / 8 days	
7	T7	72 / 3 days	2
8	T5	24 / 1 day	
9	NA	NA	
10	T5	24 / 1 day	
11	T7	72 / 3 days	
12	NA	NA	

Due to the large number of collected samples and inconsistencies among samples associated with sump system two, a subset of the samples was chosen for further analysis. Four individuals from sump system one (1, 2, 4, and 5) were chosen due to having the same collection site (Chapter 2, Section 2.2, Table 2.1), which increased their likelihood of experiencing similar environments (depths and water quality) throughout their life stages. Additionally, four timepoints and two bleached timepoints (T0, T3, T6, T9, B1, and B4) were selected to analyse changes occurring throughout the heating timeframe (Table 3.1).

3.3.4. Whole transcriptomic library preparation

Total RNA was extracted from a subset of the samples (four individuals from sump one (1, 2, 4, and 5) and six conditions (Table 3.3) using a Qiagen RNeasy Plus Mini Kit by following manufacturer instructions and suspended in RNase-free water. The purity of extracted RNA was verified by using a spectrophotometer (Nanodrop ND-1000), and concentrations were determined by using an Invitrogen Qubit Fluorometer with RNA High Sensitivity (HS) and Broad Range (BR) Assay kits. The integrity and concentration were substantiated with the Agilent 2200 Tapestation by using the Agilent High Sensitivity RNA ScreenTape System. The 500ng of RNA per sample in a concentration of 20ng/µl required by the Australian Genome Research Facility (AGRF) RNA sequencing for whole transcriptome library creation was obtained by dilution with RNase-free water (2µl - 12µl) based upon the concentration of the extracted RNA. The prepared samples were sent to AGRF for library preparation.

Table 3.3. Conditions chosen for further analysis. A breakdown of the conditions chosen for further analysis and their subsequent description.

Condition	Description
T0	Last 24 hrs @ 26ºC
T3	72 hrs (3 days) @ 34ºC
T6	144 hrs (6 days) @ 34ºC
T9	216 hrs (9 days) @ 34ºC
B1	First time bleached
B4	72 hrs (3 days) bleached

3.3.5 Bioinformatic analysis

Raw sequence quality control was evaluated with FastQC (https://www.bioinformatics.babraham.ac.uk/projects/fastqc/), and then MultiQC (Ewels et al., 2016) was used to combine the FastQC analysis for multi-sequence quality control. Reads were mapped to a *Heliofungia actiniformis* reference genome and transcriptome, obtained from https://coral.genome.edu.au. Read mapping was performed using bowtie2 and the RNA-seq by Expectation-Maximization (RSEM) package (Li & Dewey, 2011) was used to quantify gene expression levels from RNA-seq data.

A table of counts at the gene level was generated from the reads of all the gene isoforms (Supplementary Table S3.1), and the R BiocManager (Robinson et al., 2009) package tximport (Love et al., 2018) was used to import and summarise the transcript abundance from the table counts. The R

Bioconductor package DESeq2 (Love., 2014) was then utilised to create a DESeq object that measured the differential gene expression between the different stages of regeneration by comparing time to genotype. The counts were then normalised dependent on dispersion and size factors, and a variance stabilising transformation (VST) was performed. Principal component analysis (PCA) was conducted for data quality control and overall characterisation of gene expressions throughout the regeneration timepoints.

A series of pairwise-contrast tests were used to analyse the Differentially Expressed Genes (DEGs) in each pair of sequential timepoints (T0 vs T1, T1 vs T4, etc). Only the genes with a q-value lower than 0.05 were considered significantly differentially expressed to control the false discovery rate (FDR). GO Enrichment analysis was then performed on the gene sets to identify over-represented (or under-represented) GO terms by using annotations for the gene sets and regarding the GO terms with p-value < 0.001 as significantly enriched.

3.4. Results

3.4.1. Principal Component Analysis (PCA) of transcriptomic data

The transcriptomic data were obtained after sample analysis and next-gen library preparation. Filtered individual reads were mapped against assembled transcriptome, and data were subjected to principal component analyses (PCA) for quality control and characterisation of gene expression throughout bleaching timepoints. The dominant reason for sample variation in gene expression was the genotype (individual). This dominance is exhibited in PC1, PC2, and PC3 accounting for 31%, 30%, and 24% of the variance, respectively (Fig 3.1A, B, & C). All three of these PC axes largely captured individual genotype differences. Not until PC4 (6%) and PC5 (2%) do we see variation by the experimental condition with little to no connection to individual genotype (Figure 3.2D). A plot of PC4 vs PC5 shows a clear separation by condition (Figure 3.2E). Overall, the progression from PC1 to PC5 shows a clear connection between individuals that gradually becomes a strong correlation between conditions. This variation by genotype is also observed in soft corals (Al-Shaer et al., 2023; Farag et al., 2016) and was also observed in the regeneration experiment (Chapter 2 of this thesis). The PCA results highlight individual inclusion in the model, which could make it possible to identify and analyse differentially expressed genes (DEGs) across six timepoints with the adjusted p-value < 0.05.

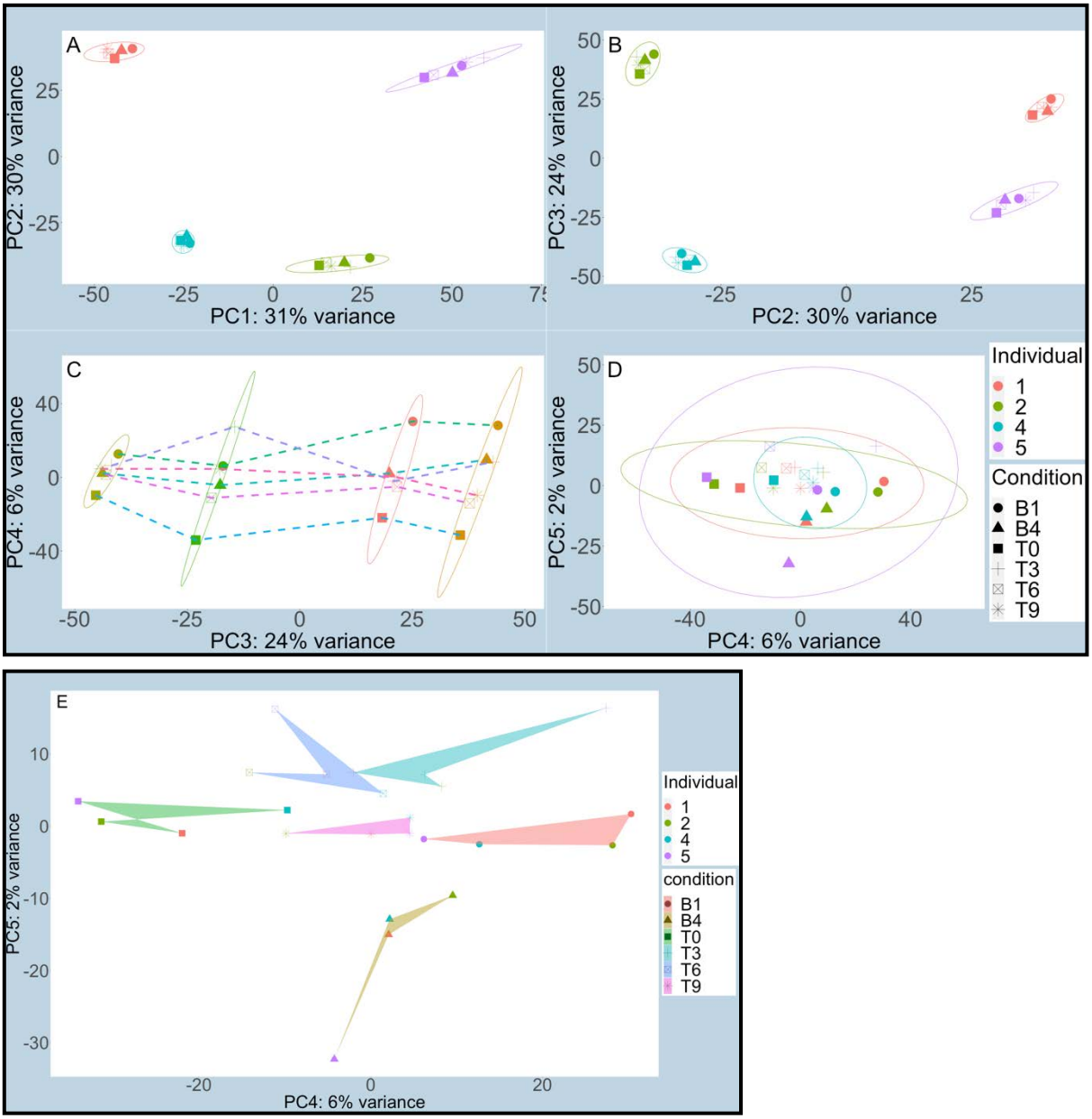

Figure 3.1A-E. Principal Component Analysis (PCA) of bleaching individuals at different time points. PCA plot of samples from *H. actiniformis* individuals (identified by colours) at different heating and bleaching time points (identifiable by symbols). (A) A comparison of the highest principal component levels (31% vs 30%; PC1). (B) A comparison of component levels 30% vs 24% (PC2). (C) Compares component levels 24% vs 6% (PC3). (D, E) Comparison of the lowest principal component levels (6% vs 2%; PC4; D) and (E) polygons around points are convex hulls coloured by a particular condition. The graphical plot and the ellipses were generated by ggplot2 R package implemented with stat ellipse function. The axis titles represent principal component along with their respective percentage of variation. The ellipses represent the orientation and spread of points according to the method of stat_ellipse().

3.4.2. Differentially gene expression through heat-stress bleaching

The strong genotypic effect that leans towards individual variation observed in the PCA allowed for the identification and analysis of DEGs across the conditions. Analysis of the differentially expressed genes (p-value <0.05) illustrated a great many genes differentially expressed between T0 and T3

followed by a gradual decline in activity after the first three days at a high temperature, followed by a steady increase in activity up to B1 (Figure 3.2). Collectively, 7,595 genes were found to be differentially expressed with the highest abundance being between the heated condition pair T0 and T3 (2,504 upregulated and 2,314 downregulated) which signifies the rise in temperature from 26°C (the temperature at T0) to 34°C (the temperature at T3) and keeping constant at 34°C for three days. The second highest abundance of DEGs was observed during bleaching condition pair B1 and B4 (1,023 upregulated and 805 downregulated), which indicates the total expulsion of symbionts from the coral host, causing the complete whitening of the coral host. After three days at 34°C (condition pair T3_T6), a small number of DEGs were observed (73 upregulated and 31 downregulated); however, the number of DEGs increased with the increase of time at 34°C. For example, the number of DEGs tripled at the T6_T9 pair, then almost doubled by the T9_B1 pair and finally almost quadrupled at the B1_B4 condition pair when compared to the T9_B1 pair (Figure 3.2). This highlights the activation of survival pathways on encountering the expulsion of symbionts from the host.

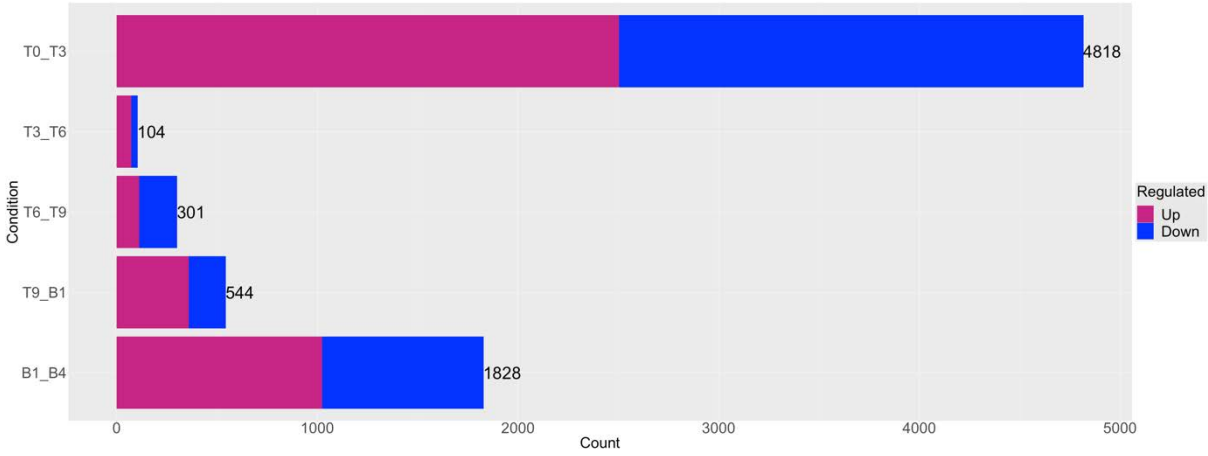

Figure 3.2. Differentially Expressed Genes (DEGs) during coral bleaching. The number of upregulated and downregulated genes through sequential pairs of the heating conditions of *H. actiniformis*, at an adjusted p-value (p-value<0.05). The abbreviations of the timepoints are T0 = last day at 26°C; T3 = 72 hours (3 days) at 34°C; T6 = 144 hours (6 days) at 34°C; T9 = 216 hours (9 days) at 34°C; B1 = First time bleached; B4 = 72 hours (3 days) bleached.

3.4.3. Gene Ontology (GO) enrichment of DEGs

The GO enrichment analysis produced 137 GO terms (BP = 71, MF = 34, CC = 29) across all pairs of consecutive conditions; however, some GO terms were observed at several conditions, which made for a total of 180 (with the same GO terms) across all pairs of consecutive conditions (Supplementary Table S3.2). The heated condition pair T0 to T3 (0_3) had the most GO terms (58 across all ontologies), followed closely by condition pair T6 to T9 (6_9; 45 GO terms across all ontologies). This pattern was almost the same as the heated condition to bleached pair T9 to B1 (9_B1; 40 GO

terms across all ontologies; Figure. 3.3; and Supplementary Table S3.2). The lowest number of GO terms was seen at the heating condition pair T3 to T6 (3_6; 13 GO terms across all ontologies), followed by the bleached condition pair B1_B4 (24 GO terms across all ontologies). The dip in GO term quantity in the heating condition T3 to T6 supports the pattern exhibited within the DEGs, which highlights the possible ability of corals to withstand heat stress for a few days before death or symbiont expulsion. However, the gene expression patterns during more extended periods of heat stress than a few hours or up to three days have not been studied so far (Phillip A. Cleves et al., 2020; Phillip A Cleves et al., 2020; Mayfield et al., 2011; McLachlan et al., 2021; McLachlan et al., 2020), making this study valuable and challenging to compare against past research.

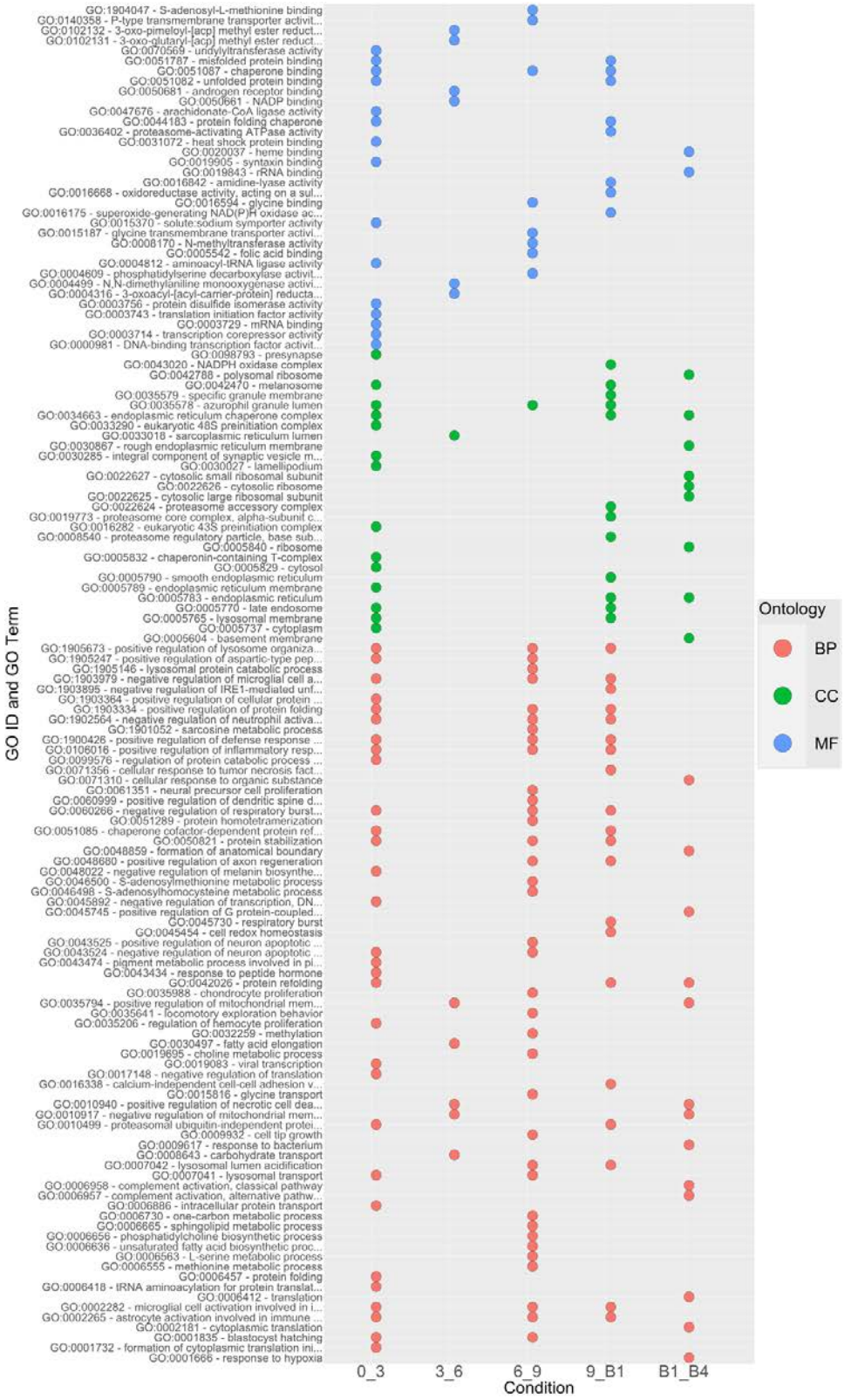

Figure 3.3. Significantly enrichment GO terms of *H. actiniformis* during bleaching. The significant (p-value < 0.005) GO IDs with their corresponding GO terms with highest p-values separated by ontology per timepoint pair. GO Terms are in order of p-value (decreasing). Condition pair 0_3 represents a comparison of heated conditions T0 (Last day at 26°C) to T3 (3 days at 34°C). Condition heated pair T3 to T6 (6 days at 34°C) are represented by 3_6. Condition 6_9 represents heated condition pair T6 to T9 (9 days at 34°C). Heated to bleached condition pair T9 to B1 (First time bleached) are represented by 9_B1. B1_B4 represents bleached condition pair B1 to B4 (3 days bleached).

3.4.4. Gene activity during the different conditions

Analysis of DEGs was performed to understand activated and deactivated functions during the heating and bleaching processes. It was hypothesized that corals under heat stress deactivate routine processes and activate stress-related functions, healing, or survival.

3.4.4.1. Activity between the last day at 26°C (T0) and 3 days at 34°C (T3)

It was hypothesised for this condition pair that there would be more activity in the T0 condition than in the T3 condition. Almost a quarter (22%) of enriched terms upregulated in condition T0 were associated with basal functions, which were allocated to enriched terms with over 100 genes that had less than 5% similarity (GO:0006457, GO:0006886, GO:0043434, GO:0045892, GO:0005737, GO:0005829, GO:0098793, GO:0000981). During the T0 condition, a further 11% of the enriched terms were purely associated with the gene eukaryotic initiation factor (GO:0001732, GO:0016282, GO:0033290, GO:0003743), which is known to be involved in DNA repair and chromatin stabilisation in *Acropora palmata* during heat stress related bleaching (Dixon et al., 2020). The upregulation of such genes during thermal stress and bleaching has been reported as a novel finding in coral *Montastraea faveolata* (DeSalvo, 2010; Michael K DeSalvo et al., 2010; M. K. DeSalvo et al., 2010; Desalvo et al., 2008). DnaJ homologs (GO:0031072, GO:0034663, GO:0003714, GO:0042026, GO:0044183, GO:0051787, GO:0051082, GO:0051085, GO:1903364) and heat shock genes (GO:0031072, GO:0034663, GO:0003714, GO:0042470, GO:0044183, GO:0051787, GO:0051082, GO:0051085, GO:1903364) were upregulated in 25% of the T0 enriched terms. These two genes play roles in stress responses and wound healing across the animal kingdom and have often been implicated in responses to various stressors in cnidarians (Brockes & Kumar, 2008; Poss, 2010; Su et al., 2022). A heat shock family member that plays a vital role in the folding of genes (such as actin and tubulin) in heat-stressed Scleractinia corals (T-complex gene) was also upregulated in 11% of the enriched terms (GO:0003729, GO:0005832, GO:0044183, GO:0051082) (Louis et al., 2017). The upregulation of endoplasmic reticulum (ER) associated genes was observed in 22% of enriched terms (GO:0044183, GO:0051082, GO:0051787, GO:0031072, GO:0034663, GO:0051085, GO:0042026, GO:0003756), which has been observed to be upregulated after 24 hrs of hypo-saline stress in *Acropora millepora* (Aguilar et al., 2019; Dixon et al., 2020), provides an environment for gene folding and plays a vital role in signal transduction in mammals (Darling & Cook, 2014; Ron & Walter, 2007). Serine-associated genes (such as Serine-tRNA ligase and Serine/threonine-gene), which are associated with death in corals and have increased expression during thermal stress in *A. millepora,* were expressed in 17% of enriched terms (GO:0006418, GO:0030027, GO:0003729, GO:0004812, GO:0031072, GO:0019083), (Bellantuono et al., 2012; Petrou et al., 2021). The gene E3 ubiquitin-gene ligase was expressed in 19% of GO terms (GO:0017148, GO:0099576, GO:1903364, GO:0003729, GO:0019905, GO:0031072, GO:0051787) and is strongly involved in

cellular stress response, in gene turnover, and homeostasis which is imperative in coral high-temperature acclimation (Phillip A. Cleves et al., 2020; Phillip A Cleves et al., 2020; Mayfield et al., 2018). A gene associated with the expulsion of symbionts, promotion of symbiont photosynthesis, and translocation of photosynthetic products (ATPase) was expressed in 11% of GO terms (GO:1903364, GO:0042470, GO:0019905, GO:0019083) in the T0 condition (Barott et al., 2015; Petrou et al., 2021). Hypoxia was upregulated in 8% of the GO terms (GO:0034663, GO:0051082, GO:0099576) enriched in the T0 condition. Hypoxia is a key contributing agent of mass coral bleaching-induced mortality worldwide. It is assumed that corals possess Hypoxia-Inducible Factor (HIF) mediated by Hypoxia Response System (HRS) that is differentially expressed under heat stress conditions (Altieri et al., 2017; Deleja et al., 2022; Hughes et al., 2020; Nelson & Altieri, 2019). Other genes that were of interest due to being mentioned in other heat stress studies, but were expressed in less than 5% of a single GO term in the T0 condition (therefore could be outliers) were 40S ribosomal gene & RNA binding (GO:0003729), MAPK/ERK (GO:0019083), proteasome subunit (GO:0010499), major facilitator (GO:0042470, GO:0048022), apoptotic protease-activating factor (GO:0031072), kelch-like gene (GO:0030027), integrin beta (GO:0030027, GO:0042470), glutamine (GO:0006418, GO:0004812), and alanine (GO:0006418, GO:0004812).

Most GO terms upregulated in the T3 condition were involved with longer term responses to stress. At least 50% of the GO terms upregulated in the T3 condition within the T0 to T3 pair were only associated with the gene progranulin (GO:1905247, GO:0060266, GO:0106016, GO:1900426, GO:0002265, GO:0002282, GO:0001835, GO:1902564, GO:1903334, GO:1903979, GO:1905673) and the other 50% of the GO terms are made up of at least 35% progranulin. This gene regulates cell growth, survival, repair, and inflammation across the animal kingdom and has been seen in several studies to regulate the immune response in the soft coral, *Xenia* (Hu et al., 2019, 2020; Townley et al., 2018). Other genes of interest expressed within the second 50% of GO terms in the T3 condition involved DnaJ homolog, E3 ubiquitin-gene ligase, zinc finger, homeobox gene, hypoxia, heat shock gene, gene white, primary facilitator, and endoplasmic reticulum chaperone. However, these genes were expressed at less than 5% within individual GO terms, therefore, could be outliers.

As hypothesised, the results in the condition pair T0-T3 were somewhat predictable regarding the quantity and variety of genes expressed. The first condition constitutes the end of acclimation temperature (26°C), showing the healthy state of corals with normal functions, proven by the vast number of GO terms with more than 100 completely different genes. The second condition, heat stress temperature for three days, shows decreased functions, proven by over 50% of the enriched GO terms mostly expressing a single gene (progranulin).

3.4.4.2. Activity between 3 days at 34°C (T3) and 6 days at 34°C (T6)

Predominant gene functions differentially expressed between the T3 to T6 condition pair were involved in production, storage, and binding of calcium. All the enriched terms during the heat condition pair T3 to T6 were upregulated at the T3 condition and down regulated at the T6 condition, except for sarcoplasmic reticulum lumen (GO:0033018), which was upregulated at the T6 condition and down regulated at the T3 condition (Supplementary Table S3.2). This pattern indicates that most functions during these two heat conditions occur during the T3 condition. The functions of this condition pair were mainly associated with the regulation of the mitochondrial membrane (GO:0010917 & GO:0035794). The structural integrity of the mitochondrial membrane is known to become compromised due to ROS resulting in dysfunction and eventually apoptosis during bleaching (Blackstone, 2009; Downs et al., 2002; Tchernov et al., 2011; Weis, 2008; Weis et al., 2008). Other functions involved fatty acids (GO:0030497) and methyl ester reduction (GO:0035794 & GO:0102132), which have been found to increase calcification rate during heat stress in corals (such as *Porites*), resulting in abnormal skeletal morphology (von Xylander et al., 2023). The binding of NADP (GO:0050661) and androgen receptors (GO:0050681) were also experienced during the T3 condition, which has been reported to control calcium levels (Heinlein & Chang, 2002). The sarcoplasmic reticulum lumen that is upregulated in the T6 condition is a form of muscle cells dedicated to handling calcium required for the contraction and relaxation of necessary muscles (Rossi et al., 2022). It is possible that its upregulating helps to deal with extra calcium produced during the T3 condition. The only GO term overrepresented in the T6 condition of this comparison pair (sarcoplasmic reticulum lumen; GO:0033018) constituted two genes, endoplasmin, a heat shock gene generally found in humans whose function is binding ATP/calcium/RNA/virion/gene phosphatase (Koch et al., 1988). Furthermore, calreticulin is a significant calcium storage gene within the endoplasmic reticulum lumen with a high capacity for calcium binding sites (Varricchio et al., 2017). It indicates that the T3 condition produces extra calcium stored and bound during the T6 condition under heat stress.

3.4.4.3. Activity between 6 days at 34°C (T6) and 9 days at 34°C (T9)

Glycine was the primary function in the T6 condition within the T6 to T9 comparison. 60% of the GO terms in the T6 condition only contained the gene Glycine N-methyltransferase (GO:0005542, GO:0016594, GO:0046498, GO:0046500, GO:1901052, GO:1904047) and the other 40% of the GO terms contained a minimum of 43% glycine N-methyltransferase genes plus a maximum of four other genes, per GO term. Glycine is vital for amino acid metabolism in corals, such as *A. millepora*, and is considered a critical osmolyte for corals as it has been observed in at least 90% of the organic solutes in *Fungia*, *Pocillopora*, *Montipora* and *Tubastrea* (Aguilar et al., 2019). The other genes of interest were serine hydroxymethyltransferase (GO:0006730, GO:0051289) which works together with glycine and is considered critical in the genomic blueprint of coral metaorganisms (Ngugi et al.,

2020), and S-adenosylmethionine synthase isoform (GO:0006555, GO:0006730, GO:0051289) which is vital in cell function and survival in mammals (e.g., mice and humans) and has been reported to be downregulated during antibiotic treatment (but not in the heat treatment in the same study) in *Pocillopora* (Connelly et al., 2022). The other genes that were expressed during this condition involved methylenetetrahydrofolate reductase (GO:0006730), thymidine kinase, cytosolic and transient receptor potential cation channel (GO:0051289), and betaine--homocysteine S-methyltransferase which are only associated with mammals (such as mice and humans) and have not been previously recorded in corals.

The primary function in the T9 condition within the T6 to T9 comparison pair was progranulin. In the T9 condition, 53% of GO terms solely contained progranulin (GO:0001835, GO:0002265, GO:0002282, GO:0007042, GO:0035641, GO:0035988, GO:0043525, GO:0048680, GO:0060266, GO:0060999, GO:0061351, GO:0106016, GO:1900426, GO:1902564, GO:1903334, GO:1903979, GO:1905146, GO:1905247, GO:1905673) and a further five GO terms contained a minimum of 35% progranulin function (GO:0007041, GO:0035578, GO:0043524, GO:0050821, GO:0051087). Two GO terms only contained phosphoethanolamine N-methyltransferase (GO:0009932 & GO:0019695), which is mainly found in coral seagrass sediment, an essential step in choline biosynthesis in plants (Mou et al., 2002) and is widely distributed across the animal kingdom, especially in rotifers, annelids and sponges (Michellod et al., 2022). One of the GO terms constituted L-tryptophan decarboxylase (GO:0004609) which is a group of enzymes in charge of converting tryptophan into tryptamine (Qiao et al., 2022) which was found negative for oxidase in coral trout (Gai et al., 2022). There were four types of transporters amongst three GO terms, proton-coupled amino acid transporter, which is an amino acid transporter found in the transmembrane of insects, small mammals and humans ((Thwaites & Anderson, 2011)) and sodium- and chloride-dependent glycine transporter (GO:0015187 & GO:0015816) which recaptures and transports glycine in the brain of small mammals, humans and zebrafish and maintains glycine levels by removing glycine and terminating glycinergic transmission (Ganser & Dallman, 2009) and has been seen to provide a model in which homeostatic plasticity restores rhythmic motor behaviours in zebrafish (Mongeon et al., 2008). Cadmium/zinc-transporting ATPase and sodium/potassium-transporting ATPase subunit transport sodium and potassium ions in the gills and kidneys of zebrafish, rainbow trout and catfish when exposed to more acidic pH levels (Marx et al., 2022) (GO:0140358). The GO term unsaturated fatty acid biosynthetic processes (GO:0006636) comprised four functions that had never been reported in coral research, and all had roles in fatty acid metabolism in the brains of mammals. Other genes of interest encountered in this condition were DnaJ (GO:0050821 & GO:0051087), hypoxia (GO:0043524 & GO:0051087), endoplasmic reticulum (GO:0051087 & GO:0006636), E3 ubiquitin-gene ligase (GO:0007041 & GO:0051087), serine (GO:0050821 & GO:0006563), Glycine N-methyltransferase (GO:0032259 & GO:0006555), prosaposin (GO:0006665), heat shock (GO:0051087), T-complex (GO:0050821),

ankyrin-2 (GO:0050821), synaptic vesicle membrane gene (GO:0035578), and zinc finger (GO:0043524 & GO:0050821) amongst others.

3.4.4.4. Activity between 9 days at 34°C (T9) and first day bleached (B1).

The functions of 75% of the GO terms enriched in the T9 condition were mainly focused on producing regulators to destroy degraded genes. In the T9 condition, 38% of the GO terms contained NADPH oxidase complex (GO:0043020) in which superoxide-generating NAD(P)H oxidase (GO:0016175) only had cytochrome. This gene is involved in the first line of defence on facing an array of stressors (e.g., thermal stress) in cnidarians such as *Hydra* sp. and sea anemone Nematostella vectensis (Rosic et al., 2010). The sole function of endoplasmic reticulum chaperone BiP was to negatively regulate IRE1-mediated unfolding (GO:1903895) and gene refolding (GO:0042026), which was significantly upregulated in a further 38% of GO terms (GO:0005783, GO:0005790, GO:0016668, GO:0016842, GO:0034663, GO:0044183, GO:0051082, GO:0051085, GO:0051787). The BiP binds, folds, and matures newly-synthesized genes as they are translocated in the endoplasmic reticulum (ER); hence it plays a role in the unfolded gene response (UPR) process as a mechanism against stress events (Bailly & Waring, 2019; Lewy et al., 2017) which is also a member of the HSP70 family (Bailly & Waring, 2019; Otero et al., 2010). This gene is reportedly activated in mammalian cancer cells (Bailly & Waring, 2019; Eugene et al., 2020; Jaud et al., 2020). The increased activity of BiP is observed in jellyfish symbiosis (Castillo-Medina et al., 2022) and in the coral *A. millepora* (Petrou et al., 2021)during heat stress of not more than two days. The sole function of GO terms proteasome-activating ATPase activity (GO:0036402), proteasome accessory complex (GO:0022624), and proteasome regulatory particle (GO:0008540) was to regulate 26S proteasome, which is vital homeostasis of gene and amino acid, and controlling cell cycle, DNA replication, transcription, signal transduction, and stress responses. GO term calcium-independent cell-cell adhesion (GO:0016338) contained a Down syndrome cell adhesion molecule-like gene 1 homolog and proteasome core complex (GO:0019773), the function of which is observed to be elevated under heat stress in anemones (Oakley et al., 2017), foraminifera (Stuhr, Blank-Landeshammer, et al., 2018; Stuhr, Meyer, et al., 2018), *D. melanogaster* (Kristensen et al., 2016), mice (Bartelt et al., 2018), and corals (Maor-Landaw et al., 2014; Traylor-Knowles et al., 2017). However, it is decreased in *A. millepora* (Petrou et al., 2021) and *C. elegans* (Gómez-Orte et al., 2018; Pispa et al., 2020). A proteasome is a gene complex containing catalytic core particles mainly used as a pathway for gene degradation in *C. elegance* (Pispa et al., 2020).

The primary gene of the B1 condition from the T9 to B1 comparison pair was progranulin. Except for proteasomal ubiquitin-independent gene (GO:0010499), all the GO terms within the B1 condition contained at least 45% progranulin, and 69% of the GO terms had the sole function of progranulin (GO:0002265, GO:0002282, GO:0060266, GO:0106016, GO:1900426, GO:1902564, GO:1903334,

GO:1903979, GO:1905673, GO:0007042, GO:0048680). Progranulin is recently known to suppress cellular apoptosis and inflammation (Jian et al., 2013; Zhou et al., 2015) but has not been reported in thermal stress studies. Respiratory burst (GO:0045730) also contained (apart from progranulin) mitochondrial cytochrome and neutrophil cytosol, which participate in cell death. The cytosolic cytochromes initiate apoptosis and can be found in mammals' neutrophil cytosol (a gene also upregulated within this GO term) (Maianski et al., 2004; Newmeyer & Ferguson-Miller, 2003). The GO term chaperone binding (GO:0051087) also contained DnaJ, endoplasmic reticulum resident gene, and Parkin coregulated gene gene homolog. The latter of which can prevent cell death in an array of stress mechanisms, initiates the removal of depolarized mitochondria in a pathway dependent on the mitochondrial serine-threonine kinase, and promotes the degradation of substrates to prevent unwanted effects in humans (McWilliams & Muqit, 2017; Meschede et al., 2020; Nguyen et al., 2016; Pickrell & Youle, 2015; Whitworth & Pallanck, 2017). However, this gene (parkin coregulated gene gene homolog) has not been reported in corals. Late endosome (GO:0005770) also contained primary facilitator, prosaposin, Notch genes, ADP-ribosylation, and syntaxin-7. Primary facilitators are a superfamily comprising secondary active transporters that use electrochemical gradients to function in plants (Hwang et al., 2016; Saier Jr et al., 2009). Prosaposin has been observed to be upregulated along with Notch genes in *Acropora* symbionts (Shinzato et al., 2020; Zhou et al., 2020). Notch genes regulate cell identity, apoptosis, and wound regeneration, are involved in developmental pathways between coral tips and their base (Kaniewska et al., 2015; Shumaker et al., 2019), get activated during heat stress in *A. hyanthus* (Hemond et al., 2014; Louis et al., 2017), and downregulated in heat-stressed *S. pistillata* (Maor-Landaw et al., 2014) and *A. millepora* (Kaniewska et al., 2015). The gene ADP-ribosylation has been observed in the *Symbiodiniaceae* of *S. pistillata* during bleaching (Weston et al., 2012). Syntaxin-7 is known to transport genes from the plasma membrane to the early vacuolar endosome (Prekeris et al., 1999). Gene stabilization (GO:0050821) also contained T-complex and calreticulin along with two other genes which are only found in wheat (peptidyl-prolyl cis-trans isomerase) or human saliva (large proline-rich gene). T-complex belongs to the HSP60 family and is mainly found in eukaryotes, bacteria, and humans (Lewis et al., 1992; Yu et al., 2018). The gene calreticulin initiates oxidative stress and cell death when downregulated in bovine (Liu et al., 1997) and in heat-stressed embryos of the coral *M. faveolata* (Voolstra et al., 2009).

3.4.4.5. Activity between day 1 bleached (B1) and 3 days bleached (B4).

More activity was observed in the B4 condition than in the B1 condition. The genes in every GO term enriched in the B1 condition were at least 50% 40S or 60S ribosomal gene. In the B1 condition, two of the GO terms did not constitute 100% 40S or 60S ribosomal gene: rough endoplasmic reticulum membrane (GO:0030867) contained 50% 40S or 60S ribosomal gene and the other 50% involved N-acetylaspartate synthetase, translocon associated gene and SUN domain-containing ossification factor. The latter is required for bone modelling during late embryogenesis and regulates collagen synthesis

in rodents, humans, and reef fish (Ryu et al., 2020). The second GO term was a translation (GO:0006412), whose genes were 63% 40S or 60S ribosomal gene, and the other 37% contained E3 ubiquitin-gene ligase, RING finger binding and RNA binding genes. RING finger binding is one of the most prominent E3 ubiquitin ligase families with 340 validated human members and has a role in DNA binding and recognition (Cai et al., 2022). Eukaryotic ribosomes constitute small (40S) or large (60S) subunits. The 40S ribosomal subunit is required to decode genetic messages, and the 60S ribosomal subunit catalyses peptide bond formation (Fox et al., 2019; Gregory et al., 2019). The 40S and 60S ribosomal genes are downregulated in corals, such as *A. aspera* (Deisenroth & Zhang, 2011; Rosic et al., 2014; Xirodimas et al., 2008). Some studies have found ribosomal gene expression to decrease in short-term heat stress but increase in longer-term heat stress (Bellantuono et al., 2012; Desalvo et al., 2008; Vidal-Dupiol et al., 2009).

The B4 condition expressed more functions than expected. Only 20% of the GO terms had the function complement C3 (GO:0006957, GO:0006958, and GO:0045745), which has a vital role in innate immunity in heat-stressed corals, such as *Porites* (Louis et al., 2017) and has been known to be upregulated in response to heat stress in corals, such as *A. aspera* (van De Water et al., 2015). Another 20% of the GO terms only had the function of a heme-binding gene (GO:0010917, G:0010940, and GO:0035794). This gene can stimulate mitochondrial permeability and accelerate necrotic cell death under stress in hard corals, such as *A. millepora* (Petrou et al., 2021). The GO term, cellular response to an organic substance, was too generalised (GO:0071310), and the last 53% of GO terms contained a minimum of three functions. The complement activation classical pathway (GO:0042026) GO term comprised three genes, heat shock gene, endoplasmic reticulum chaperone, and DnaJ. These played roles in stress responses across the animal kingdom, especially under heat stress in cnidarians and were also upregulated in two other GO terms (GO:0005783 and GO:0034663) in the B4 condition. Progranulin (GO:0009617 and GO:0005783) and E3 ubiquitin-gene ligase (GO:0009617 and GO:0005604) were also significantly upregulated under the B4 condition, both of which maintain internal stability while adjusting external conditions (Phillip A. Cleves et al., 2020; Phillip A Cleves et al., 2020; Hu et al., 2020; Mayfield et al., 2018; Townley et al., 2018). E3 ubiquitin-gene ligase is a family of over 700 genes that conjugate ubiquitin to target genes resulting in a range of cellular responses, including DNA repair. This family participates in homeostasis, inhibiting apoptosis, and regulation of cell death (Humphreys et al., 2021). A third gene that was significantly upregulated in the B4 condition was hypoxia (GO:0001666 and GO:0034663), showing that the coral was not receiving enough oxygen at the tissue level to maintain adequate homeostasis (Altieri et al., 2017; Deleja et al., 2022; Hughes et al., 2020; Nelson & Altieri, 2019). Other significantly upregulated genes constituted notch genes and homeobox genes (GO:0048859), which play crucial roles in cell identification and cell-fate decisions during tissue homeostasis (Phillip A. Cleves et al., 2020; Phillip A Cleves et al., 2020; Hu et al., 2020; Mayfield et al., 2018; Townley et

al., 2018); TNF receptors, toll-like receptors (GO:0009617), neuroglobin, and endoplasmin (GO:0001666) which are either crucial in immunity, activate cell death pathways and induce genes involved in survival or protect from hypoxia by binding and increasing oxygen availability (Deisenroth & Zhang, 2011; Rosic et al., 2014; Xirodimas et al., 2008); and heme-binding genes and cytochrome, which play vital roles in homeostasis, cellular metabolism and various oxygen related functions in corals, such as *A. aspera* (GO:0020037) (van De Water et al., 2015). The increase in these genes' functions indicates the corals' ability to survive in the absence of symbionts.

3.4.5. Patterns throughout the conditions in genes of interest during bleaching

Rigorous analysis of the functions within the enriched terms disclosed patterns within some of the genes of interest; therefore, based on previous work that implicated these groups of genes in heat stress and or bleaching, further insight into these patterns was conducted.

3.4.5.1. Patterns found in the heat stress genes of *H. actiniformis*.

The results from the first timepoints support the hypothesis of the "core cnidarian heat stress response" system. In 2018 (and further supported in 2019), (Cziesielski et al., 2018; Cziesielski, Schmidt-Roach, & Aranda, 2019) were Cziesielski stated that the first biomarkers of heat stress constitute HSPs and ROS, both of which were found within the experiment's initial timepoints (T0-T3). The increase in B-crystallin, lipid peroxide (LPO), and total glutathione (GSH) was also found within the first two timepoints, which, according to Cziesielski, are important antioxidants produced in corals during heat and light stress as they can trigger nitric oxide production. Also, following Cziesielski, some genes with essential roles in heat shock stress response were upregulated during the heat-increasing timepoints (Table 3.3). Some other genes associated with heat shock stress were upregulated at timepoints with subsequent increased heat (Table 3.3). The vital genes in cnidarian heat stress, such as Peroxidasin, C/EBP, and EF-hand (Cziesielski et al., 2018; Cziesielski, Schmidt-Roach, & Aranda, 2019) were all upregulated during the first two timepoints (T0 & T3)—other biomarkers of heat stress involved caspase-3, TRAF3, and apoptotic responses. The apoptotic response was upregulated during the first and last timepoints before bleaching.

Table 3.4. Upregulated genes of interest in heat-stress response of *H. actiniformis*. Genes that were upregulated during different heat-stress timepoints with their individual roles. Providing support to the core cnidarian heat stress response theory suggested by Cziesielski in 2018.

Gene	Role	Upregulated Timepoint
Ribosomal RNA	Gene biosynthesis	T3, B1
Ferritin	Oxidative stress	T3
Thioredoxin	Oxidative stress	T0, T9, B1
Actin	Cytoskeleton structure	T0, T3
Rab7	Membrane trafficking	T0
Carbonic anHydrase	Skeletal growth	T0, T3

3.4.5.2. Patterns found in L-serine metabolic process vs glycine binding genes.

Coral hosts provide algae with shelter and inorganic nutrients in turn for a certain amount of help gene creation during times of stress, such as heat and bleaching stress (Phillip A. Cleves et al., 2020; Phillip A Cleves et al., 2020). For example, in *Aiptasia*, a symbiotic anemone, *Symbiodiniaceae* has been found to catalyse glycine/serine biosynthesis from food-derived choline allowing the host cnidarian to have a decreased demand for dietary choline. Serine is known to be a critical component in amino acid interconversions as it can use phosphoserine aminotransferase (PSAT, AIPGENE17104) to catalyse and convert glutamate to 2-oxoglutarate. This conversion may serve as the main consequence to provide amino acid groups for the biosynthesis of amino acids (Cui et al., 2019). Within these results, patterns of expression for genes under the L-serine metabolic process GO term (GO:0006563) are consistent with the theory that symbiont hosts might use symbiont-derived glucose to assimilate waste ammonium into amino acids (Cui et al., 2019). The genes involved in serine metabolic processes from 3-phosphoglycerate (one of the intermediates of glycolysis) were upregulated through to timepoint T6 (Figure 3.4). However, these genes were downregulated from timepoint T6 to T9 (start of bleaching), consistent with findings of Guoxin Cui. Another theory of Cui shows that serine may serve as a metabolic intermediate to produce other amino acids. Our research showed that five of the six intermediates in the alternative glycine/serine biosynthesis pathway were significantly enriched during heating and bleaching of the corals, which suggest that Cui's theory remains consistent even through stressors. The abundance of serine metabolic process genes decreased from T0 (last 24 hrs at 26°C) to T9 (8 days at 34°C, the last timepoint before bleaching) and then plateaus. In contrast, glycine genes significantly increased from T0-T9 and plateaued at the same level as the serine genes. Their abundance did not change from timepoint T9 till bleaching timepoints as both serine and glycine remained steady (Figure 3.5).

Serine and glycine switch from being upregulated to being downregulated at the same timepoint. Serine is upregulated during the heating condition, from the timepoints T0-T6 and then

downregulated during the bleaching phase of the experiment, from the T9-B4 timepoints, while in contrast, the glycine genes are all downregulated in the heated timepoints T0-T6 and upregulated when the bleaching process begins (T9) to B4, the last bleaching timepoint (Figure 3.4). This is also consistent with one of the findings by Ivanio Amelio that serine activity leads to glycine activity (Figure 3.6) as serine is upregulated at the first timepoints and glycine is upregulated at the final timepoints (Amelio et al., 2014). They were making it a clear switch from serine to glycine. All the metabolic intermediates in the de novo serine biosynthesis pathway were highly enriched in the symbiotic coral, *Heliofungia* (Figure 3.6).

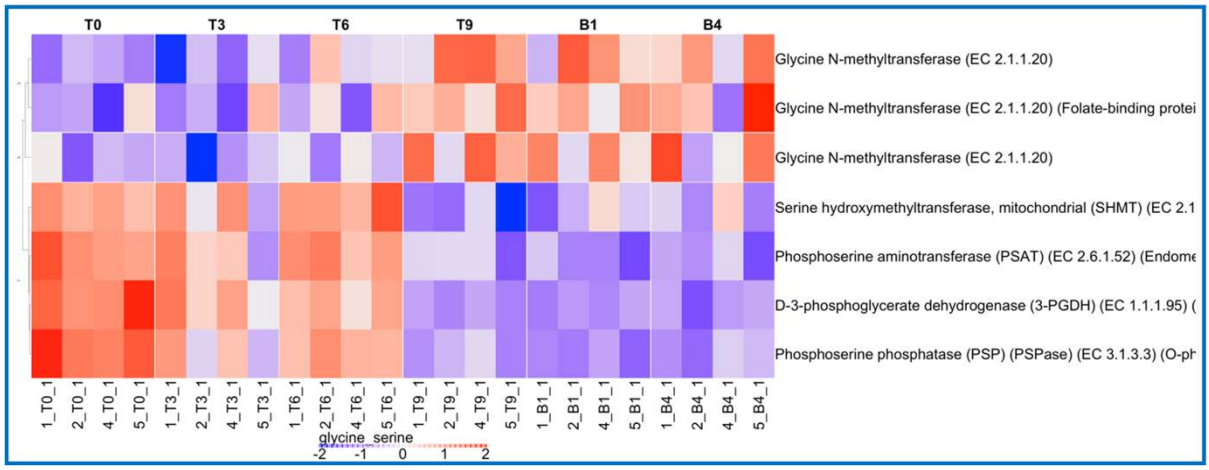

Figure 3.4. Heatmap of genes associated with L-serine metabolic process (GO:0006563) and glycine binding (GO:0016594). Heatmap showing the correlation between glycine binding and L-serine metabolic processes. The abbreviations of the conditions are divided into three sections: first section is the individual number, second section is the condition, and third section is the sample number. For example, 1_T0_1 means individual coral number 1, condition is T0 (last day at 26°C) and the sample number is number 1. Other condition abbreviations are: T3 = 72 hours (3 days) at 34°C; T6 = 144 hours (6 days) at 34°C; T9 = 216 hours (9 days) at 34°C; B1 = First time bleached; B4 = 72 hours (3 days) bleached.

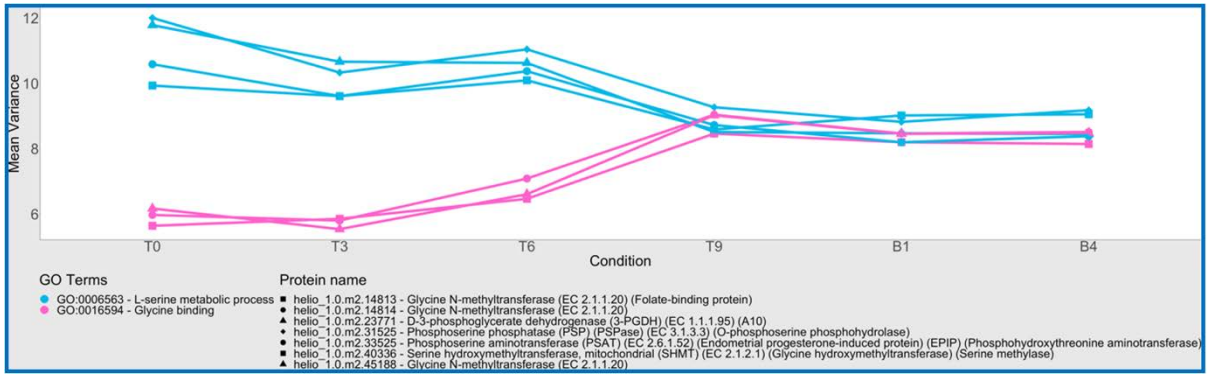

Figure 3.5. A comparison of gene functions associated with L-serine metabolic process (GO:0006563) and glycine transport (GO:0015816). The abbreviations of the conditions are T0 = last day at 26°C; T3 = 72 hours (3 days) at 34°C; T6 = 144 hours (6 days) at 34°C; T9 = 216 hours (9 days) at 34°C; B1 = First time bleached; B4 = 72 hours (3 days) bleached.

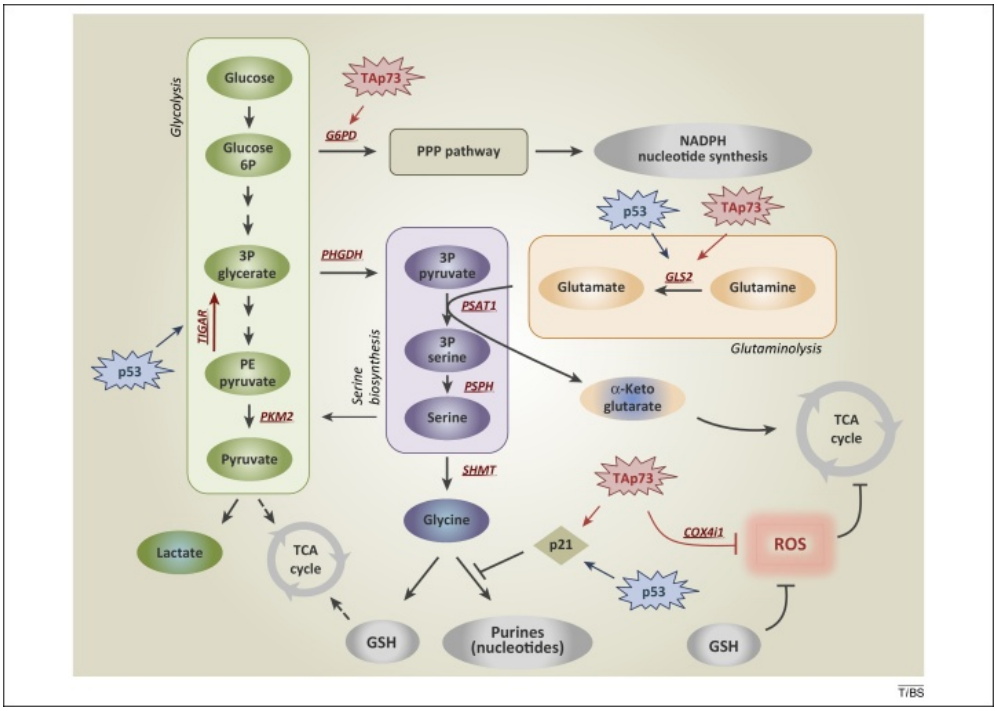

Figure 3.6. ***De novo*** **serine biosynthesis pathway (Amelio et al., 2014).** Visual figure explaining the working of serine biosynthesis pathway, created by Ivanio Amelio. It explains conversion of glucose into NADPH, serine, and pyruvate through respective pathways. Abbreviations: glycerate-3-phosphate (3P glycerate), phosphoglycerate dehydrogenase (PHGDH), pyruvate kinase M2 (PKM2), pentose phosphate pathway (PPP), reactive oxygen species (ROS), cytochrome C oxidase subunit 4 isoform 1 (COX4i1), glucose-6-phosphate dehydrogenase (G6PD), glutaminase-2 (GLS-2), glutathione (GSH), phosphoserine aminotransferase 1 (PSAT-1), phosphoserine phosphatase (PSPH), TP53-inducible glycolysis and apoptosis regulator (TIGAR).

3.4.5.3. Patterns found in endoplasmic reticulum chaperone complex genes.

The endoplasmic reticulum chaperone complex has a clear pattern. All eight genes associated with the GO term GO:0034663 follow the same path throughout the experiment, i.e., all of them increased for the first 48 hours at 34ºC (T0 to T3) then decreased over the next three days (total of five days) at 34ºC (T6) (Figure 3.7). For the following three days (totalling eight days at 34ºC) the genes either slightly decreased or stabilised, followed by an apparent increase to the first bleaching point and a significant decrease by the end of the bleaching period (Figure 3.7). Despite minimal changes for most of the genes (except for BiP), the pattern is clear and consistent throughout all the genes expressed within the endoplasmic reticulum chaperone complex. BiP is an ER-located member of the HSP70 molecular chaperones family, and it has two significant domains that interconnect to control the affinity and duration of polypeptide binding (Gething, 1999). It interacts with DnaJ to facilitate gene folding and assists other genes in membrane fusion during karyogamy (Gething, 1999). BiP is a vital regulator of unfolded gene response (UPR) and its target. Its expression is upregulated when UPR transcription factors are associated with the UPR element in its DNA promoter region (Wang et al., 2017). BiP binds to and blocks the activation of caspase-7, an apoptotic gene, and etoposide-induced apoptosis (Wang et al., 2017).

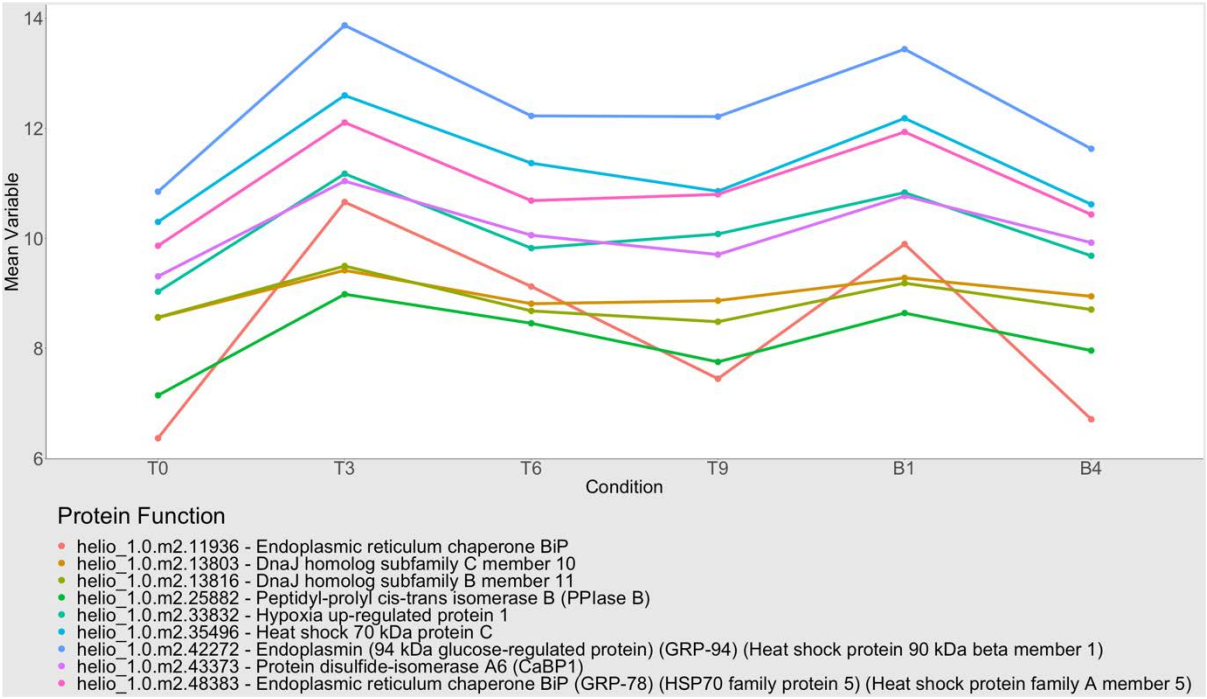

Figure 3.7. Gene functions associated with endoplasmic reticulum chaperone complex (GO:0034663) throughout the heating conditions. The abbreviations of the conditions: T0 = last day at 26°C; T3 = 72 hours (3 days) at 34°C; T6 = 144 hours (6 days) at 34°C; T9 = 216 hours (9 days) at 34°C; B1 = First time bleached; B4 = 72 hours (3 days) bleached. Abbreviations of the gene functions: BiP = Binding-immunoglobulin gene, GRP = glucose-regulated gene, HSP70 = Heat shock 70 family gene 5 and the gene functions are stated as *Heliofungia* gene id followed by gene name.

3.5. Discussion

This study employed RNAseq analysis to explore gene expression in the cnidarian coral *Heliofungia actiniformis* across a time course from acclimation temperature through the climb of temperature to a level that induced heat stress and continued until the corals exhibited complete bleaching.

The selected samples from sump one provides an invaluable snapshot of coral responses throughout the heating timeframe, permitting a degree of control over environmental variables. Future research would benefit from improved systems stability, such as sump two, achieved through more rigorous monitoring and timely responses to changing conditions. Overall, our study underscores the significant impact of environmental changes on coral health and bleaching patterns, highlighting the need for a multifaceted approach to understand and mitigate coral bleaching in continuous environmental change. The findings underline the influence of temperature and other environmental stressors, such as ammonia levels, thus serving as a steppingstone for future studies.

3.5.1. Variation between coral genotypes dominates variation in gene expression.

This study aimed to delve into the intricacies of gene expression variations and thermal stress reactions in corals experiencing bleaching. Our work resonates with past studies as it reiterated that transcriptional variability in corals is a multifaceted process significantly affected by the individual source colony (Luz, 2020; Rodriguez et al., 2008; Xu, 2022). The study utilised Principal Component Analysis (PCA) on transcriptomic data, a statistical procedure identifying multivariate data's most significant variation sources to reveal that the primary source of variation was attributable to the coral's genotype. This genetic dominance was notably pronounced in the first two principal components, accounting for 61% of the variance combined. However, as the experiment progressed, a clear separation based on the condition was observed by the fourth principal component, implying that environmental factors started to overshadow genotypic differences in driving gene expression responses. This observation supports the understanding that the influence of the environment induces gene expression alterations that can supersede innate genotypic variability.

In pursuing a more profound understanding of gene expression variations in response to thermal stress, we focused on analysing differentially expressed genes (DEGs) throughout the bleaching process. The stark individual variation observed in the PCA analysis was again apparent in our DEG analysis, underlining the complex relationship between genotype and environmental conditions. Initially a significant slowing of the rate of change during the three days at high temperatures was noted, which suggested a possible shock response to sudden thermal stress, with the coral's cellular machinery undergoing drastic adjustments reflected in wide-scale changes in gene expression. This period of decline was followed by a dramatic shift in gene expression between conditions T0 and T3 (2,504 upregulated and 2,314 downregulated), a crucial phase marking the temperature increase from 26ºC to 34ºC and its maintenance for three days.

Interestingly, another surge in DEGs occurred during the total expulsion of symbionts and the ensuing complete bleaching of the coral host. During this period, the upregulation of 1,023 genes and downregulation of 805 genes could be interpreted as an attempt by the coral host to survive without its symbiotic partners, possibly through the activation of alternative metabolic pathways and stress survival mechanisms. To complement our DEG analysis and provide a detailed look into the functional implications of the gene expression changes, we performed Gene Ontology (GO) enrichment analysis. This analysis allowed us to categorise differentially expressed genes according to biological process (BP), molecular function (MF), and cellular component (CC). An initial increase in GO terms (indicative of a broad functional response) with the first temperature rise followed by a dip in GO term numbers under sustained thermal stress and post-bleaching conditions was observed. This dip might indicate a survival strategy employed by the coral, potentially involving the reduction

of metabolic activities and a shutdown of non-essential biological processes to conserve energy. During the final bleaching stage, another significant decrease in GO terms was recorded, which might reflect a severe survival response after its symbionts entirely abandon the coral.

Overall, our study offers a meticulous and comprehensive exploration of the profound effect of environmental stressors on coral genomic activity. We have elucidated the complex interplay of genotype and environmental condition in driving gene expression changes in corals through PCA, DEG analysis, and GO enrichment analysis.

3.5.2. Genomic coping mechanisms in corals exposed to sustained thermal stress.

Under the influence of sustained thermal conditions, corals undergo significant shifts in gene activity, highlighting adaptive survival strategies. During the initial acclimation phase at 26°C, our study, drawing from the work of Mayfield et al. (2018) and Darling & Cook (2014), observed that the primary focus of gene expression was on gene turnover and folding, with genes such as E3 ubiquitin-gene ligase and ER being prominently expressed. Similarly, genes associated with chromatin stabilization and symbiont photosynthesis, such as eukaryotic initiation factor and ATPase (Barott et al., 2015; DeSalvo, 2010; Michael K DeSalvo et al., 2010; M. K. DeSalvo et al., 2010), were also noted for their increased activity, indicating an effort to maintain coral health under emerging stress.

As the corals were exposed to the heat stress temperature of 34°C for three days, there was a notable change in gene activation from gene-related functions to survival-related genes. The work of Hu et al. (2019, 2020) illuminates Progranulin's role in this phase, which was observed to be the critical gene expressed. Progranulin, known for its role in regulating cell growth, survival, repair, and inflammation, is suggested to be the coral's primary line of defence against heat stress. Continued exposure to heat stress for six days prompted the expression of additional genes, mainly those associated with regulating the mitochondrial membrane, which prevents apoptosis, as Blackstone (2009) and Weis et al. (2008) suggested. Concurrently, genes related to increasing calcium and calcification levels were upregulated, which was achieved by increasing fatty acids and methyl ester reduction activity (von Xylander et al., 2023).

Interestingly, nine days of thermal stress resulted in the upregulation of Progranulin and transport genes, such as the glycine transporter. The work of Ganser & Dallman (2009) and Mongeon et al. (2008) highlights the role of these transporters in maintaining glycine levels. Additionally, there was a significant upregulation of the cytochrome gene (Rosic et al., 2010) and the endoplasmic reticulum chaperone BiP (Petrou et al., 2021), providing further insight into the coral's defence mechanisms against prolonged heat stress.

3.5.3. Coral bleaching: Insights into genetic activation and survival strategy

During the initial 24 hours of bleaching, a strong shift in transcriptional activity ensued. The upregulation of 427 genes associated with 25 Gene Ontology (GO) terms revealed that the coral, bereft of symbiont assistance, launched into a systematic clean-up. The three most crucial gene classifications involved in this process were the 40S or 60S ribosomal gene, progranulin, and proteasome. Various genes also played supporting roles, including cytochrome, neutrophil cytosol, and DnaJ. In the heat of this genetic chaos, the 40S or 60S ribosomal genes held sway, being the most abundantly expressed genes. Critical to decoding genetic messages and catalysing peptide-bond formations during stress and recovery periods, these genes played a pivotal role in resuming translation after stress events (Bellantuono et al., 2012; Desalvo et al., 2008; Vidal-Dupiol et al., 2009). Our study corroborated previous research by Darriere et al., 2022 and revealed the novel finding that during bleaching, the expression of ribosomal genes increased as it has not been documented before in cnidarian heat stress. However, the release of ribosomal genes has been associated with recovery after heat shock in plants (Merret et al., 2017), therefore a similar function could be associated within this cnidarian coral.

At the same time, progranulin and proteasome, recognised suppressors of cellular apoptosis and inflammation, were activated to function at an elevated level. Progranulin, integral to rapidly dividing cells' growth, division, and survival, has connections to heat stress, making it a co-chaperone of heat shock genes 70 (HSP70) (Wang et al., 2021). Conversely, proteasome breaks down HSP70-bound genes and is a critical part of tissue-specific gene degradation during heat stress (McLoughlin et al., 2019; Pispa et al., 2020). As the bleaching advanced to its final stages, genetic activation was observed. The resultant functions could be primarily categorised into two mechanisms: survival and death. For instance, the activation of hypoxia and heme-binding genes highlighted the onset of apoptosis (Altieri et al., 2017; Deleja et al., 2022; Hughes et al., 2020; Nelson & Altieri, 2019; Petrou et al., 2021), while a range of other genes such as complement C3, heat shock gene, and endoplasmic reticulum chaperone came into play to aid in survival (Phillip A. Cleves et al., 2020; Phillip A Cleves et al., 2020; Deisenroth & Zhang, 2011; Hu et al., 2020; Humphreys et al., 2021; Louis et al., 2017; Mayfield et al., 2018; Rosic et al., 2014; Townley et al., 2018; van De Water et al., 2015; Xirodimas et al., 2008).

Corals exhibit dynamic genetic responses as thermal stress intensifies, leading to bleaching. Efforts to maintain cellular homeostasis, promote cellular repair, and mitigate thermal stress effects are evident with the upregulation of genes associated with glycine, progranulin, and ATPase. Furthermore, the endoplasmic reticulum chaperone BiP activation indicates its potential role in gene regulation and

stress response. Consequently, these genes could be significant targets for conservation strategies supporting coral survival under ongoing thermal stress. In the last 24 hours of bleaching, when the coral turns completely white, there is an upsurge in function activation associated with death or survival. Here, mechanisms related to repairing or stabilising the organism or to apoptosis and necrosis are observed. For example, hypoxia and heme-binding genes, involved in apoptosis, are activated as the corals undergo cell death. The genes complement C3, heat shock gene, endoplasmic reticulum chaperone, DnaJ, progranulin, E3 ubiquitin-gene ligase, notch genes, homeobox genes, and cytochrome, work in concert to aid survival, attempting to re-stabilise the corals and inhibit apoptosis and necrosis. Compared to the first, the increase in function numbers in the final bleached condition could suggest that the coral relies on its symbionts for survival during thermal stressors, possibly decreasing its functions to conserve energy. However, once bleached, the coral must fend for itself, activating functions to increase its immunity that possibly leads to a significant depletion of energy, and other functions activating begin initiating necrosis in areas deemed unnecessary for survival.

This study highlights corals' remarkable adaptability and capacity to deploy various survival strategies amidst severe thermal stress and bleaching impacts. However, the urgent need to mitigate escalating temperatures threatening coral reefs worldwide cannot be ignored, and effective conservation strategies should focus on understanding and targeting these essential genes.

3.5.4. Unravelling the interplay between amino acid metabolism and heat stress response in corals

The intricate interplay of various genes during heat stress conditions in corals is critical for their survival, adaptation, and resilience. Two key areas of research are examining the patterns across the stages of heat stress, including the onset, progression, and bleaching, and a comparative analysis of specific genes implicated in heat stress response with findings from other studies.

Under the heat stress condition, an early upregulation of heat stress response genes, such as heat shock genes (HSPs) and reactive oxygen species (ROS), have been noted (Cziesielski et al., 2018; Cziesielski et al., 2019) which supports the proposed “core cnidarian heat stress response” system, with additional markers such as B-crystallin, lipid peroxide (LPO), and total glutathione (GSH) playing integral roles in modulating oxidative stress and damage induced by heat stress. Further findings during the early heat stress phase included upregulation of Peroxidasin, C/EBP, EF-hand, biomarkers of heat stress like caspase-3 and TRAF3, and apoptotic responses, hinting towards programmed cell death in the coral’s response to thermal stress. Additionally, a significant metabolic shift was noted from the upregulation of serine metabolic processes to their downregulation and the subsequent increase in glycine gene activity, in sync with the theories presented by Cui et al., 2019

and Amelio and others regarding metabolic conversions between these two amino acids in response to heat stress.

Meanwhile, endoplasmic reticulum (ER) chaperone complex genes exhibited an initial increase in expression under elevated temperature, followed by a decrease and eventual stabilization, with BiP, a part of the HSP70 family, demonstrating significant changes. Therefore, BiP has a crucial role in managing unfolded genes and regulating the unfolded gene response (UPR) during heat stress, including potential involvement in apoptosis regulation through its interaction with caspase-7. Compared to other heat stress studies, we supported Czielsielskis' hypothesis of the "core cnidarian heat stress response" system (Cziesielski et al., 2018; Cziesielski et al., 2019). Additionally, patterns of expression for genes under the L-serine metabolic process GO term was consistent with the theory that symbiont hosts might use symbiont-derived glucose to assimilate waste ammonium into amino acids (Cui et al., 2019). The results also endorsed the hypothesis that serine may serve as a metabolic intermediate to produce other amino acids and supported Ivanio Amelio's theory that serine activity leads to glycine activity during heat stress conditions. A clear pattern was observed in the endoplasmic reticulum chaperone complex, as all its genes followed the same path throughout the experiment, suggesting that it could be involved throughout the heat stress period as a maintenance tool. It exhibited interactions with DnaJ, UPR, and BiP, and by default HSP70, and was found to bind and block activation apoptosis.

In summary, the findings provide a comprehensive perspective on the dynamic changes in gene expression and metabolic adaptations in corals as they experience and respond to heat stress. These insights contribute to understanding the fundamental shifts in the coral's survival strategy under thermal stress. They can serve as a foundation for future research to develop interventions to protect corals against the ongoing threat of climate change.

3.5.5. Bridging the Gap: Translating coral heat stress response into conservation strategies

As highlighted in the preceding sections, the significant alterations in corals' genetic and metabolic responses under thermal stress offer critical insights into the mechanisms underlying coral heat stress responses and bleaching. These findings hold profound significance for understanding coral biology and ecology and potentially offer applications for future conservation efforts.

Firstly, by mapping changes in gene expression in response to heat stress, we gain a clearer understanding of how corals perceive and respond to increased temperatures at the cellular level. The observed patterns, particularly in genes of interest such as heat shock genes (HSPs), reactive oxygen

species (ROS), and those associated with the endoplasmic reticulum chaperone complex, reinforce the existence of a "core cnidarian heat stress response" system. These complex networks of stress response genes act as the corals' frontline defence against thermal stress, suggesting potential targets for interventions aimed at enhancing coral resilience to heat stress. The upregulation of antioxidant and apoptosis-related genes further expands our knowledge of the defensive strategies employed by corals under stress. The antioxidant defence system's role is particularly noteworthy, as it counters the damaging effects of ROS generated under stress conditions. In contrast, the upregulation of apoptosis, a form of programmed cell death, may represent a strategy to remove cells with irreparable damage. The interconnectedness of these stress response pathways illustrates the complexity of coral biology and the intricate balancing act these organisms perform in response to environmental stressors.

The metabolic adaptations, specifically the switch in serine and glycine metabolic processes, offer another layer of insight. This metabolic switch, which appears to coincide with the onset of bleaching, suggests a strategy by which corals may regulate their metabolic resources under stress. A better understanding of these metabolic changes could reveal opportunities to support corals during periods of high thermal stress. Moreover, the utility of tools such as Principal Coordinate Analysis (PCoA), Gene Ontology (GO), and Differential Expression Gene (DEG) analysis, demonstrated in this study, underscores the power of 'omics' approaches in ecological research. These methods provide a multidimensional view of coral responses, giving us a far richer and more nuanced picture of coral biology than what is achievable through traditional methods. Furthermore, the advent of these techniques offers an unprecedented opportunity to explore other stress response mechanisms in corals and other marine organisms, which could pave the way for novel conservation strategies.

As climate change continues to intensify, the insights gleaned from this research have the potential to be directly applied to coral reef conservation. Strategies could be developed to identify corals with more robust heat stress response systems and promote their growth, leading to reefs that are more resilient in the face of rising ocean temperatures. Additionally, understanding the metabolic adaptations in response to heat stress could inform efforts to provide targeted nutritional support to corals during periods of elevated thermal stress. Overall, this comprehensive investigation into coral gene expression and metabolic adaptations under heat stress deepens our understanding of coral responses to environmental stressors, thus presenting a crucial step forward in our quest to safeguard these valuable marine ecosystems. As the findings of this research are further validated and applied, we may yet turn the tide on coral bleaching and ensure the continued survival of these remarkable organisms in our warming oceans.

3.6. Conclusion

In conclusion, this comprehensive study on coral response to thermal stress and bleaching has provided significant insights into corals' intricate and dynamic interplay of metabolic and gene expression adaptations. Our research substantiates not only existing theories, such as Cziesielski's proposed "core cnidarian heat stress response system" and Amelio's postulation of serine leading to glycine activity but also reveals several novel findings that will guide future studies in this field.

A striking revelation from our study is the apparent hibernation-like state of the corals under sustained heat stress. As the temperature gradually increases to reach heat stress levels, we observe a noticeable decrease in the activation of biological functions, potentially as an energy conservation strategy. This hypothesized 'hibernation state' persists until around the seventh day of heat stress, providing the coral with a window of endurance through short-term thermal stress. Simultaneously, we noted an unusual surge in the number of Gene Ontology (GO) terms, though not functions, commencing from day six at heat stress and lasting until the onset of bleaching, which could indicate a shift in the coral's metabolic or stress response mechanisms, gearing up for the upcoming bleaching event.

Interestingly, following the onset of complete bleaching, we observed a pronounced reduction in the activation of GO terms and functions, potentially signifying an energy conservation mode during this critical phase. Our study also unveiled the activation of several functions previously undocumented in coral research but noted in mammalian studies, mostly in disease contexts. These unprecedented findings hint at unknown, complex physiological responses in corals during heat stress and bleaching, necessitating further investigation.

Our findings underscore the need for continued, intensive research into coral responses to heat stress. By understanding the coral's physiological and genetic adaptability to such stressors, we can strive towards more effective conservation strategies. Given the current pace of global climate change, efforts to understand and protect these vital marine organisms are more urgent than ever. The knowledge derived from our study adds to the pool of valuable information that researchers and conservationists can utilize in their quest to mitigate the effects of climate change on these invaluable marine ecosystems.

Chapter 4: Heat stress and bleaching: a symbiont perspective?

4.1. Abstract

The survival and functioning of coral reef systems are based on the symbiotic association between dinoflagellate symbionts (*Symbiodiniaceae* spp.) and cnidarian coral hosts. Coral bleaching involves the breakdown of such associations due to stress and increasingly frequent mass bleaching events are associated with global warming. However, despite two decades of research into coral bleaching, it still needs to be determined precisely how temperature affects this symbiotic association at the cellular level. Therefore, this study reports essential findings on gene expression changes in the *Symbiodiniaceae Cladocopium* during heat-stress bleaching of the coral host *H. actiniformis*. In this regard, the experiment was conducted on the coral *Heliofungia actiniformis* increased tank temperature by one-degree Celsius every 24 hours from acclimatisation temperature (26ºC) until the heat-stress temperature (34ºC) was reached. Transcriptomic analysis showed a robust genotypic connection followed by a strong connection by condition, which supported the results from the other two studies in this project. GO term analysis only showed activity in the first two timepoints, the last 24-hours at acclimation temperature and the first 24-hours at the heat-stress temperature, and the last two timepoints, the bleaching timepoints. The genes activated during those timepoints are associated with survival and host-symbiont communication. Most of the activated genes were also activated at similar timepoints in the host study, and some of them were also activated during different regeneration stages, such as hsp70 and 60S ribosome. It is seen that *H. actiniformis* activates similar genes when regenerating and attempting to survive heat-stress.

4.2. Introduction

The leading cause of global degradation of coral reefs is due to bleaching via the breakdown of the symbiosis between corals and their *Symbiodiniaceae* endosymbionts (Blackstone & Golladay, 2018; Hughes et al., 2017; M. J. van Oppen & L. L. Blackall, 2019; M. J. H. van Oppen & L. L. Blackall, 2019). It is hypothesised that changes in coral-associated bacterial communities may be associated with bleaching through heat stress (Bourne et al., 2008; Grottoli et al., 2018; Lee et al., 2016; Ziegler et al., 2017) or may be associated to other environmental characteristics, such as Reactive oxygen species (ROS) (Diaz et al., 2016; Hadaidi et al., 2017; Tracy et al., 2015).

The ecologically diverse coral reef ecosystems provide habitats for various marine organisms and are considered economically significant. These ecosystems rely on the stable endosymbiosis (intracellular symbiosis) between dinoflagellate algae of the family *Symbiodiniaceae* and their cnidarian host animals (Phillip A. Cleves et al., 2020; Cui et al., 2019; Ishii et al., 2019; Weis, 2008). Algal endosymbionts enable corals to thrive in nutrient-poor waters by providing photosynthetically derived energy and metabolic building blocks. Metabolic exchange is central to the ecological success of the symbiotic association between coral and dinoflagellate, which also plays a role in host-symbiont recognition and specificity (Davy et al., 2012).

Most symbiotic coral hosts acquire symbionts from the environment in a process that involves the initial phases of phagocytosis, followed by formation of a stable intracellular structure called symbiosome (Allemand & Furla, 2018; Miller et al., 2007; Mydlarz et al., 2016). This system is believed to have a vital role in the symbiotic partnerships of many animals and plants, such as marine invertebrates (Nyholm & Graf, 2012) and cnidarian-*Symbiodiniaceae* (Davy et al., 2012). The innate immune system of cnidarians, like other organisms, differentiates between mutualistic and parasitic microbes to establish a beneficial symbiotic association (Mansfield & Gilmore, 2019; McFall-Ngai et al., 2013; Merselis et al., 2018). It is reported that complement pathways of the innate immune system play a role in identifying symbionts and regulating cnidarian-flagellate symbiosis (Davies et al., 2023; Poole et al., 2016). The system also maintains a healthy holobiont by balancing the relationship between the host and symbionts; however, environmental changes can add stress and dysbiosis to such relationships (Davies et al., 2023; Nyholm & Graf, 2012; Poole et al., 2016; Rosset et al., 2021).

The detection of beneficial or parasitic microorganisms occurs by recognising either microbe-associated molecular patterns (MAMPs) or pathogen-associated molecular patterns (PAMPs) by the host. In some corals and anemones, host-symbiont recognition involves lectin-glycan interactions (Davy et al., 2012; Hirsch, 1999; Mansfield & Gilmore, 2019; Meints & Pardy, 1980; Nyholm &

McFall-Ngai, 2004; Poole et al., 2016). In cnidarians, millectin, along with other lectins (such as PdC-lectin), may be involved in the recognition of symbionts or pathogens (Jimbo et al., 2000; Koike et al., 2004; Kvennefors et al., 2010; Vidal-Dupiol et al., 2009; Zhou et al., 2018) and also involves certain receptors (pattern recognition receptors (PRRs), complement C3 receptors, scavenger receptors (SRs)), TGFb pathways, and Rab5 genes (Allemand & Furla, 2018; Chen & Ten Dijke, 2016; Davy et al., 2012; Detournay et al., 2012; Lehnert et al., 2014; Mansfield & Gilmore, 2019; Neubauer et al., 2016; Rodriguez-Lanetty et al., 2006; Vidal-Dupiol et al., 2009; Wood-Charlson et al., 2006).

Nitric oxide (NO) and reactive oxygen species (ROS) levels have been found to increase due to heat stress events and symbiont photosynthesis suppression by photosystem II (Detournay et al., 2012; Weis, 2008). However, the source or target of NO and the cause of symbiont loss are unknown (Detournay et al., 2012; Hawkins et al., 2013). Bleached corals and anemones have shown an upregulation of genes involved in immunity and inflammation (e.g., Elk-1, Irf, Kruppel-like factors, MyD88, NF-κB, TRAF3) and cell stress and death (e.g., Rab, NOS, caspase, and catalase). However, the role of other biological pathways found through RNA-seq analysis in bleaching and loss of symbiotic association is unclear (Mansfield & Gilmore, 2019).

The genotypes of *Symbiodiniaceae* are considered critical for deciding the ability of a particular host to tolerate the range of environmental stress. Nine genetically distinct clades were found, named from A to I; all (except E, H, and I) were observed in corals. In 2018, the *Symbiodinium* clades were divided into (among others) seven main *Symbiodiniaceae* genera: *Symbiodinium*, *Breviolum*, *Cladocopium*, *Durusdinium*, *Effrenium*, *Fugacium*, and *Gerakladium* (LaJeunesse et al., 2018). The most-abundant genus observed in corals at the Great Barrier Reef is *Cladocopium* (Al-Hammady et al., 2022; Rosset et al., 2021). Anemones generally host *Effrenium* (Al-Hammady et al., 2022), and foraminifera is home to *Fugacium* and *Gerakladium* (Stuhr, Blank-Landeshammer, et al., 2018; Stuhr, Meyer, et al., 2018). Various studies have observed that *Symbiodiniaceae* genus in coral hosts may influence the susceptibility of the coral host to thermal bleaching (Berkelmans & Van Oppen, 2006; Fisher et al., 2012; LaJeunesse et al., 2010; Rowan, 2004). The differences in temperature tolerance between species have been found; however, it is hard to know its reason as the same type does not typically inhabit the same host species (Fisher et al., 2012).

A substantial amount of research has focused on the process of coral bleaching. Despite two decades of research about coral bleaching resulting from symbiont loss due to heat stress, it still needs to be determined how the symbiosis falls apart at the cellular level (Cziesielski et al., 2018; McDermott, 2020). Hence, comprehending the molecular mechanisms involved in the breakdown of symbiosis during heat stress could help predict and prevent the process of bleaching (McDermott, 2020). Moreover, understanding the involvement of molecular signalling pathways in the homeostasis of

symbiosis and controlling the balance in host-symbiont affiliations could be critical in designing new approaches to ensure the survival of coral reefs. Also, by looking at the symbiont transcriptome during heat stress and cross referencing this with gene activity in the host it is possible to gain insights into the role of the symbiont within the process.

This chapter aims to observe changes in gene expression through symbiont ejection from the host during thermal-induced bleaching. This study is focused on the transcriptome of the symbiont, and it hypothesises that changes in gene expressions of *H. actiniformis* corals on the way to bleaching at high temperatures are like other symbiotic-dependent animals. It also hypothesises that this genus of cnidaria involves some novel genes and pathways. This chapter aims to explain the relationship between symbionts and *H. actiniformis* corals during thermal-induced bleaching.

4.3. Materials and methods

4.3.1. Experimental design

The symbiont analysis was performed on the samples collected during the heat shock bleaching experiment (Chapter 3, Section 3.2). In addition to the samples and data recorded for analysis as previously described (in Chapter 3, Section 3.2), pulse amplification modulated (PAM) fluorometer measurements were recorded for each coral prior to every sampling to analyse the photosynthetic efficiency of photosystem II (PS II) within the endosymbiotic *Symbiodiniacea* spp. The next-gen library was obtained from the previous bleaching chapter (Chapter 3, Section 3.3.4) and the same four individuals (1, 2, 4, and 5) and six conditions from said chapter were analysed.

4.3.2. Photosynthetic measurements

The photophysiological response of the inhabiting photosymbionts. was assessed in *H. actiniformis* corals with Pulse Amplitude Modulated (PAM) fluorometry and its associated software (Nobes et al., 2008). PAM fluorometry is a non-destructive and non-invasive technique used to estimate algal health by measuring changes in the photochemical effectiveness of photosystem II (PSII) (Howe et al., 2017). Light-adapted measurements were recorded in triplicate from each individual (and averaged) every 24-hours before sampling to ensure maximum tentacle extension and potential quantum yield (ratio of maximum to variable fluorescence: Fv/Fm). This study employs PAM fluorometry on *H. actiniformis* corals to analyse the effect of heat-stress on coral zooxanthellae regarding bleaching (Bhagooli & Hidaka, 2004). This method has also been utilised for coral reef macroalgae and microphytobenthic communities (Uthicke, 2006) and to evaluate the adaptation of the algal endosymbionts (Ralph & Gademann, 2005). Therefore, PAM fluorometry measurements manifest the

proficiency of PSII and are an accepted indicator of stress in corals, with Fv/Fm yields proportional to coral health (Nobes et al., 2008).

4.3.3. Bioinformatic analysis

Raw sequence quality control was evaluated with FastQC (https://www.bioinformatics.babraham.ac.uk/projects/fastqc/), and then MultiQC (Ewels et al., 2016) was used to combine the FastQC analysis for multi-sample quality control. Raw reads were mapped to a kraken database of major symbiont genera and the *H. actiniformis* coral host genome mentioned in section 3.3.5 to analyse the most dominant symbiont in *H. actiniformis* samples. This process involved creating Kraken-compatible references and then using kraken to clarify all raw reads according to their *Symbiodiniaceae* genus of origin.

After identifying the dominant symbiont, a "Marine Omics Symbiont-Host" RNASeq pipeline http://github.com/marine-omics/morp tool (Hass et al., 2013) was used to co-analyse all reads from the host and symbiont. This pipeline first creates a combined reference transcriptome for the host (*H. actiniformis*) and symbiont (in this case, *Cladocopium*, *Symbiont* C1), indexes this and then maps all reads to it using bowtie2. The use of a combined transcriptome ensures that any reads with ambiguous mapping (i.e. that could map to host or symbiont) can be clearly identified and the ambiguity accounted for. The symbiont transcriptome and its annotation were downloaded from the reefgenomics site http://symbs.reefgenomics.org/download/). After aligning reads, gene expression level was determined from aligned RNA-seq by using RNA-seq by Expectation-Maximization (RSEM) package (Li & Dewey, 2011). The number of alignments for each FLAG type in the resulting bam files was counted using samtools flagstat. A table of counts was generated from the reads of all the gene isoforms, and the R BiocManager (Robinson et al., 2009) package tximport (Love et al., 2018) was used to import and summarise the transcript abundance from the table counts.

The R Bioconductor package DESeq2 (Love., 2014) was then utilised to create a DESeq object that measured the differential gene expression between the different heat shock and bleaching conditions. The counts were normalised dependent on dispersion and size factors, and a variance stabilizing transformation (VST) was performed. The normalisation and statistical steps were performed separately for the host and symbiont data. Principal component analysis (PCA) was conducted for data quality control and to characterise gene expressions in the *Symbiodinium* throughout the heat shock and bleached timepoints.

A pairwise-contrast test was used to analyse the Differentially Expressed Genes (DEGs) by grouping two sequential timepoints (T0 vs T3, T3 vs T6). To manage the false discovery rate (FDR), genes with a q-value lower than 0.001 were deemed significantly differentially expressed. GO Enrichment

analysis was implemented on the gene sets to identify over-represented or under-represented GO terms by using annotations for the gene sets. The GO terms with p-value < 0.001 were considered as significantly enriched.

4.4. Results

All corals had similar bleaching timepoints within each sump system, as explained in the bleaching chapter (Chapter 3: Section: 3.4 & Table: 3.2). However, the issues associated with sump system two (Chapter 3: Section: 3.3.3) meant a subset of samples needed to be chosen for further analysis. Four individuals and six-timepoints chosen for the bleaching study were also chosen for this study (Chapter 3: Section: 3.4 & Table: 3.1).

4.4.1. Symbiont health analysis

Pulse Amplitude Modulated (PAM) fluorometry readings of the *H. actiniformis* tentacles decreased as the tentacles were bleached. Most individuals resulted in numbers too low to analyse after the T9 timepoint, except for one of the four individuals having a result in the B1 condition (Figure 4.1). All PAM readings of the corals decreased steadily throughout the heat-stress conditions. Therefore, the PAM data showed similar patterns in all the individuals throughout the timepoints. Corals are thought to be able to acclimate to changes in growth radiance, such as those experienced after physical disturbances (Gardner et al., 2015). Light is the primary energy source for reef-building zooxanthellate corals (Anthony & Hoegh-Guldberg, 2003). Therefore, decreasing PAM readings may influence the health and energy levels of the symbionts inhabiting the *H. actiniformis* coral host. Studies in fluorescence analysis showed differences in photosynthetic performance at different sites of the same corals, for example, along the length of coral branches (Ulstrup et al., 2006). Therefore, the bleaching of tentacles throughout the timepoints affected the capability of collecting readings and may show a decrease in the photosynthetic performance of the inhabiting symbionts.

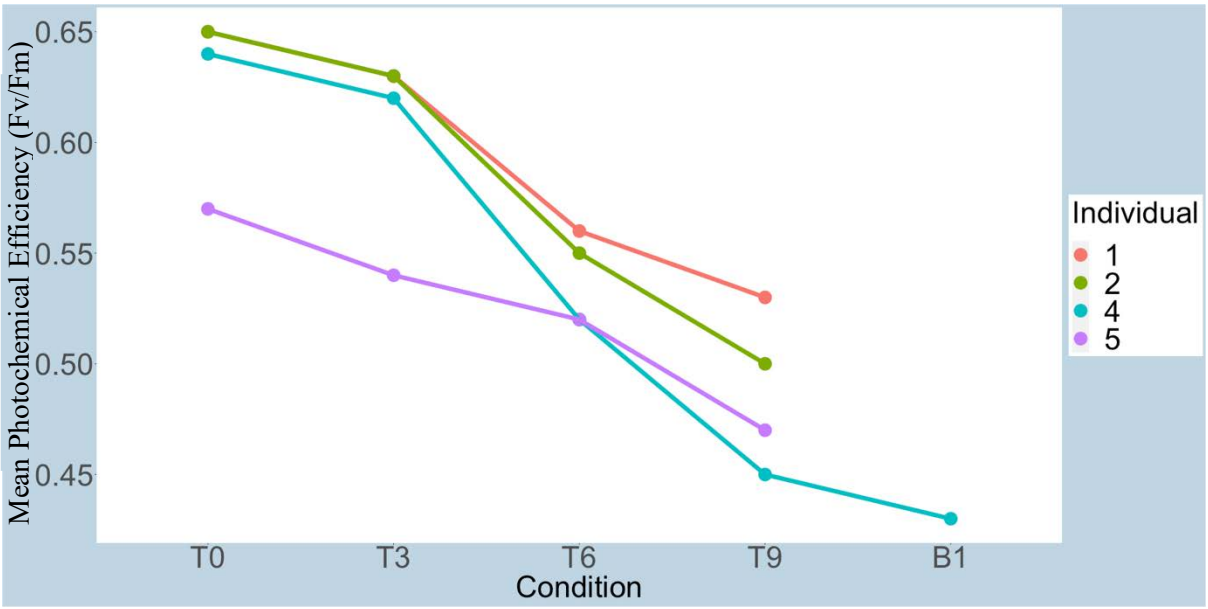

Figure 4.1. PAM fluorometer readings of symbionts in heat-stressed *H. actiniformis*. Mean of triplicate PAM readings from exposed tentacles of *H. actiniformis* corals exposed to heat-stress bleaching. The abbreviations of the conditions are: T0 (last day at 26°C); T3 (72 hours (3 days) at 34°C); T6 (144 hours (6 days) at 34°C); T9 (216 hours (9 days) at 34°C); B1 (First time bleached).

4.4.2. *Symbiodiniaceae* dominance in *H. actiniformis* host samples

The reads analysed in this section all came from the *Cladocopium* symbiont which was the most dominant symbiont in the *H. actiniformis* corals, with a raw read number of 14,690,496 across all samples (Figure 4.2), as reported previously for corals on the Great Barrier Reef (GBR) (Al-Hammady et al., 2022; Rosset et al., 2021). The second most dominant *Symbiodiniaceae* found was *Fugacium* with a relative abundance level of 145,236 (Figure 4.2). Surprisingly, *Durusdinium* was found to be the second to last most dominant with a relative abundance level of 28,818 (Figure 4.2), which was previously found as second most dominant type in GBR corals (Al-Hammady et al., 2022; Rosset et al., 2021).

It is hypothesised that the number of symbionts probably decreases with the increase in temperature and bleaching of the host (Figures 4.2). *Cladocopium* (C1) counts were arranged regarding different heating and bleaching timepoints, revealing an apparent decrease in counts when comparing through timepoints. The number of classified reads in some B4 timepoints reached zero (Figures 4.2). A substantial decrease of reads was found from the healthy coral timepoint (T0) to the first 24 hours at 34°C (T3), which kept decreasing until the bleaching timepoint (B4), except for individual one at timepoint T6 (Figure 4.2).

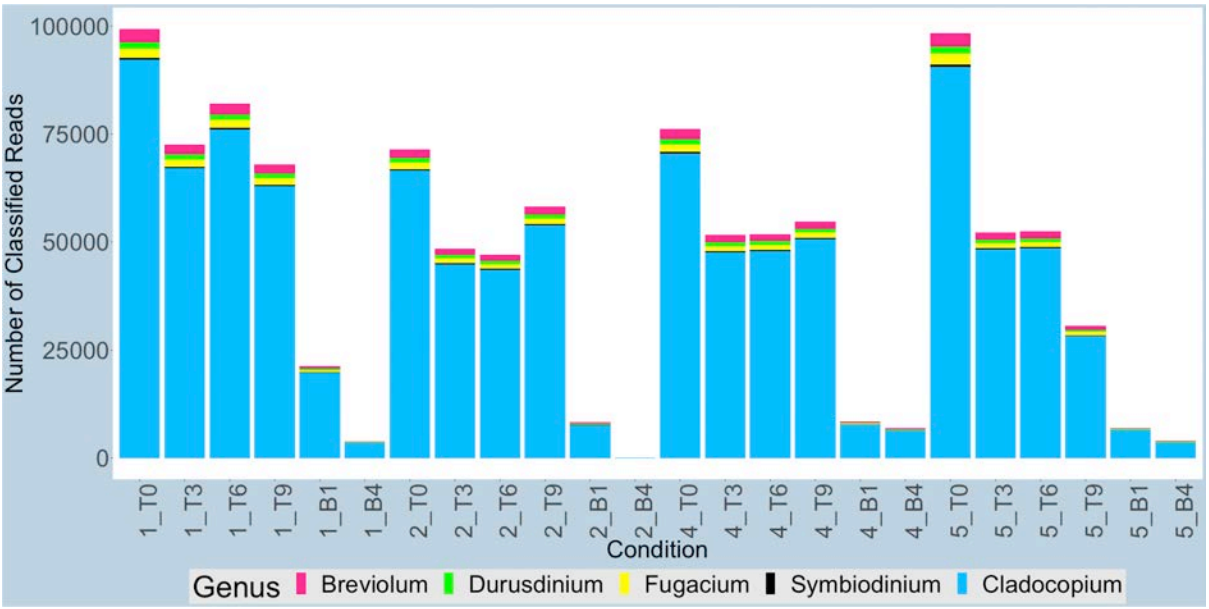

Figure 4.2. Symbiont types present in *H. actiniformis* samples. The dominance of symbiont (y-axis) is present in individual samples separated by condition (x-axis). The abbreviations of the conditions are composed of two parts: the first part depicts individual numbers, and the second part represents the condition. For example, 1_T0 means individual coral number 1 in condition T0 (last day at 26°C). Other condition abbreviations are: T3 = 72 hours (3 days) at 34°C; T6 = 144 hours (6 days) at 34°C; T9 = 216 hours (9 days) at 34°C; B1 = First time bleached; B4 = 72 hours (3 days) bleached.

4.4.3. Principal Component Analysis (PCA) of transcriptomic data

The PCA on normalised, variance stabilised data showed that the dominant source of sample variation in gene expression was found to be the condition as exhibited in principal components 1 (PC1), 2 (PC2), and 3 (PC3) with a variance of 76%,15%, and 3% respectively (Figure 4.3A, B, and C). The dominance by condition is unmistakable in PCA2 (Figure 4.3A) and PCA3 (Figure 4.3B). Principal component 4 (PC4), which accounts for 1%, exhibited a stronger connection via host genotype (Figure 4.3E). The high variability between samples in the B4 condition may be due to the scarce abundance of symbionts at this stage of the experiment causing a higher error rate in the analysis. Some potential reasons why this may have occurred are mentioned in the discussion.

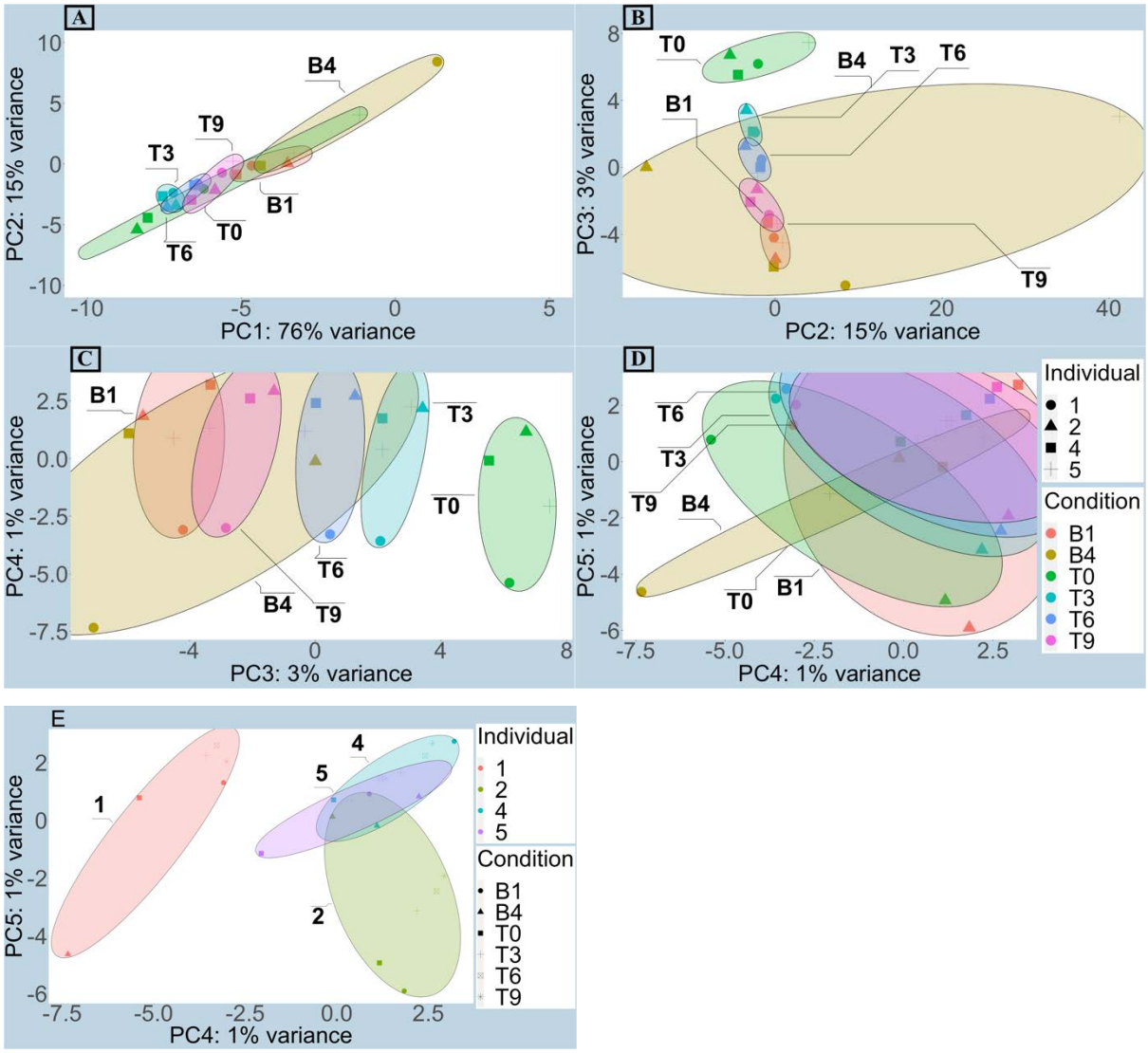

Figure 4.3A-E. Principal Component Analysis (PCA) of the expulsion of symbionts during heat-stress at different time points. PCA plot of the symbionts from the samples collected from *H. actiniformis* individuals (identified by symbols) at different heating and bleaching time points (identifiable by colour). (A) Compares the highest principal component levels (76% vs 15%; PC1). (B) A comparison of component levels 15% vs 3% (PC2). (C) Comparison of component levels 3% vs 1% (PC3). (D & E) Comparison of the lowest principal component levels (1% vs 1%; PC4; D & E). Plot E shows individual by colour and condition by symbol. The ggplot2 R package implemented with stat ellipse function generated the graphical plot and the ellipses. The axis titles represent the principal component and their respective variation percentage. The ellipses represent the orientation and spread of points according to the method of stat_ellipse().

4.4.4. Differential gene expression through heat stressed *Symbiodiniaceae*

The individual variations observed in the PCA allowed for the identification and analysis of DEGs across various conditions. DEG analysis clearly identifies two major transition points in gene expression. These first of these are the onset of heating as evidenced by the 2,262 DEGs between timepoint pair T0 (26°C) and T3 (34°C for three days) (Figure 4.4). The second is the onset of bleaching as demonstrated by the 2,492 DEGs were observed during bleaching condition pair B1 and

B4 (1,493 upregulated and 999 downregulated), timepoint depicting the total expulsion of symbionts from the coral host. In comparison, the transitions at intermediate timepoints show relatively little change, for example after three days at 34°C (condition pair T3_T6), a small number of DEGs were observed (16 upregulated and 23 downregulated); and the number remained stable over the next timepoint pair (T6_T9: 12 upregulated and 36 downregulated) followed by a decrease in the last heating timepoint and first bleaching timepoint comparison pair (T9_B1: 3 upregulated). The number of DEGs in the B1_B4 pair was expected to be like that of the T9_B1 pair; however, it is surprisingly much higher.

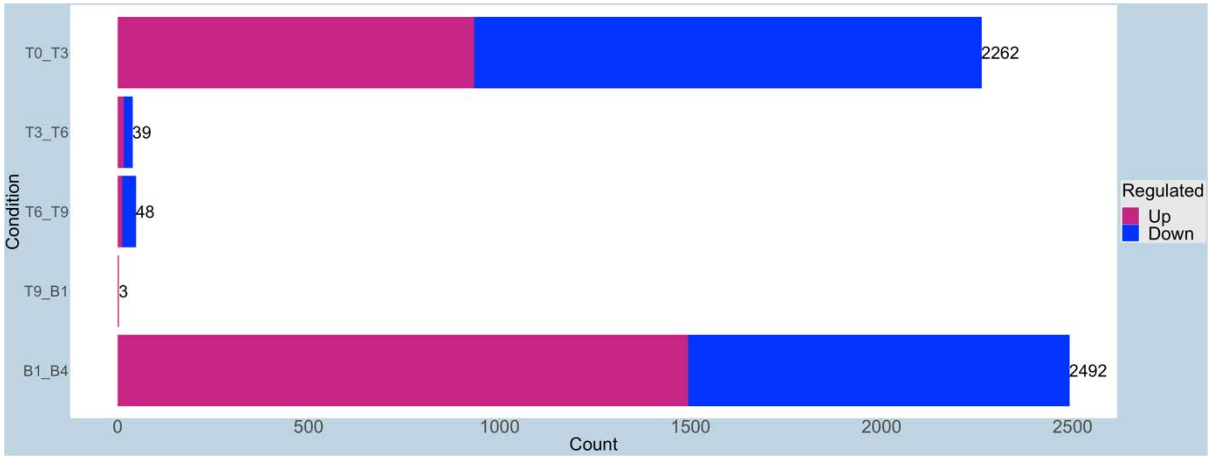

Figure 4.4. Differentially Expressed Genes (DEGs). Upregulated and downregulated genes through sequential timepoint pairs of the heating conditions of *Cladocopium* symbionts in the *H. actiniformis* coral at an adjusted p-value (p-value<0.05). The abbreviations of the timepoints are T0 = last day at 26°C; T3 = 72 hours (3 days) at 34°C; T6 = 144 hours (6 days) at 34°C; T9 = 216 hours (9 days) at 34°C; B1 = First time bleached; B4 = 72 hours (3 days) bleached.

4.4.5. Gene Ontology (GO) terms through heat-stressed *Symbiodiniaceae*

The gene ontology (GO) enrichment analysis produced 16 GO terms (BP = 7, MF = 7, CC = 2) across all pairs of consecutive conditions (Figure 4.5). Analysis of GO terms during heating protocol showed that symbiont GO terms activated in the first step and last step of the experimental protocols (T0-T3 and B1-B4). The bleached condition pair B1 to B4 had the most considerable quantity of GO terms (11 across all ontologies), double that of GO terms activated in the first condition pair T0 to T3 (5 GO terms across all ontologies). At the onset of the heating process, the symbionts respond by activating GO terms primarily related to the biosynthesis of macromolecules and organonitrogen compounds and the intra- and extra-cellular transport of ions and genes. At the same time, genes catalytic activities and GO terms related to the lumen are repressed. During the first bleaching event, several GO terms related to cell-cell adhesion, tissue remodelling, response to external stimuli and oxidation of fatty acid and lipids are activated. However, those related to glycogene metabolism, response to radiation and DNA damaging checkpoint are suppressed. Interestingly, HSP90 genes appear activated

exclusively at the second bleaching event, while non-coding RNA-related GO terms and some developmental GO terms are suppressed.

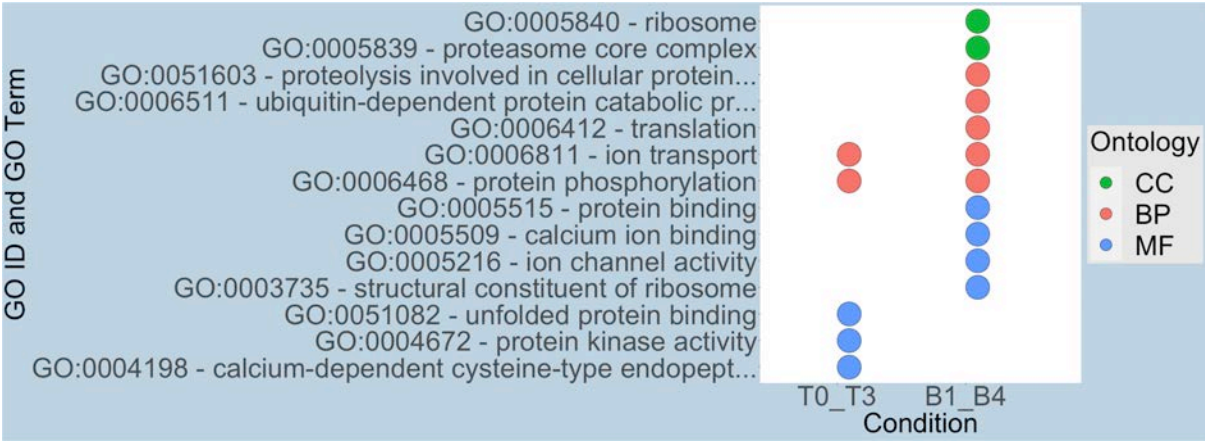

Figure 4.5. Significantly enriched GO terms of the inhabiting symbionts in *H. actiniformis* during bleaching. The significant (p-value < 0.001) GO IDs and GO terms with the highest p-values separated by ontology per timepoint pair are shown. GO Terms are in order of p-value (decreasing) from top to bottom. Condition pair T0_T3 compares heated conditions T0 (Last day at 26°C) to T3 (3 days at 34°C). Condition bleached pair B1_B4 represents bleached condition pair B1 to B4 (3 days bleached).

4.4.6. Gene activity during the different conditions

Analysis of genes within the significant GO terms was performed to understand activated and deactivated functions during the heating and bleaching processes. It was hypothesized that symbionts under heat stress would activate genes related to stress or survival.

4.4.6.1. Activity between the last day at 26°C (T0) and the first day at 34°C (T3)

The last timepoint at 26°C and the first at the heat-stress temperature (34°C) had five enriched terms containing 222 gene families. Among the 222 gene families, 50% belong to the enriched term gene kinase activity (GO:0004672) (Supplement Table S4.1) and (81%) were upregulated within the BP and MF ontologies at the T0 timepoint. Another 12% of the 222 gene families that were also (71%) upregulated in the T0 timepoint belong to the BP ontology were related to the enriched term ion transport gene (GO:0006811) (Supplement Table S4.1). The remaining 28% of enriched terms constitutes gene families associated with survival. For example, enriched terms in the MF ontology included those related to unfolded gene binding (GO:0051082), which contained four gene families (DnaJ, HSP90, calreticulin, prefolding subunit), that were upregulated in the T0 timepoint (Supplement Table S4.1). These four gene families are associated with the preventing the export of misfolded genes by assisting in the folding genes and degradation of terminally misfolded genes in Scleractinia corals, such as *Porites lobata* (Lock et al., 2022). Another enriched term in the MF ontology, calcium-dependent cysteine-type endopeptide (GO:0004198), was solely made up of

calpain family cystine protease (Supplement Table S4.1), a family with critical roles in regulating pathological cell death (Nakagawa & Yuan, 2000). Calpains allow corals to use cellular calcium levels to modulate the expression of hypoxia-inducible factor (HIF) targets under the condition of hypoxia (Bhattacharya et al., 2016; Levy et al., 2011), which shifts cell-death mediators from anti-apoptotic to pro-apoptotic states (Nakagawa & Yuan, 2000; Rosic et al., 2014). The list of shared *Symbiodinium* genes observed in this timepoint pair is at minimum 50% associated with the establishment of symbiosis through calcium-dependent gene kinases, which initiate signalling necessary for communication between eukaryotic cells (Nagamune & Sibley, 2006). Ion transport genes are also involved in host-symbiont interaction and are well-represented in *Symbiodinium* proteomes (Liu et al., 2018). An upregulation in ion transport has been shown to aid corals, such as *Pocillopora damicornis*, with low pH exposure (Vidal-Dupiol et al., 2009). Therefore, it might also be aiding the *H. actiniformis* under heat-stress. In summary, the genes activated during the last 24-hours at acclimation temperature and the first 24-hours at heat-stress temperature are associated with host-symbiont communication and survival.

4.4.6.2. Activity between day 1 bleached (B1) and 3 days bleached (B3).

The bleached timepoints (B1_B4) produced eleven enriched terms containing 578 genes across all ontologies (259 upregulated in B1, 318 upregulated in B4). A minimum of 22% of genes (primarily upregulated in the B4 timepoint) were associated with ribosome genes (Supplement Table 4.1) in a variety of enriched terms (GO:0003735, GO:0005840, and GO:0006412), which are commonly associated with heat-stress shuffling from *Cladocopium* to *Durusdinium* symbionts (Cunning & Baker, 2020). An upregulation of ribosomes is generally considered an indicator of cell proliferation (López-Maury et al., 2008); however, it has also been observed in cytoplasmic stress granules in eukaryotes (Buchan & Parker, 2009).

Another 19% of genes were associated with ion transport genes (Supplement Table 4.1) within two enriched terms (GO:0005216 and GO:0006811), which were mainly upregulated in the first bleached timepoint (B1). Another 12% of genes performed functions related to cell-matrix adhesion, translation, photosynthesis, lipid metabolism, and calcium ion transport (GO:0005216, GO:0005509, GO:0005515, GO:0006468, and GO:0006811) (Guzman et al., 2019; von Marschall et al., 2012) as they were associated with EF-hand domain (Supplement Table 4.1).

Eleven percent were gene kinase (Supplement Table 4.1) which were primarily upregulated in the B1 timepoint within a variety of enriched terms (GO:0005509, GO:0005515, GO:0006468, and GO:0006811), and six percent were ankyrin repeat across three enriched terms (GO:0005509, GO:0005515, GO:0005509). Ankyrin repeat genes are known as being one of the most copious and universal genes throughout the animal kingdom, which perform regulatory and structurally critical

roles and are associated with host-microbe interactions (Brüwer et al., 2017; Fan et al., 2012; Gauthier et al., 2016; Hentschel et al., 2012; Thomas et al., 2010) and with host immune evasion (Gauthier et al., 2016). They also inhibit the antiviral response of the algal host during heat-stress through interactions with viral infection pathways (Blanié et al., 2010; Guo et al., 2011) and neutralising host innate immunity of host systems by preventing apoptosis of cells and affecting the ubiquitination system of the coral host (Al-Khodor et al., 2010; Herbert et al., 2015; Revilla et al., 1998). Furthermore, ankyrin repeat genes are considered host epigenome-modifying genes in the coral microbiome and have been found to help mediate gene-gene interactions in eukaryotic cells (Barno et al., 2021; Robbins et al., 2019).

The last 30% constituted a wide variety of gene families, such as ubiquitin family, ATP synthase, calpain family, hsp90, ATPase, DnaJ, Cyclin, Kelch, and zinc finger; all of which were upregulated in the host bleaching study (Chapter 3: Section 3.4.4). The upregulated functions during bleaching timepoints suggest they activated symbiont metabolism throughout the coral host as there is an enrichment of symbiont-related functions, such as ATP synthesis and photosynthesis. The functions observed in these timepoints indicate host-symbiont communication and survival, like those observed in the study's first two timepoints. These results suggest a mutual effort of the host and symbionts for host survival, as the "expulsion" of symbionts during bleaching leads to the death of the host.

4.5. Discussion

4.5.1. Photosynthetic Efficiency and Symbiont Health

This study aimed to assess the impact of heat stress on the photosynthetic efficiency and symbiont health within the coral species *H. actiniformis*. The photosynthetic efficiency was evaluated using PAM fluorometry, which measures photosystem II (PSII) efficiency, a key component in the photosynthetic process.

Throughout the heat stress experiment, there was a significant decrease in the photochemical efficiency of the symbionts within the coral host. This decrease was most noticeable during the bleaching phase, indicating a severe disruption to the photosynthetic capacity of the symbionts. The high-temperature stress resulted in significant physiological changes, causing damage to PSII and a subsequent decrease in photosynthetic performance. This outcome is in alignment with several previous studies that reported a reduction in the photosynthetic performance of symbionts as a direct result of thermal stress, leading to coral bleaching events (Bhagooli & Hidaka, 2004; Gardner et al., 2015; Ulstrup et al., 2006). Coral health and survival rely heavily on the symbiotic relationship with

their resident symbionts, with photosynthetic activity playing a crucial role. The heat-induced stress causing the reduction in PAM readings could be attributed to several physiological changes within the symbionts. The decrease in the symbiont population, likely due to cellular damage and subsequent expulsion from the coral host, led to an overall reduction in the coral's photosynthetic capability. Beyond the observed decline in photosynthetic efficiency, this disruption is physically manifested by the visible bleaching of the coral host. Coral bleaching is a stress response occurring when the symbiotic relationship between the coral and symbionts breaks down, which often leads to the expulsion of the symbionts and loss of pigmentation in the coral host, giving them a 'bleached' appearance.

Further analyses indicated that the level of bleaching correlated strongly with the severity of the reduction in photosynthetic efficiency. This observation supports that coral bleaching and decreases photosynthetic efficiency are intimately connected. The loss of photosynthetic capacity in the symbionts like reduces the availability of essential nutrients to the coral host, which then triggers the bleaching response. These results shed light on the impact of heat stress on *H. actiniformis* and its symbionts, they also raise additional questions. For instance, why do some symbionts fare better than others under heat stress? What factors contribute to the resilience of specific symbionts, and can these factors be manipulated to enhance the overall resilience of the coral-symbiont relationship? Further studies exploring these questions provide valuable insights into the mechanisms of coral resilience under stress, which could be pivotal in protecting coral reefs against global climate change.

4.5.2. Symbiont Diversity and Dominance

The analysis of the symbiont communities within the *H. actiniformis* corals revealed a distinct dominance of the *Cladocopium* symbionts, reaffirming the findings from earlier research which identified *Cladocopium* as the predominant symbiont in corals inhabiting the Great Barrier Reef (GBR) (Al-Hammady et al., 2022; Rosset et al., 2021). This dominance of *Cladocopium* underscores its potential adaptability to the conditions present in the GBR and, perhaps, higher symbiotic compatibility with the coral host species in this region.

A compelling finding of this research was the identification of *Fugacium* as the second most prevalent symbiont, a significant presence in the *H. actiniformis* coral species within the Great Barrier Reef (GBR). The high prevalence of *Fugacium*, rather than the commonly seen *Durusdinium*, is fascinating and opens new avenues of inquiry about the symbiont's role under thermal stress and its influence on the overall resilience of the coral. This pattern also highlights the dynamic nature of the symbiont community composition in the coral, possibly due to anthropogenic environmental factors, such as temperature variations. As part of the heat-stress experiment, the symbiont populations experienced a

significant decrease, as represented effectively in Figures 4.2 and 4.3. This decline is consistent with our understanding of the effects of increased temperature on the symbiotic relationship between corals and their symbionts. Elevated thermal stress commonly prompts the expulsion of symbionts from their coral hosts, leading to coral bleaching due to a substantial reduction in the symbiont population size (Aichelman et al., 2024; Hughes, Anderson, et al., 2018; Hughes, Kerry, et al., 2018).

However, the data revealed an interesting anomaly in the trend - individual one at timepoint T6 exhibited an increase in the symbiont population. This divergence from the declining trend may suggest a unique resilience or acclimatization mechanism in certain individual corals. The fact that this coral could maintain, and even increase, its symbiont population under thermal stress points to potential inherent differences in coral resistance to heat stress. This observation calls for further investigations to understand why and how some coral individuals demonstrate resilience to heat stress while others succumb. The elucidation of these mechanisms could unlock new strategies to enhance coral resilience amidst the mounting challenge of global climate change.

4.5.3. Challenges in measuring changes in gene expression with bleaching

In this experiment small decreases in overall symbiont abundance (as measured by numbers of mapped reads; Figure 4.2) occurred during timepoints T0-T9 followed by a dramatic loss of symbionts at timepoints B1 and later. This poses a major challenge for data normalisation in a dual host-symbiont analysis because the fraction of reads attributable to symbionts undergoes such large changes, especially at the transition from T9 to the first bleaching timepoint. A partial solution (chich I implemented in this chapter) can be obtained by performing normalisation separately on the symbiont fractions, thereby allowing for overall changes in symbiont abundance. Nevertheless, even when this measure is taken it must be acknowledged that such large changes in symbiont abundance will stretch the assumptions of normalisation. One issue is that read counts in bleached samples may be so low that they are subject to greater random variation as seen in the PCA for the B4 timepoint in figure 4.3. Another issue is that bleaching might result in an overall change in the species composition of symbionts thereby driving changes that might be falsely interpreted as being due to molecular activity within the dominant symbiont (Cladocopium).

Although it is impossible to rule out the many sources of bias that can come from a bleaching experiment the results of Figure 4.4 are reassuring. In this figure the numbers of genes up and down regulated are approximately the same, indicating that results are not driven by bulk changes in symbiont number (which would lead to a preponderance of down-regulated genes).

4.5.4. Gene Activity: A tale of survival

The supplementary data provided, coupled with a Gene Ontology (GO) analysis, has allowed for a comprehensive assessment of gene function and response within the SymbC1 symbiont during periods of heat stress. This in-depth examination of differentially expressed genes (DEGs), their biological processes (BP), molecular functions (MF), and cellular components (CC) presents a tale of survival under stress conditions.

Notably, two molecular functions emerged prominently from this analysis: calcium-dependent cysteine-type endopeptidase activity (GO:0004198) and gene kinase activity (GO:0004672). Under increasing temperature conditions from T0 to T3, genes linked with the Calpain family of cysteine proteases, associated with the first function, exhibited an upregulation. This observation suggests the essential role this gene family might play in maintaining cellular homeostasis during heat stress. At the same time, an upsurge was noted in genes related to gene kinase activity. As the linchpin of cellular regulation and signal transduction, these genes also responded dynamically to the changing conditions between T0 and T3, emphasizing their integral role in the symbiont's stress response mechanism.

Further inspection of the DEGs provided intriguing revelations. Certain SymbC1 scaffolds like SymbC1.scaffold6019.2 and SymbC1.scaffold1244.8 showcased the presence of the EF-hand domain, denoting genes with the capability to bind calcium ions. This discovery aligns with the increased activity of calcium-dependent endopeptidase under specific conditions. The gene activity underwent a considerable shift as the heat stress continued to prevail. Genes associated with host-microbe interactions, ribosome generation, and ion transport became increasingly active, possibly as a survival strategy to mitigate the bleaching effects. The enrichment of ATP synthesis and photosynthesis functions suggested that the symbionts, despite the adversities, remained metabolically active, trying to sustain their host during the bleaching event.

The significance of gene kinase activity under T0 and T3 conditions was further emphasized by the upregulation of numerous genes exhibiting this function. These enzymes control various cellular processes while acting as molecular switches through gene phosphorylation, indicating a possible shift in the cellular environment in response to heat stress. Moreover, the biological process of gene phosphorylation (GO:0006468) was also noteworthy. Genes associated with this process, vital for virtually all cellular activities, showed an upregulation under T0 and T3 conditions. This observation indicated an enhanced need for gene phosphorylation, possibly hinting at increased cellular signalling or other phosphorylation-dependent processes as a response to heat stress. A variety of genes belonging to unique families like Zinc finger, C3HC4 type (RING finger), cyclic nucleotide-binding

domain, EF-hand domain pair, Gene kinase domain, Poly (ADP-ribose) polymerase catalytic domain, WWE domain, KH domain, HEAT repeats, and MYND finger; SET domain, showed a distinct upregulation under either T0 or T3 conditions. This gene diversity signifies the vast array of cellular processes activated in response to heat stress, potentially contributing to a shift in the cellular environment.

Transitioning from T0 to T3 was marked by significant shifts in gene activity and associated cellular processes. Enhanced activity of genes related to GO:0006468 (Gene phosphorylation) and GO:0006811 (Ion transport) suggested an amplified stress response with altered cellular signalling and ion transport. Interestingly, the onset of stress led to an upregulation of genes associated with GO:0051082 (Unfolded gene binding) and GO:0003735 (Structural constituent of the ribosome), involved in gene folding and synthesis, respectively. This response indicated an increased need for gene folding or a reaction to gene misfolding. The variability in ribosomal gene expression further suggested changes in gene synthesis, hinting at possible alterations in the ribosomal function or structure.

In conclusion, the gene ontology analysis vividly depicted survival and adaptation. The complex web of responses unveiled the intricate mechanisms that the SymbC1 symbiont harnesses to tackle heat stress, highlighting the pivotal roles that certain molecular functions and genes play in ensuring survival in a changing environment.

4.6. Conclusion: A multidimensional response to heat stress - The symbiont-host interplay

The cumulative insights from this research unravel a complex and multifaceted response of the SymbC1 symbionts and their host, *H. actiniformis*, to heat stress conditions. The significant shifts observed in cellular processes, notably gene synthesis, folding, modification, and ion transport, propose a robust and versatile response mechanism to thermal stress. These changes suggest an adaptive transition in the symbionts, characterized by heightened cellular signalling, varied gene expression, and increased gene-gene interactions.

This study underscores the importance of understanding the intricate molecular mechanisms of coral symbionts under different thermal stress conditions. These insights serve as a foundation for future research to design targeted interventions for coral reef conservation. It further magnifies the delicate equilibrium of marine ecosystems and the potential ramifications of thermal stress brought upon by global warming on these invaluable habitats. The data led us to an unexpected finding: The *Cladocopium* symbiont emerged as the most dominant species within the *H. actiniformis* corals,

contrary to our initial assumptions. However, the second most abundant symbiont was the *Fugacium*, a divergence from the common trend observed on the Great Barrier Reef, where *Durusdinium* is typically the second most dominant. The relatively high prevalence of the *Fugacium* symbiont offers intriguing hints about its potential role in augmenting the host coral's resilience to thermal stress, inviting more research into the symbiotic dynamics of these coral systems.

The complex interplay between the symbiont and its host under heat-stress conditions is at the heart of the findings. This interaction involves various responses, including alterations in gene expression, activation of stress responses, and shifts in metabolic activity, all aimed at fostering survival under stress. In essence, our understanding of the symbiont's molecular mechanisms and the host's resilience strategies, shaped by this study, brings us closer to comprehending the coral's response to thermal stress. This knowledge, in turn, stands to guide future conservation strategies, directing policymaking and efforts aimed at safeguarding our invaluable coral reef ecosystems in an era of changing climate.

Chapter 5: General Discussion: Unveiling the intricacies of coral biology.

This study was formulated around the comprehensive exploration of *Heliofungia actiniformis*, a cnidarian species better known for its anemone-like appearance and significant role in coral reef ecosystems. The primary focus was an in-depth analysis of the molecular processes involved in regeneration and bleaching, predominantly under conditions of heat-associated stress, which is developing as a significant threat to coral reefs globally due to climate change. The reason for choosing *H. actiniformis* as the study organism was twofold. Firstly, *H. actiniformis* has a unique biology among cnidarians, characterized by its large solitary polyp life form that regenerates quickly, which makes it an excellent model for studies related to coral biology (Knittweis, 2008). Secondly, like other cnidarians, it plays a crucial role in sustaining the health and balance of coral reef ecosystems, making its study vital for the broader understanding of these complex environments (Knittweis, 2008). Generally, it has vast potential to become a model species due to robustness and speedy recovery timeframes that allow for fast experimental re-creation.

The overarching goal was to understand the molecular processes of this species in its response to different stressors. Corals, including *H. actiniformis*, are threatened by various processes, such as pollution, and destructive fishing practices. One of the most immediate and severe threats is the rising sea temperatures associated with global warming, leading to heat-associated stress in corals, often culminating in coral bleaching (Gilbert et al., 2010; Hoegh-Guldberg et al., 2007). Coral bleaching, the expulsion of symbiotic algae from the coral host causing corals to turn completely white, is a significant concern in rising sea temperatures (Dai & Horng, 2009). It signifies a coral under stress, and while bleaching does not instantly kill corals, it leaves them more susceptible to disease and other threats, leading to increased mortality rates. Mass bleaching events can lead to extensive coral reef death in the worst-case scenarios. Thus, understanding the molecular processes that underpin the bleaching response in corals can provide vital insights into how corals respond to thermal stress and identify potential strategies to enhance coral resilience in the face of climate change.

The capability of corals to regenerate is a fundamental biological process that allows them to recover from physical damage. This regenerative capacity is particularly crucial in the face of frequent physical disturbances, ranging from storm events to predation (Gilbert et al., 2010; Hoegh-Guldberg et al., 2007). However, our understanding of the molecular mechanisms that facilitate this regeneration in corals, particularly in *H. actiniformis*, is limited. Therefore, a detailed investigation into these mechanisms was an integral part of this research. Beyond advancing our knowledge of coral biology, the results of these investigations carry far-reaching implications. Corals, including *H. actiniformis*, play a critical role in marine ecosystems (Fisher et al., 2012; Slattery et al., 2019). These corals provide habitat and shelter for many marine organisms, contribute to the recycling of nutrients, assist in carbon and nitrogen fixing, and help protect coastlines from storm damage. Coral reefs offer economic benefits, including tourism, fisheries, and medicines (Fisher et al., 2012; Slattery et al., 2019). An improved understanding of the biological mechanisms that help corals cope with environmental and physical stressors can inform strategies to protect and conserve these vital ecosystems.

5.1. *H. actiniformis* as a model coral facilitates new discoveries.

This study was methodologically progressive, incorporating innovative techniques to illuminate complex aspects of the biology of *H. actiniformis*, specifically in the context of tentacle regeneration and heat-induced bleaching. The regeneration experiment would have been far more difficult without the very large tentacles of *H. actiniformis*, and this size advantage was also apparent in the bleaching experiment where it facilitated easy and accurate measurement of bleaching progression. The central aim of the methodology was to expose and detail the hidden complexities in the coral's biological response to physical and environmental stressors and to outline the significant role that genetic variations play in coral resilience. In the study of tentacle regeneration, a pioneering approach was adopted, where we designed and carried out a pilot experiment, which ensured that timepoints chosen for RNA sequencing captured all relevant stages. As a biological process, tentacle regeneration has multiple variables influencing its onset and progression. For example, parameters such as the location and size of the coral, which were overlooked in previous studies (Hughes, Anderson, et al., 2018; Hughes, Kerry, et al., 2018), were considered critical factors for our

research. Our methodology allowed us to systematically analyse these variables and establish a more accurate and elaborate timeline for the regeneration process.

As the pilot experiment unfolded, we observed the distinctive interplay of these factors and their direct bearing on the regeneration outcome. We formulated an in-depth heat stress sampling regime in the chapters dedicated to heat-induced bleaching (Chapters 3 & 4). The basis for selecting this methodology was to unravel the corals' biological responses as they transition from acclimation temperatures to complete bleaching. This transition, we believed, would be marked by significant changes in gene expression, a hypothesis that could only be validated through methodical and precise sampling.

In the sampling regimen, we tracked the gene expression changes in *H. actiniformis* under increasing heat stress. The data gathered gave us a comprehensive understanding of the coral's biological adjustments in response to escalating temperatures. The findings deepened our comprehension of the coral's thermal tolerance mechanisms by showing that previously unknown molecular mechanisms are initiated throughout the bleaching process and served as a valuable scientific resource, contributing to the collective understanding of heat-induced bleaching in corals. The impact of the genotype on gene expression variations was another significant finding across our analyses (DeSalvo et al., 2010). These genotype-based variations underscored the premise that the coral's genetic diversity could be instrumental in determining its resilience to stress (Al-Shaer et al., 2023; Farag et al., 2016). Recognizing the crucial role of genetic variability opens exciting avenues for future research. Investigations can now explore how these genetic differences could be harnessed or manipulated to bolster coral resilience to environmental stressors.

In summary, the methodologies adopted in this thesis were innovative and highly consequential, both for our current research and future investigations. They provided us with the tools to examine the intricate biological processes in *H. actiniformis*, offering invaluable insights into the coral's stress response mechanisms and regenerative capabilities. Moreover, they have set the stage for further research, particularly in genetic variability, which could enhance coral resilience amid rising global temperatures.

5.2. Consolidation of insights and their broader implications

Our comprehensive study offers an in-depth view of the biology of the mushroom coral *Heliofungia actiniformis*, specifically in terms of tentacle regeneration, thermal stress responses, and symbiont-host dynamics. This multifaceted research expands our knowledge of these complex marine organisms and establishes a solid groundwork for subsequent research and conservation efforts. Our probe into *H. actiniformis* regeneration revealed an intricate network of genetic and cellular processes that assist in healing from physical harm. Distinct, time-sensitive regulation of genes involved in wound healing, inflammation, apoptosis, antiviral responses, and regulation of cell and tissue polarity was evident, which showcases the sophistication of the regeneration process, where various genes and pathways are activated at different stages of tissue repair. The ATP-binding mechanism emerged as an intriguing commonality, potentially influencing several facets of regeneration, including drug resistance and protection against predatory toxins (Huls et al., 2009; Kimura et al., 2012; Shao et al., 2020).

Our inquiry into the thermal stress response of *H. actiniformis* yielded new insights, as we were able to disentangle the effects of heat stress and bleaching, which are separate molecular processes that commonly co-occur. Noticeable shifts in gene expression profiles and metabolic activity suggest that corals prepare for bleaching events by conserving energy at a molecular level (Cui et al., 2019). Furthermore, that corals initiate specific metabolic and gene expression adaptations that have only previously been observed in diseased mammals (Hector et al., 2022; Kers et al., 2018; Woodhams et al., 2020).

The *Symbiodiniaceae*, *Cladocopium* emerged as the most dominant species within the *H. actiniformis* corals (LaJeunesse et al., 2018). However, the second most abundant *Symbiodiniaceae* was the *Fugacium*, a divergence from the common trend on the Great Barrier Reef where *Durusdinium* is usually the second most dominant (Al-Hammady et al., 2022; Rosset et al., 2021). The *Fugacium* prevalence hints at its potential role in strengthening the host's resilience to thermal stress (Berkelmans & Van Oppen, 2006; Fisher et al., 2012; LaJeunesse et al., 2010; Rowan, 2004).

These interrelated discoveries, collected across distinct yet interconnected aspects of coral biology, emphasize the delicate balance and complex interactions within the coral holobiont.

They spotlight the coral's remarkable resilience strategies and the adaptable nature of the host and its symbionts in the presence of environmental stressors (LaJeunesse et al., 2018; Robison & Warner, 2006). Importantly, these insights can guide future research into unexplored realms of coral biology, such as the physiological implications of a hibernation-like state, the role of the *Symbiodiniaceae*, *Fugacium*, and the function of ATP binding in coral regeneration. On a larger scale, these findings contribute to enhancing coral conservation strategies. As global warming poses a significant threat to coral reef ecosystems, a thorough understanding of the coral's genetic, cellular, and physiological responses to stress is imperative for devising effective mitigation tactics. Thus, the knowledge amassed from this research significantly aids this cause, offering critical scientific evidence to inform policy-making and conservation initiatives to protect these vital marine ecosystems.

5.3. Charting the course for future explorations

An intriguing area that warrants further investigation is the observed genotype-based variations in gene expression. Throughout the studies conducted as part of this thesis, the influence of genotype on gene expression patterns became increasingly evident (Fisher et al., 2012). This variation in gene expression across different genotypes suggests a complex interplay between the genetic constitution of an organism and its response to stressors. Understanding these genotype-phenotype connections in more depth could elucidate the genetic basis for differences in stress resilience among coral populations (Fisher et al., 2012). Could specific genotypes better withstand heat stress or facilitate more efficient regeneration? Answering such questions could identify genetic markers of resilience, providing a new dimension to coral conservation efforts. Genetic approaches, including genome sequencing and population genetics studies, could be employed to dissect these genotype-phenotype relationships and provide critical knowledge for conserving these vital ecosystems.

In parallel, an in-depth investigation into the roles played by different symbiont species during thermal stress could further illuminate the intricacies of the coral-symbiont relationship. Our findings have taken a step towards understanding how heat stress and bleaching affect symbionts and their coral hosts by looking at them separately and providing evidence that they generally experience the stress independently. Supported by the symbionts

and coral hosts only having three significantly enriched terms: unfolded gene binding (GO:0051082); translation (GO:0006412); and ribosome (GO:0005840) in common during heat stress and bleaching. Further insights into how these pathways are linked and how the interactions between host and symbiont result in bleaching could possibly be obtained via transcriptomics. Research dedicated towards understanding what molecular mechanisms symbiont species possess that allow them to cope with heat stress and how symbionts contribute to their host's health and survival abilities during heat stress could provide nuanced insights into the roles of different symbiont species in coral health and resilience. These types of findings could open the door for potential interventions to bolster coral survival under increased temperatures.

Thus far, our studies have primarily focused on the impact of heat stress on coral health and resilience (Cziesielski et al., 2018; McDermott, 2020). However, in the natural environment, corals are simultaneously subjected to a combination of these stressors (Grottoli et al., 2018; Ziegler et al., 2017). Therefore, there is a pressing need for comprehensive studies that evaluate the synergistic impact of multiple environmental stressors on coral health and resilience bleaching (Fisch et al., 2019; Pinzón et al., 2015; Thomas & Palumbi, 2017; Wall et al., 2021; Wall et al., 2019). Future research should assess the cumulative impact of these stressors and understand how they interact to influence coral health (Howells et al., 2016; Matsuda et al., 2020). Such research would not only paint a more accurate picture of the challenges corals face in their natural habitats but also aid in developing practical and holistic conservation strategies.

In conclusion, this study has made significant strides in understanding the complex biology of *H. actiniformis* and highlighted several exciting directions for future research. The findings underscore the intricate relationships within the coral holobiont, the dynamic genomic responses of the coral to environmental changes, and the remarkable resilience of these organisms in the face of challenging environmental stressors. However, the path towards effective coral conservation is a long one. It necessitates a multidisciplinary approach involving biologists, climate scientists, policymakers, and local communities. Through such collaborations, we hope to translate our scientific understanding of coral biology into tangible conservation strategies, preserving the vital coral reef ecosystems for future generations.

References

Aguilar, C., Raina, J. B., Fôret, S., Hayward, D. C., Lapeyre, B., Bourne, D. G., & Miller, D. J. (2019). Transcriptomic analysis reveals gene homeostasis breakdown in the coral Acropora millepora during hypo-saline stress. *BMC Genomics*, *20*(1), 148. https://doi.org/10.1186/s12864-019-5527-2

Aichelman, H.E., Huzar, A.K., Wuitchik, D.M., Atherton, K.F., Wright, R.M., Dixon, G., Schlatter, E., Haftel, N., & Davies, S.W. (2024). Symbiosis modulates gene expression of symbionts, but not coral hosts, under thermal challenge. *Molecular Ecology*, *33*(8), p.e17318. https://doi.org/10.1111/mec.17318

Ainsworth, T., Hoegh-Guldberg, O., Heron, S., Skirving, W., & Leggat, W. (2008). Early cellular changes are indicators of pre-bleaching thermal stress in the coral host. *Journal of Experimental Marine Biology and Ecology*, *364*(2), 63-71. https://doi.org/10.1016/j.jembe.2008.06.032

Akimenko, M.-A. & Ekker, M. (1995). Anterior duplication of the Sonic hedgehog expression pattern in the pectoral fin buds of zebrafish treated with retinoic acid. *Developmental biology*, *170*(1), 243-247. https://doi.org/10.1006/dbio.1995.1211

Akimenko, M.-A., Johnson, S. L., Westerfield, M., & Ekker, M. (1995). Differential induction of four msx homeobox genes during fin development and regeneration in zebrafish. *Development*, *121*(2), 347-357. https://doi.org/10.1242/dev.121.2.347

Al-Hammady, M. A., Silva, T. F., Hussein, H. N., Saxena, G., Modolo, L. V., Belasy, M. B., Westphal, H., & Farag, M. A. (2022). How do algae endosymbionts mediate for their coral host fitness under heat stress? A comprehensive mechanistic overview. *Algal Research*, 102850. https://doi.org/10.1016/j.algal.2022.102850

Al-Khodor, S., Price, C. T., Kalia, A., & Kwaik, Y. A. (2010). Functional diversity of ankyrin repeats in microbial genes. *Trends in Microbiology*, *18*(3), 132-139. https://www.cell.com/ajhg/abstract/S0966-842X(09)00252-2

Al-Shaer, L., Leach, W., Baban, N., Yagodich, M., Gibson, M. C., & Layden, M. J. (2023). Environmental and molecular regulation of asexual reproduction in the sea anemone Nematostella vectensis. *bioRxiv*, 2023.2001. 2027.525773. https://doi.org/10.1098/rsos.230152

Alappat, S., Zhang, Z. Y., & Chen, Y. P. (2003). Msx homeobox gene family and craniofacial development. *Cell Res*, *13*(6), 429-442. https://doi.org/10.1038/sj.cr.7290185

Allemand, D. & Furla, P. (2018). How does an animal behave like a plant? Physiological and molecular adaptations of zooxanthellae and their hosts to symbiosis. *Comptes rendus*

biologies, *341*(5), 276-280. https://www.sciencedirect.com/science/article/pii/S1631069118300520?via%3Dihub

Allemand, D. & Osborn, D. (2019). Ocean acidification impacts on coral reefs: From sciences to solutions. *Regional Studies in Marine Science*, *28*, 100558. https://doi.org/10.1016/j.rsma.2019.100558

Altieri, A. H., Harrison, S. B., Seemann, J., Collin, R., Diaz, R. J., & Knowlton, N. (2017). Tropical dead zones and mass mortalities on coral reefs. *Proceedings of the National Academy of Sciences*, *114*(14), 3660-3665. https://doi.org/10.1073/pnas.1621517114

Alvarado, A. S. & Tsonis, P. A. (2006). Bridging the regeneration gap: genetic insights from diverse animal models. *Nature reviews. Genetics*, *7*(11), 873-884. https://doi.org/10.1038/nrg1923

Amelio, I., Cutruzzolá, F., Antonov, A., Agostini, M., & Melino, G. (2014). Serine and glycine metabolism in cancer. *Trends in biochemical sciences (Amsterdam. Regular ed.)*, *39*(4), 191-198. https://doi.org/10.1016/j.tibs.2014.02.004

Amiel, A. R., Johnston, H. T., Nedoncelle, K., Warner, J. F., Ferreira, S., & Röttinger, E. (2015). Characterization of Morphological and Cellular Events Underlying Oral Regeneration in the Sea Anemone, Nematostella vectensis. *International Journal of Molecular Sciences*, *16*(12), 28449-28471. https://doi.org/10.3390/ijms161226100

Anthony, K. R. N., & Hoegh-Guldberg, O. (2003). Variation in Coral Photosynthesis, Respiration and Growth Characteristics in Contrasting Light Microhabitats: An Analogue to Plants in Forest Gaps and Understoreys? *Functional Ecology*, *17*(2), 246–259. http://www.jstor.org/stable/3599181

Arias-Mejias, S. M., Warda, K. Y., Quattrocchi, E., Alonso-Quinones, H., Sominidi-Damodaran, S., & Meves, A. (2020). The role of integrins in melanoma: A review. *International journal of dermatology*, *59*(5), 525-534. https://doi.org/10.1111/ijd.14850

Authority, G. B. R. M. P. A. (2019). *Great Barrier Reef Outlook Report 2019*. Great Barrier Reef Marine Park Authority. https://elibrary.gbrmpa.gov.au/jspui/bitstream/11017/3474/13/Outlook-Report-2019-Intro.pdf

Avila-Magaña, V., Kamel, B., DeSalvo, M., Gómez-Campo, K., Enríquez, S., Kitano, H., Rohlfs, R. V., Iglesias-Prieto, R., & Medina, M. (2021). Elucidating gene expression adaptation of phylogenetically divergent coral holobionts under heat stress. *Nature Communications*, *12*(1), 5731-5731. https://doi.org/10.1038/s41467-021-25950-4

Bailly, C. & Waring, M. J. (2019). Pharmacological effectors of GRP78 chaperone in cancers. *Biochemical Pharmacology*, *163*, 269-278. https://doi.org/https://doi.org/10.1016/j.bcp.2019.02.038

Baird, A. H., Keith, S. A., Woolsey, E., Yoshida, R., & Naruse, T. (2017). Rapid coral mortality following unusually calm and hot conditions on Iriomote, Japan. *F1000Research*, *6*. https://doi.org/10.12688/f1000research.12660.2

Bak, R. P. (1977). Coral reefs and their zonation in Netherlands Antilles: modern and ancient reefs. https://archives.datapages.com/data/specpubs/carbona1/data/a045/a045/0001/0000/0003.htm

Bak, R. P. & Meesters, E. H. (1999). Population structure as a response of coral communities to global change. *American Zoologist*, *39*(1), 56-65. https://doi.org/10.1093/icb/39.1.56

Bak, R. P. & Steward-Van Es, Y. (1980). Regeneration of superficial damage in the scleractinian corals Agaricia agaricites f. purpurea and Porites astreoides. *Bulletin of Marine Science*, *30*(4), 883-887. https://www.ingentaconnect.com/content/umrsmas/bullmar/1980/00000030/00000004/art00010

Barno, A. R., Villela, H. D., Aranda, M., Thomas, T., & Peixoto, R. S. (2021). Host under epigenetic control: A novel perspective on the interaction between microorganisms and corals. *BioEssays*, *43*(10), 2100068. https://doi.org/10.1002/bies.202100068

Barott, K. L., Venn, A. A., Perez, S. O., Tambutté, S., & Tresguerres, M. (2015). Coral host cells acidify symbiotic algal microenvironment to promote photosynthesis. *Proceedings of the National Academy of Sciences*, *112*(2), 607-612. https://doi.org/10.1073/pnas.1413483112

Barros, Y., Lucas, C. C., & Soares, M. O. (2021). An urban intertidal reef is dominated by fleshy macroalgae, sediment, and bleaching of a resilient coral (Siderastrea stellata). *Marine Pollution Bulletin*, *173*(Pt A), 112967-112967. https://doi.org/10.1016/j.marpolbul.2021.112967

Barshis, D. J., Ladner, J. T., Oliver, T. A., Seneca, F. O., Traylor-Knowles, N., & Palumbi, S. R. (2013). Genomic basis for coral resilience to climate change. *Proceedings of the National Academy of Sciences*, *110*(4), 1387-1392. https://doi.org/10.1073/pnas.1210224110

Bartelt, A., Widenmaier, S. B., Schlein, C., Johann, K., Goncalves, R. L., Eguchi, K., Fischer, A. W., Parlakgül, G., Snyder, N. A., & Nguyen, T. B. (2018). Brown adipose tissue thermogenic adaptation requires Nrf1-mediated proteasomal activity. *Nature medicine*, *24*(3), 292-303. https://doi.org/10.1038/nm.4481

Baumgarten, S., Simakov, O., Esherick, L. Y., Liew, Y. J., Lehnert, E. M., Michell, C. T., Li, Y., Hambleton, E. A., Guse, A., & Oates, M. E. (2015). The genome of Aiptasia, a sea anemone model for coral symbiosis. *Proceedings of the National Academy of Sciences*, *112*(38), 11893-11898. https://doi.org/10.1073/pnas.1513318112

Bellantuono, A. J., Granados-Cifuentes, C., Miller, D. J., Hoegh-Guldberg, O., & Rodriguez-Lanetty, M. (2012). Coral thermal tolerance: tuning gene expression to resist thermal stress. *PLoS One*, *7*(11), e50685. https://doi.org/10.1371/journal.pone.0050685

Bely, A. E. (2014). Early events in annelid regeneration: a cellular perspective. *American Zoologist*, *54*(4), 688-699. https://doi.org/10.1093/icb/icu109

Berkelmans, R. & Van Oppen, M. J. (2006). The role of zooxanthellae in the thermal tolerance of corals: a 'nugget of hope'for coral reefs in an era of climate change. *Proceedings of the Royal*

Society B: Biological Sciences, *273*(1599), 2305-2312. https://www.ncbi.nlm.nih.gov/pmc/articles/PMC1636081/pdf/rspb20063567.pdf

Berthet, S., Demont-Caulet, N., Pollet, B., Bidzinski, P., Cézard, L., Le Bris, P., Borrega, N., Hervé, J., Blondet, E., Balzergue, S., Lapierre, C., & Jouanin, L. (2011). Disruption of LACCASE4 and 17 Results in Tissue-Specific Alterations to Lignification of Arabidopsis thaliana Stems. *The Plant cell*, *23*(3), 1124-1137. https://doi.org/10.1105/tpc.110.082792

Bhagooli, R., & Hidaka, M. (2004). Release of zooxanthellae with intact photosynthetic activity by the coral Galaxea fascicularis in response to high temperature stress. *Marine Biology*, *145*, 329-337. https://doi.org/10.1007/s00227-004-1309-7

Bhattacharya, D., Agrawal, S., Aranda, M., Baumgarten, S., Belcaid, M., Drake, J. L., Erwin, D., Foret, S., Gates, R. D., Gruber, D. F., Kamel, B., Lesser, M. P., Levy, O., Liew, Y. J., MacManes, M., Mass, T., Medina, M., Mehr, S., Meyer, E., & Falkowski, P. G. (2016). Comparative genomics explains the evolutionary success of reef-forming corals. *Elife*, *5*, e13288. https://doi.org/10.7554/eLife.13288

Bideau, L., Kerner, P., Hui, J., Vervoort, M., & Gazave, E. (2021). Animal regeneration in the era of transcriptomics. *Cellular and Molecular Life Sciences*, *78*(8), 3941-3956. https://doi.org/10.1007/s00018-021-03760-7

Bieri, T., Onishi, M., Xiang, T., Grossman, A. R., & Pringle, J. R. (2016). Relative Contributions of Various Cellular Mechanisms to Loss of Algae during cnidarian Bleaching. *PLoS One*, *11*(4), e0152693-e0152693. https://doi.org/10.1371/journal.pone.0152693

Blackstone, N. (2009). Mitochondria and the redox control of development in cnidarians. Seminars in cell & developmental biology, https://doi.org/10.1016/j.semcdb.2008.12.006

Blackstone, N. W. & Golladay, J. M. (2018). Why do corals bleach? Conflict and conflict mediation in a host/symbiont community. *BioEssays*, *40*(8), 1800021. https://doi.org/10.1002/bies.201800021

Blanié, S., Gelfi, J., Bertagnoli, S., & Camus-Bouclainville, C. (2010). MNF, an ankyrin repeat gene of myxoma virus, is part of a native cellular SCF complex during viral infection. *Virology Journal*, *7*(1), 1-5. https://doi.org/10.1186/1743-422X-7-56

Boehm, A.-M. & Bosch, T. C. G. (2012). Migration of multipotent interstitial stem cells in Hydra. *Zoology (Jena)*, *115*(5), 275-282. https://doi.org/10.1016/j.zool.2012.03.004

Boros, K., Lacaud, G., & Kouskoff, V. (2011). The transcription factor Mxd4 controls the proliferation of the first blood precursors at the onset of hematopoietic development in vitro. *Experimental hematology*, *39*(11), 1090-1100. https://doi.org/10.1016/j.exphem.2011.07.007

Bourne, D., Iida, Y., Uthicke, S., & Smith-Keune, C. (2008). Changes in coral-associated microbial communities during a bleaching event. *The ISME Journal*, *2*(4), 350-363. https://www.nature.com/articles/ismej2007112.pdf

Bourne, D. G., Morrow, K. M., & Webster, N. S. (2016). Insights into the coral microbiome: underpinning the health and resilience of reef ecosystems. *Annual review of microbiology*, *70*, 317-340. https://doi.org/10.1146/annurev-micro-102215-095440

Bradshaw, B., Thompson, K., & Frank, U. (2015). Distinct mechanisms underlie oral vs aboral regeneration in the cnidarian Hydractinia echinata. *Elife*, *4*, e05506-e05506. https://doi.org/10.7554/eLife.05506

Brockes, J. P. & Kumar, A. (2002). Plasticity and reprogramming of differentiated cells in amphibian regeneration. *Nature Reviews Molecular Cell Biology*, *3*(8), 566-574. https://doi.org/10.1038/nrm881

Brockes, J. P. & Kumar, A. (2008). Comparative aspects of animal regeneration. *Annual review of cell and developmental biology*, *24*(1), 525-549. https://doi.org/10.1146/annurev.cellbio.24.110707.175336

Brockes, J. P., Kumar, A., & Velloso, C. P. (2001). Regeneration as an evolutionary variable. *The Journal of Anatomy*, *199*(1-2), 3-11. https://doi.org/10.1017/S0021878201008299

Brüwer, J. D., Agrawal, S., Liew, Y. J., Aranda, M., & Voolstra, C. R. (2017). Association of coral algal symbionts with a diverse viral community responsive to heat shock. *BMC microbiology*, *17*(1), 1-11. https://doi.org/10.1186/s12866-017-1084-5

Bryant, S. V. E., Gardiner, T., & Miller, D. (2002). Vertebrate limb regeneration and the origin of limb stem cells. *International Journal of Developmental Biology*, *46*, 887-896. https://escholarship.org/uc/item/7rv1c4qq

Buchan, J. R. & Parker, R. (2009). Eukaryotic stress granules: the ins and outs of translation. *Molecular cell*, *36*(6), 932-941. https://www.cell.com/AJHG/fulltext/S1097-2765(09)00861-2

Burriesci, M. S., Raab, T. K., & Pringle, J. R. (2012). Evidence that glucose is the major transferred metabolite in dinoflagellate–cnidarian symbiosis. *Journal of Experimental Biology*, *215*(19), 3467-3477. https://doi.org/10.1242/jeb.070946

Burton, P. M. & Finnerty, J. R. (2009). Conserved and novel gene expression between regeneration and asexual fission in Nematostella vectensis. *Development genes and evolution*, *219*(2), 79-87. https://link.springer.com/article/10.1007/s00427-009-0271-2

Cai, C., Tang, Y.-D., Zhai, J., & Zheng, C. (2022). The RING finger gene family in health and disease. *Signal Transduction and Targeted Therapy*, *7*(1), 300. https://doi.org/10.1038/s41392-022-01152-2

Cameron, C. M. & Edmunds, P. J. (2014). Effects of simulated fish predation on small colonies of massive Porites spp. and Pocillopora meandrina. *Marine Ecology Progress Series*, *508*, 139-148. https://doi.org/10.3354/meps10862

Carnevali, C. M. D. & Bonasoro, F. (2001). Introduction to the biology of regeneration in echinoderms. *Microscopy research and technique*, *55*(6), 365-368. https://doi.org/10.1002/jemt.1184

Cary, G. A., Wolff, A., Zueva, O., Pattinato, J., & Hinman, V. F. (2019). Analysis of sea star larval regeneration reveals conserved processes of whole-body regeneration across the metazoa. *BMC biology*, *17*(1), 16-16. https://doi.org/10.1186/s12915-019-0633-9

Castillo-Medina, R. E., Islas-Flores, T., & Villanueva, M. (2022). Light-stimulated dephosphorylation of the BiP-like gene, SmicHSP75 (SBiP1) from Symbiodinium microadriaticum is inhibited by elevated but not low temperature and suggests regulation of the chaperone function. *Acta Biochimica Polonica*, *69*(1), 155-164. https://doi.org/10.18388/abp.2020_5788

Chan, E. C., Liu, G. S., Roulston, C. L., Lim, S. Y., & Dusting, G. J. (2014). NADPH Oxidase in Tissue Repair and Regeneration. In I. Laher (Ed.), *Systems Biology of Free Radicals and Antioxidants* (pp. 2517-2537). Springer Berlin Heidelberg. https://doi.org/10.1007/978-3-642-30018-9_97

Chang, H.-C., Shapiro, J. S., Jiang, X., Senyei, G., Sato, T., Geier, J., Sawicki, K. T., & Ardehali, H. (2021). Augmenter of liver regeneration regulates cellular iron homeostasis by modulating mitochondrial transport of ATP-binding cassette B8. *Elife*, *10*. https://doi.org/10.7554/ELIFE.65158

Chavanich, S., Viyakarn, V., Loyjiw, T., Pattaratamrong, P., & Chankong, A. (2009). Mass bleaching of soft coral, Sarcophyton spp. in Thailand and the role of temperature and salinity stress. *ICES journal of marine science*, *66*(7), 1515-1519. https://doi.org/10.1093/icesjms/fsp048

Chen, R., Mukhtar, I., Wei, S., Wu, S., & Chen, J. (2022). Morphological and molecular features of early regeneration in the marine annelid Ophryotrocha xiamen. *Scientific Reports*, *12*(1), 1799. https://doi.org/10.1038/s41598-022-04870-3

Chen, W. & Ten Dijke, P. (2016). Immunoregulation by members of the TGFβ superfamily. *Nature Reviews Immunology*, *16*(12), 723-740. https://www.nature.com/articles/nri.2016.112

Chera, S., de Rosa, R., Miljkovic-Licina, M., Dobretz, K., Ghila, L., Kaloulis, K., & Galliot, B. (2006). Silencing of the Hydra serine protease inhibitor Kazal1 gene mimics the human SPINK1 pancreatic phenotype. *Journal of cell science*, *119*(5), 846-857. https://doi.org/10.1242/jcs.02807

Chera, S., Ghila, L., Dobretz, K., Wenger, Y., Bauer, C., Buzgariu, W., Martinou, J.-C., & Galliot, B. (2009). Apoptotic cells provide an unexpected source of Wnt3 signaling to drive Hydra head regeneration. *Developmental Cell*, *17*(2), 279-289. https://www.cell.com/developmental-cell/pdf/S1534-5807(09)00298-6.pdf

Chiori, R., Jager, M., Denker, E., Wincker, P., Da Silva, C., Le Guyader, H., Manuel, M., & Quéinnec, E. (2009). Are Hox Genes Ancestrally Involved in Axial Patterning? Evidence from the Hydrozoan Clytia hemisphaerica (Cnidaria). *PLoS One*, *4*(1), e4231. https://doi.org/10.1371/journal.pone.0004231

Christensen, R. N., & Tassava, R. A. (2000). Apical epithelial cap morphology and fibronectin gene expression in regenerating axolotl limbs. *Developmental dynamics*, *217*(2), 216-224. https://doi.org/10.1002/(SICI)1097-0177(200002)217:2<216::AID-DVDY8>3.0.CO;2-8

Cleves, P. A., Krediet, C. J., Lehnert, E. M., Onishi, M., & Pringle, J. R. (2020). Insights into coral bleaching under heat stress from analysis of gene expression in a sea anemone model system. *Proceedings of the National Academy of Sciences - PNAS*, *117*(46), 28906-28917. https://doi.org/10.1073/pnas.2015737117 (From the Cover)

Cleves, P. A., Shumaker, A., Lee, J., Putnam, H. M., & Bhattacharya, D. (2020). Unknown to known: Advancing knowledge of coral gene function. *Trends in genetics*, *36*(2), 93-104. https://www.cell.com/trends/genetics/fulltext/S0168-9525(19)30238-0?_returnURL=https%3A%2F%2Flinkinghub.elsevier.com%2Fretrieve%2Fpii%2FS0168952519302380%3Fshowall%3Dtrue

Connelly, M. T., McRae, C. J., Liu, P.-J., Martin, C. E., & Traylor-Knowles, N. (2022). Antibiotics Alter Pocillopora Coral-Symbiodiniaceae-Bacteria Interactions and Cause Microbial Dysbiosis During Heat Stress. *Frontiers In Marine Science*, *8*, 814124. https://doi.org/10.3389/fmars.2021.814124

Costanza, R., De Groot, R., Sutton, P., Van der Ploeg, S., Anderson, S. J., Kubiszewski, I., Farber, S., & Turner, R. K. (2014). Changes in the global value of ecosystem services. *Global environmental change*, *26*, 152-158. https://doi.org/10.1016/j.gloenvcha.2014.04.002

Cuervo, R., Hernández-Martínez, R., Chimal-Monroy, J., Merchant-Larios, H., & Covarrubias, L. (2012). Full regeneration of the tribasal Polypterus fin. *Proceedings of the National Academy of Sciences - PNAS*, *109*(10), 3838-3843. https://doi.org/10.1073/pnas.1006619109

Cui, G., Liew, Y. J., Li, Y., Kharbatia, N., Zahran, N. I., Emwas, A.-H., Eguiluz, V. M., & Aranda, M. (2019). Host-dependent nitrogen recycling as a mechanism of symbiont control in Aiptasia. *PLoS genetics*, *15*(6), e1008189-e1008189. https://doi.org/10.1371/journal.pgen.1008189

Cunning, R., & Baker, A. C. (2020). Thermotolerant coral symbionts modulate heat stress-responsive genes in their hosts. *Molecular Ecology*, *29*(15), 2940-2950. https://doi.org/10.1111/mec.15526

Cziesielski, M. J., Liew, Y. J., Cui, G., Schmidt-Roach, S., Campana, S., Marondedze, C., & Aranda, M. (2018). Multi-omics analysis of thermal stress response in a zooxanthellate cnidarian reveals the importance of associating with thermotolerant symbionts. *Proceedings of the Royal Society. B, Biological sciences*, *285*(1877), 20172654-20172654. https://doi.org/10.1098/rspb.2017.2654

Cziesielski, M. J., Schmidt-Roach, S., & Aranda, M. (2019). The past, present, and future of coral heat stress studies. *Ecology and evolution*, *9*(17), 10055-10066. https://doi.org/10.1002/ece3.5576

Dai, C., & Horng, S. (2009). Scleractinia fauna of Taiwan II. *The robust group. National Taiwan University, Taipei*, 1-162.

Dani, V., Priouzeau, F., Mertz, M., Mondin, M., Pagnotta, S., Lacas-Gervais, S., Davy, S. K., & Sabourault, C. (2017). Expression patterns of sterol transporters NPC1 and NPC2 in the cnidarian–dinoflagellate symbiosis. *Cellular Microbiology*, *19*(10), e12753. https://doi.org/10.1111/cmi.12753

Darling, N. J., & Cook, S. J. (2014). The role of MAPK signalling pathways in the response to endoplasmic reticulum stress. *Biochimica et Biophysica Acta (BBA)-Molecular Cell Research*, *1843*(10), 2150-2163. https://doi.org/10.1016/j.bbamcr.2014.01.009

Darriere, T., Jobet, E., Zavala, D., Escande, M. L., Durut, N., de Bures, A., Blanco-Herrera, F., Vidal, E. A., Rompais, M., Carapito, C., Gourbiere, S., & Sáez-Vásquez, J. (2022). Upon heat stress processing of ribosomal RNA precursors into mature rRNAs is compromised after cleavage at primary P site in Arabidopsis thaliana. *RNA Biol*, *19*(1), 719-734. https://doi.org/10.1080/15476286.2022.2071517

Davies, S. W., Gamache, M. H., Howe-Kerr, L. I., Kriefall, N. G., Baker, A. C., Banaszak, A. T., Bay, L. K., Bellantuono, A. J., Bhattacharya, D., & Chan, C. X. (2023). Building consensus around the assessment and interpretation of Symbiodiniaceae diversity. *PeerJ*, *11*, e15023. https://peerj.com/articles/15023/

Davy, S., Burchett, S., Dale, A., Davies, P., Davy, J., Muncke, C., Hoegh-Guldberg, O., & Wilson, W. (2006). Viruses: agents of coral disease? *Diseases of aquatic organisms*, *69*(1), 101-110. https://www.int-res.com/articles/dao2006/69/d069p101.pdf

Davy, S. K., Allemand, D., & Weis, V. M. (2012). Cell Biology of cnidarian-Dinoflagellate Symbiosis. *Microbiology and Molecular Biology Reviews*, *76*(2), 229-261. https://doi.org/10.1128/MMBR.05014-11

Day, J. (2019). Planning and managing the Great Barrier Reef Marine Park. *The Great Barrier Reef: Biology, Environment and Management*, 169-181. https://books.google.com.au/books?hl=en&lr=&id=_NmGDwAAQBAJ&oi=fnd&pg=PA169&dq=Day,+J.+(2019).+Planning+and+managing+the+Great+Barrier+Reef+Marine+Park.+The+Great+Barrier+Reef:+Biology,+Environment+and+Management,+169-181.+&ots=ebFEtMT8RV&sig=hmbgXHm814H_N5Voka9DYgupYsk#v=onepage&q=Day%2C%20J.%20(2019).%20Planning%20and%20managing%20the%20Great%20Barrier%20Reef%20Marine%20Park.%20The%20Great%20Barrier%20Reef%3A%20Biology%2C%20Environment%20and%20Management%2C%20169-181.&f=false

Deisenroth, C. & Zhang, Y. (2011). The ribosomal gene-Mdm2-p53 pathway and energy metabolism: bridging the gap between feast and famine. *Genes & cancer*, *2*(4), 392-403. https://doi.org/10.1177/1947601911409737

Deleja, M., Paula, J. R., Repolho, T., Franzitta, M., Baptista, M., Lopes, V., Simão, S., Fonseca, V. F., Duarte, B., & Rosa, R. (2022). Effects of Hypoxia on Coral Photobiology and Oxidative Stress. *Biology (Basel)*, *11*(7). https://doi.org/10.3390/biology11071068

DeSalvo, M., Estrada, A., Sunagawa, S., & Medina, M. (2012). Transcriptomic responses to darkness stress point to common coral bleaching mechanisms. *Coral Reefs*, *31*, 215-228. https://doi.org/10.1007/s00338-011-0833-4

DeSalvo, M. K. (2010). *cDNA microarray-based studies of thermal stress-induced bleaching in the Caribbean corals Montastraea faveolata and Acropora palmata* UC Merced]. https://escholarship.org/uc/item/3wj093bn

DeSalvo, M. K., Sunagawa, S., Fisher, P. L., Voolstra, C. R., IGLESIAS-PRIETO, R., & Medina, M. (2010). Coral host transcriptomic states are correlated with Symbiodinium genotypes. *Molecular Ecology*, *19*(6), 1174-1186. https://doi.org/10.1111/j.1365-294X.2010.04534.x

DeSalvo, M. K., Sunagawa, S., Voolstra, C. R., & Medina, M. (2010). Transcriptomic responses to heat stress and bleaching in the elkhorn coral Acropora palmata. *Marine ecology. Progress series (Halstenbek)*, *402*, 97-113. https://doi.org/10.3354/meps08372

Desalvo, M. K., Voolstra, C. R., Sunagawa, S., Schwarz, J. A., Stillman, J. H., Coffroth, M. A., Szmant, A. M., & Medina, M. (2008). Differential gene expression during thermal stress and bleaching in the Caribbean coral Montastraea faveolata. *Molecular Ecology*, *17*(17), 3952-3971. https://doi.org/10.1111/j.1365-294X.2008.03879.x

Detournay, O., Schnitzler, C. E., Poole, A., & Weis, V. M. (2012). Regulation of cnidarian–dinoflagellate mutualisms: Evidence that activation of a host TGFβ innate immune pathway promotes tolerance of the symbiont. *Developmental and comparative immunology*, *38*(4), 525-537. https://doi.org/10.1016/j.dci.2012.08.008

Diaz, J. M., Hansel, C. M., Apprill, A., Brighi, C., Zhang, T., Weber, L., McNally, S., & Xun, L. (2016). Species-specific control of external superoxide levels by the coral holobiont during a natural bleaching event. *Nature Communications*, *7*(1), 13801. https://doi.org/10.1038/ncomms13801

Diaz-Rodriguez, P., López-Álvarez, M., Serra, J., González, P., & Landín, M. (2019). Current stage of marine ceramic grafts for 3D bone tissue regeneration. *Marine drugs*, *17*(8), 471. https://doi.org/10.3390/md17080471

Dixon, G., Abbott, E. and Matz, M. (2020). Meta-analysis of the coral environmental stress response: Acropora corals show opposing responses depending on stress intensity. *Molecular Ecology*, *29*(15), pp.2855-2870. https://doi.org/10.1111/mec.15535

Downs, C., Fauth, J. E., Halas, J. C., Dustan, P., Bemiss, J., & Woodley, C. M. (2002). Oxidative stress and seasonal coral bleaching. *Free Radical Biology and Medicine*, *33*(4), 533-543. https://doi.org/10.1016/S0891-5849(02)00907-3

DuBuc, T. Q., Traylor-Knowles, N., & Martindale, M. Q. (2014). Initiating a regenerative response; cellular and molecular features of wound healing in the cnidarian Nematostella vectensis. *BMC biology*, *12*(1), 24-24. https://doi.org/10.1186/1741-7007-12-24

Duffy, D. J. (2011). Modulation of Wnt signaling: A route to speciation? *Communicative & integrative biology*, *4*(1), 59-61. https://doi.org/10.4161/cib.13712

Duffy, D. J., Plickert, G., Kuenzel, T., Tilmann, W., & Frank, U. (2010). Wnt signaling promotes oral but suppresses aboral structures in Hydractinia metamorphosis and regeneration. *Development*, *137*(18), 3057-3066. https://doi.org/10.1242/dev.046631

Eguchi, G., Eguchi, Y., Nakamura, K., Yadav, M. C., Millán, J. L., & Tsonis, P. A. (2011). Regenerative capacity in newts is not altered by repeated regeneration and ageing. *Nature Communications*, *2*(1), 384. https://doi.org/10.1038/ncomms1389

Emanuel, K., Sundararajan, R., & Williams, J. (2008). Hurricanes and global warming: Results from downscaling IPCC AR4 simulations. *Bulletin of the American Meteorological Society*, *89*(3), 347-368. https://doi.org/10.1175/BAMS-89-3-347

Emanuel, K. A. (2013). Downscaling CMIP5 climate models shows increased tropical cyclone activity over the 21st century. *Proceedings of the National Academy of Sciences*, *110*(30), 12219-12224. https://doi.org/10.1073/pnas.1301293110

Eming, S. A., Hammerschmidt, M., Krieg, T., & Roers, A. (2009). Interrelation of immunity and tissue repair or regeneration. *Seminars in cell & developmental biology*, *20*(5), 517-527. https://doi.org/10.1016/j.semcdb.2009.04.009

Endo, T., Bryant, S. V., & Gardiner, D. M. (2004). A stepwise model system for limb regeneration. *Developmental biology*, *270*(1), 135-145. https://doi.org/10.1016/j.ydbio.2004.02.016

Erofeeva, T. V., Grigorenko, A. P., Gusev, F. E., Kosevich, I. A., & Rogaev, E. I. (2022). Studying of Molecular Regulation of Developmental Processes of Lower Metazoans Exemplified by Cnidaria Using High-Throughput Sequencing. *Biochemistry (Moscow)*, *87*(3), 269-293. https://doi.org/10.1134/S0006297922030075

Eugene, S. P., Reddy, V. S., & Trinath, J. (2020). Endoplasmic Reticulum Stress and Intestinal Inflammation: A Perilous Union [Mini Review]. *Frontiers in Immunology*, *11*. https://doi.org/10.3389/fimmu.2020.543022

Ewels, P., Magnusson, M., Lundin, S., Käller, M. (2016). MultiQC: Summarize analysis results for multiple tools and samples in a single report. Bioinformatics 32, 3047– 3048. https://doi.org/10.1093/bioinformatics/btw354

Fan, L., Reynolds, D., Liu, M., Stark, M., Kjelleberg, S., Webster, N. S., & Thomas, T. (2012). Functional equivalence and evolutionary convergence in complex communities of microbial sponge symbionts. *Proceedings of the National Academy of Sciences*, *109*(27), E1878-E1887. https://doi.org/10.1073/pnas.1203287109

Farag, M. A., Porzel, A., Al-Hammady, M. A., Hegazy, M.-E. F., Meyer, A., Mohamed, T. A., Westphal, H., & Wessjohann, L. A. (2016). Soft Corals Biodiversity in the Egyptian Red Sea: A Comparative MS and NMR Metabolomics Approach of Wild and Aquarium Grown Species. *Journal of proteome research*, *15*(4), 1274-1287. https://doi.org/10.1021/acs.jproteome.6b00002

Fatima, J., Ara, G., Afzal, M., & Siddique, Y. H. (2024). Hydra as a research model. *Toxin reviews*, 1-21. https://doi.org/10.1080/15569543.2024.2306544

Ferrari, J. & Vavre, F. (2011). Bacterial symbionts in insects or the story of communities affecting communities. *Philosophical Transactions of the Royal Society B: Biological Sciences*, *366*(1569), 1389-1400. https://www.ncbi.nlm.nih.gov/pmc/articles/PMC3081568/pdf/rstb20100226.pdf

Fisch, J., Drury, C., Towle, E. K., Winter, R. N., & Miller, M. W. (2019). Physiological and reproductive repercussions of consecutive summer bleaching events of the threatened Caribbean coral Orbicella faveolata. *Coral Reefs*, *38*, 863-876. https://doi.org/10.1007/s00338-019-01817-5

Fisher, E. M., Fauth, J. E., Hallock, P., & Woodley, C. M. (2007). Lesion regeneration rates in reef-building corals Montastraea spp. as indicators of colony condition. *Marine ecology. Progress series (Halstenbek)*, *339*, 61-71. https://doi.org/10.3354/meps339061

Fisher, P., Malme, M., & Dove, S. (2012). The effect of temperature stress on coral–Symbiodinium associations containing distinct symbiont types. *Coral Reefs*, *31*, 473-485. https://doi.org/10.1007/s00338-011-0853-0

Forsman, Z. H., Ritson-Williams, R., Tisthammer, K. H., Knapp, I. S. S., & Toonen, R. J. (2020). Host-symbiont coevolution, cryptic structure, and bleaching susceptibility, in a coral species complex (Scleractinia; Poritidae). *Scientific Reports*, *10*(1), 16995-16995. https://doi.org/10.1038/s41598-020-73501-6

Fox, J. M., Rashford, R. L., & Lindahl, L. (2019). Co-Assembly of 40S and 60S Ribosomal Genes in Early Steps of Eukaryotic Ribosome Assembly. *Int J Mol Sci*, *20*(11). https://doi.org/10.3390/ijms20112806

Fraguas, S., Barberán, S., & Cebrià, F. (2011). EGFR signaling regulates cell proliferation, differentiation and morphogenesis during planarian regeneration and homeostasis. *Developmental biology*, *354*(1), 87-101. https://doi.org/10.1016/j.ydbio.2011.03.023

Fumagalli, M. R., Zapperi, S., & La Porta, C. A. M. (2018). Regeneration in distantly related species: common strategies and pathways. *NPJ systems biology and applications*, *4*(1), 5-5. https://doi.org/10.1038/s41540-017-0042-z

Gai, C., Liu, J., Zheng, X., Xu, L., & Ye, H. (2022). Identification of Vibrio ponticus as a bacterial pathogen of coral trout Plectropomus leopardus [Brief Research Report]. *Frontiers in Cellular and Infection Microbiology*, *12*. https://doi.org/10.3389/fcimb.2022.1089247

Galliot, B. (2000). Conserved and divergent genes in apex and axis development of cnidarians. *Current opinion in genetics & development*, *10*(6), 629-637. https://doi.org/https://doi.org/10.1016/S0959-437X(00)00141-6

Galliot, B., & Chera, S. (2010). The Hydra model: disclosing an apoptosis-driven generator of Wnt-based regeneration. *Trends in cell biology*, *20*(9), 514-523. https://www.cell.com/trends/cell-biology/fulltext/S0962-8924(10)00099-1?_returnURL=https%3A%2F%2Flinkinghub.elsevier.com%2Fretrieve%2Fpii%2FS0962892410000991%3Fshowall%3Dtrue

Galliot, B. & Ghila, L. (2010). Cell plasticity in homeostasis and regeneration. *Molecular reproduction and development*, *77*(10), 837-855. https://doi.org/10.1002/mrd.21206

Galliot, B. & Schmid, V. (2002). cnidarians as a model system for understanding evolution and regeneration. *International Journal of Developmental Biology*, *46*(1), 39-48. https://ijdb.ehu.eus/article/pdf/11902686

Ganser, L. R., & Dallman, J. E. (2009). Glycinergic synapse development, plasticity, and homeostasis in zebrafish. *Frontiers in molecular neuroscience*, *2*, 30. Retrieved 2009, from http://europepmc.org/abstract/MED/20126315

García-González, M., Muñoz Guzón, F. M., González-Cantalapiedra, A., González-Fernández, P. M., Otero Pérez, R., & Serra Rodríguez, J. A. (2020). Application of shark teeth–derived bioapatites as a bone substitute in veterinary orthopedics. preliminary clinical trial in dogs and cats. *Frontiers in Veterinary Science*, *7*, 574017. https://doi.org/10.3389/fvets.2020.574017

Gardner, S. G., Nielsen, D. A., Petrou, K., Larkum, A. W. D., & Ralph, P. J. (2015). Characterisation of coral explants: a model organism for cnidarian–dinoflagellate studies. *Coral Reefs*, *34*(1), 133-142. https://doi.org/10.1007/s00338-014-1240-4

Gauthier, M.-E. A., Watson, J. R., & Degnan, S. M. (2016). Draft Genomes Shed Light on the Dual Bacterial Symbiosis that Dominates the Microbiome of the Coral Reef Sponge Amphimedon queenslandica [Original Research]. *FRONTIERS IN MARINE SCIENCE*, *3*. https://doi.org/10.3389/fmars.2016.00196

Gegner, H. M., Rädecker, N., Ochsenkühn, M., Barreto, M. M., Ziegler, M., Reichert, J., Schubert, P., Wilke, T., & Voolstra, C. R. (2019). High levels of floridoside at high salinity link osmoadaptation with bleaching susceptibility in the cnidarian-algal endosymbiosis. *Biology open*, *8*(12). https://doi.org/10.1242/bio.045591

Gehrke, A. R., Neverett, E., Luo, Y.-J., Brandt, A., Ricci, L., Hulett, R. E., Gompers, A., Ruby, J. G., Rokhsar, D. S., & Reddien, P. W. (2019). Acoel genome reveals the regulatory landscape of whole-body regeneration. *Science*, *363*(6432), eaau6173. https://www.science.org/doi/full/10.1126/science.aau6173

Gething, M.-J. (1999). Role and regulation of the ER chaperone BiP. *Seminars in cell & developmental biology*, *10*(5), 465-472. https://doi.org/10.1006/scdb.1999.0318

Gilbert, S.F., 2000. An introduction to early developmental processes. In *Developmental Biology. 6th edition*. Sinauer Associates. https://doi.org/https://www.ncbi.nlm.nih.gov/books/NBK9971/

Gilbert, S. F., McDonald, E., Boyle, N., Buttino, N., Gyi, L., Mai, M., Prakash, N., & Robinson, J. (2010). Symbiosis as a source of selectable epigenetic variation: taking the heat for the big guy. *Philosophical Transactions of the Royal Society B: Biological Sciences*, *365*(1540), 671-678. https://doi.org/10.1098/rstb.2009.0245

Godwin, J. W., & Brockes, J. P. (2006). Regeneration, tissue injury and the immune response. *Journal of anatomy*, *209*(4), 423-432. https://doi.org/10.1111/j.1469-7580.2006.00626.x

Gómez-Orte, E., Cornes, E., Zheleva, A., Sáenz-Narciso, B., De Toro, M., Iñiguez, M., López, R., San-Juan, J.-F., Ezcurra, B., & Sacristán, B. (2018). Effect of the diet type and temperature on the C. elegans transcriptome. *Oncotarget*, *9*(11), 9556. https://www.ncbi.nlm.nih.gov/pmc/articles/PMC5839384/

Gregory, B., Rahman, N., Bommakanti, A., Shamsuzzaman, M., Thapa, M., Lescure, A., Zengel, J. M., & Lindahl, L. (2019). The small and large ribosomal subunits depend on each other for stability and accumulation. *Life Sci Alliance*, *2*(2). https://doi.org/10.26508/lsa.201800150

Grottoli, A. G., Dalcin Martins, P., Wilkins, M. J., Johnston, M. D., Warner, M. E., Cai, W.-J., Melman, T. F., Hoadley, K. D., Pettay, D. T., & Levas, S. (2018). Coral physiology and microbiome dynamics under combined warming and ocean acidification. *PLoS One*, *13*(1), e0191156. https://journals.plos.org/plosone/article/file?id=10.1371/journal.pone.0191156&type=printable

Gufler, S., Artes, B., Bielen, H., Krainer, I., Eder, M. K., Falschlunger, J., Bollmann, A., Ostermann, T., Valovka, T., Hartl, M., Bister, K., Technau, U., & Hobmayer, B. (2018). β-Catenin acts in a position-independent regeneration response in the simple eumetazoan Hydra. *Developmental biology*, *433*(2), 310-323. https://doi.org/10.1016/j.ydbio.2017.09.005

Guo, C.-J., Chen, W.-J., Yuan, L.-Q., Yang, L.-S., Weng, S.-P., Yu, X.-Q., & He, J.-G. (2011). The viral ankyrin repeat gene (ORF124L) from infectious spleen and kidney necrosis virus attenuates nuclear factor-κ B activation and interacts with I κ B kinase β. *Journal of general virology*, *92*(7), 1561-1570. https://doi.org/10.1099/vir.0.031120-0

Gurtner, G. C., Werner, S., Barrandon, Y., & Longaker, M. T. (2008). Wound repair and regeneration : Regeneration medicine. *Nature (London)*, *453*(7193), 314-321. https://www.nature.com/articles/nature07039

Guzman, C., Atrigenio, M., Shinzato, C., Aliño, P., & Conaco, C. (2019). Warm seawater temperature promotes substrate colonization by the blue coral, Heliopora coerulea. *PeerJ*, *7*, e7785.

Haas, B.J., Papanicolaou, A., Yassour, M., Grabherr, M., Blood, P.D., Bowden, J., Couger, M.B., Eccles, D., Li, B., Lieber, M., Macmanes, M.D., Ott, M., Orvis, J., Pochet, N., Strozzi, F., Weeks, N., Westerman, R., William, T., Dewey, C.N., Henschel, R., Leduc, R.D., Friedman,

N., Regev, A. (2013). De novo transcript sequence reconstruction from RNA-seq using the Trinity platform for reference generation and analysis. Nat. Protoc. 8, 1494–1512. https://doi.org/10.1038/nprot.2013.084

Hadaidi, G., Röthig, T., Yum, L. K., Ziegler, M., Arif, C., Roder, C., Burt, J., & Voolstra, C. R. (2017). Stable mucus-associated bacterial communities in bleached and healthy corals of Porites lobata from the Arabian Seas. *Scientific Reports*, *7*(1), 1-11. https://doi.org/10.1038/srep45362

Hambleton, E. A., Jones, V. A. S., Maegele, I., Kvaskoff, D., Sachsenheimer, T., & Guse, A. (2019). Sterol transfer by atypical cholesterol-binding NPC2 genes in coral-algal symbiosis. *Elife*, *8*, e43923. https://doi.org/10.7554/eLife.43923

Han, M. J., An, J. Y., & Kim, W. S. (2001). Expression patterns of Fgf-8 during development and limb regeneration of the axolotl. *Developmental dynamics*, *220*(1), 40-48. https://doi.org/10.1002/1097-0177(2000)9999:9999<::AID-DVDY1085>3.0.CO;2-8

Hawkins, T. D., Bradley, B. J., & Davy, S. K. (2013). Nitric oxide mediates coral bleaching through an apoptotic-like cell death pathway: evidence from a model sea anemone-dinoflagellate symbiosis. *The FASEB journal*, *27*(12), 4790-4798. https://faseb.onlinelibrary.wiley.com/doi/abs/10.1096/fj.13-235051

Hawkins, T. D., & Davy, S. K. (2012). Nitric oxide production and tolerance differ among Symbiodinium types exposed to heat stress. *Plant and Cell Physiology*, *53*(11), 1889-1898. https://watermark.silverchair.com/pcs127.pdf?token=AQECAHi208BE49Ooan9kkhW_Ercy7Dm3ZL_9Cf3qfKAc485ysgAAAr8wggK7BgkqhkiG9w0BBwagggKsMIICqAIBADCCAqEGCSqGSIb3DQEHATAeBglghkgBZQMEAS4wEQQM271PzlqmP1atjZwfAgEQgIICcgXbh68UgWTHx6uBlSfRFrgTxQDyCPvpGBBPk-Sz6LIHJpfWAzZTfEqtUBniky2sB96yoPv9V6gvC0qLGIFxwqQ-goS0czuRZi5hcOer_evKWwwe7cM5mFSAHDQBLF-mui69NGIVvZ4z_3sWLvpK0yoECnSw99471nSOneWRa1UOUeO4DYP-UJUZ4upv7ksnmg36ev6pfO9f1Fy3PPofz5mNxJ_IaryXNtJHPDoNm-XpbrFsjQ7IcqP-9lLppr9b3GN2sfTNLl74Ru4NCO9JDetS_coo2VoCSG6FgmfCCtL1cgQXyfQ5jWIV8qjA7drhECgGGWg_xGJW9zMzp1Ir2qCMffQdtDV355qq0QzgA2yZVwuf5AQAXp6oN3o5c1dIFygd86vNiX1gPytxybil1P2b6L1xRLnvPHVoqJmWKAtfu8K9lLlMbMWUAj7N9-RhDK8lUtCT_B9GiBw-4ErL65hJr-khziGJSr7e-jXKMh0JaY1CFlw5KFpaaW1iZOOq37o-7AYZFs7Q4L7BOcXC84-5cI7vyXbRIiLAu7tVnUKdorhV3DqthdzD6mGJmdwYZ1vFZSvxHsrDcf1LfHJYXKnXkOC5CzHNUi_zL8-2sm_9tG_sH8HgNUIe3QkKggXxOn-drYf55_I4EKAfDvXijBEeO7ltn3PuzSvlpbkOSKGfMKOHAsl4_kk1DGFqI9TL1jr9XIXSQViqDML2Co14dTPqq08T71JwzuOe_XBXMhI-pLdAj-

DV9Gw5pGwMY_HeY_fNr6GeebRksHffnip-PC4Veo8rXPsHcqXAXwWqtNQpDT5zPyASDmkdFkyQqM57NG8t

Hector, T. E., Hoang, K. L., Li, J., & King, K. C. (2022). Symbiosis and host responses to heating. *Trends in Ecology & Evolution*. https://www.cell.com/trends/ecology-evolution/abstract/S0169-5347(22)00078-7

Hemond, E. M., Kaluziak, S. T., & Vollmer, S. V. (2014). The genetics of colony form and function in Caribbean Acropora corals. *BMC Genomics*, *15*(1), 1-21. https://doi.org/10.1186/1471-2164-15-1133

Hentschel, U., Piel, J., Degnan, S. M., & Taylor, M. W. (2012). Genomic insights into the marine sponge microbiome. *Nature Reviews Microbiology*, *10*(9), 641-654. https://doi.org/10.1038/nrmicro2839

Herbert, M. H., Squire, C. J., & Mercer, A. A. (2015). Poxviral ankyrin genes. *Viruses*, *7*(2), 709-738.

Higuchi, T., Yuyama, I., & Nakamura, T. (2015). The combined effects of nitrate with high temperature and high light intensity on coral bleaching and antioxidant enzyme activities. *Regional Studies in Marine Science*, *2*, 27-31. https://doi.org/10.1016/j.rsma.2015.08.012

Hirsch, A. M. (1999). Role of lectins (and rhizobial exopolysaccharides) in legume nodulation. *Current opinion in plant biology*, *2*(4), 320-326. https://doi.org/10.1016/S1369-5266(99)80056-9

Hoegh-Guldberg, O., Mumby, P. J., Hooten, A. J., Steneck, R. S., Greenfield, P., Gomez, E., Harvell, C. D., Sale, P. F., Edwards, A. J., & Caldeira, K. (2007). Coral reefs under rapid climate change and ocean acidification. *Science*, *318*(5857), 1737-1742. https://www.science.org/doi/abs/10.1126/science.1152509

Hoegh-Guldberg, O., Poloczanska, E. S., Skirving, W., & Dove, S. (2017). Coral Reef Ecosystems under Climate Change and Ocean Acidification [Review]. *FRONTIERS IN MARINE SCIENCE*, *4*. https://doi.org/10.3389/fmars.2017.00158

Holstein, T. W. (2022). The role of cnidarian developmental biology in unraveling axis formation and Wnt signaling. *Developmental biology*, *487*, 74-98. https://doi.org/10.1016/j.ydbio.2022.04.005

Holstein, T. W. (2023). The Hydra stem cell system – Revisited. *Cells & Development*, *174*, 203846. https://doi.org/https://doi.org/10.1016/j.cdev.2023.203846

Holstein, T. W., Hobmayer, E., & Technau, U. (2003). Cnidarians: An evolutionarily conserved model system for regeneration? *Developmental dynamics*, *226*(2), 257-267. https://doi.org/10.1002/dvdy.10227

Howells, E. J., Abrego, D., Meyer, E., Kirk, N. L., & Burt, J. A. (2016). Host adaptation and unexpected symbiont partners enable reef-building corals to tolerate extreme temperatures. *Global Change Biology*, *22*(8), 2702-2714. https://doi.org/10.1111/gcb.13250

Howells, E. J., Bauman, A. G., Vaughan, G. O., Hume, B. C., Voolstra, C. R., & Burt, J. A. (2020). Corals in the hottest reefs in the world exhibit symbiont fidelity not flexibility. *Molecular Ecology*, *29*(5), 899-911. https://doi.org/10.1111/mec.15372

Howells, E. J., Beltran, V. H., Larsen, N. W., Bay, L. K., Willis, B. L., & van Oppen, M. J. H. (2011). Coral thermal tolerance shaped by local adaptation of photosymbionts. *Nature Climate Change*, *2*(2), 116-120. https://doi.org/10.1038/nclimate1330

Hu, G., Lee, H., Price, S. M., Shen, M. M., & Abate-Shen, C. (2001). Msx homeobox genes inhibit differentiation through upregulation of cyclin D1. https://doi.org/10.1242/dev.128.12.2373

Hu, M., Zheng, X., Fan, C., & Zheng, Y. (2019). *Single cell lineage dynamics of the endosymbiotic cell type in a soft coral Xenia species*. https://doi.org/10.1101/2019.12.12.874602

Hu, M., Zheng, X., Fan, C., & Zheng, Y. (2020). Lineage dynamics of the endosymbiotic cell type in the soft coral Xenia. *Nature*, *582*. https://doi.org/10.1038/s41586-020-2385-7

Huang, C., Morlighem, J.-É. R., Cai, J., Liao, Q., Perez, C. D., Gomes, P. B., Guo, M., Rádis-Baptista, G., & Lee, S. M.-Y. (2017). Identification of long non-coding RNAs in two anthozoan species and their possible implications for coral bleaching. *Scientific Reports*, *7*(1), 5333. https://doi.org/10.1038/s41598-017-02561-y

Hughes, D. J., Alderdice, R., Cooney, C., Kühl, M., Pernice, M., Voolstra, C. R., & Suggett, D. J. (2020). Coral reef survival under accelerating ocean deoxygenation. *Nature Climate Change*, *10*(4), 296-307. https://doi.org/10.1038/s41558-020-0737-9

Hughes, T. P., Anderson, K. D., Connolly, S. R., Heron, S. F., Kerry, J. T., Lough, J. M., Baird, A. H., Baum, J. K., Berumen, M. L., & Bridge, T. C. (2018). Spatial and temporal patterns of mass bleaching of corals in the Anthropocene. *Science*, *359*(6371), 80-83. https://core.ac.uk/download/146457240.pdf

Hughes, T. P., Kerry, J. T., Álvarez-Noriega, M., Álvarez-Romero, J. G., Anderson, K. D., Baird, A. H., Babcock, R. C., Beger, M., Bellwood, D. R., & Berkelmans, R. (2017). Global warming and recurrent mass bleaching of corals. *Nature*, *543*(7645), 373-377. https://core.ac.uk/download/143898379.pdf

Hughes, T. P., Kerry, J. T., Baird, A. H., Connolly, S. R., Dietzel, A., Eakin, C. M., Heron, S. F., Hoey, A. S., Hoogenboom, M. O., & Liu, G. (2018). Global warming transforms coral reef assemblages. *Nature*, *556*(7702), 492-496. https://www.nature.com/articles/s41586-018-0041-2

Huls, M., Russel, F. G., & Masereeuw, R. (2009). The role of ATP binding cassette transporters in tissue defense and organ regeneration. *Journal of Pharmacology and Experimental Therapeutics*, *328*(1), 3-9. https://doi.org/10.1124/jpet.107.132225

Humphreys, L. M., Smith, P., Chen, Z., Fouad, S., & D'Angiolella, V. (2021). The role of E3 ubiquitin ligases in the development and progression of glioblastoma. *Cell Death & Differentiation*, *28*(2), 522-537. https://doi.org/10.1038/s41418-020-00696-6

Hwang, J.-U., Song, W.-Y., Hong, D., Ko, D., Yamaoka, Y., Jang, S., Yim, S., Lee, E., Khare, D., & Kim, K. (2016). Plant ABC transporters enable many unique aspects of a terrestrial plant's lifestyle. *Molecular Plant*, *9*(3), 338-355. https://www.cell.com/molecular-plant/fulltext/S1674-2052(16)00036-8

Ishii, Y., Maruyama, S., Takahashi, H., Aihara, Y., Yamaguchi, T., Yamaguchi, K., Shigenobu, S., Kawata, M., Ueno, N., & Minagawa, J. (2019). Global Shifts in Gene Expression Profiles Accompanied with Environmental Changes in cnidarian-Dinoflagellate Endosymbiosis. *G3 (Bethesda, Md.)*, *9*(7), 2337-2347. https://doi.org/10.1534/g3.118.201012

Iten, L. E., & Bryant, S. V. (1973). Forelimb regeneration from different levels of amputation in the newt, Notophthalmus viridescens: Length, rate, and stages. *Wilhelm Roux'Archiv fur Entwicklungsmechanik der Organismen*, *173*(4), 263-282. https://doi.org/10.1007/BF00575834

Janusz, G., Pawlik, A., Świderska-Burek, U., Polak, J., Sulej, J., Jarosz-Wilkołazka, A., & Paszczyński, A. (2020). Laccase properties, physiological functions, and evolution. *International Journal of Molecular Sciences*, *21*(3), 966. https://doi.org/10.3390/ijms21030966

Jaud, M., Philippe, C., Di Bella, D., Tang, W., Pyronnet, S., Laurell, H., Mazzolini, L., Rouault-Pierre, K., & Touriol, C. (2020). Translational Regulations in Response to Endoplasmic Reticulum Stress in Cancers. *Cells*, *9*(3), 540. https://www.mdpi.com/2073-4409/9/3/540

Jaźwińska, A., & Blanchoud, S. (2020). Towards deciphering variations of heart regeneration in fish. *Current Opinion in Physiology*, *14*, 21-26. https://doi.org/https://doi.org/10.1016/j.cophys.2019.11.007

Jian, J., Konopka, J., & Liu, C. (2013). Insights into the role of progranulin in immunity, infection, and inflammation. *Journal of leukocyte biology*, *93*(2), 199-208. https://doi.org/10.1189/jlb.0812429

Jimbo, M., Yanohara, T., Koike, K., Koike, K., Sakai, R., Muramoto, K., & Kamiya, H. (2000). The D-galactose-binding lectin of the octocoral Sinularia lochmodes: characterization and possible relationship to the symbiotic dinoflagellates. *Comparative Biochemistry and Physiology Part B: Biochemistry and Molecular Biology*, *125*(2), 227-236. https://doi.org/10.1016/S0305-0491(99)00173-X

Kabil, S. H., Haridy, M. F., & Farid, M. R. (2019). Effect of High Light Intensity Bleaching Protocol versus Descending Light Intensities Bleaching Protocol on Post Bleaching Teeth Sensitivity: A Randomized Clinical Trial. *Open access Macedonian journal of medical sciences*, *7*(13), 2173-2181. https://doi.org/10.3889/oamjms.2019.588

Kalafatić, M., Kovačević, G., Ljubešić, N., & Šunjić, H. (2001). Effects of ciprofloxacin on green Hydra and endosymbiotic alga. *Periodicum biologorum*, *103*(3), 267-272. https://www.croris.hr/crosbi/publikacija/prilog-casopis/96645

Kaniewska, P., Chan, C. K., Kline, D., Ling, E. Y., Rosic, N., Edwards, D., Hoegh-Guldberg, O., & Dove, S. (2015). Transcriptomic Changes in Coral Holobionts Provide Insights into Physiological Challenges of Future Climate and Ocean Change. *PLoS One*, *10*(10), e0139223. https://doi.org/10.1371/journal.pone.0139223

Kawakami, Y., Esteban, C. R., Raya, M., Kawakami, H., Belmonte, J. C. I., Marti, M., & Dubova, I. (2006). Wnt/[beta]-catenin signaling regulates vertebrate limb regeneration. *Genes & development*, *20*(23), 3232. https://genesdev.cshlp.org/content/20/23/3232.short

Kenkel, C. D., Aglyamova, G., Alamaru, A., Bhagooli, R., Capper, R., Cunning, R., deVillers, A., Haslun, J. A., Hédouin, L., Keshavmurthy, S., Kuehl, K. A., Mahmoud, H., McGinty, E. S., Montoya-Maya, P. H., Palmer, C. V., Pantile, R., Sánchez, J. A., Schils, T., Silverstein, R. N., . . . Matz, M. V. (2011). Development of gene expression markers of acute heat-light stress in reef-building corals of the genus Porites. *PLoS One*, *6*(10), e26914. https://doi.org/10.1371/journal.pone.0026914

Kenkel, C. D., Sheridan, C., Leal, M. C., Bhagooli, R., Castillo, K. D., Kurata, N., McGinty, E., Goulet, T. L., & Matz, M. V. (2014). Diagnostic gene expression biomarkers of coral thermal stress. *Molecular ecology resources*, *14*(4), 667-678. https://doi.org/10.1111/1755-0998.12218

Kers, J. G., Velkers, F. C., Fischer, E. A., Hermes, G. D., Stegeman, J. A., & Smidt, H. (2018). Host and environmental factors affecting the intestinal microbiota in chickens. *Frontiers in Microbiology*, *9*, 235. https://www.ncbi.nlm.nih.gov/pmc/articles/PMC5820305/pdf/fmicb-09-00235.pdf

Kerswell, A. P., & Jones, R. J. (2003). Effects of hypo-osmosis on the coral Stylophora pistillata: nature and cause of 'low-salinity bleaching'. *Marine ecology. Progress series (Halstenbek)*, *253*, 145-154. https://doi.org/10.3354/meps253145

Kimura, N., Hakamada, K., Ikenaga, S.-K., Umehara, Y., Toyoki, Y., & Sasaki, M. (2012). Gene expression of ATP-binding cassette transporters during liver regeneration after 90% hepatectomy in rats. *International journal of molecular medicine*, *30*(1), 28-34. https://doi.org/10.3892/ijmm.2012.972

Kitchen, S. A., Poole, A. Z., & Weis, V. M. (2017). Sphingolipid metabolism of a sea anemone is altered by the presence of dinoflagellate symbionts. *The Biological Bulletin*, *233*(3), 242-254. https://www.journals.uchicago.edu/doi/abs/10.1086/695846

Kitchen, S. A., & Weis, V. M. (2017). The sphingosine rheostat is involved in the cnidarian heat stress response but not necessarily in bleaching. *Journal of Experimental Biology*, *220*(Pt 9), 1709-1720. https://doi.org/10.1242/jeb.153858

Klosin, A., Casas, E., Hidalgo-Carcedo, C., Vavouri, T., & Lehner, B. (2017). Transgenerational transmission of environmental information in C. elegans. *Science*, *356*(6335), 320-323. https://www.science.org/doi/full/10.1126/science.aah6412

Knittweis, L. (2008). Population Demographics and Life History Characteristics of Heliofungia actiniformis: A Fungiid Coral Species Exploited for the Live Coral Aquarium Trade in the Spermonde Archipelago, Indonesia. *Centre for Tropical Marine Ecology*. http://nbn-resolving.de/urn:nbn:de:gbv:46-diss000110060

Knittweis, L., Jompa, J., Richter, C., & Wolff, M. (2009). Population dynamics of the mushroom coral Heliofungia actiniformis in the Spermonde Archipelago, South Sulawesi, Indonesia. *Coral Reefs*, *28*(3), 793-804. https://doi.org/10.1007/s00338-009-0513-9

Knittweis, L., Kraemer, W. E., Timm, J., & Kochzius, M. (2009). Genetic structure of Heliofungia actiniformis (Scleractinia: Fungiidae) populations in the Indo-Malay Archipelago: implications for live coral trade management efforts. *Conservation Genetics*, *10*(1), 241-249. https://doi.org/10.1007/s10592-008-9566-5

Koch, G. L., Macer, D. R., & Wooding, F. B. (1988). Endoplasmin is a reticuloplasmin. *J Cell Sci*, *90 (Pt 3)*, 485-491. https://doi.org/10.1242/jcs.90.3.485

Kochman-Gino, N.-R., Grover, R., Rottier, C., Ferrier-Pagès, C., & Fine, M. (2021). The reef building coral Stylophora pistillata uses stored carboHydrates to maintain ATP levels under thermal stress. *Coral Reefs*, *40*. https://doi.org/10.1007/s00338-021-02174-y

Koike, K., Jimbo, M., Sakai, R., Kaeriyama, M., Muramoto, K., Ogata, T., Maruyama, T., & Kamiya, H. (2004). Octocoral chemical signaling selects and controls dinoflagellate symbionts. *The Biological Bulletin*, *207*(2), 80-86. https://www.journals.uchicago.edu/doi/10.2307/1543582

Koumans, J., & Akster, H. (1995). Myogenic cells in development and growth of fish. *Comparative Biochemistry and Physiology Part A: Physiology*, *110*(1), 3-20. https://doi.org/10.1016/0300-9629(94)00150-R

Kramarsky-Winter, E., & Loya, Y. (2000). Tissue regeneration in the coral Fungia granulosa : the effect of extrinsic and intrinsic factors. *Marine Biology*, *137*(5-6), 867-873. https://doi.org/10.1007/s002270000416

Kristensen, T. N., Kjeldal, H., Schou, M. F., & Nielsen, J. L. (2016). Proteomic data reveal a physiological basis for costs and benefits associated with thermal acclimation. *Journal of Experimental Biology*, *219*(7), 969-976. https://doi.org/10.1242/jeb.132696

Kvennefors, E. C. E., Leggat, W., Kerr, C. C., Ainsworth, T. D., Hoegh-Guldberg, O., & Barnes, A. C. (2010). Analysis of evolutionarily conserved innate immune components in coral links immunity and symbiosis. *Developmental & Comparative Immunology*, *34*(11), 1219-1229.

LaJeunesse, T. C., Parkinson, J. E., Gabrielson, P. W., Jeong, H. J., Reimer, J. D., Voolstra, C. R., & Santos, S. R. (2018). Systematic Revision of Symbiodiniaceae Highlights the Antiquity and Diversity of Coral Endosymbionts. *Current Biology*, *28*(16), 2570-2580.e2576. https://doi.org/https://doi.org/10.1016/j.cub.2018.07.008

LaJeunesse, T. C., Smith, R., Walther, M., Pinzón, J., Pettay, D. T., McGinley, M., Aschaffenburg, M., Medina-Rosas, P., Cupul-Magaña, A. L., & Pérez, A. L. (2010). Host–symbiont

recombination versus natural selection in the response of coral–dinoflagellate symbioses to environmental disturbance. *Proceedings of the Royal Society B: Biological Sciences*, *277*(1696), 2925-2934. https://www.ncbi.nlm.nih.gov/pmc/articles/PMC2982020/pdf/rspb20100385.pdf

LaJeunesse, T.C., Wiedenmann, J., Casado-Amezúa, P., D'ambra, I., Turnham, K.E., Nitschke, M.R., Oakley, C.A., Goffredo, S., Spano, C.A., Cubillos, V.M. and Davy, S.K. (2022). Revival of Philozoon Geddes for host-specialized dinoflagellates,'zooxanthellae', in animals from coastal temperate zones of northern and southern hemispheres. *European Journal of Phycology*, *57*(2), pp.166-180. https://doi.org/10.1080/09670262.2021.1914863

Lawson, C. A., Possell, M., Seymour, J. R., Raina, J.-B., & Suggett, D. J. (2019). Coral endosymbionts (Symbiodiniaceae) emit species-specific volatilomes that shift when exposed to thermal stress. *Scientific Reports*, *9*(1), 1-11. https://doi.org/10.1038/s41598-019-53552-0

Lee, S. T., Davy, S. K., Tang, S.-L., & Kench, P. S. (2016). Mucus sugar content shapes the bacterial community structure in thermally stressed Acropora muricata. *Frontiers in Microbiology*, *7*, 371. https://www.ncbi.nlm.nih.gov/pmc/articles/PMC4805648/pdf/fmicb-07-00371.pdf

Lehnert, E. M., Mouchka, M. E., Burriesci, M. S., Gallo, N. D., Schwarz, J. A., & Pringle, J. R. (2014). Extensive differences in gene expression between symbiotic and aposymbiotic cnidarians. *G3 (Bethesda, Md.)*, *4*(2), 277-295. https://doi.org/10.1534/g3.113.009084

Leisegang, M. S., Babelova, A., Wong, M. S. K., Helfinger, V., Weißmann, N., Brandes, R. P., & Schröder, K. (2016). The NADPH Oxidase Nox2 Mediates Vitamin D-Induced Vascular Regeneration in Male Mice. *Endocrinology (Philadelphia)*, *157*(10), 4032-4040. https://doi.org/10.1210/en.2016-1257

Lesser, M. P. (2010). Coral Bleaching: Causes and Mechanisms. In (pp. 405-419). Springer Netherlands. https://doi.org/10.1007/978-94-007-0114-4_23

Levin, M., Anavy, L., Cole, A. G., Winter, E., Mostov, N., Khair, S., Senderovich, N., Kovalev, E., Silver, D. H., Feder, M., Fernandez-Valverde, S. L., Nakanishi, N., Simmons, D., Simakov, O., Larsson, T., Liu, S.-Y., Jerafi-Vider, A., Yaniv, K., Ryan, J. F., . . . Yanai, I. (2016). The mid-developmental transition and the evolution of animal body plans. *Nature (London)*, *531*(7596), 637-641. https://doi.org/10.1038/nature16994

Levin, R. A., Voolstra, C. R., Weynberg, K. D., & Van Oppen, M. J. H. (2017). Evidence for a role of viruses in the thermal sensitivity of coral photosymbionts. *The ISME Journal*, *11*(3), 808-812. https://doi.org/10.1038/ismej.2016.154

Levy, O., Kaniewska, P., Alon, S., Eisenberg, E., Karako-Lampert, S., Bay, L., Reef, R., Rodriguez-Lanetty, M., Miller, D., & Hoegh-Guldberg, O. (2011). Complex diel cycles of gene expression in coral-algal symbiosis. *Science*, *331*(6014), 175-175. https://www.science.org/doi/abs/10.1126/science.1196419

Lewis, V. A., Hynes, G. M., Zheng, D., Saibil, H., & Willison, K. (1992). T-complex polypeptide-1 is a subunit of a heteromeric particle in the eukaryotic cytosol. *Nature*, *358*(6383), 249-252. https://doi.org/10.1038/358249a0

Lewy, T. G., Grabowski, J. M., & Bloom, M. E. (2017). Focus: Infectious diseases: BiP: master regulator of the unfolded gene response and crucial factor in flavivirus biology. *The Yale journal of biology and medicine*, *90*(2), 291. https://www.ncbi.nlm.nih.gov/pmc/articles/PMC5482305/

Li, B. & Dewey, C.N. (2011). RSEM: accurate transcript quantification from RNA - Seq data34 with or without a reference genome. BMC Bioinformatics.12: 1–16. doi:10.1186/1471-2105-12-323 https://doi.org/10.1186/1471-2105-12-323

Li, Q., Wang, X., Korzhev, M., Schröder, H. C., Link, T., Tahir, M. N., Diehl-Seifert, B., & Müller, W. E. (2015). Potential biological role of laccase from the sponge Suberites domuncula as an antibacterial defense component. *Biochimica et Biophysica Acta (BBA)-General Subjects*, *1850*(1), 118-128. https://doi.org/10.1016/j.bbagen.2014.10.007

Lirman, D. (2000). Lesion regeneration in the branching coral Acropora palmata: effects of colonization, colony size, lesion size, and lesion shape. *Marine ecology. Progress series (Halstenbek)*, *197*, 209-215. https://doi.org/10.3354/meps197209

Liu, C., Huang, M., Han, C., Li, H., Wang, J., Huang, Y., Chen, Y., Zhu, J., Fu, G., Yu, H., Lei, Z., & Chu, X. (2021). A narrative review of the roles of muscle segment homeobox transcription factor family in cancer. *Ann Transl Med*, *9*(9), 810. https://doi.org/10.21037/atm-21-220

Liu, H., Bowes, R. C., van de Water, B., Sillence, C., Nagelkerke, J. F., & Stevens, J. L. (1997). Endoplasmic reticulum chaperones GRP78 and calreticulin prevent oxidative stress, Ca2+ disturbances, and cell death in renal epithelial cells. *Journal of Biological Chemistry*, *272*(35), 21751-21759. https://www.jbc.org/article/S0021-9258(19)65619-X/fulltext

Liu, H., Stephens, T. G., González-Pech, R. A., Beltran, V. H., Lapeyre, B., Bongaerts, P., Cooke, I., Aranda, M., Bourne, D. G., & Forêt, S. (2018). Symbiodinium genomes reveal adaptive evolution of functions related to coral-dinoflagellate symbiosis. *Communications Biology*, *1*(1), 95. https://doi.org/10.1038/s42003-018-0098-3

Liu, S. Y., Selck, C., Friedrich, B., Lutz, R., Vila-Farré, M., Dahl, A., Brandl, H., Lakshmanaperumal, N., Henry, I., & Rink, J. C. (2013). Reactivating head regrowth in a regeneration-deficient planarian species. *Nature (London)*, *500*(7460), 81-84. https://doi.org/10.1038/nature12414

Lock, C., Bentlage, B., & Raymundo, L. J. (2022). Calcium homeostasis disruption initiates rapid growth after micro-fragmentation in the scleractinian coral <em>Porites lobata</em&gt. *bioRxiv*, 2022.2002.2028.482414. https://doi.org/10.1101/2022.02.28.482414

López-Maury, L., Marguerat, S., & Bähler, J. (2008). Tuning gene expression to changing environments: from rapid responses to evolutionary adaptation. *Nature Reviews Genetics*, *9*(8), 583-593. https://doi.org/10.1038/nrg2398

Louis, Y. D., Bhagooli, R., Kenkel, C. D., Baker, A. C., & Dyall, S. D. (2017). Gene expression biomarkers of heat stress in scleractinian corals: Promises and limitations. *Comparative biochemistry and physiology. Toxicology & pharmacology*, *191*, 63-77. https://doi.org/10.1016/j.cbpc.2016.08.007

Love, M.I., Anders S, Huber W. (2014). Differential analysis of count data - the DESeq2 package. Genome Biology. doi:110.1186/s13059-014-0550-8

Love M, Soneson C, Robinson M, Patro R, Parker A, Thompson RC, et al. (2018) Import and summarize transcript-level estimates for transcript- and gene-level analysis. p. 5. Available: https://git.bioconductor.org/packages/tximport

Lu, C., Zhang, J., Nie, Z., Chen, J., Zhang, W., Ren, X., Yu, W., Liu, L., Jiang, C., & Zhang, Y. (2013). Study of microRNAs related to the liver regeneration of the whitespotted bamboo shark, Chiloscyllium plagiosum. *BioMed research international*, *2013*. https://doi.org/10.1155/2013/795676

Lust, K., & Tanaka, E. M. (2019). A comparative perspective on brain regeneration in amphibians and teleost fish. *Developmental neurobiology*, *79*(5), 424-436. https://doi.org/10.1002/dneu.22665

Luz, B. L. P., Capel, K. C. C., Zilberberg, C., Flores, A. A. V., Migotto, A. E., & Kitahara, M. V. (2018). A polyp from nothing: The extreme regeneration capacity of the Atlantic invasive sun corals Tubastraea coccinea and T. tagusensis (Anthozoa, Scleractinia). *Journal of Experimental Marine Biology and Ecology*, *503*, 60-65. https://doi.org/10.1016/j.jembe.2018.02.002

Luz, B. L. P. Z., Jia; Moya, Aurelie; Kitahara, Marcelo V.; Miller, David J. (2020). Gene expression in Tubastraea coccinea during regeneration.

Maddaluno, L., Urwyler, C., & Werner, S. (2017). Fibroblast growth factors: key players in regeneration and tissue repair. *Development (Cambridge)*, *144*(22), 4047-4060. https://doi.org/10.1242/dev.152587

Maianski, N. A., Geissler, J., Srinivasula, S. M., Alnemri, E. S., Roos, D., & Kuijpers, T. W. (2004). Functional characterization of mitochondria in neutrophils: a role restricted to apoptosis. *Cell Death & Differentiation*, *11*(2), 143-153. https://doi.org/10.1038/sj.cdd.4401320

Mansfield, K. M., & Gilmore, T. D. (2019). Innate immunity and cnidarian-Symbiodiniaceae mutualism. *Developmental and comparative immunology*, *90*, 199-209. https://doi.org/10.1016/j.dci.2018.09.020

Maor-Landaw, K., Karako-Lampert, S., Ben-Asher, H. W., Goffredo, S., Falini, G., Dubinsky, Z., & Levy, O. (2014). Gene expression profiles during short-term heat stress in the red sea coral

Stylophora pistillata. *Global Change Biology*, *20*(10), 3026-3035. https://doi.org/10.1111/gcb.12592

Mariscal, R. N., McLean, R. B., & Hand, C. (1977). The form and function of cnidarian spirocysts: 3. Ultrastructure of the thread and the function of spirocysts. *Cell and tissue research*, *178*, 427-433. https://doi.org/10.1007/BF00219566

Marques, I. J., Lupi, E., & Mercader, N. (2019). Model systems for regeneration: zebrafish. *Development (Cambridge)*, *146*(18). https://doi.org/10.1242/dev.167692

Marx, M. T. S., Souza, C. d. F., Almeida, A. P. G., Descovi, S. N., Bianchini, A. E., Martos-Sitcha, J. A., Martínez-Rodríguez, G., Antoniazzi, A. Q., & Baldisserotto, B. (2022). Expression of Ion Transporters and Na+/K+-ATPase and H+-ATPase Activities in the Gills and Kidney of Silver Catfish (Rhamdia quelen) Exposed to Different pHs. *Fishes*, *7*(5), 261. https://www.mdpi.com/2410-3888/7/5/261

Matsuda, S. B., Huffmyer, A. S., Lenz, E. A., Davidson, J. M., Hancock, J. R., Przybylowski, A., Innis, T., Gates, R. D., & Barott, K. L. (2020). Coral bleaching susceptibility is predictive of subsequent mortality within but not between coral species. *Frontiers in Ecology and Evolution*, *8*, 178. https://doi.org/10.3389/fevo.2020.00178

Matus, D. Q., Magie, C. R., Pang, K., Martindale, M. Q., & Thomsen, G. H. (2008). The Hedgehog gene family of the cnidarian, Nematostella vectensis, and implications for understanding metazoan Hedgehog pathway evolution. *Developmental biology*, *313*(2), 501-518. https://doi.org/https://doi.org/10.1016/j.ydbio.2007.09.032

Matus, D. Q., Pang, K., Daly, M., & Martindale, M. Q. (2007). Expression of Pax gene family members in the anthozoan cnidarian, Nematostella vectensis. *Evolution & development*, *9*(1), 25-38. https://doi.org/10.1111/j.1525-142X.2006.00135.x

Matus, D. Q., Thomsen, G. H., & Martindale, M. Q. (2007). FGF signaling in gastrulation and neural development in Nematostella vectensis, an anthozoan cnidarian. *Development genes and evolution*, *217*(2), 137-148. https://doi.org/10.1007/s00427-006-0122-3

Mayfield, A. B., Chen, Y. J., Lu, C. Y., & Chen, C. S. (2018). The proteomic response of the reef coral Pocillopora acuta to experimentally elevated temperatures. *PLoS One*, *13*(1), e0192001. https://doi.org/10.1371/journal.pone.0192001

Mayfield, A. B., Wang, L.-H., Tang, P.-C., Fan, T.-Y., Hsiao, Y.-Y., Tsai, C.-L., & Chen, C.-S. (2011). Assessing the impacts of experimentally elevated temperature on the biological composition and molecular chaperone gene expression of a reef coral. *PLoS One*, *6*(10), e26529. https://doi.org/10.1371/journal.pone.0026529

McClanahan, T., & Maina, J. (2003). Response of coral assemblages to the interaction between natural temperature variation and rare warm-water events. *Ecosystems*, *6*, 551-563. https://doi.org/10.1007/s10021-002-0104-x

McClanahan, T. R., Ateweberhan, M., Muhando, C. A., Maina, J., & Mohammed, M. S. (2007). Effects of climate and seawater temperature variation on coral bleaching and mortality. *Ecological Monographs*, *77*(4), 503-525. https://www-jstor-org.elibrary.jcu.edu.au/stable/pdf/27646104

McDermott, A. (2020). A microscopic mystery at the heart of mass-coral bleaching. *Proceedings of the National Academy of Sciences - PNAS*, *117*(5), 2232-2235. https://doi.org/10.1073/pnas.1921846117

McFall-Ngai, M., Hadfield, M. G., Bosch, T. C., Carey, H. V., Domazet-Lošo, T., Douglas, A. E., Dubilier, N., Eberl, G., Fukami, T., & Gilbert, S. F. (2013). Animals in a bacterial world, a new imperative for the life sciences. *Proceedings of the National Academy of Sciences*, *110*(9), 3229-3236. https://www.pnas.org/doi/pdf/10.1073/pnas.1218525110

McLachlan, R. H., Dobson, K. L., Schmeltzer, E. R., Thurber, R. V., & Grottoli, A. G. (2021). A review of coral bleaching specimen collection, preservation, and laboratory processing methods. *PeerJ*, *9*, e11763. https://www.proquest.com/docview/2549715345/fulltextPDF?pq-origsite=primo&sourcetype=Scholarly%20Journals

McLachlan, R. H., Price, J. T., Solomon, S. L., & Grottoli, A. G. (2020). Thirty years of coral heat-stress experiments: a review of methods. *Coral Reefs*, *39*(4), 885-902. https://doi.org/10.1007/s00338-020-01931-9

McLoughlin, F., Kim, M., Marshall, R. S., Vierstra, R. D., & Vierling, E. (2019). HSP101 Interacts with the Proteasome and Promotes the Clearance of Ubiquitylated Gene Aggregates. *Plant Physiol*, *180*(4), 1829-1847. https://doi.org/10.1104/pp.19.00263

McWilliams, T. G., & Muqit, M. M. (2017). PINK1 and Parkin: emerging themes in mitochondrial homeostasis. *Current opinion in cell biology*, *45*, 83-91. https://doi.org/10.1016/j.ceb.2017.03.013

Meints, R., & Pardy, R. L. (1980). Quantitative demonstration of cell surface involvement in a plant-animal symbiosis: lectin inhibition of reassociation. *Journal of cell science*, *43*(1), 239-251. https://doi.org/10.1242/jcs.43.1.239

Merselis, D. G., Lirman, D., & Rodriguez-Lanetty, M. (2018). Symbiotic immuno-suppression: is disease susceptibility the price of bleaching resistance? *PeerJ*, *6*, e4494. https://www.proquest.com/docview/2026319675/fulltextPDF?pq-origsite=primo&sourcetype=Scholarly%20Journals

Meschede, J., Šadić, M., Furthmann, N., Miedema, T., Sehr, D. A., Müller-Rischart, A. K., Bader, V., Berlemann, L. A., Pilsl, A., Schlierf, A., Barkovits, K., Kachholz, B., Rittinger, K., Ikeda, F., Marcus, K., Schaefer, L., Tatzelt, J., & Winklhofer, K. F. (2020). The parkin-coregulated gene product PACRG promotes TNF signaling by stabilizing LUBAC. *Sci Signal*, *13*(617). https://doi.org/10.1126/scisignal.aav1256

Meyer, B., Wurm, J. P., Koetter, P., Leisegang, M. S., Schilling, V., Buchhaupt, M., Held, M., Bahr, U., Karas, M., Heckel, A., Bohnsack, M. T., Woehnert, J., & Entian, K.-D. (2011). The Bowen-Conradi syndrome gene Nep1 (Emg1) has a dual role in eukaryotic ribosome biogenesis, as an essential assembly factor and in the methylation of psi 1191 in yeast 18S rRNA. *Nucleic acids research*, *39*(4), 1526-1537. https://www.ncbi.nlm.nih.gov/pmc/articles/PMC3045603/pdf/gkq931.pdf

Meyer, E., Aglyamova, G., & Matz, M. (2011). Profiling gene expression responses of coral larvae (Acropora millepora) to elevated temperature and settlement inducers using a novel RNA-Seq procedure. *Molecular Ecology*, *20*(17), 3599-3616. https://doi.org/10.1111/j.1365-294X.2011.05205.x

Michellod, D., Bien, T., Birgel, D., Jensen, M., Kleiner, M., Fearn, S., Zeidler, C., Gruber-Vodicka, H. R., Dubilier, N., & Liebeke, M. (2022). De novo phytosterol synthesis in animals. *bioRxiv*, 2022.2004. 2022.489198. DOI: 10.1126/science.add783

Miller, D. J., Hemmrich, G., Ball, E. E., Hayward, D. C., Khalturin, K., Funayama, N., Agata, K., & Bosch, T. C. (2007). The innate immune repertoire in Cnidaria-ancestral complexity and stochastic gene loss. *Genome Biology*, *8*, 1-13. https://doi.org/10.1186/gb-2007-8-4-r59

Minowada, G., Jarvis, L. A., Chi, C. L., Neubüser, A., Sun, X., Hacohen, N., Krasnow, M. A., & Martin, G. R. (1999). Vertebrate Sprouty genes are induced by FGF signaling and can cause chondrodysplasia when overexpressed. *Development (Cambridge)*, *126*(20), 4465-4475. https://doi.org/10.1242/dev.126.20.4465

Mongeon, R., Gleason, M. R., Masino, M. A., Fetcho, J. R., Mandel, G., Brehm, P., & Dallman, J. E. (2008). Synaptic homeostasis in a zebrafish glial glycine transporter mutant. *Journal of neurophysiology*, *100*(4), 1716-1723. https://doi.org/10.1152/jn.90596.2008

Mou, Z., Wang, X., Fu, Z., Dai, Y., Han, C., Ouyang, J., Bao, F., Hu, Y., & Li, J. (2002). Silencing of phosphoethanolamine N-methyltransferase results in temperature-sensitive male sterility and salt hypersensitivity in Arabidopsis. *The Plant cell*, *14*(9), 2031-2043. https://doi.org/10.1105/tpc.001701

Moya, A., Huisman, L., Forêt, S., Gattuso, J. P., Hayward, D. C., Ball, E. E., & Miller, D. J. (2015). Rapid acclimation of juvenile corals to CO2-mediated acidification by upregulation of heat shock gene and Bcl-2 genes. *Molecular Ecology*, *24*(2), 438-452. https://doi.org/10.1111/mec.13021

Murad, R., Macias-Muñoz, A., Wong, A., Ma, X., & Mortazavi, A. (2021). Coordinated gene expression and chromatin regulation during Hydra head regeneration. *Genome Biology and Evolution*, *13*(12), evab221. https://doi.org/10.1093/gbe/evab221

Mydlarz, L. D., Fuess, L., Mann, W., Pinzón, J. H., & Gochfeld, D. J. (2016). Cnidarian immunity: from genomes to phenomes. *The cnidaria, past, present and future: the world of medusa and her sisters*, 441-466. https://doi.org/10.1007/978-3-319-31305-4_28

Nagamune, K., & Sibley, L. D. (2006). Comparative genomic and phylogenetic analyses of calcium ATPases and calcium-regulated genes in the apicomplexa. *Molecular biology and evolution*, *23*(8), 1613-1627. https://doi.org/10.1093/molbev/msl026

Nagelkerken, I. A., & Bak, R. P. M. (1998). Differential regeneration of artificial lesions among sympatric morphs of the Caribbean corals Porites astreoides and Stephanocoenia michelinii. *Marine ecology. Progress series (Halstenbek)*, *163*, 279-283. https://doi.org/10.3354/meps163279

Nakagawa, T., & Yuan, J. (2000). Cross-talk between two cysteine protease families. Activation of caspase-12 by calpain in apoptosis. *J Cell Biol*, *150*(4), 887-894. https://doi.org/10.1083/jcb.150.4.887

Nakatani, Y., Kawakami, A., & Kudo, A. (2007). Cellular and molecular processes of regeneration, with special emphasis on fish fins. *Development, growth & differentiation*, *49*(2), 145-154. https://doi.org/10.1111/j.1440-169X.2007.00917.x

Nallasamy, S., Kaya Okur, H. S., Bhurke, A., Davila, J., Li, Q., Young, S. L., Taylor, R. N., Bagchi, M. K., & Bagchi, I. C. (2019). Msx Homeobox Genes Act Downstream of BMP2 to Regulate Endometrial Decidualization in Mice and in Humans. *Endocrinology*, *160*(7), 1631-1644. https://doi.org/10.1210/en.2019-00131

Negri, A., Marshall, P., & Heyward, A. (2007). Differing effects of thermal stress on coral fertilization and early embryogenesis in four Indo Pacific species. *Coral Reefs*, *26*, 759-763. https://doi.org/10.1007/s00338-007-0258-2

Nelson, H. R., & Altieri, A. H. (2019). Oxygen: the universal currency on coral reefs. *Coral Reefs*, *38*(2), 177-198. https://doi.org/10.1007/s00338-019-01765-0

Neubauer, E. F., Poole, A. Z., Detournay, O., Weis, V. M., & Davy, S. K. (2016). The scavenger receptor repertoire in six cnidarian species and its putative role in cnidarian-dinoflagellate symbiosis. *PeerJ*, *4*, e2692. https://www.ncbi.nlm.nih.gov/pmc/articles/PMC5119243/pdf/peerj-04-2692.pdf

Newmeyer, D. D., & Ferguson-Miller, S. (2003). Mitochondria: releasing power for life and unleashing the machineries of death. *Cell*, *112*(4), 481-490. https://www.cell.com/cell/fulltext/S0092-8674(03)00116-8

Ngugi, D. K., Ziegler, M., Duarte, C. M., & Voolstra, C. R. (2020). Genomic blueprint of glycine betaine metabolism in coral metaorganisms and their contribution to reef nitrogen budgets. *Iscience*, *23*(5), 101120. https://www.cell.com/iscience/fulltext/S2589-0042(20)30305-9

Nguyen, T. N., Padman, B. S., & Lazarou, M. (2016). Deciphering the molecular signals of PINK1/Parkin mitophagy. *Trends in cell biology*, *26*(10), 733-744. https://www.cell.com/trends/cell-biology/abstract/S0962-8924(16)30051-4

Nitschke, M.R., Craveiro, S.C., Brandão, C., Fidalgo, C., Serôdio, J., Calado, A.J. and Frommlet, J.C. (2020a). Description of Freudenthalidium gen. nov. and Halluxium gen. nov. to formally

recognize clades Fr3 and H as genera in the family Symbiodiniaceae (Dinophyceae). *Journal of Phycology*, *56*(4), pp.923-940. https://doi.org/10.1111/jpy.12999

Nitschke, M.R., Fidalgo, C., Simões, J., Brandão, C., Alves, A., Serôdio, J. and Frommlet, J.C. (2020b). Symbiolite formation: a powerful in vitro model to untangle the role of bacterial communities in the photosynthesis-induced formation of microbialites. *The ISME Journal*, *14*(6), pp.1533-1546. https://doi.org/10.1038/s41396-020-0629-z

Núñez-Pons, L., Bertocci, I., & Baghdasarian, G. (2017). Symbiont dynamics during thermal acclimation using cnidarian-dinoflagellate model holobionts. *Marine environmental research*, *130*, 303-314. https://doi.org/10.1016/j.marenvres.2017.08.005

Nyholm, S. V., & Graf, J. (2012). Knowing your friends: invertebrate innate immunity fosters beneficial bacterial symbioses. *Nature Reviews Microbiology*, *10*(12), 815-827. https://www.ncbi.nlm.nih.gov/pmc/articles/PMC3870473/pdf/nihms531725.pdf

Nyholm, S. V., & McFall-Ngai, M. (2004). The winnowing: establishing the squid–vibrio symbiosis. *Nature Reviews Microbiology*, *2*(8), 632-642. https://www.nature.com/articles/nrmicro957

Oakley, C. A., & Davy, S. K. (2018). Cell biology of coral bleaching. *Coral bleaching: patterns, processes, causes and consequences*, 189-211. https://link.springer.com/chapter/10.1007/978-3-319-75393-5_8

Oakley, C. A., Durand, E., Wilkinson, S. P., Peng, L., Weis, V. M., Grossman, A. R., & Davy, S. K. (2017). Thermal Shock Induces Host Proteostasis Disruption and Endoplasmic Reticulum Stress in the Model Symbiotic cnidarian Aiptasia. *Journal of proteome research*, *16*(6), 2121-2134. https://doi.org/10.1021/acs.jproteome.6b00797

Oren, U., Benayahu, Y., & Loya, Y. (1997). Effect of lesion size and shape on regeneration of the Red Sea coral Favia favus. *Marine ecology. Progress series (Halstenbek)*, *146*(1/3), 101-107. https://doi.org/10.3354/meps146101

Otero, J.H., Lizák, B. and Hendershot, L.M. (2010). Life and death of a BiP substrate. In *Seminars in cell & developmental biology* (Vol. 21, No. 5, pp. 472-478). Academic Press. https://doi.org/10.1016/j.semcdb.2009.12.008

Pajaud, J., Kumar, S., Rauch, C., Morel, F., & Aninat, C. (2012). Regulation of Signal Transduction by Glutathione Transferases. *International Journal of Hepatology*, *2012*, 137676. https://doi.org/10.1155/2012/137676

Pajaud, J., Ribault, C., Ben Mosbah, I., Rauch, C., Henderson, C., Bellaud, P., Aninat, C., Loyer, P., Morel, F., & Corlu, A. (2015). Glutathione transferases P1/P2 regulate the timing of signaling pathway activations and cell cycle progression during mouse liver regeneration. *Cell Death & Disease*, *6*(1), e1598-e1598. https://doi.org/10.1038/cddis.2014.562

Passamaneck, Y. J., & Martindale, M. Q. (2012). Cell proliferation is necessary for the regeneration of oral structures in the anthozoan cnidarian Nematostella vectensis. *BMC developmental biology*, *12*(1), 34-34. https://doi.org/10.1186/1471-213X-12-34

Patel, S. U., Hauser, P., & Ronan, J. (2022). Metabolomic Signatures of Ocean Acidification Stress in the Coral Acropora millepora. *The FASEB journal*, *36*(S1), n/a. https://doi.org/10.1096/fasebj.2022.36.S1.R6327

Peiris, T. H., Hoyer, K. K., & Oviedo, N. J. (2014). Innate immune system and tissue regeneration in planarians: An area ripe for exploration. *Seminars in immunology*, *26*(4), 295-302. https://doi.org/10.1016/j.smim.2014.06.005

Pellettieri, J., Fitzgerald, P., Watanabe, S., Mancuso, J., Green, D. R., & Sánchez Alvarado, A. (2010). Cell death and tissue remodeling in planarian regeneration. *Developmental biology*, *338*(1), 76-85. https://doi.org/10.1016/j.ydbio.2009.09.015

Petersen, H. O., Höger, S. K., Looso, M., Lengfeld, T., Kuhn, A., Warnken, U., Nishimiya-Fujisawa, C., Schnölzer, M., Krüger, M., Özbek, S., Simakov, O., & Holstein, T. W. (2015). A Comprehensive Transcriptomic and Proteomic Analysis of Hydra Head Regeneration. *Molecular biology and evolution*, *32*(8), 1928-1947. https://doi.org/10.1093/molbev/msv079

Petrou, K., Nunn, B. L., Padula, M. P., Miller, D. J., & Nielsen, D. A. (2021). Broad scale proteomic analysis of heat-destabilised symbiosis in the hard coral Acropora millepora. *Scientific Reports*, *11*(1), 19061-19061. https://doi.org/10.1038/s41598-021-98548-x

Pickrell, A.M. and Youle, R.J. (2015). The roles of PINK1, parkin, and mitochondrial fidelity in Parkinson's disease. *Neuron*, *85*(2), pp.257-273. https://www.cell.com/neuron/fulltext/S0896-6273(14)01088-5

Pinzón, J.H., Kamel, B., Burge, C.A., Harvell, C.D., Medina, M., Weil, E. and Mydlarz, L.D. (2015). Whole transcriptome analysis reveals changes in expression of immune-related genes during and after bleaching in a reef-building coral. *Royal Society open science*, *2*(4), p.140214. https://doi.org/10.1098/rsos.140214

Pispa, J., Matilainen, O. and Holmberg, C.I. (2020). Tissue-specific effects of temperature on proteasome function. *Cell Stress and Chaperones*, *25*(3), pp.563-572.Plotnikov, A., Zehorai, E., Procaccia, S., & Seger, R. (2011). The MAPK cascades: Signaling components, nuclear roles and mechanisms of nuclear translocation. *Biochimica et biophysica acta. Molecular cell research*, *1813*(9), 1619-1633. https://doi.org/10.1016/j.bbamcr.2010.12.012

Polato, N. R., Voolstra, C. R., Schnetzer, J., DeSalvo, M. K., Randall, C. J., Szmant, A. M., Medina, M., & Baums, I. B. (2010). Location-specific responses to thermal stress in larvae of the reef-building coral Montastraea faveolata. *PLoS One*, *5*(6), e11221. https://journals.plos.org/plosone/article/file?id=10.1371/journal.pone.0011221&type=printable

Pollock, F. J., Morris, P. J., Willis, B. L., & Bourne, D. G. (2011). The Urgent Need for Robust Coral Disease Diagnostics. *PLOS Pathogens*, *7*(10), e1002183. https://doi.org/10.1371/journal.ppat.1002183

Poole, A. Z., Kitchen, S. A., & Weis, V. M. (2016). The role of complement in cnidarian-dinoflagellate symbiosis and immune challenge in the sea anemone Aiptasia pallida. *Frontiers in Microbiology*, *7*, 519. https://www.ncbi.nlm.nih.gov/pmc/articles/PMC4840205/pdf/fmicb-07-00519.pdf

Portune, K. J., Voolstra, C. R., Medina, M., & Szmant, A. M. (2010). Development and heat stress-induced transcriptomic changes during embryogenesis of the scleractinian coral Acropora palmata. *Marine genomics*, *3*(1), 51-62. https://www.sciencedirect.com/science/article/pii/S1874778710000073?via%3Dihub

Poss, K. D. (2010). Advances in understanding tissue regenerative capacity and mechanisms in animals. *Nature reviews. Genetics*, *11*(10), 710-722. https://doi.org/10.1038/nrg2879

Poss, K. D., Wilson, L. G., & Keating, M. T. (2002). Heart Regeneration in Zebrafish. *Science (American Association for the Advancement of Science)*, *298*(5601), 2188-2190. https://doi.org/10.1126/science.1077857

Prekeris, R., Yang, B., Oorschot, V., Klumperman, J., & Scheller, R. H. (1999). Differential roles of syntaxin 7 and syntaxin 8 in endosomal trafficking. *Mol Biol Cell*, *10*(11), 3891-3908. https://doi.org/10.1091/mbc.10.11.3891

Pryor, S. H., Hill, R., Dixson, D. L., Fraser, N. J., Kelaher, B. P., & Scott, A. (2020). Anemonefish facilitate bleaching recovery in a host sea anemone. *Scientific Reports*, *10*(1), 18586. https://doi.org/10.1038/s41598-020-75585-6

Qiao, C., Chen, F., Liu, Z., Huang, T., Li, W., Zhang, G., & Luo, Y. (2022). Functional characterization of a catalytically promiscuous tryptophan decarboxylase from camptothecin-producing Camptotheca acuminata [Original Research]. *Frontiers in Plant Science*, *13*. https://doi.org/10.3389/fpls.2022.987348

Reddy, P. C., Gungi, A., & Unni, M. (2019). Cellular and Molecular Mechanisms of Hydra Regeneration. *Results Probl Cell Differ*, *68*, 259-290. https://doi.org/10.1007/978-3-030-23459-1_12

Reif, W.-E. (1978). Types of morphogenesis of the dermal skeleton in fossil sharks. *Paläontologische Zeitschrift*, *52*(1-2), 110-128. https://link.springer.com/article/10.1007/BF03006733

Reimschuessel, R. (2001). A fish model of renal regeneration and development. *42*(4), 285-291. https://doi.org/10.1093/ilar.42.4.285

Reimschuessel, R., Bennett, R.O., May, E.B. and Lipsky, M.M. (1993). Pathological alterations and new nephron development in rainbow trout (Oncorhynchus mykiss) following tetrachloroethylene contamination. *Journal of Zoo and Wildlife Medicine*, pp.503-507.Reimschuessel, R. and Biggs, K. (1996). Zebrafish model for nephron regeneration following injury. In *Cold Spring Harbor Symposium on Zebrafish Development and Genetics. Cold Spring Harbor, New York, April* (pp. 24-28). Revilla, Y., Callejo, M., Rodrıguez, J. M., Culebras, E., Nogal, M. L., Salas, M. L., Vinuela, E., & Fresno, M. (1998). Inhibition of

nuclear factor κB activation by a virus-encoded IκB-like gene. *Journal of Biological Chemistry*, *273*(9), 5405-5411. https://www.jbc.org/article/S0021-9258(17)47126-2/fulltext

Reynolds, J. M., Bruns, B. U., Fitt, W. K., & Schmidt, G. W. (2008). Enhanced photoprotection pathways in symbiotic dinoflagellates of shallow-water corals and other cnidarians. *Proceedings of the National Academy of Sciences - PNAS*, *105*(36), 13674-13678. https://doi.org/10.1073/pnas.0805187105

Ribeiro, A. O., de Oliveira, A. C., Costa, J. M., Nachtigall, P. G., Herkenhoff, M. E., Campos, V. F., Delella, F. K., & Pinhal, D. (2022). MicroRNA roles in regeneration: Multiple lessons from zebrafish. *Developmental dynamics*, *251*(4), 556-576. https://doi.org/https://doi.org/10.1002/dvdy.421

Richier, S., Rodriguez-Lanetty, M., Schnitzler, C. E., & Weis, V. M. (2008). Response of the symbiotic cnidarian Anthopleura elegantissima transcriptome to temperature and UV increase. *Comparative biochemistry and physiology. Part D, Genomics & proteomics*, *3*(4), 283-289. https://doi.org/10.1016/j.cbd.2008.08.001

Richter, K., Haslbeck, M., & Buchner, J. (2010). The heat shock response: life on the verge of death. *Molecular cell*, *40*(2), 253-266. https://www.cell.com/molecular-cell/fulltext/S1097-2765(10)00782-3

Rieger, S., & Sagasti, A. (2011). Hydrogen peroxide promotes injury-induced peripheral sensory axon regeneration in the zebrafish skin. *PLoS biology*, *9*(5), e1000621. https://doi.org/10.1371/journal.pbio.1000621

Roach, T. N., Dilworth, J., Jones, A. D., Quinn, R. A., & Drury, C. (2021). Metabolomic signatures of coral bleaching history. *Nature Ecology & Evolution*, *5*(4), 495-503. https://doi.org/10.1038/s41559-020-01388-7

Robbins, S. J., Singleton, C. M., Chan, C. X., Messer, L. F., Geers, A. U., Ying, H., Baker, A., Bell, S. C., Morrow, K. M., Ragan, M. A., Miller, D. J., Forêt, S., Voolstra, C. R., Tyson, G. W., & Bourne, D. G. (2019). A genomic view of the reef-building coral Porites lutea and its microbial symbionts. *Nature microbiology*, *4*(12), 2090-2100. https://doi.org/10.1038/s41564-019-0532-4

Roberty, S., & Plumier, J.-C. (2022). Bleaching physiology: who's the 'weakest link'—host vs. symbiont? *Emerging Topics in Life Sciences*, *6*(1), 17-32. https://doi.org/10.1042/ETLS20210228

Robinson, M.D., McCarthy, D.J., Smyth, G.K. (2009). edgeR: A Bioconductor package for differential expression analysis of digital gene expression data. Bioinformatics 26, 139–140. https://doi.org/10.1093/bioinformatics/btp616

Robison, J. D., & Warner, M. E. (2006). Differential impacts of photoacclimation and thermal stress on the photobiology of four different phylotypes of Symbiodinium (pyrrhophyta) 1. *Journal of phycology*, *42*(3), 568-579. https://doi.org/10.1111/j.1529-8817.2006.00232.x

Rodriguez, R. J., Henson, J., Van Volkenburgh, E., Hoy, M., Wright, L., Beckwith, F., Kim, Y.-O., & Redman, R. S. (2008). Stress tolerance in plants via habitat-adapted symbiosis. *The ISME Journal*, *2*(4), 404-416. https://www.nature.com/articles/ismej2007106.pdf

Rodriguez-Lanetty, M., Phillips, W. S., & Weis, V. M. (2006). Transcriptome analysis of a cnidarian–dinoflagellate mutualism reveals complex modulation of host gene expression. *BMC Genomics*, *7*(1), 1-11. https://doi.org/10.1186/1471-2164-7-23

Ron, D., & Walter, P. (2007). Signal integration in the endoplasmic reticulum unfolded gene response. *Nature Reviews Molecular Cell Biology*, *8*(7), 519-529. July 2007. https://doi.org/10.1038/nrm2199

Rosic, N., Kaniewska, P., Chan, C.-K. K., Ling, E. Y. S., Edwards, D., Dove, S., & Hoegh-Guldberg, O. (2014). Early transcriptional changes in the reef-building coral Acropora aspera in response to thermal and nutrient stress. *BMC Genomics*, *15*, 1-17. https://doi.org/10.1186/1471-2164-15-1052

Rosic, N. N., Pernice, M., Dunn, S., Dove, S., & Hoegh-Guldberg, O. (2010). Differential regulation by heat stress of novel cytochrome P450 genes from the dinoflagellate symbionts of reef-building corals. *Appl Environ Microbiol*, *76*(9), 2823-2829. https://doi.org/10.1128/aem.02984-09

Rosset, S. L., Oakley, C. A., Ferrier-Pagès, C., Suggett, D. J., Weis, V. M., & Davy, S. K. (2021). The molecular language of the cnidarian–dinoflagellate symbiosis. *Trends in Microbiology*, *29*(4), 320-333. https://www.cell.com/trends/microbiology/abstract/S0966-842X(20)30232-8

Röttinger, E. (2021). Nematostella vectensis , an Emerging Model for Deciphering the Molecular and Cellular Mechanisms Underlying Whole-Body Regeneration. *Cells (Basel, Switzerland)*, *10*(10), 2692. https://doi.org/10.3390/cells10102692

Rowan, R. (2004). Thermal adaptation in reef coral symbionts. *Nature*, *430*(7001), 742-742. https://www.nature.com/articles/430742a.pdf

Rowe, R., & Goldspink, G. (1969). Muscle fibre growth in five different muscles in both sexes of mice. *Journal of anatomy*, *104*(Pt 3), 519. https://www.ncbi.nlm.nih.gov/pmc/articles/PMC1231952/

Rowlerson, A., & Veggetti, A. (2001). Cellular mechanisms of post-embryonic muscle growth in aquaculture species. In *Muscle development and growth.* (pp. 103-140). Academic Press. https://cir.nii.ac.jp/crid/1574231875094328448

Ryu, T., Veilleux, H. D., Munday, P. L., Jung, I., Donelson, J. M., & Ravasi, T. (2020). An epigenetic signature for within-generational plasticity of a reef fish to ocean warming. *FRONTIERS IN MARINE SCIENCE*, *7*, 284. https://doi.org/10.3389/fmars.2020.00284

Safaie, A., Silbiger, N. J., McClanahan, T. R., Pawlak, G., Barshis, D. J., Hench, J. L., Rogers, J. S., Williams, G. J., & Davis, K. A. (2018). High frequency temperature variability reduces the

risk of coral bleaching. *Nature Communications*, *9*(1), 1671. https://doi.org/10.1038/s41467-018-04074-2

Saier Jr, M. H., Yen, M. R., Noto, K., Tamang, D. G., & Elkan, C. (2009). The transporter classification database: recent advances. *Nucleic acids research*, *37*(suppl_1), D274-D278. https://doi.org/10.1093/nar/gkn862

Sato, M., Nanami, A., Bayne, C. J., Makino, M., & Hori, M. (2020). Changes in the potential stocks of coral reef ecosystem services following coral bleaching in Sekisei Lagoon, southern Japan: implications for the future under global warming. *Sustainability Science*, *15*(3), 863-883. https://doi.org/10.1007/s11625-019-00778-6

Schneider, E., & Hunke, S. (1998). ATP-binding-cassette (ABC) transport systems: Functional and structural aspects of the ATP-hydrolyzing subunits/domains. *FEMS Microbiology Reviews*, *22*(1), 1-20. https://doi.org/10.1111/j.1574-6976.1998.tb00358.x

Sehring, I. M., & Weidinger, G. (2020). Recent advancements in understanding fin regeneration in zebrafish. *Wiley Interdisciplinary Reviews: Developmental Biology*, *9*(1), e367. https://wires.onlinelibrary.wiley.com/doi/pdfdirect/10.1002/wdev.367?download=true

Seifert, A. W., & Muneoka, K. (2018). The blastema and epimorphic regeneration in mammals. *Dev Biol*, *433*(2), 190-199. https://doi.org/10.1016/j.ydbio.2017.08.007

Sen, C. K., & Ghatak, S. (2015). miRNA control of tissue repair and regeneration. *Am J Pathol*, *185*(10), 2629-2640. https://doi.org/10.1016/j.ajpath.2015.04.001

Seveso, D., Montano, S., Strona, G., Orlandi, I., Galli, P., & Vai, M. (2014). The susceptibility of corals to thermal stress by analyzing Hsp60 expression. *Marine environmental research*, *99*, 69-75. https://doi.org/10.1016/j.marenvres.2014.06.008

Shao, Y., Wang, X.-B., Zhang, J.-J., Li, M.-L., Wu, S.-S., Ma, X.-Y., Wang, X., Zhao, H.-F., Li, Y., Zhu, H. H., Irwin, D. M., Wang, D.-P., Zhang, G.-J., Ruan, J., & Wu, D.-D. (2020). Genome and single-cell RNA-sequencing of the earthworm Eisenia andrei identifies cellular mechanisms underlying regeneration. *Nature Communications*, *11*(1), 2656. https://doi.org/10.1038/s41467-020-16454-8

Shende, P., Bhandarkar, S., & Prabhakar, B. (2019). Heat Shock Genes and their Protective Roles in Stem Cell Biology. *Stem cell reviews*, *15*(5), 637-651. https://doi.org/10.1007/s12015-019-09903-5

Shinzato, C., Khalturin, K., Inoue, J., Zayasu, Y., Kanda, M., Kawamitsu, M., Yoshioka, Y., Yamashita, H., Suzuki, G., & Satoh, N. (2020). Eighteen Coral Genomes Reveal the Evolutionary Origin of Acropora Strategies to Accommodate Environmental Changes. *Molecular biology and evolution*, *38*(1), 16-30. https://doi.org/10.1093/molbev/msaa216

Shumaker, A., Putnam, H. M., Qiu, H., Price, D. C., Zelzion, E., Harel, A., Wagner, N. E., Gates, R. D., Yoon, H. S., & Bhattacharya, D. (2019). Genome analysis of the rice coral Montipora capitata. *Scientific Reports*, *9*(1), 2571. https://doi.org/10.1038/s41598-019-39274-3

Sikes, J. M., & Newmark, P. A. (2013). Restoration of anterior regeneration in a planarian with limited regenerative ability. *Nature (London)*, *500*(7460), 77-80. https://doi.org/10.1038/nature12403

Singh, S. P., Holdway, J. E., & Poss, K. D. (2012). Regeneration of amputated zebrafish fin rays from de novo osteoblasts. *Developmental Cell*, *22*(4), 879-886. https://www.cell.com/developmental-cell/fulltext/S1534-5807(12)00129-3?script=true&code=cell-site

Sire, J.-Y. A., Marie-Andree. (2004). Scale development in fish: a review, with description of sonic hedgehog (shh) expression in the zebrafish (Danio rerio). *International Journal of Developmental Biology*, *48*, 233-247. http://jysire.free.fr/PDF/PDF%202001-2005/2004%20Scale%20Devt%20IJDB.pdf

Slattery, M., Pankey, M. S., & Lesser, M. P. (2019). Annual thermal stress increases a soft coral's susceptibility to bleaching. *Scientific Reports*, *9*(1), 1-10. https://doi.org/10.1038/s41598-019-44566-9

Sottile, M. L., & Nadin, S. B. (2018). Heat shock genes and DNA repair mechanisms: an updated overview. *Cell stress & chaperones*, *23*(3), 303-315. https://doi.org/10.1007/s12192-017-0843-4

Spakova, I., Zelko, A., Rabajdova, M., Kolarcik, P., Rosenberger, J., Zavacka, M., Marekova, M., Madarasova Geckova, A., van Dijk, J. P., & Reijneveld, S. A. (2020). MicroRNA molecules as predictive biomarkers of adaptive responses to strength training and physical inactivity in haemodialysis patients. *Scientific Reports*, *10*(1), 15597. https://doi.org/10.1038/s41598-020-72542-1

Steele, R. E., David, C. N., & Technau, U. (2011). A genomic view of 500 million years of cnidarian evolution. *Trends in genetics*, *27*(1), 7-13. https://www.cell.com/trends/genetics/abstract/S0168-9525(10)00208-8

Steichele, M., Sauermann, L., Pan, Q., Moneer, J., de la Porte, A., Heß, M., Mercker, M., Strube, C., Jenewein, M. and Böttger, A., 2024. HvNotch coordinates two independent pattern forming systems during head regeneration in Hydra by supporting a lateral inhibition process restricting the tentacle system. *bioRxiv*, pp.2024-02. https://doi.org/10.1101/2024.02.02.578611

Steinberg, R. K., Johnston, E. L., Bednarek, T., Dafforn, K. A., & Ainsworth, T. D. (2021). Its What's on the Inside That Counts: An Effective, Efficient, and Streamlined Method for Quantification of Octocoral Symbiodiniaceae and Chlorophyll. *FRONTIERS IN MARINE SCIENCE*, *8*. https://doi.org/10.3389/fmars.2021.710730

Stewart, Z. K., Pavasovic, A., Hock, D. H., & Prentis, P. J. (2017). Transcriptomic investigation of wound healing and regeneration in the cnidarian Calliactis polypus. *Scientific Reports*, *7*(1), 41458-41458. https://doi.org/10.1038/srep41458

Strader, M. E. Q., Kate M. (2022). The role of gene expression and symbiosis in reef-building coral acquired heat tolerance. *Nature Communications*, *13*. https://doi.org/10.1038/s41467-022-32217-z

Stuhr, M., Blank-Landeshammer, B., Reymond, C. E., Kollipara, L., Sickmann, A., Kucera, M., & Westphal, H. (2018). Disentangling thermal stress responses in a reef-calcifier and its photosymbionts by shotgun proteomics. *Scientific Reports*, *8*(1), 3524. https://doi.org/10.1038/s41598-018-21875-z

Stuhr, M., Meyer, A., Reymond, C. E., Narayan, G. R., Rieder, V., Rahnenführer, J., Kucera, M., Westphal, H., Muhando, C. A., & Hallock, P. (2018). Variable thermal stress tolerance of the reef-associated symbiont-bearing foraminifera Amphistegina linked to differences in symbiont type. *Coral Reefs*, *37*, 811-824. https://doi.org/10.1007/s00338-018-1707-9

Su, F., Yang, H., & Sun, L. (2022). A Review of Histocytological Events and Molecular Mechanisms Involved in Intestine Regeneration in Holothurians. *Biology*, *11*(8), 1095. https://www.mdpi.com/2079-7737/11/8/1095

https://mdpi-res.com/d_attachment/biology/biology-11-01095/article_deploy/biology-11-01095.pdf?version=1658499131

Suggett, D. J., & Smith, D. J. (2020). Coral bleaching patterns are the outcome of complex biological and environmental networking. *Global Change Biology*, *26*(1), 68-79. https://doi.org/10.1111/gcb.14871

Suggett, D. J., Warner, M. E., Smith, D. J., Davey, P., Hennige, S., & Baker, N. R. (2008). Photosynthesis and production of hydrogen peroxide by Symbiodinium (pyrrhophyta) phylotypes with different thermal tolerances 1. *Journal of phycology*, *44*(4), 948-956. https://onlinelibrary.wiley.com/doi/10.1111/j.1529-8817.2008.00537.x

Sully, S., Burkepile, D. E., Donovan, M., Hodgson, G., & Van Woesik, R. (2019). A global analysis of coral bleaching over the past two decades. *Nature Communications*, *10*(1), 1264. https://doi.org/10.1038/s41467-019-09238-2

Sun, Y., & Ripps, H. (1992). Rhodopsin regeneration in the normal and in the detached/replaced retina of the skate. *Experimental eye research*, *55*(5), 679-689. https://doi.org/10.1016/0014-4835(92)90173-P

Szabó, M., Larkum, A. W. D., & Vass, I. (2020). A Review: The Role of Reactive Oxygen Species in Mass Coral Bleaching. In (pp. 459-488). Springer International Publishing. https://doi.org/10.1007/978-3-030-33397-3_17

Tanaka, Elly M., & Reddien, Peter W. (2011). The Cellular Basis for Animal Regeneration. *Developmental Cell*, *21*(1), 172-185. https://doi.org/https://doi.org/10.1016/j.devcel.2011.06.016

Tawk, M., Tuil, D., Torrente, Y., Vriz, S., & Paulin, D. (2002). High-efficiency gene transfer into adult fish: a new tool to study fin regeneration. *genesis*, *32*(1), 27-31. https://doi.org/10.1002/gene.10025

Tchernov, D., Kvitt, H., Haramaty, L., Bibbyd, T. S., Gorbunov, M. Y., Rosenfeld, H., & Falkowski, P. G. (2011). Apoptosis and the selective survival of host animals following thermal bleaching in zooxanthellate corals. *Proceedings of the National Academy of Sciences - PNAS*, *108*(24), 9905-9909. https://doi.org/10.1073/pnas.1106924108

Tedeschi, J. N., Kennington, W., Tomkins, J. L., Berry, O., Whiting, S., Meekan, M. G., & Mitchell, N. J. (2016). Heritable variation in heat shock gene expression: a potential mechanism for adaptation to thermal stress in embryos of sea turtles. *Proceedings of the Royal Society B: Biological Sciences*, *283*(1822), 20152320. https://doi.org/10.1098/rspb.2015.2320

Thomas, L., & Palumbi, S. R. (2017). The genomics of recovery from coral bleaching. *Proceedings of the Royal Society B: Biological Sciences*, *284*(1865), 20171790. https://doi.org/10.1098/rspb.2017.1790

Thomas, T., Rusch, D., DeMaere, M. Z., Yung, P. Y., Lewis, M., Halpern, A., Heidelberg, K. B., Egan, S., Steinberg, P. D., & Kjelleberg, S. (2010). Functional genomic signatures of sponge bacteria reveal unique and shared features of symbiosis. *The ISME Journal*, *4*(12), 1557-1567. https://doi.org/10.1038/ismej.2010.74

Thummasan, M., Casareto, B. E., Ramphul, C., Suzuki, T., Toyoda, K., & Suzuki, Y. (2021). Physiological responses (Hsps 60 and 32, caspase 3, H2O2 scavenging, and photosynthetic activity) of the coral Pocillopora damicornis under thermal and high nitrate stresses. *Marine Pollution Bulletin*, *171*, 112737. https://doi.org/10.1016/j.marpolbul.2021.112737

Thwaites, D. T., & Anderson, C. M. (2011). The SLC36 family of proton-coupled amino acid transporters and their potential role in drug transport. *Br J Pharmacol*, *164*(7), 1802-1816. https://doi.org/10.1111/j.1476-5381.2011.01438.x

Tiozzo, S., & Copley, R. R. (2015). Reconsidering regeneration in metazoans: an evo-devo approach. *Frontiers in Ecology and Evolution*, *3*. https://doi.org/10.3389/fevo.2015.00067

Tomanek, L. (2010). Variation in the heat shock response and its implication for predicting the effect of global climate change on species' biogeographical distribution ranges and metabolic costs. *Journal of Experimental Biology*, *213*(6), 971-979. https://doi.org/10.1242/jeb.038034

Tomczyk, S., Fischer, K., Austad, S., & Galliot, B. (2015). Hydra, a powerful model for aging studies. *Invertebrate reproduction & development*, *59*(sup1), 11-16. https://doi.org/10.1080/07924259.2014.927805

Townley, R. A., Boeve, B. F., & Benarroch, E. E. (2018). Progranulin: Functions and neurologic correlations. *Neurology*, *90*(3), 118-125. https://doi.org/10.1212/wnl.0000000000004840

Tracy, A. M., Koren, O., Douglas, N., Weil, E., & Harvell, C. D. (2015). Persistent shifts in C aribbean coral microbiota are linked to the 2010 warm thermal anomaly. *Environmental*

Microbiology Reports, *7*(3), 471-479. https://ami-journals.onlinelibrary.wiley.com/doi/10.1111/1758-2229.12274

Traylor-Knowles, N., Rose, N. H., Sheets, E. A., & Palumbi, S. R. (2017). Early Transcriptional Responses during Heat Stress in the Coral Acropora hyacinthus. *The Biological bulletin (Lancaster)*, *232*(2), 91-100. https://doi.org/10.1086/692717

Tucker, A. S., & Fraser, G. J. (2014). Evolution and developmental diversity of tooth regeneration. Seminars in cell & developmental biology. https://doi.org/10.1016/j.semcdb.2013.12.013

Ulstrup, K., Ralph, P., Larkum, A., & Kühl, M. (2006). Intra-colonial variability in light acclimation of zooxanthellae in coral tissues of Pocillopora damicornis. *Marine Biology*, *149*, 1325-1335. https://doi.org/10.1007/s00227-006-0286-4

Umesono, Y., Tasaki, J., Nishimura, Y., Hrouda, M., Kawaguchi, E., Yazawa, S., Nishimura, O., Hosoda, K., Inoue, T., & Agata, K. (2013). The molecular logic for planarian regeneration along the anterior-posterior axis. *Nature (London)*, *500*(7460), 73-76. https://doi.org/10.1038/nature12359

Van De Water, J. A., Leggat, W., Bourne, D. G., Van Oppen, M. J., Willis, B. L., & Ainsworth, T. D. (2015). Elevated seawater temperatures have a limited impact on the coral immune response following physical damage. *Hydrobiologia*, *759*, 201-214. https://doi.org/10.1007/s10750-015-2243-z

Van der Burg, C. A., Pavasovic, A., Gilding, E. K., Pelzer, E. S., Surm, J. M., Smith, H. L., Walsh, T. P., & Prentis, P. J. (2020). The rapid regenerative response of a model sea anemone species Exaiptasia pallida is characterised by tissue plasticity and highly coordinated cell communication. *Marine Biotechnology*, *22*(2), 285-307. https://doi.org/10.1007/s10126-020-09951-w

Van der Burg, C. A., & Prentis, P. J. (2021). The Tentacular Spectacular: Evolution of Regeneration in Sea Anemones. *Genes*, *12*(7), 1072. https://www.mdpi.com/2073-4425/12/7/1072

https://mdpi-res.com/d_attachment/genes/genes-12-01072/article_deploy/genes-12-01072-v3.pdf?version=1626743083

Van Oppen, M. J., & Blackall, L. L. (2019). Coral microbiome dynamics, functions and design in a changing world. *Nature Reviews Microbiology*, *17*(9), 557-567. https://doi.org/10.1038/s41579-019-0223-4

Van Oppen, M. J. H., & Blackall, L. L. (2019). Coral microbiome dynamics, functions and design in a changing world. *Nature Reviews Microbiology*, *17*(9), 557-567. https://doi.org/10.1038/s41579-019-0223-4

Van Woesik, R., Houk, P., Isechal, A. L., Idechong, J. W., Victor, S., & Golbuu, Y. (2012). Climate-change refugia in the sheltered bays of P alau: analogs of future reefs. *Ecology and evolution*, *2*(10), 2474-2484. https://doi.org/10.1002/ece3.363

Varricchio, L., Falchi, M., Dall'Ora, M., De Benedittis, C., Ruggeri, A., Uversky, V. N., & Migliaccio, A. R. (2017). Calreticulin: Challenges Posed by the Intrinsically Disordered Nature of Calreticulin to the Study of Its Function [Hypothesis and Theory]. *Frontiers in Cell and Developmental Biology*, *5*. https://doi.org/10.3389/fcell.2017.00096

Vidal-Dupiol, J., Adjeroud, M., Roger, E., Foure, L., Duval, D., Mone, Y., Ferrier-Pages, C., Tambutte, E., Tambutte, S., Zoccola, D., Allemand, D., & Mitta, G. (2009). Coral bleaching under thermal stress: Putative involvement of host/symbiont recognition mechanisms. *BMC physiology*, *9*(1), 14-14. https://doi.org/10.1186/1472-6793-9-14

Vogg, M. C., Galliot, B., & Tsiairis, C. D. (2019). Model systems for regeneration: Hydra. *Development*, *146*(21). https://doi.org/10.1242/dev.177212

Von Marschall, Z., Mok, S., Phillips, M. D., McKnight, D. A., & Fisher, L. W. (2012). Rough endoplasmic reticulum trafficking errors by different classes of mutant dentin sialophosphogene (DSPP) cause dominant negative effects in both dentinogenesis imperfecta and dentin dysplasia by entrapping normal DSPP. *Journal of Bone and Mineral Research*, *27*(6), 1309-1321. https://doi.org/10.1002/jbmr.1573

Von Xylander, N. S. H., Young, S. A., Cole, C., Smith, T. K., & Allison, N. (2023). Sterols, free fatty acids, and total fatty acid content in the massive Porites spp. corals cultured under different pCO2 and temperature treatments. *Coral Reefs*, *42*(2), 551-566. https://doi.org/10.1007/s00338-023-02356-w

Voolstra, C. R., Schnetzer, J., Peshkin, L., Randall, C. J., Szmant, A. M., & Medina, M. (2009). Effects of temperature on gene expression in embryos of the coral Montastraea faveolata. *BMC Genomics*, *10*, 1-9. https://doi.org/10.1186/1471-2164-10-627

Vorontsova, M. A., & Liosner, L. D. (1960). *Asexual propagation and regeneration*. https://cir.nii.ac.jp/crid/1130000794903357952

Wall, C. B., Ricci, C. A., Wen, A. D., Ledbetter, B. E., Klinger, D. E., Mydlarz, L. D., Gates, R. D., & Putnam, H. M. (2021). Shifting baselines: Physiological legacies contribute to the response of reef corals to frequent heatwaves. *Functional ecology*, *35*(6), 1366-1378. https://doi.org/10.1111/1365-2435.13795

Wall, C. B., Ritson-Williams, R., Popp, B. N., & Gates, R. D. (2019). Spatial variation in the biochemical and isotopic composition of corals during bleaching and recovery. *Limnology and Oceanography*, *64*(5), 2011-2028. https://doi.org/10.1002/lno.11166

Wang, J., Lee, J., Liem, D., & Ping, P. (2017). HSPA5 Gene encoding Hsp70 chaperone BiP in the endoplasmic reticulum. *Gene*, *618*, 14-23. https://doi.org/10.1016/j.gene.2017.03.005

Wang, X. M., Zeng, P., Fang, Y. Y., Zhang, T., & Tian, Q. (2021). Progranulin in neurodegenerative dementia. *Journal of Neurochemistry*, *158*(2), 119-137. https://onlinelibrary.wiley.com/doi/pdfdirect/10.1111/jnc.15378?download=true

Warner, J., Amiel, A., Johnston, H., & Röttinger, E. (2020). Regeneration is a partial redeployment of the embryonic gene network. https://hal.science/hal-03021512/document

Warner, J. F., Johnston, H., Amiel, A. R., Nedoncelle, K., Carvalho, J. E., & Röttinger, E. (2021). Whole body regeneration deploys a rewired embryonic gene regulatory network logic. In. Cold Spring Harbor: Cold Spring Harbor Laboratory Press. https://doi.org/10.1101/658930

Weis, V. M. (2008). Cellular mechanisms of cnidarian bleaching: Stress causes the collapse of symbiosis. *Journal of Experimental Biology*, *211*(19), 3059-3066. https://doi.org/10.1242/jeb.009597

Weis, V. M. (2022). Seminal Early Studies on the Mechanisms of Coral Bleaching. In (Vol. 243, pp. 12-13): The University of Chicago Press Chicago, IL. https://www.journals.uchicago.edu/doi/full/10.1086/721689x

Weis, V. M., Davy, S. K., Hoegh-Guldberg, O., Rodriguez-Lanetty, M., & Pringle, J. R. (2008). Cell biology in model systems as the key to understanding corals. *Trends in ecology & evolution (Amsterdam)*, *23*(7), 369-376. https://doi.org/10.1016/j.tree.2008.03.004

Wenger, Y., & Galliot, B. (2013). Punctuated emergences of genetic and phenotypic innovations in eumetazoan, bilaterian, euteleostome, and hominidae ancestors. *Genome Biology and Evolution*, *5*(10), 1949-1968. https://doi.org/10.1093/gbe/evt142

Weston, A. J., Dunlap, W. C., Shick, J. M., Klueter, A., Iglic, K., Vukelic, A., Starcevic, A., Ward, M., Wells, M. L., Trick, C. G., & Long, P. F. (2012). A Profile of an Endosymbiont-enriched Fraction of the Coral Stylophora pistillata Reveals Genes Relevant to Microbial-Host Interactions*. *Molecular & Cellular Proteomics*, *11*(6), M111.015487. https://doi.org/https://doi.org/10.1074/mcp.M111.015487

White, A. T., Vogt, H. P., & Arin, T. (2000). Philippine coral reefs under threat: the economic losses caused by reef destruction. *Marine Pollution Bulletin*, *40*(7), 598-605. https://doi.org/10.1016/S0025-326X(00)00022-9

Whitworth, A. J., & Pallanck, L. J. (2017). PINK1/Parkin mitophagy and neurodegeneration—what do we really know in vivo? *Current opinion in genetics & development*, *44*, 47-53. https://doi.org/10.1016/j.gde.2017.01.016

Wood-Charlson, E. M., Hollingsworth, L. L., Krupp, D. A., & Weis, V. M. (2006). Lectin/glycan interactions play a role in recognition in a coral/dinoflagellate symbiosis. *Cellular Microbiology*, *8*(12), 1985-1993. https://doi.org/10.1111/j.1462-5822.2006.00765.x

Woodhams, D. C., Bletz, M. C., Becker, C. G., Bender, H. A., Buitrago-Rosas, D., Diebboll, H., Huynh, R., Kearns, P. J., Kueneman, J., & Kurosawa, E. (2020). Host-associated microbiomes are predicted by immune system complexity and climate. *Genome Biology*, *21*, 1-20. https://doi.org/10.1186/s13059-019-1908-8

Xiang, T., Nelson, W., Rodriguez, J., Tolleter, D., & Grossman, A. R. (2015). Symbiodinium transcriptome and global responses of cells to immediate changes in light intensity when

grown under autotrophic or mixotrophic conditions. *The Plant journal : for cell and molecular biology*, *82*(1), 67-80. https://doi.org/10.1111/tpj.12789

Xirodimas, D. P., Sundqvist, A., Nakamura, A., Shen, L., Botting, C., & Hay, R. T. (2008). Ribosomal genes are targets for the NEDD8 pathway. *EMBO reports*, *9*(3), 280-286. https://doi.org/10.1038/embor.2008.10

Xu, J., Mead, O., Moya, A., Caglar, C., Miller, D.J., Adamski, M. and Adamska, M. (2023). Wound healing and regeneration in the reef building coral Acropora millepora. *Frontiers in Ecology and Evolution*, *10*, p.979278.Yang, E. V., Gardiner, D. M., Carlson, M. R. J., Nugas, C. A., & Bryant, S. V. (1999). Expression of Mmp-9 and related matrix metallogenease genes during axolotl limb regeneration. *Developmental dynamics*, *216*(1), 2-9. https://doi.org/10.3389/fevo.2022.979278

Yu, T.-y., Lu, M.-x., & Cui, Y.-d. (2018). Characterization of T-complex polypeptide 1 (TCP-1) from the Chilo suppressalis HSP60 family and its expression in response to temperature stress. *Journal of Integrative Agriculture*, *17*(5), 1032-1039. https://doi.org/https://doi.org/10.1016/S2095-3119(17)61775-1

Zaragoza, W. J., Krediet, C. J., Meyer, J. L., Canas, G., Ritchie, K. B., & Teplitski, M. (2014). Outcomes of infections of sea anemone Aiptasia pallida with Vibrio spp. pathogenic to corals. *Microbial ecology*, *68*, 388-396. https://doi.org/10.1007/s00248-014-0397-2

Zhang, Y., Zhou, Z., Wang, L., & Huang, B. (2018). Transcriptome, expression, and activity analyses reveal a vital heat shock gene 70 in the stress response of stony coral Pocillopora damicornis. *Cell Stress and Chaperones*, *23*, 711-721. https://doi.org/10.1007/s12192-018-0883-4

Zheng, H., Ying, H., Wiedemeyer, R., Yan, H., Quayle, S. N., Ivanova, E. V., Paik, J.-H., Zhang, H., Xiao, Y., & Perry, S. R. (2010). PLAGL2 regulates Wnt signaling to impede differentiation in neural stem cells and gliomas. *Cancer cell*, *17*(5), 497-509. https://www.cell.com/action/showPdf?pii=S1535-6108%2810%2900147-9

Zhou, J., Lin, Z. J., Cai, Z. H., Zeng, Y. H., Zhu, J. M., & Du, X. P. (2020). Opportunistic bacteria use quorum sensing to disturb coral symbiotic communities and mediate the occurrence of coral bleaching. *Environmental Microbiology*, *22*(5), 1944-1962. https://doi.org/10.1111/1462-2920.15009

Zhou, M., Tang, W., Fu, Y., Xu, X., Wang, Z., Lu, Y., Liu, F., Yang, X., Wei, X., & Zhang, Y. (2015). Progranulin protects against renal ischemia/reperfusion injury in mice. *Kidney international*, *87*(5), 918-929. https://doi.org/10.1038/ki.2014.403

Zhou, Z., Zhao, S., Ni, J., Su, Y., Wang, L., & Xu, Y. (2018). Effects of environmental factors on C-type lectin recognition to zooxanthellae in the stony coral Pocillopora damicornis. *Fish & shellfish immunology*, *79*, 228-233. https://doi.org/10.1016/j.fsi.2018.05.026

Ziegler, M., Seneca, F. O., Yum, L. K., Palumbi, S. R., & Voolstra, C. R. (2017). Bacterial community dynamics are linked to patterns of coral heat tolerance. *Nature Communications*, *8*(1), 14213. https://doi.org/10.1038/ncomms14213

Zimmerman, A. M., & Lowery, M. S. (1999). Hyperplastic development and hypertrophic growth of muscle fibers in the white seabass (Atractoscion nobilis). *Journal of Experimental Zoology*, *284*(3), 299-308. https://doi.org/10.1002/(SICI)1097-010X(19990801)284:3<299::AID-JEZ7>3.0.CO;2-6

Appendices

Chapter 2 – Appendix

Pilot Experiment

Introduction

This pilot experiment was carried out to identify the best time points for sampling *Heliofungia* during the regeneration experiment that will take place later.

Methods

Four *Heliofungia actiniformis* corals were chosen from a stock of *Heliofungia* located at the Australian Institute of Marine Sciences (AIMS). The four individuals were separated into two tanks, two corals per tank, and kept at 27ºC with artificially created normal daylight hours and left to acclimate for fourteen days. Post-acclimatisation, randomly chosen tentacles were severed from each of the specimens. A Canon mirrorless M6 camera was set up to document the regenerative growth of the amputated tentacles by continuously taking photos for a set amount of time (between 1-7hrs, in the first 24hrs). Each day of the experiment started with a 1-3hrs continuous photo "video" documenting the first hours in each new 24hr cycle and hourly photos following the videos. The photos were analysed daily to assess the degree of regeneration.

Results

Looking at the continuous photos, the main healing occurs within the first 24 hours of amputation. The wounds close, creating a sort of scab-like formation and the tentacles refill with water within the first two hours (fig.1). By the end of the first 24 hours, the "scab" starts turning into a smooth surface with "pinch" like ending (fig 2). In the following 24-48 hours, the "scab" disappears, leaving a nubbin with no sign of damage (fig. 3), other than the absence of a tentacle "head" (white tip at the top of the tentacle). The tip started to show on day four (fig. 4) and it took ten days to grow from nubbin lid to tentacle "head". In total it took the Heliofungia fourteen days to completely regenerate their tentacles regardless of whether they were damaged at the base or at a distance from the base.

Figure. A2.1. Morphological stages of tentacle regeneration in *H. actiniformis*. The regeneration process is illustrated in temporal order. (A) Formation of a "scab" like structure showing the accumulation of bubbles toward the end of scab formation (around 2 hours PA). (B) Formation of "pinched" ends of nubbins (around 24 hours PA). (C) The formation of smooth regenerating stump ends (48 hours PA). The formation of acrosome with the appearance of white tentacle tips (96 hours PA).

Table A2.1. Times post-amputation of observed morphological stages of tentacle regeneration of *H. actiniformis*. Observed morphological stages of tentacle regeneration during a pilot regeneration experiment on individual H. actiniformis corals at the Australian Institute of Marine Sciences (AIMS). Photographs were collected every minute for several hours/days and timelapse videos were created to ascertain the actual physical changes and how long they took to materialise.

Time point	Time PA (hrs)	Morphological stage
T1	**2**	**Closing of wound "scab" (rough)**
T2	**24**	**Nubbin ending (smooth) started**
T3	**48**	**Nubbin ending (smooth) completed**
T4	**96 (4 days)**	**Tip first show**
T5	**240 (10 days)**	**Tip finishes forming**
T6	**4 weeks?**	**Line appears (end of regeneration)**

Discussion

When severing the tentacles, it was found that the Heliofungia specimens reacted differently to damage than wild specimens. The wild specimens pulled their tentacles in as soon as one was cut, but the aquarium specimens did not. This leads to the possibility that there may also be a difference in regeneration procedure or gene expressions in wild raised vs aquarium raised Heliofungia regeneration. Heliofungia appears to have four distinct phases in the regeneration procedure of its tentacles at very specific time points, these are the closing/scabbing of the wound within two hours, 72 hours to completely smooth wound closure (scab has gone), formation of the tip after four days and finally tip finishes forming by day ten.

Chapter 2: Supplementary Data

Table S2.1. Summary of mapped reads. List of mapped reads, before and after quality filtering and the number of counts for each sample.

Sample		T0_1	T0_2	T0_4	T0_5	T1_1	T1_4	T1_5	T4_1	T4_2	T4_4	T4_5	T6_1	T6_2	T6_4	T7_1	T7_2	T7_4	T7_5	T9_1	T9_2	T9_4	T9_5
Total Number of Reads		15194842	204332024	174425410	193210240	13131846	13963041	15564630	178323874	11642629	185527714	13630134	201540390	212737134	16258117	126719884	167382534	165807750	194907242	184549852	141207338	159652004	151866024
No. of Mapped Reads	Pre-filtering	48094566	126148010	109667892	95586026	15992702	74396572	91484130	130380938	87929938	96151700	83958428	114983610	121830856	102522580	62132964	94276798	100749692	117700706	94137978	80934392	94008192	83321106
	Post-filtering	14151916	74110215	62306528	75613878	5789920	51840119	56775876	65190469	43964969	69294154	49136247	74409846	80888515	57913599	48646965	60857900	59684575	69614891	70900473	50530075	57931756	57181409
Number of Counts	hello_1.0.m2.1	0.09	0.00	0.00	0.00	0.00	0.50	0.50	0.00	0.00	0.00	0.50	0.00	0.00	0.00	0.00	0.00	0.00	0.00	0.00	0.00	0.00	0.00
	hello_1.0.m2.10	51.29	773.59	470.21	408.33	46.57	405.08	307.16	858.73	539.78	503.57	386.03	727.39	860.61	748.43	305.62	776.26	564.98	533.59	391.48	536.02	584.03	410.77
	hello_1.0.m2.100	1.62	0.00	2.00	0.00	0.00	0.00	2.00	0.23	0.14	4.32	0.00	0.00	4.38	0.00	0.00	0.00	0.00	0.00	0.00	2.00	3.09	0.00
	hello_1.0.m2.1000	100.27	202.47	117.29	496.42	97.85	230.32	55.18	294.01	72.86	665.81	729.53	834.86	167.84	212.14	464.40	373.94	324.41	1171.88	596.73	331.95	342.05	2383.57
	hello_1.0.m2.10000	1.74	85.09	76.00	14.40	0.00	65.00	43.11	93.00	26.72	1.00	16.46	5.00	51.43	77.00	4.98	25.75	94.01	25.47	2.00	24.03	78.00	13.43
	hello_1.0.m2.10001	1.00	2.00	67.00	6.00	4.00	100.00	15.63	117.34	6.00	5.00	18	3.00	1.00	104.00	0.00	4.98	181.00	34.00	5.00	7.00	119.00	13.00
	hello_1.0.m2.10002	0.00	0.00	0.00	0.00	0.00	3.86	0.00	0.00	0.00	7.22	0.00	0.00	0.00	0.00	0.00	0.00	0.00	0.00	0.00	1.51	0.00	0.00
	hello_1.0.m2.10003	0.00	0.00	1.00	0.00	0.00	3.00	1.00	1.28	0.00	1.13	4.00	0.00	0.00	1.00	1.00	0.00	3.00	3.00	0.00	0.00	1.00	3.00
	hello_1.0.m2.10004	5.00	35.72	23.84	12.00	2.00	13.02	76.29	24.29	12.99	8.98	6.02	6.58	53.00	17.46	5.91	20.76	9.76	5.22	9.79	28.03	19.00	3.99
	hello_1.0.m2.10005	2.00	0.00	189.16	68.00	0.00	143.56	84.82	199.46	0.00	0.00	143.62	0.00	0.00	257.48	0.00	0.00	450.74	278.06	0.00	0.00	254.66	193.11
	hello_1.0.m2.10006	0.00	0.00	2.00	0.00	0.00	0.00	0.00	0.00	1.00	0.00	0.00	0.00	0.00	2.00	0.00	0.00	0.00	0.00	0.00	0.00	0.00	0.00
	hello_1.0.m2.10007	2.00	82.00	99.00	112.00	5.00	119.00	103.00	219.00	54.00	44.00	179.00	56.00	32.00	195.00	29.00	90.00	133.00	296.00	28.00	72.00	143.00	190.00
	hello_1.0.m2.10008	64.93	213.17	159.47	160.35	15.60	223.39	138.25	400.16	126.43	193.16	227.93	239.21	208.84	368.09	131.79	281.85	270.76	312.59	174.46	165.10	323.95	117.70
	hello_1.0.m2.10009	41.29	626.74	19.39	330.96	52.67	62.13	28.73	60.13	290.99	245.05	297.22	344.83	742.03	28.93	187.02	282.50	51.20	260.14	210.82	315.88	42.81	122.18
	hello_1.0.m2.1001	2.15	4.28	4.47	2.65	0.00	4.65	0.00	23.17	1.15	27.83	17.07	34.18	4.14	13.40	15.08	7.27	5.60	27.92	18.36	10.13	19.04	71.54
	hello_1.0.m2.10010	634.20	9224.29	2791.51	1535.56	722.54	2934.96	372.87	3151.81	3128.20	2417.04	1343.79	2671.93	6147.86	3237.79	2100.52	5885.06	6900.05	2231.88	2519.25	6363.82	4913.82	2296.12
	hello_1.0.m2.10011	3.00	14.00	20.00	10.00	0.00	19.15	41.00	24.85	10.00	14.00	9.00	17.36	8.00	41.41	4.00	29.05	25.00	26.00	11.09	13.00	43.87	6.46
	hello_1.0.m2.10012	0.00	0.00	1.29	0.00	0.00	0.00	0.00	0.00	0.00	0.00	0.00	0.00	0.00	0.00	0.00	0.00	0.00	0.00	0.00	0.00	0.00	0.00
	hello_1.0.m2.10013	0.00	0.00	0.00	0.00	0.00	0.00	0.00	1.00	0.00	0.00	0.00	0.00	0.00	0.00	0.00	0.00	0.00	0.00	0.00	0.00	1.00	0.00
	hello_1.0.m2.10014	0.00	0.00	1.84	0.00	0.00	2.76	6.18	1.52	2.00	0.00	1.38	0.00	0.00	1.52	0.00	0.00	4.27	4.94	0.00	0.00	1.34	1.89
	hello_1.0.m2.10015	8.53	2.54	4.32	4.73	0.00	2.06	0.00	6.00	14.84	35.39	20.00	32.13	14.65	0.15	9.27	32.51	1.05	28.13	12.51	21.78	3.08	17.85
	hello_1.0.m2.10016	0.00	0.00	0.00	0.00	1.28	0.00	0.00	1.39	0.00	12.95	1.55	5.28	0.00	0.00	0.00	0.00	1.40	1.77	9.08	1.53	1.04	0.00
	hello_1.0.m2.10017	59.15	617.60	277.02	306.05	60.22	157.35	147.51	261.22	390.13	436.73	492.37	639.98	786.68	276.28	340.36	647.18	281.66	627.37	598.95	491.56	249.59	432.00
	hello_1.0.m2.10018	23.41	80.00	337.59	65.86	13.00	365.10	121.37	397.84	80.73	140.97	201.72	136.26	74.99	680.33	58.12	170.46	654.71	297.84	84.42	111.21	447.59	161.24
	hello_1.0.m2.10019	8.86	23.17	126.79	0.00	27.51	0.00	0.00	63.99	9.30	81.51	0.00	62.31	34.36	54.14	42.76	48.90	0.00	0.00	47.52	5.15	32.69	0.00
	hello_1.0.m2.1002	86.53	169.22	511.05	184.62	42.88	473.54	272.10	775.09	125.51	353.00	193.27	462.34	118.88	616.07	276.41	164.48	398.17	271.97	309.07	145.05	451.03	89.62
	hello_1.0.m2.10020	6.89	7.91	9.78	2.62	0.00	3.11	0.00	15.52	0.00	0.00	2.62	5.77	1.42	8.10	1.41	5.86	6.60	1.85	2.83	2.95	5.57	3.90
	hello_1.0.m2.10021	27.59	131.39	257.80	53.38	17.14	123.85	60.08	272.95	46.79	129.30	62.80	105.94	78.35	231.60	63.83	109.10	206.02	94.12	74.30	74.60	210.85	120.50
	hello_1.0.m2.10022	0.00	7.00	33.97	2.00	0.00	17.00	0.00	26.00	1.00	2.00	3.00	2.00	0.00	31.00	0.00	2.00	16.00	5.00	3.00	4.00	16.00	5.00
	hello_1.0.m2.10023	0.00	0.00	0.00	0.00	0.00	0.00	0.00	0.00	0.00	0.00	0.00	0.00	0.00	0.00	1.20	1.27	0.00	0.00	2.47	1.44	0.00	4.00
	hello_1.0.m2.10024	10.00	1.00	0.00	15.00	0.00	7.00	10.38	6.18	0.00	8.00	8.00	9.00	7.00	8.00	1.00	9.00	4.00	12.00	4.00	7.00	6.00	4.00
	hello_1.0.m2.10025	0.00	6.02	3.00	14.01	0.00	2.00	7.00	2.00	0.00	10.01	21.00	2.00	2.00	2.00	1.00	5.00	0.00	6.04	6.04	6.00	2.07	9.00
	hello_1.0.m2.10026	143.76	796.05	366.71	495.30	109.66	243.56	405.22	457.43	394.90	473.67	457.41	677.69	591.33	424.74	313.20	439.61	410.64	668.05	574.09	368.74	400.38	378.86
	hello_1.0.m2.10027	0.00	0.00	0.00	0.00	0.00	0.00	1.00	0.00	0.00	0.00	0.00	0.00	0.00	0.00	0.00	0.00	0.00	0.00	0.00	0.00	0.00	0.00
	hello_1.0.m2.10028	0.00	0.00	0.00	0.00	0.00	0.00	0.00	1.00	0.00	0.00	0.00	0.00	0.00	0.00	0.00	0.00	0.00	0.00	0.00	0.00	0.00	0.00
	hello_1.0.m2.10029	0.00	5.84	11.79	0.00	0.00	2.47	7.34	9.18	1.43	3.46	2.13	7.14	3.18	12.48	0.00	6.80	0.00	6.21	3.76	3.81	10.51	1.55
	hello_1.0.m2.1003	1.67	6.95	0.00	0.00	0.00	0.00	2.61	0.99	4.74	14.06	0.00	17.41	1.73	1.56	0.00	4.88	0.00	6.21	6.05	8.12	0.00	1.02
	hello_1.0.m2.10030	0.00	0.00	0.00	0.00	0.00	0.00	0.00	2.00	0.00	0.00	0.00	4.00	4.00	0.00	1.00	0.00	0.00	1.00	0.00	0.00	0.00	0.00
	hello_1.0.m2.10031	721.33	2583.14	1800.80	1282.00	1736.40	2957.87	3500.96	1764.59	1693.66	1859.95	1146.35	2227.60	2342.85	1534.94	971.61	1461.92	3618.22	1864.29	1626.90	1382.37	1969.87	2840.41
	hello_1.0.m2.10032	3.87	14.15	3.20	9.18	1.16	3.94	16.36	2.60	2.02	23.79	3.86	33.18	6.19	10.29	12.07	9.04	19.87	6.64	14.88	4.06	14.90	1.33
	hello_1.0.m2.10033	2975.73	5146.76	3205.80	3336.64	994.49	3916.66	1972.81	4660.25	6401.79	4829.08	3601.51	6063.67	5529.12	5634.08	2711.43	4251.62	4849.27	4796.99	4091.14	3189.85	3819.77	3046.86
	hello_1.0.m2.10034	260.62	1087.09	1276.91	833.01	164.72	862.46	468.07	996.52	525.56	522.86	939.74	813.51	1045.83	736.84	521.39	615.93	760.57	1194.84	759.16	610.67	933.82	409.85
	hello_1.0.m2.10035	16.35	36.95	36.26	22.92	2.00	32.20	61.96	16.78	7.14	87.70	23.60	116.62	42.00	73.41	53.96	49.49	179.63	37.43	63.01	27.20	78.54	21.74
	hello_1.0.m2.10036	1466.00	3366.00	3336.00	3286.00	770.00	1019.00	2527.00	2312.00	702.00	1663.00	1765.00	2126.00	3384.00	1710.00	1212.00	1337.00	1122.00	2110.00	1558.00	1321.00	1537.00	736.00
	hello_1.0.m2.10037	47.68	336.56	232.02	258.40	40.84	180.63	185.01	243.93	254.56	367.70	283.51	429.93	480.60	394.84	164.51	322.51	372.99	380.37	240.22	226.95	369.56	298.93

Table S2.2. Significantly Enriched GO terms in tentacle regeneration of *H. actiniformis*. List of significantly enriched GO terms per timepoint and grouped by ontology.

Ontology	Timepoint					Go ID	GO Term
	0_1	1_4	4_6	6_7	7_9		
Biological Process (BP)						GO:0002540	leukotriene production involved in inflamation
						GO:0006820	anion transport
						GO:0010634	positive regulation of epithelial cell m...
						GO:0010718	positive regulation of epithelial to mes...
						GO:0018401	peptidyl-proline hydroxylation to 4-hydr...
						GO:0030574	collagen catabolic process
						GO:0032348	negative regulation of aldosterone biosy...
						GO:0032720	negative regulation of tumor necrosis fa...
						GO:0034765	regulation of ion transmembrane transpor...
						GO:0045646	regulation of erythrocyte differentiatio...
						GO:0050803	regulation of synapse structure or activ...
						GO:0052027	modulation by symbiont of host signal tr...
						GO:0060022	hard palate development
						GO:0061044	negative regulation of vascular wound he...
						GO:0070374	positive regulation of ERK1 and ERK2 cas...
						GO:0071805	potassium ion transmembrane transport
						GO:1901753	leukotriene A4 biosynthetic process
						GO:1904999	positive regulation of leukocyte adhesio...
						GO:2000065	negative regulation of cortisol biosynth...
						GO:0009408	response to heat
						GO:0051085	chaperone cofactor-dependent protein ref...
						GO:0006749	glutathione metabolic process
						GO:0023019	signal transduction involved in regulati...
						GO:0042554	superoxide anion generation
						GO:0046330	positive regulation of JNK cascade
						GO:0060213	positive regulation of nuclear-transcrib...
						GO:0070534	protein K63-linked ubiquitination
						GO:0097400	interleukin-17-mediated signaling pathwa...
						GO:1900153	positive regulation of nuclear-transcrib...
						GO:2000255	negative regulation of male germ cell pr...
						GO:0045893	positive regulation of transcription, DN...
						GO:1900122	positive regulation of receptor binding
						GO:1903665	negative regulation of asexual reproduct...
						GO:0030435	sporulation resulting in formation of a ...
						GO:0031288	sorocarp morphogenesis
						GO:0042590	antigen processing and presentation of e...
						GO:0046274	lignin catabolic process
						GO:0050923	regulation of negative chemotaxis
						GO:0051603	proteolysis involved in cellular protein...
						GO:0002576	platelet degranulation
						GO:0006633	fatty acid biosynthetic process
						GO:0015721	bile acid and bile salt transport
						GO:0015747	urate transport
						GO:0032310	prostaglandin secretion
						GO:0038183	bile acid signaling pathway
						GO:0048661	positive regulation of smooth muscle cel...
						GO:0070730	cAMP transport
						GO:0071716	leukotriene transport
						GO:0140115	export across plasma membrane
						GO:0150104	transport across blood-brain barrier
Cellular Component (CC)						GO:0008076	voltage-gated potassium channel complex
						GO:0045211	postsynaptic membrane
						GO:0060076	excitatory synapse
						GO:0009898	cytoplasmic side of plasma membrane
						GO:0035631	CD40 receptor complex
						GO:0043020	NADPH oxidase complex
						GO:0005581	collagen trimer
						GO:0005615	extracellular space
						GO:0005576	extracellular region
						GO:0005788	endoplasmic reticulum lumen
						GO:0031410	cytoplasmic vesicle
						GO:0032579	apical lamina of hyaline layer
						GO:0070062	extracellular exosome
						GO:0016323	basolateral plasma membrane
						GO:0031088	platelet dense granule membrane
						GO:0098591	external side of apical plasma membrane

Molecular Function (MF)						
					GO:0000978	RNA polymerase II cis-regulatory region ...
					GO:0000981	DNA-binding transcription factor activit...
					GO:0004051	arachidonate 5-lipoxygenase activity
					GO:0004052	arachidonate 12(S)-lipoxygenase activity
					GO:0004222	metalloendopeptidase activity
					GO:0005313	L-glutamate transmembrane transporter ac...
					GO:0005326	neurotransmitter transmembrane transport...
					GO:0015293	symporter activity
					GO:0016706	2-oxoglutarate-dependent dioxygenase act...
					GO:0031418	L-ascorbic acid binding
					GO:1904315	transmitter-gated ion channel activity i...
					GO:0051082	unfolded protein binding
					GO:0004364	glutathione transferase activity
					GO:0004667	prostaglandin-D synthase activity
					GO:0005109	frizzled binding
					GO:0016175	superoxide-generating NAD(P)H oxidase ac...
					GO:0031996	thioesterase binding
					GO:0042802	identical protein binding
					GO:0043565	sequence-specific DNA binding
					GO:0004867	serine-type endopeptidase inhibitor acti...
					GO:0009374	biotin binding
					GO:0030020	extracellular matrix structural constitu...
					GO:0052716	hydroquinone:oxygen oxidoreductase activ...
					GO:0001409	guanine nucleotide transmembrane transpo...
					GO:0004315	3-oxoacyl-[acyl-carrier-protein] synthas...
					GO:0008559	ABC-type xenobiotic transporter activity
					GO:0015132	prostaglandin transmembrane transporter ...
					GO:0015143	urate transmembrane transporter activity
					GO:0015431	ABC-type glutathione S-conjugate transpo...
					GO:0015432	ABC-type bile acid transporter activity
					GO:0015562	efflux transmembrane transporter activit...
					GO:0015662	ion transmembrane transporter activity, ...
					GO:0016404	15-hydroxyprostaglandin dehydrogenase (N...
					GO:0031177	phosphopantetheine binding
					GO:0034634	glutathione transmembrane transporter ac...
					GO:0043225	ATPase-coupled inorganic anion transmemb...
					GO:0050111	mycocerosate synthase activity

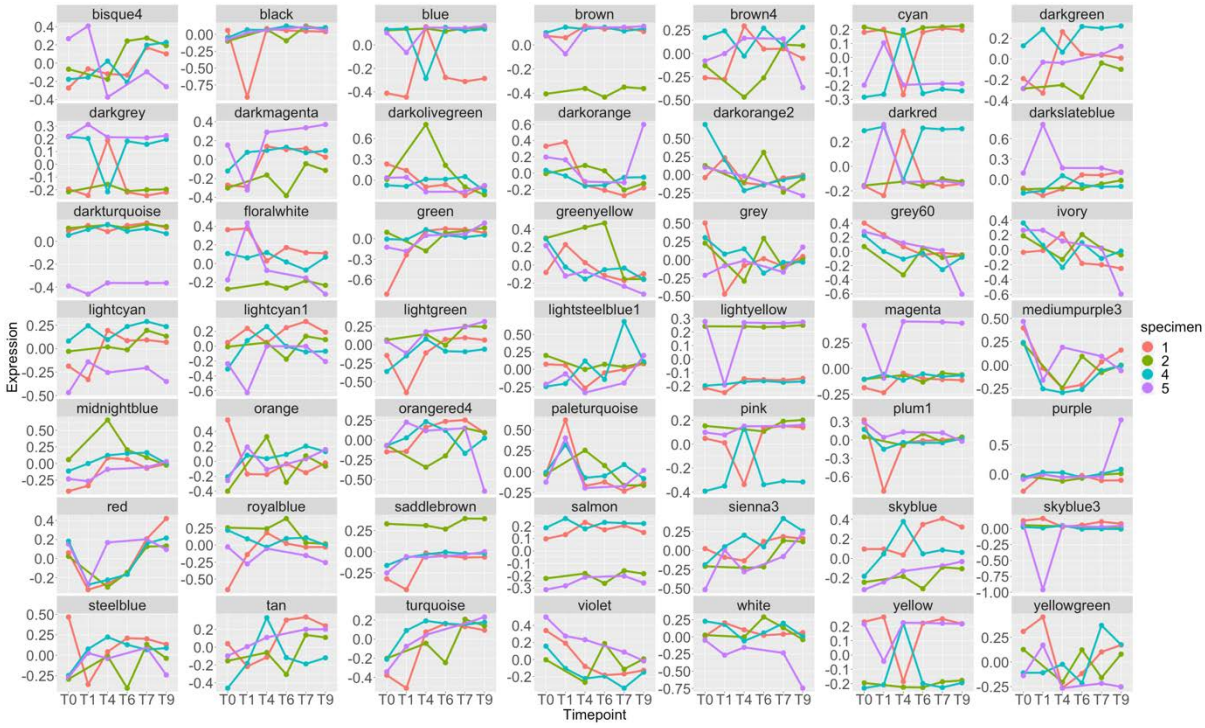

Figure S2.1. Expression level patterns of eigengenes (WGCNA) of every module throughout the regeneration stages of *Heliofungia actiniformis*. T0 = timepoint 0 (primary amputation); T1 = timepoint 1, 1-hour post-amputation ("scab" formation); T4 = timepoint 4, 24 hours post-amputation ("pinched" appearance); T6 = timepoint 6, 72 hours post-amputation (smooth stump ending); T7 = timepoint 7, 96 hours post-amputation (beginning of tip formation); T9 = timepoint 9, 10 days post-amputation (fully regenerated acrosome, end of regeneration).

Table S2.3. Significantly enriched gene ontology pathways for modules of co-regulated genes (WGCNA) in tentacle regeneration of *H. actiniformis*. Weighted gene co-expression network analysis (WGCNA) investigating the relationship between co-expression modules by identifying genes with related expression configurations and their relationship with the various tentacle regeneration timepoints of H. actiniformis. The GO terms are grouped by module colour and identify the GO ID, number of module genes, p-value associated with each GO term and related ontology.

Module	No of module genes	GO ID	GO Term	Annotated	Significant	Expected	P-value	Ontology
bisque4	**45**	GO:0019695	choline metabolic process	11	3	0.02	5.10E-07	BP
bisque4	**45**	GO:0032259	methylation	344	5	0.52	3.60E-05	BP
bisque4	**45**	GO:0035999	tetrahydrofolate interconversion	15	3	0.02	1.40E-06	BP
black	**1,155**	GO:0030322	stabilization of membrane potential	39	7	1.02	6.10E-05	BP
black	**1,155**	GO:0034150	toll-like receptor 6 signaling pathway	10	4	0.26	8.60E-05	BP
black	**1,155**	GO:0022841	potassium ion leak channel activity	41	7	1.09	9.00E-05	MF
blue	**2,189**	GO:0005524	ATP binding	2738	167	122.32	1.30E-05	MF
brown	**1,854**	GO:0032196	transposition	126	10	4.68	3.30E-06	BP
brown	**1,854**	GO:0090461	glutamate homeostasis	7	4	0.26	6.00E-05	BP
brown	**1,854**	GO:1901526	positive regulation of mitophagy	6	4	0.22	2.70E-05	BP
brown4	**45**	GO:0002755	MyD88-dependent toll-like receptor signa...	36	3	0.06	3.20E-05	BP
brown4	**45**	GO:0042325	regulation of phosphorylation	1596	7	2.73	9.90E-08	BP
brown4	**45**	GO:0042495	detection of triacyl bacterial lipopepti...	7	2	0.01	6.00E-05	BP
brown4	**45**	GO:0051965	positive regulation of synapse assembly	95	4	0.16	2.00E-05	BP
brown4	**45**	GO:0090050	positive regulation of cell migration in...	21	4	0.04	4.20E-08	BP
brown4	**45**	GO:0009986	cell surface	1193	9	1.82	5.30E-05	CC
brown4	**45**	GO:0035354	Toll-like receptor 1-Toll-like receptor ...	7	2	0.01	4.70E-05	CC
brown4	**45**	GO:0036458	hepatocyte growth factor binding	6	4	0.01	8.10E-11	MF
darkgrey	**431**	GO:0002230	positive regulation of defense response ...	30	4	0.24	8.80E-05	BP
darkgrey	**431**	GO:0005779	integral component of peroxisomal membra...	11	3	0.08	7.00E-05	CC
darkorange	**319**	GO:0031514	motile cilium	247	13	2.1	5.60E-05	CC
darkorange	**319**	GO:0036064	ciliary basal body	157	10	1.34	9.90E-07	CC
darkorange2	**46**	GO:0006418	tRNA aminoacylation for protein translat...	49	4	0.07	1.20E-05	BP
darkorange2	**46**	GO:0032048	cardiolipin metabolic process	9	2	0.01	7.90E-05	BP
darkorange2	**46**	GO:0004826	phenylalanine-tRNA ligase activity	5	2	0.01	2.20E-05	MF
green	**1,508**	GO:0006886	intracellular protein transport	758	61	34.64	1.10E-05	BP
green	**1,508**	GO:0033137	negative regulation of peptidyl-serine p...	15	6	0.69	3.10E-05	BP
green	**1,508**	GO:0051056	regulation of small GTPase mediated sign...	224	21	10.24	1.50E-05	BP
green	**1,508**	GO:0005654	nucleoplasm	2384	177	106.16	3.30E-06	CC
green	**1,508**	GO:0005730	nucleolus	891	66	39.68	2.50E-06	CC
green	**1,508**	GO:0005737	cytoplasm	12709	664	565.93	7.70E-07	CC
green	**1,508**	GO:0005813	centrosome	552	46	24.58	2.10E-06	CC
green	**1,508**	GO:0005819	spindle	510	37	22.71	1.80E-05	CC
green	**1,508**	GO:0005829	cytosol	3508	231	156.21	1.60E-10	CC
green	**1,508**	GO:0005096	GTPase activator activity	153	21	6.61	2.70E-06	MF
green	**1,508**	GO:0008017	microtubule binding	184	25	7.94	1.50E-06	MF
green	**1,508**	GO:0031267	small GTPase binding	170	25	7.34	8.20E-08	MF
green	**1,508**	GO:0045296	cadherin binding	134	18	5.79	1.90E-05	MF
greenyellow	**855**	GO:0006457	protein folding	237	19	6.75	7.60E-05	BP
greenyellow	**855**	GO:0032543	mitochondrial translation	36	9	1.02	5.60E-07	BP
greenyellow	**855**	GO:0070536	protein K63-linked deubiquitination	25	6	0.71	5.80E-05	BP
greenyellow	**855**	GO:0016272	prefoldin complex	8	4	0.22	3.70E-05	CC
greenyellow	**855**	GO:0046540	U4/U6 x U5 tri-snRNP complex	30	8	0.83	1.10E-06	CC
greenyellow	**855**	GO:0071005	U2-type precatalytic spliceosome	42	8	1.16	1.70E-05	CC
greenyellow	**855**	GO:0071013	catalytic step 2 spliceosome	68	11	1.88	1.40E-05	CC
greenyellow	**855**	GO:0004596	peptide alpha-N-acetyltransferase activi...	5	4	0.13	2.30E-06	MF
greenyellow	**855**	GO:0047631	ADP-ribose diphosphatase activity	14	5	0.37	2.00E-05	MF
grey60	**618**	GO:0006749	glutathione metabolic process	83	10	1.57	3.80E-06	BP
grey60	**618**	GO:0007584	response to nutrient	166	11	3.15	1.50E-05	BP
grey60	**618**	GO:0010632	regulation of epithelial cell migration	300	19	5.68	1.20E-07	BP
grey60	**618**	GO:0042178	xenobiotic catabolic process	9	4	0.17	1.50E-05	BP
grey60	**618**	GO:0051597	response to methylmercury	33	8	0.63	1.40E-07	BP
grey60	**618**	GO:0061580	colon epithelial cell migration	27	8	0.51	2.50E-08	BP
grey60	**618**	GO:0097065	anterior head development	36	7	0.68	4.30E-06	BP
grey60	**618**	GO:0005764	lysosome	743	38	13.95	1.30E-08	CC
grey60	**618**	GO:0003943	N-acetylgalactosamine-4-sulfatase activi...	27	8	0.54	3.80E-08	MF
grey60	**618**	GO:0004065	arylsulfatase activity	39	8	0.78	8.50E-07	MF
grey60	**618**	GO:0004364	glutathione transferase activity	37	8	0.74	5.50E-07	MF
lightcyan1	**51**	GO:0033152	immunoglobulin V(D)J recombination	13	2	0.02	9.90E-05	BP
lightsteelblue1	**71**	GO:0042102	positive regulation of T cell proliferat...	54	3	0.09	9.80E-05	BP
lightsteelblue1	**71**	GO:0045577	regulation of B cell differentiation	8	2	0.01	7.50E-05	BP
lightsteelblue1	**71**	GO:0060396	growth hormone receptor signaling pathwa...	9	2	0.01	9.60E-05	BP
lightsteelblue1	**71**	GO:0004714	transmembrane receptor protein tyrosine ...	527	9	0.89	4.70E-06	MF
lightyellow	**560**	GO:0023019	signal transduction involved in regulati...	24	4	0.24	9.40E-05	BP
lightyellow	**560**	GO:0070534	protein K63-linked ubiquitination	140	8	1.42	9.50E-05	BP
lightyellow	**560**	GO:0035631	CD40 receptor complex	76	7	0.79	1.50E-05	CC

magenta	**958**	GO:0032092	positive regulation of protein binding	174	12	3.16	8.30E-05	BP
magenta	**958**	GO:0033690	positive regulation of osteoblast prolif...	117	12	2.12	1.50E-06	BP
magenta	**958**	GO:0043932	ossification involved in bone remodeling	107	12	1.94	5.60E-07	BP
magenta	**958**	GO:0045669	positive regulation of osteoblast differ...	176	14	3.19	4.20E-06	BP
magenta	**958**	GO:0060071	Wnt signaling pathway, planar cell polar...	180	13	3.27	4.10E-06	BP
magenta	**958**	GO:0060122	inner ear receptor cell stereocilium org...	136	12	2.47	7.10E-06	BP
magenta	**958**	GO:0090090	negative regulation of canonical Wnt sig...	230	14	4.17	8.40E-05	BP
magenta	**958**	GO:0090103	cochlea morphogenesis	123	12	2.23	2.50E-06	BP
magenta	**958**	GO:0090177	establishment of planar polarity involve...	134	12	2.43	6.10E-06	BP
magenta	**958**	GO:0005581	collagen trimer	322	19	5.9	8.60E-06	CC
magenta	**958**	GO:0004397	histidine ammonia-lyase activity	5	3	0.09	5.70E-05	MF
magenta	**958**	GO:0005109	frizzled binding	159	13	2.88	6.80E-06	MF
magenta	**958**	GO:0017147	Wnt-protein binding	160	13	2.9	7.30E-06	MF
mediumpurple3	**76**	GO:0099509	regulation of presynaptic cytosolic calc...	6	2	0.01	3.50E-05	BP
orangered4	**86**	GO:0006578	amino-acid betaine biosynthetic process	18	3	0.04	4.60E-05	BP
paleturquoise	**215**	GO:0009408	response to heat	110	8	0.75	1.50E-06	BP
paleturquoise	**215**	GO:0030574	collagen catabolic process	61	5	0.42	6.10E-05	BP
paleturquoise	**215**	GO:0060022	hard palate development	7	3	0.05	1.10E-05	BP
paleturquoise	**215**	GO:0051082	unfolded protein binding	80	6	0.53	1.50E-05	MF
purple	**923**	GO:0001501	skeletal system development	529	36	13.33	1.30E-08	BP
purple	**923**	GO:0001568	blood vessel development	754	35	19	3.10E-08	BP
purple	**923**	GO:0003341	cilium movement	240	44	6.05	3.70E-13	BP
purple	**923**	GO:0003351	epithelial cilium movement involved in e...	48	10	1.21	2.30E-05	BP
purple	**923**	GO:0003356	regulation of cilium beat frequency	13	6	0.33	5.70E-06	BP
purple	**923**	GO:0006165	nucleoside diphosphate phosphorylation	140	6	3.53	1.30E-05	BP
purple	**923**	GO:0007018	microtubule-based movement	415	68	10.46	7.40E-07	BP
purple	**923**	GO:0007288	sperm axoneme assembly	19	9	0.48	2.80E-10	BP
purple	**923**	GO:0009142	nucleoside triphosphate biosynthetic pro...	44	7	1.11	1.30E-05	BP
purple	**923**	GO:0009887	animal organ morphogenesis	1348	65	33.96	1.50E-05	BP
purple	**923**	GO:0030199	collagen fibril organization	138	15	3.48	2.20E-06	BP
purple	**923**	GO:0030282	bone mineralization	242	15	6.1	5.20E-08	BP
purple	**923**	GO:0030317	flagellated sperm motility	140	20	3.53	7.30E-08	BP
purple	**923**	GO:0032963	collagen metabolic process	132	10	3.33	2.50E-06	BP
purple	**923**	GO:0034446	substrate adhesion-dependent cell spread...	74	8	1.86	9.00E-05	BP
purple	**923**	GO:0035082	axoneme assembly	86	29	2.17	7.60E-06	BP
purple	**923**	GO:0036159	inner dynein arm assembly	24	9	0.6	3.60E-09	BP
purple	**923**	GO:0043589	skin morphogenesis	15	7	0.38	3.30E-08	BP
purple	**923**	GO:0045494	photoreceptor cell maintenance	49	9	1.23	3.20E-06	BP
purple	**923**	GO:0060285	cilium-dependent cell motility	200	34	5.04	3.70E-10	BP
purple	**923**	GO:0061512	protein localization to cilium	46	11	1.16	7.90E-09	BP
purple	**923**	GO:0070208	protein heterotrimerization	6	6	0.15	2.50E-10	BP
purple	**923**	GO:0071230	cellular response to amino acid stimulus	65	10	1.64	4.90E-06	BP
purple	**923**	GO:0071869	response to catecholamine	103	5	2.59	2.00E-06	BP
purple	**923**	GO:0085029	extracellular matrix assembly	70	11	1.76	9.30E-06	BP
purple	**923**	GO:0002177	manchette	11	6	0.29	1.50E-07	CC
purple	**923**	GO:0005584	collagen type I trimer	7	6	0.19	2.50E-09	CC
purple	**923**	GO:0005737	cytoplasm	12709	395	340.26	8.40E-06	CC
purple	**923**	GO:0005856	cytoskeleton	2252	151	60.29	1.70E-07	CC
purple	**923**	GO:0005874	microtubule	346	34	9.26	9.60E-12	CC
purple	**923**	GO:0005930	axoneme	153	45	4.1	3.60E-24	CC
purple	**923**	GO:0030286	dynein complex	66	17	1.77	2.00E-05	CC
purple	**923**	GO:0030992	intraciliary transport particle B	20	6	0.54	1.00E-05	CC
purple	**923**	GO:0031514	motile cilium	247	55	6.61	1.30E-20	CC
purple	**923**	GO:0036064	ciliary basal body	157	29	4.2	1.80E-16	CC
purple	**923**	GO:0036126	sperm flagellum	156	24	4.18	4.10E-14	CC
purple	**923**	GO:0036156	inner dynein arm	7	4	0.19	1.70E-05	CC
purple	**923**	GO:0097546	ciliary base	22	7	0.59	1.10E-06	CC
purple	**923**	GO:0097729	9+2 motile cilium	166	30	4.44	5.60E-08	CC
purple	**923**	GO:0004017	adenylate kinase activity	10	5	0.24	1.90E-06	MF
purple	**923**	GO:0004550	nucleoside diphosphate kinase activity	14	7	0.34	1.40E-08	MF
purple	**923**	GO:0005375	copper ion transmembrane transporter act...	10	4	0.24	6.30E-05	MF
purple	**923**	GO:0008017	microtubule binding	184	17	4.45	2.60E-06	MF
purple	**923**	GO:0008569	ATP-dependent microtubule motor activity...	40	12	0.97	1.10E-10	MF
purple	**923**	GO:0031177	phosphopantetheine binding	20	5	0.48	9.30E-05	MF
purple	**923**	GO:0045505	dynein intermediate chain binding	46	9	1.11	1.30E-06	MF
purple	**923**	GO:0048407	platelet-derived growth factor binding	17	9	0.41	5.40E-11	MF
purple	**923**	GO:0051959	dynein light intermediate chain binding	42	9	1.02	5.80E-07	MF

red	**1,433**	GO:0006820	anion transport	2800	119	110.05	9.20E-08	BP
red	**1,433**	GO:0010634	positive regulation of epithelial cell m...	233	25	9.16	3.30E-11	BP
red	**1,433**	GO:0010718	positive regulation of epithelial to mes...	70	16	2.75	9.50E-09	BP
red	**1,433**	GO:0018401	peptidyl-proline hydroxylation to 4-hydr...	26	12	1.02	7.30E-11	BP
red	**1,433**	GO:0030903	notochord development	29	7	1.14	5.80E-05	BP
red	**1,433**	GO:0031408	oxylipin biosynthetic process	22	7	0.86	1.40E-05	BP
red	**1,433**	GO:0034220	ion transmembrane transport	1292	120	50.78	2.30E-05	BP
red	**1,433**	GO:0034765	regulation of ion transmembrane transpor...	513	38	20.16	1.20E-12	BP
red	**1,433**	GO:0035235	ionotropic glutamate receptor signaling ...	17	6	0.67	3.10E-05	BP
red	**1,433**	GO:0035725	sodium ion transmembrane transport	193	27	7.59	3.40E-10	BP
red	**1,433**	GO:0042391	regulation of membrane potential	663	66	26.06	6.50E-11	BP
red	**1,433**	GO:0042590	antigen processing and presentation of e...	29	8	1.14	1.10E-05	BP
red	**1,433**	GO:0045646	regulation of erythrocyte differentiatio...	37	8	1.45	7.70E-05	BP
red	**1,433**	GO:0050803	regulation of synapse structure or activ...	380	19	14.93	2.50E-08	BP
red	**1,433**	GO:0050877	nervous system process	1513	97	59.46	5.30E-08	BP
red	**1,433**	GO:0050957	equilibrioception	9	5	0.35	1.00E-05	BP
red	**1,433**	GO:0050982	detection of mechanical stimulus	189	27	7.43	1.50E-09	BP
red	**1,433**	GO:0051260	protein homooligomerization	285	23	11.2	9.80E-05	BP
red	**1,433**	GO:0060004	reflex	34	9	1.34	1.80E-06	BP
red	**1,433**	GO:0060012	synaptic transmission, glycinergic	16	6	0.63	2.10E-05	BP
red	**1,433**	GO:0070374	positive regulation of ERK1 and ERK2 cas...	254	28	9.98	9.10E-07	BP
red	**1,433**	GO:0071294	cellular response to zinc ion	28	7	1.1	8.10E-05	BP
red	**1,433**	GO:0071805	potassium ion transmembrane transport	245	33	9.63	1.50E-12	BP
red	**1,433**	GO:0098700	neurotransmitter loading into synaptic v...	29	7	1.14	8.70E-05	BP
red	**1,433**	GO:1900122	positive regulation of receptor binding	9	7	0.35	4.70E-09	BP
red	**1,433**	GO:1902476	chloride transmembrane transport	96	17	3.77	1.80E-07	BP
red	**1,433**	GO:1903665	negative regulation of asexual reproduct...	5	4	0.2	1.10E-05	BP
red	**1,433**	GO:0000139	Golgi membrane	845	57	33.41	3.70E-05	CC
red	**1,433**	GO:0001518	voltage-gated sodium channel complex	11	5	0.43	3.60E-05	CC
red	**1,433**	GO:0005576	extracellular region	4029	253	159.29	2.50E-07	CC
red	**1,433**	GO:0005615	extracellular space	2244	141	88.72	1.10E-07	CC
red	**1,433**	GO:0005788	endoplasmic reticulum lumen	200	28	7.91	7.50E-09	CC
red	**1,433**	GO:0005887	integral component of plasma membrane	2933	197	115.96	7.60E-07	CC
red	**1,433**	GO:0005892	acetylcholine-gated channel complex	46	9	1.82	6.70E-05	CC
red	**1,433**	GO:0008076	voltage-gated potassium channel complex	103	21	4.07	5.10E-10	CC
red	**1,433**	GO:0016021	integral component of membrane	7564	427	299.05	6.10E-09	CC
red	**1,433**	GO:0032281	AMPA glutamate receptor complex	15	6	0.59	1.40E-05	CC
red	**1,433**	GO:0032809	neuronal cell body membrane	56	10	2.21	6.00E-05	CC
red	**1,433**	GO:0034706	sodium channel complex	35	14	1.38	1.90E-05	CC
red	**1,433**	GO:0034707	chloride channel complex	59	16	2.33	7.70E-08	CC
red	**1,433**	GO:0043005	neuron projection	2125	120	84.01	7.90E-09	CC
red	**1,433**	GO:0045211	postsynaptic membrane	502	53	19.85	2.30E-09	CC
red	**1,433**	GO:0060076	excitatory synapse	215	14	8.5	7.20E-05	CC
red	**1,433**	GO:0099060	integral component of postsynaptic speci...	84	16	3.32	1.10E-05	CC
red	**1,433**	GO:1902711	GABA-A receptor complex	32	10	1.27	2.60E-07	CC
red	**1,433**	GO:1903561	extracellular vesicle	728	46	28.78	8.30E-05	CC
red	**1,433**	GO:0004890	GABA-A receptor activity	37	11	1.47	1.20E-07	MF
red	**1,433**	GO:0004971	AMPA glutamate receptor activity	12	6	0.48	2.90E-06	MF
red	**1,433**	GO:0005248	voltage-gated sodium channel activity	32	9	1.27	2.90E-06	MF
red	**1,433**	GO:0005251	delayed rectifier potassium channel acti...	51	12	2.03	5.40E-07	MF
red	**1,433**	GO:0005262	calcium channel activity	311	33	12.36	3.40E-08	MF
red	**1,433**	GO:0005313	L-glutamate transmembrane transporter ac...	27	7	1.07	6.70E-05	MF
red	**1,433**	GO:0005326	neurotransmitter transmembrane transport...	11	6	0.44	1.50E-06	MF
red	**1,433**	GO:0015280	ligand-gated sodium channel activity	84	16	3.34	9.80E-10	MF
red	**1,433**	GO:0015293	symporter activity	227	21	9.02	3.70E-08	MF
red	**1,433**	GO:0022848	acetylcholine-gated cation-selective cha...	57	11	2.26	1.30E-05	MF
red	**1,433**	GO:0022851	GABA-gated chloride ion channel activity	18	7	0.72	3.30E-06	MF
red	**1,433**	GO:0030246	carbohydrate binding	572	62	22.73	5.30E-09	MF
red	**1,433**	GO:0031418	L-ascorbic acid binding	35	12	1.39	5.10E-09	MF
red	**1,433**	GO:1904315	transmitter-gated ion channel activity i...	97	24	3.85	2.20E-09	MF
royalblue	**541**	GO:0001732	formation of cytoplasmic translation ini...	23	6	0.42	2.80E-06	BP
royalblue	**541**	GO:0000777	condensed chromosome kinetochore	17	5	0.29	1.90E-05	CC
royalblue	**541**	GO:0005663	DNA replication factor C complex	6	3	0.1	9.50E-05	CC
royalblue	**541**	GO:0005730	nucleolus	891	36	15.2	4.10E-05	CC
royalblue	**541**	GO:0005852	eukaryotic translation initiation factor...	21	6	0.36	1.00E-06	CC
royalblue	**541**	GO:0016282	eukaryotic 43S preinitiation complex	22	6	0.38	1.40E-06	CC
royalblue	**541**	GO:0033290	eukaryotic 48S preinitiation complex	22	6	0.38	1.40E-06	CC
royalblue	**541**	GO:0003743	translation initiation factor activity	59	9	0.95	3.90E-07	MF
salmon	**804**	GO:0007250	activation of NF-kappaB-inducing kinase ...	83	8	1.41	8.10E-05	BP
sienna3	**169**	GO:0031048	heterochromatin assembly by small RNA	40	6	0.21	5.60E-08	BP
sienna3	**169**	GO:0031380	nuclear RNA-directed RNA polymerase comp...	38	6	0.2	3.90E-08	CC
skyblue	**246**	GO:0046537	2,3-bisphosphoglycerate-independent phos...	10	3	0.05	1.90E-05	MF

tan	**815**	GO:0006418	tRNA aminoacylation for protein translat...	49	10	0.85	4.30E-06	BP
tan	**815**	GO:0007156	homophilic cell adhesion via plasma memb...	458	21	7.96	5.70E-05	BP
tan	**815**	GO:0035002	liquid clearance, open tracheal system	13	4	0.23	5.70E-05	BP
tan	**815**	GO:0045217	cell-cell junction maintenance	22	5	0.38	5.60E-05	BP
tan	**815**	GO:1904274	tricellular tight junction assembly	10	4	0.17	1.70E-05	BP
tan	**815**	GO:0061689	tricellular tight junction	10	4	0.17	1.50E-05	CC
tan	**815**	GO:0000049	tRNA binding	63	7	1.07	9.20E-05	MF
tan	**815**	GO:0004812	aminoacyl-tRNA ligase activity	52	10	0.88	7.30E-06	MF
turquoise	**8,352**	GO:0000422	autophagy of mitochondrion	60	31	13.24	6.10E-06	BP
turquoise	**8,352**	GO:0002181	cytoplasmic translation	77	34	16.99	1.10E-06	BP
turquoise	**8,352**	GO:0006099	tricarboxylic acid cycle	30	17	6.62	4.00E-05	BP
turquoise	**8,352**	GO:0006412	translation	532	182	117.39	7.90E-15	BP
turquoise	**8,352**	GO:0007017	microtubule-based process	808	212	178.28	5.90E-05	BP
turquoise	**8,352**	GO:0007281	germ cell development	239	66	52.74	3.10E-05	BP
turquoise	**8,352**	GO:0008625	extrinsic apoptotic signaling pathway vi...	52	20	11.47	4.60E-05	BP
turquoise	**8,352**	GO:0015031	protein transport	1636	480	360.98	1.90E-05	BP
turquoise	**8,352**	GO:0032981	mitochondrial respiratory chain complex ...	34	19	7.5	1.90E-05	BP
turquoise	**8,352**	GO:0005737	cytoplasm	12709	3115	2812.01	6.00E-10	CC
turquoise	**8,352**	GO:0005739	mitochondrion	1351	423	298.92	3.60E-05	CC
turquoise	**8,352**	GO:0005743	mitochondrial inner membrane	336	125	74.34	7.00E-05	CC
turquoise	**8,352**	GO:0005765	lysosomal membrane	370	122	81.87	1.30E-05	CC
turquoise	**8,352**	GO:0005789	endoplasmic reticulum membrane	888	266	196.48	9.30E-05	CC
turquoise	**8,352**	GO:0005829	cytosol	3508	952	776.19	9.40E-12	CC
turquoise	**8,352**	GO:0005840	ribosome	142	85	31.42	2.50E-08	CC
turquoise	**8,352**	GO:0022625	cytosolic large ribosomal subunit	25	20	5.53	1.30E-09	CC
turquoise	**8,352**	GO:0022627	cytosolic small ribosomal subunit	12	10	2.66	1.20E-05	CC
turquoise	**8,352**	GO:0003723	RNA binding	1350	395	285.6	1.50E-08	MF
turquoise	**8,352**	GO:0003735	structural constituent of ribosome	115	74	24.33	1.50E-23	MF
violet	**196**	GO:0035641	locomotory exploration behavior	40	5	0.21	1.90E-06	BP
white	**292**	GO:0006269	DNA replication, synthesis of RNA primer	6	3	0.06	1.50E-05	BP
white	**292**	GO:0006270	DNA replication initiation	27	11	0.25	5.50E-09	BP
white	**292**	GO:0006271	DNA strand elongation involved in DNA re...	15	6	0.14	7.50E-09	BP
white	**292**	GO:0006281	DNA repair	789	28	7.28	9.20E-06	BP
white	**292**	GO:0007049	cell cycle	1927	66	17.77	2.40E-09	BP
white	**292**	GO:0030174	regulation of DNA-dependent DNA replicat...	10	5	0.09	1.50E-08	BP
white	**292**	GO:0033314	mitotic DNA replication checkpoint	7	3	0.06	2.60E-05	BP
white	**292**	GO:0051301	cell division	940	35	8.67	1.20E-10	BP
white	**292**	GO:0071897	DNA biosynthetic process	177	9	1.63	8.20E-05	BP
white	**292**	GO:1900264	positive regulation of DNA-directed DNA ...	5	3	0.05	7.60E-06	BP
white	**292**	GO:1902969	mitotic DNA replication	29	5	0.27	8.60E-05	BP
white	**292**	GO:0000775	chromosome, centromeric region	140	9	1.23	9.20E-05	CC
white	**292**	GO:0000785	chromatin	471	15	4.14	7.60E-05	CC
white	**292**	GO:0005634	nucleus	6635	102	58.29	5.30E-05	CC
white	**292**	GO:0005663	DNA replication factor C complex	6	3	0.05	1.30E-05	CC
white	**292**	GO:0005813	centrosome	552	17	4.85	9.40E-07	CC
white	**292**	GO:0031390	Ctf18 RFC-like complex	5	3	0.04	6.60E-06	CC
white	**292**	GO:0042555	MCM complex	11	6	0.1	1.90E-10	CC
white	**292**	GO:0042575	DNA polymerase complex	14	5	0.12	9.30E-08	CC
white	**292**	GO:0043601	nuclear replisome	22	6	0.19	5.90E-08	CC
white	**292**	GO:0071162	CMG complex	10	8	0.09	1.40E-15	CC
white	**292**	GO:0003678	DNA helicase activity	313	9	2.59	4.00E-05	MF
white	**292**	GO:0003688	DNA replication origin binding	17	4	0.14	9.90E-06	MF
white	**292**	GO:0005524	ATP binding	2738	45	22.66	3.50E-06	MF
white	**292**	GO:0106310	protein serine kinase activity	569	15	4.71	8.10E-05	MF
white	**292**	GO:0106311	protein threonine kinase activity	569	15	4.71	8.10E-05	MF
yellow	**1,517**	GO:0010650	positive regulation of cell communicatio...	24	7	0.74	5.70E-06	BP
yellow	**1,517**	GO:0010960	magnesium ion homeostasis	39	8	1.2	2.10E-05	BP
yellow	**1,517**	GO:0034112	positive regulation of homotypic cell-ce...	25	7	0.77	7.70E-06	BP
yellow	**1,517**	GO:0045838	positive regulation of membrane potentia...	33	8	1.02	1.30E-05	BP
yellow	**1,517**	GO:0071286	cellular response to magnesium ion	34	8	1.05	7.10E-06	BP
yellow	**1,517**	GO:0072660	maintenance of protein location in plasm...	25	7	0.77	7.70E-06	BP
yellow	**1,517**	GO:0090314	positive regulation of protein targeting...	36	7	1.11	9.90E-05	BP
yellow	**1,517**	GO:0099612	protein localization to axon	109	11	3.37	7.60E-06	BP
yellow	**1,517**	GO:1900827	positive regulation of membrane depolari...	24	7	0.74	5.70E-06	BP
yellow	**1,517**	GO:1902260	negative regulation of delayed rectifier...	33	7	1.02	5.50E-05	BP
yellow	**1,517**	GO:2000651	positive regulation of sodium ion transm...	29	7	0.9	2.20E-05	BP
yellow	**1,517**	GO:1904399	heparan sulfate binding	37	8	1.15	1.40E-05	MF
yellowgreen	**163**	GO:0035456	response to interferon-beta	15	5	0.06	1.30E-05	BP
yellowgreen	**163**	GO:0035458	cellular response to interferon-beta	13	3	0.05	1.40E-05	BP
yellowgreen	**163**	GO:0042832	defense response to protozoan	17	5	0.06	3.80E-09	BP
yellowgreen	**163**	GO:0050830	defense response to Gram-positive bacter...	122	5	0.45	9.30E-05	BP
yellowgreen	**163**	GO:0071346	cellular response to interferon-gamma	97	7	0.36	7.40E-08	BP
yellowgreen	**163**	GO:0071356	cellular response to tumor necrosis fact...	202	6	0.75	5.30E-07	BP
yellowgreen	**163**	GO:0071360	cellular response to exogenous dsRNA	14	3	0.05	1.80E-05	BP
yellowgreen	**163**	GO:0003725	double-stranded RNA binding	44	4	0.16	1.70E-05	MF
yellowgreen	**163**	GO:0003924	GTPase activity	267	10	0.94	3.30E-08	MF
yellowgreen	**163**	GO:0005525	GTP binding	489	12	1.73	1.30E-07	MF

Chapter 3: Supplementary Data

Table S3.1. Summary of mapped reads. List of mapped reads, before and after quality filtering and the number of counts for each sample.

Sample		1_T0	1_T3	1_T6	1_T9	1_B1	1_B4	2_T0	2_T3	2_T6	2_T9	2_B1	2_B4	4_T0	4_T3	4_T6	4_T9	4_B1	4_B4	5_T0	5_T3	5_T6	5_T9	5_B1	5_B4
Total Number of Reads		71879658	93885826	77382154	91235836	110670460	87429344	92593856	115844670	86203062	96142514	86504116	154888122	87239190	83697386	102764508	78114432	91226384	98829554	93951034	78027752	84536730	79633284	80972104	191944438
Mapped Reads	Pre-filtering	16401908	35025626	32837279	37515004	65204960	57997084	38584832	54707372	42042384	42185042	55253880	105356534	31359454	40751284	47127252	36836798	58403830	62037472	23599518	34592788	39837872	44254154	52399900	113872976
	Post-filtering	32369637	19101866	25960852	36291775	41501167	30293914	31032710	45967915	33198202	37856940	30712736	51741139	17135010	32385853	40758117	29923533	32257671	33808440	12866430	31908447	33238202	29128688	28016989	74191414
Number of Counts	**helio_1.0.m2.1**	0.00	0.00	0.00	0.00	0.00	0.00	0.50	0.00	0.00	0.00	0.50	0.00	0.00	0.00	0.00	0.00	0.50	0.00	0.00	0.00	0.00	0.00	0.00	0.00
	helio_1.0.m2.10	241.24	203.75	75.57	131.27	88.89	198.19	562.19	757.18	221.90	435.69	455.23	490.13	404.62	483.85	184.85	178.43	341.56	272.45	259.15	817.46	99.55	155.94	148.75	253.27
	helio_1.0.m2.100	4.00	4.00	3.00	1.00	0.00	2.00	4.11	11.77	0.00	7.00	0.00	3.95	2.00	3.09	3.00	0.00	2.00	2.00	0.00	0.00	0.00	0.00	0.00	1.00
	helio_1.0.m2.1000	1783.82	413.71	132.11	330.92	259.29	441.46	391.65	598.04	228.31	404.68	175.39	225.42	386.71	536.34	133.99	158.29	262.69	265.18	1005.20	675.30	231.77	917.60	636.55	1286.28
	helio_1.0.m2.10000	4.00	2.00	0.00	2.00	2.00	3.00	4.00	39.01	8.40	25.76	15.78	18.30	67.00	65.00	16.00	32.00	34.99	42.00	22.00	24.58	6.83	6.00	8.71	29.00
	helio_1.0.m2.10001	1.00	4.00	1.00	2.00	0.00	1.00	1.00	8.00	2.00	10.00	4.00	5.00	100.00	70.00	44.00	38.00	58.00	34.00	19.00	9.00	2.00	20.00	13.02	15.00
	helio_1.0.m2.10002	0.00	0.00	0.00	0.00	0.00	0.00	0.00	0.00	0.00	0.00	0.00	0.00	0.00	0.00	0.00	1.89	0.00	0.00	0.00	0.00	0.00	0.00	1.81	0.00
	helio_1.0.m2.10003	0.00	0.00	0.00	0.00	0.00	1.00	0.00	0.00	0.00	0.00	5.01	3.00	0.00	3.00	0.00	0.00	0.00	2.00	0.00	0.00	0.00	1.00	0.00	2.00
	helio_1.0.m2.10004	5.12	3.96	0.00	2.00	4.00	6.99	7.86	24.74	4.00	14.10	14.00	10.41	10.00	5.00	4.00	9.51	13.17	10.00	2.62	21.00	0.00	0.00	4.00	1.00
	helio_1.0.m2.10005	1.00	0.00	0.00	0.00	0.00	0.00	0.00	0.00	0.00	0.00	0.00	0.00	199.44	109.55	81.41	165.47	120.00	96.00	146.76	66.00	39.00	101.59	125.00	117.00
	helio_1.0.m2.10006	0.00	0.00	0.00	0.00	0.00	0.00	0.00	1.00	0.00	0.00	0.00	0.00	0.00	0.00	1.00	0.00	0.00	0.00	1.00	0.00	0.00	0.00	0.00	0.00
	helio_1.0.m2.10007	23.00	16.00	11.00	17.00	13.00	23.00	72.00	108.00	41.00	84.00	35.00	58.00	100.00	226.00	71.00	66.00	92.00	117.00	151.00	216.00	75.00	100.00	80.00	211.00
	helio_1.0.m2.10008	110.38	97.93	39.52	79.76	66.19	73.01	105.26	231.22	128.94	158.57	117.72	127.00	152.45	324.39	128.52	114.62	158.48	122.74	99.22	131.59	24.07	65.08	87.07	91.95
	helio_1.0.m2.10009	86.55	81.73	24.66	42.70	60.17	52.56	117.21	280.55	122.52	102.27	142.25	111.40	26.64	28.18	12.63	3.45	8.24	9.63	98.58	442.02	51.68	51.59	71.29	81.01
	helio_1.0.m2.1001	95.91	8.06	5.00	18.49	13.54	22.97	21.53	35.84	7.39	37.63	6.88	8.01	42.22	49.30	11.48	7.52	15.29	34.57	10.18	0.00	2.20	24.52	17.12	30.77
	helio_1.0.m2.10010	2026.12	1090.45	429.91	859.24	673.00	1058.47	2577.59	8734.56	3349.05	4474.25	3071.54	3985.89	2620.67	2659.11	1525.95	1900.41	2182.34	1705.54	865.68	1754.08	378.02	1144.23	765.45	1422.23
	helio_1.0.m2.10011	2.00	0.00	0.00	3.00	3.00	1.00	3.00	9.00	2.13	3.00	5.00	5.00	2.00	7.00	2.99	2.00	3.00	6.00	4.00	0.00	0.00	3.00	0.00	0.00
	helio_1.0.m2.10012	0.00	0.00	0.00	0.00	0.00	0.00	0.00	0.00	0.00	0.00	0.00	0.00	0.00	0.00	0.00	0.00	0.00	0.00	0.00	0.00	0.00	0.00	0.00	0.00
	helio_1.0.m2.10013	0.00	0.00	0.00	0.00	0.00	0.00	0.00	0.00	0.00	0.00	0.00	0.00	1.00	0.00	0.00	0.00	0.00	0.00	0.00	0.00	0.00	0.00	0.00	0.00
	helio_1.0.m2.10014	0.00	0.00	0.00	0.00	0.00	0.00	0.00	0.00	0.00	1.97	0.00	0.00	2.36	1.45	1.59	1.53	0.00	0.00	3.48	0.00	0.00	2.41	0.00	3.00
	helio_1.0.m2.10015	15.94	14.54	0.90	11.50	5.77	14.39	29.54	24.63	3.28	21.92	6.90	7.05	0.00	1.00	0.00	0.00	0.00	0.00	12.63	0.00	0.00	11.46	12.33	11.92
	helio_1.0.m2.10016	13.73	1.89	0.00	12.23	3.32	4.23	0.00	0.00	0.59	0.00	1.29	1.38	1.28	1.16	0.00	0.00	0.00	0.00	6.00	0.00	1.10	0.00	2.00	1.55
	helio_1.0.m2.10017	210.90	267.14	63.32	145.57	110.34	196.09	299.49	421.64	151.49	259.34	250.36	175.27	110.10	121.50	71.48	64.56	112.45	58.05	187.80	554.22	71.57	193.55	144.06	198.46
	helio_1.0.m2.10018	115.34	41.98	14.00	36.15	44.00	70.51	81.96	282.21	59.00	120.55	88.58	121.53	423.51	346.72	171.03	319.23	311.10	244.04	210.25	42.00	33.99	113.00	170.10	148.59
	helio_1.0.m2.10019	0.00	26.19	17.07	35.26	23.41	4.99	19.66	13.29	49.21	12.56	23.77	15.34	43.66	0.00	0.00	0.00	33.64	20.77	0.00	0.00	0.00	0.00	0.00	0.00
	helio_1.0.m2.1002	308.23	334.19	69.13	168.44	133.38	205.53	240.04	311.31	57.52	101.47	116.54	128.33	424.14	836.97	283.20	271.35	410.18	395.44	136.15	169.30	72.04	35.03	60.20	77.79
	helio_1.0.m2.10020	3.96	1.71	0.93	1.47	0.00	1.31	0.00	2.57	0.00	3.90	0.00	1.48	0.00	23.14	4.62	9.17	5.39	5.05	0.00	0.00	0.00	1.15	1.34	2.53
	helio_1.0.m2.10021	119.11	77.93	17.75	85.24	47.60	64.45	89.37	150.96	23.10	82.11	56.50	57.64	176.49	158.42	96.16	146.43	185.23	127.06	102.95	105.29	12.49	66.64	75.91	83.61
	helio_1.0.m2.10022	3.00	0.00	0.00	1.00	0.00	1.00	3.00	1.00	4.42	2.00	0.00	0.00	9.00	18.00	12.00	14.00	11.00	8.00	4.00	9.00	3.00	1.00	1.00	3.00
	helio_1.0.m2.10023	3.24	0.00	0.00	0.00	0.00	3.93	32.66	0.00	1.52	4.32	0.00	0.00	0.00	0.00	1.24	0.00	1.23	0.00	0.00	0.00	0.00	1.10	0.00	0.00
	helio_1.0.m2.10024	0.00	0.00	0.00	1.00	4.00	1.00	0.00	0.00	5.00	3.00	1.31	1.00	0.00	2.00	1.00	1.00	3.00	0.00	0.00	0.00	2.00	0.00	4.00	1.00
	helio_1.0.m2.10025	5.00	5.01	2.00	3.00	0.00	3.00	6.00	6.00	4.00	3.00	1.00	3.00	4.00	3.00	2.00	1.00	4.00	2.00	9.00	5.00	11.00	2.00	5.00	5.00
	helio_1.0.m2.10026	409.87	293.49	115.04	217.99	184.84	261.05	286.07	569.02	170.23	331.00	208.69	249.50	307.86	334.00	154.44	233.15	240.82	223.60	422.89	716.41	186.81	253.96	261.04	341.32
	helio_1.0.m2.10027	0.00	0.00	0.00	0.00	0.00	0.00	0.00	0.00	0.00	0.00	0.00	0.00	0.00	0.00	0.00	0.00	0.00	0.00	0.00	0.00	0.00	0.00	0.00	0.00
	helio_1.0.m2.10028	0.00	0.00	0.00	0.00	0.00	0.00	0.00	0.00	0.00	0.00	0.00	0.00	0.00	0.00	0.00	0.00	0.00	0.00	0.00	0.00	0.00	0.00	0.00	0.00
	helio_1.0.m2.10029	0.00	0.00	1.10	0.02	0.00	1.25	2.32	11.15	5.62	11.39	3.42	4.84	0.00	2.90	3.95	3.41	0.00	4.00	5.64	9.31	0	1.17	1.16	0.98
	helio_1.0.m2.1003	1.00	3.07	1.55	1.06	2.39	0.00	2.85	2.38	2.45	0.00	6.87	4.05	0.00	0.00	0.00	0.00	0.00	2.05	0.00	0.00	0.00	0.00	0.94	0.00
	helio_1.0.m2.10030	1.00	0.00	0.00	0.00	0.00	0.00	0.00	0.00	0.00	1.00	0.00	0.00	0.00	1.00	0.00	0.00	1.00	0.00	0.00	0.00	2.00	0.00	0.00	0.00
	helio_1.0.m2.10031	1362.95	671.91	287.86	469.95	324.10	456.25	830.21	1813.90	540.58	836.31	721.46	700.33	1407.67	1038.16	520.05	661.94	833.93	543.84	787.91	1556.99	288.01	1196.18	649.64	979.78
	helio_1.0.m2.10032	10.05	4.04	3.09	1.18	9.19	4.14	18.58	7.25	6.99	3.23	7.91	5.22	12.17	5.09	11.91	6.01	5.11	6.18	12.89	1.41	3.08	2.88	8.15	3.92
	helio_1.0.m2.10033	3024.53	2249.47	993.08	1300.32	1017.15	1440.47	3300.38	3558.56	1675.59	2096.09	1633.88	1542.79	2466.10	2890.12	1543.87	1209.10	1673.79	1186.71	2303.73	4745.77	1416.02	1435.84	1589.76	2167.51

Table S3.2. Significantly Enriched GO terms grouped by ontology and via regeneration timepoint pairs. Condition pair T0_T3 represents a comparison of heated conditions T0 (Last day at 26°C) to T3 (3 days at 34°C). Condition heated pair T3_T6 compares heated condition T3 to T6 (6 days at 34°C). Condition pair T6_T9 represent condition T6 to T9 (9 days at 34°C). Heated to bleached condition pair T9_B1 represent a comparison between heated condition T9 and B1 (first time bleached). B1_B4 represents bleached condition pair B1 and B4 (3 days bleached). The colours exhibit the condition pair(s) the GO term is found within, in each ontology, for example, blastocyst hatching (GO:0001835) is expressed in timepoint pairs T0_T3 and T6_T9, within the biological processes (BP) ontology, while gene folding (GO:0006457) is only found in the timepoint pair T0_T3 within the BP ontology. The condition within each of the coloured squares indicates which condition the GO term was upregulated within that pair, for example, gene folding (GO:0006457) was upregulated in condition T0 while blastocyst hatching (GO:0001835) was upregulated in conditions T3 and T9. The GO terms are organised by condition.

Ontology	Condition					Go ID	Term
	T0_T3	T3_T6	T6_T9	T9_B1	B1_B4		
Biological Process (BP)	T0					GO:0001732	formation of cytoplasmic translation ini...
	T0					GO:0006418	tRNA aminoacylation for protein translat...
	T0					GO:0006457	protein folding
	T0					GO:0006886	intracellular protein transport
	T0					GO:0017148	negative regulation of translation
	T0					GO:0019083	viral transcription
	T0					GO:0035206	regulation of hemocyte proliferation
	T0					GO:0043434	response to peptide hormone
	T3					GO:0043474	pigment metabolic process involved in pi...
	T0					GO:0045892	negative regulation of transcription, DN...
	T0					GO:0048022	negative regulation of melanin biosynthe...
	T0					GO:0099576	regulation of protein catabolic process ...
	T0					GO:1903364	positive regulation of cellular protein ...
	T3		T9			GO:0001835	blastocyst hatching
	T3		T9			GO:0007041	lysosomal transport
	T3		T9			GO:0043524	negative regulation of neuron apoptotic ...
	T3		T9			GO:1905247	positive regulation of aspartic-type pep...
	T3		T9	B1		GO:0002265	astrocyte activation involved in immune ...
	T3		T9	B1		GO:0002282	microglial cell activation involved in i...
	T3		T9	B1		GO:0050821	protein stabilization
	T3		T9	B1		GO:0060266	negative regulation of respiratory burst...
	T3		T9	B1		GO:0106016	positive regulation of inflammatory resp...
	T3		T9	B1		GO:1900426	positive regulation of defense response ...
	T3		T9	B1		GO:1902564	negative regulation of neutrophil activa...
	T3		T9	B1		GO:1903334	positive regulation of protein folding
	T3		T9	B1		GO:1903979	negative regulation of microglial cell a...
	T3		T9	B1		GO:1905673	positive regulation of lysosome organiza...
	T0			B1		GO:0010499	proteasomal ubiquitin-independent protei...
	T0			T9		GO:0051085	chaperone cofactor-dependent protein ref...
	T0			T9	B4	GO:0042026	protein refolding
		T3				GO:0008643	carbohydrate transport
		T3				GO:0030497	fatty acid elongation
		T3			B4	GO:0010917	negative regulation of mitochondrial mem...
		T3			B4	GO:0010940	positive regulation of necrotic cell dea...
		T3			B4	GO:0035794	positive regulation of mitochondrial mem...
			T6			GO:0006555	methionine metabolic process
			T9			GO:0006563	L-serine metabolic process
			T9			GO:0006636	unsaturated fatty acid biosynthetic proc...
			T9			GO:0006656	phosphatidylcholine biosynthetic process
			T9			GO:0006665	sphingolipid metabolic process
			T6			GO:0006730	one-carbon metabolic process
			T9			GO:0009932	cell tip growth
			T9			GO:0015816	glycine transport
			T9			GO:0019695	choline metabolic process
			T9			GO:0032259	methylation
			T9			GO:0035641	locomotory exploration behavior
			T9			GO:0035988	chondrocyte proliferation
			T9			GO:0043525	positive regulation of neuron apoptotic ...
			T6			GO:0046498	S-adenosylhomocysteine metabolic process
			T6			GO:0046500	S-adenosylmethionine metabolic process
			T6			GO:0051289	protein homotetramerization
			T9			GO:0060999	positive regulation of dendritic spine d...
			T9			GO:0061351	neural precursor cell proliferation
			T6			GO:1901052	sarcosine metabolic process
			T9			GO:1905146	lysosomal protein catabolic process
			T9	B1		GO:0007042	lysosomal lumen acidification
			T9	B1		GO:0048680	positive regulation of axon regeneration
				T9		GO:0016338	calcium-independent cell-cell adhesion v...
				T9		GO:0045454	cell redox homeostasis
				B1		GO:0045730	respiratory burst
				T9		GO:0071356	cellular response to tumor necrosis fact...
				T9		GO:1903895	negative regulation of IRE1-mediated unf...
					B4	GO:0001666	response to hypoxia
					B1	GO:0002181	cytoplasmic translation
					B1	GO:0006412	translation
					B4	GO:0006957	complement activation, alternative pathw...
					B4	GO:0006958	complement activation, classical pathway
					B4	GO:0009617	response to bacterium
					B4	GO:0045745	positive regulation of G protein-coupled...
					B4	GO:0048859	formation of anatomical boundary
					B4	GO:0071310	cellular response to organic substance

Cellular Component (CC)	T0					GO:0005737	cytoplasm
	T3					GO:0005789	endoplasmic reticulum membrane
	T0					GO:0005829	cytosol
	T0					GO:0005832	chaperonin-containing T-complex
	T0					GO:0016282	eukaryotic 43S preinitiation complex
	T0					GO:0030027	lamellipodium
	T3					GO:0030285	integral component of synaptic vesicle m...
	T0					GO:0033290	eukaryotic 48S preinitiation complex
	T0					GO:0098793	presynapse
	T3		T9	T9		GO:0035578	azurophil granule lumen
	T3			B1		GO:0005770	late endosome
	T0			T9		GO:0042470	melanosome
	T0			T9	B4	GO:0034663	endoplasmic reticulum chaperone complex
		T6				GO:0033018	sarcoplasmic reticulum lumen
		T3		T9		GO:0005765	lysosomal membrane
				T9		GO:0005790	smooth endoplasmic reticulum
				T9		GO:0008540	proteasome regulatory particle, base sub...
				T9		GO:0019773	proteasome core complex, alpha-subunit c...
				T9		GO:0022624	proteasome accessory complex
				T9		GO:0043020	NADPH oxidase complex
				T9		GO:0035579	specific granule membrane
				T9	B4	GO:0005783	endoplasmic reticulum
					B4	GO:0005604	basement membrane
					B1	GO:0005840	ribosome
					B1	GO:0022625	cytosolic large ribosomal subunit
					B1	GO:0022626	cytosolic ribosome
					B1	GO:0022627	cytosolic small ribosomal subunit
					B1	GO:0030867	rough endoplasmic reticulum membrane
					B1	GO:0042788	polysomal ribosome
Molecular Function (MF)	T0					GO:0000981	DNA-binding transcription factor activit...
	T0					GO:0003714	transcription corepressor activity
	T0					GO:0003729	mRNA binding
	T0					GO:0003743	translation initiation factor activity
	T0					GO:0003756	protein disulfide isomerase activity
	T0					GO:0004812	aminoacyl-tRNA ligase activity
	T3					GO:0015370	solute:sodium symporter activity
	T0					GO:0019905	syntaxin binding
	T0					GO:0031072	heat shock protein binding
	T3					GO:0047676	arachidonate-CoA ligase activity
	T0					GO:0070569	uridylyltransferase activity
	T3		T9	B1		GO:0051087	chaperone binding
	T0			T9		GO:0044183	protein folding chaperone
	T0			T9		GO:0051082	unfolded protein binding
	T0			T9		GO:0051787	misfolded protein binding
		T3				GO:0004316	3-oxoacyl-[acyl-carrier-protein] reducta...
		T3				GO:0004499	N,N-dimethylaniline monooxygenase activi...
		T3				GO:0050661	NADP binding
		T3				GO:0050681	androgen receptor binding
		T3				GO:0102131	3-oxo-glutaryl-[acp] methyl ester reduct...
		T3				GO:0102132	3-oxo-pimeloyl-[acp] methyl ester reduct...
			T9			GO:0004609	phosphatidylserine decarboxylase activit...
			T6			GO:0005542	folic acid binding
			T6			GO:0008170	N-methyltransferase activity
			T9			GO:0015187	glycine transmembrane transporter activi...
			T6			GO:0016594	glycine binding
			T9			GO:0140358	P-type transmembrane transporter activit...
			T6			GO:1904047	S-adenosyl-L-methionine binding
				T9		GO:0016175	superoxide-generating NAD(P)H oxidase ac...
				T9		GO:0016668	oxidoreductase activity, acting on a sul...
				T9		GO:0016842	amidine-lyase activity
				T9		GO:0036402	proteasome-activating ATPase activity
					B1	GO:0019843	rRNA binding
					B4	GO:0020037	heme binding

Chapter 4: Supplementary Data

Table S4.1. Significantly Enriched GO terms and associated gene families. List of all the significantly enriched GO terms with all their associated gene families grouped by GO term ID. The list includes the condition pair and ontology they were expressed in and what timepoint the gene was upregulated in. Abbreviations: MF = Molecular Function, BP = Biological process, CC = Cellular Component.

Condition	Upregulated	Ontology	GO term ID/Term	Symbiont ID	Protein Family
T0_T3	T0	MF	GO:0004198 - calcium-dependent cysteine-type endopept…	SymbC1.scaffold10056.1	Calpain family cysteine protease
T0_T3	T0	MF	GO:0004198 - calcium-dependent cysteine-type endopept…	SymbC1.scaffold10510.1	Calpain family cysteine protease
T0_T3	T3	MF	GO:0004198 - calcium-dependent cysteine-type endopept…	SymbC1.scaffold11140.2	Calpain family cysteine protease
T0_T3	T3	MF	GO:0004198 - calcium-dependent cysteine-type endopept…	SymbC1.scaffold12305.1	Calpain family cysteine protease
T0_T3	T3	MF	GO:0004198 - calcium-dependent cysteine-type endopept…	SymbC1.scaffold12816.1	Calpain family cysteine protease
T0_T3	T3	MF	GO:0004198 - calcium-dependent cysteine-type endopept…	SymbC1.scaffold15905.1	Calpain family cysteine protease
T0_T3	T0	MF	GO:0004198 - calcium-dependent cysteine-type endopept…	SymbC1.scaffold475.7	Calpain family cysteine protease
T0_T3	T3	MF	GO:0004198 - calcium-dependent cysteine-type endopept…	SymbC1.scaffold6019.2	EF-hand domain pair;Calpain family cysteine protease
T0_T3	T0	MF	GO:0004198 - calcium-dependent cysteine-type endopept…	SymbC1.scaffold651.13	PBZ domain;Calpain family cysteine protease
T0_T3	T0	MF	GO:0004672 - protein kinase activity	SymbC1.scaffold1077.6	Protein kinase domain
T0_T3	T0	MF	GO:0004672 - protein kinase activity	SymbC1.scaffold1129.8	Protein kinase domain
T0_T3	T3	MF	GO:0004672 - protein kinase activity	SymbC1.scaffold1236.5	Protein kinase domain
T0_T3	T3	MF	GO:0004672 - protein kinase activity	SymbC1.scaffold1244.8	EF-hand domain pair;Protein kinase domain
T0_T3	T0	MF	GO:0004672 - protein kinase activity	SymbC1.scaffold12477.1	Protein kinase domain;EF hand
T0_T3	T0	MF	GO:0004672 - protein kinase activity	SymbC1.scaffold1504.6	Protein kinase domain
T0_T3	T0	MF	GO:0004672 - protein kinase activity	SymbC1.scaffold1522.6	Protein kinase domain
T0_T3	T0	MF	GO:0004672 - protein kinase activity	SymbC1.scaffold1598.8	Protein kinase domain
T0_T3	T0	MF	GO:0004672 - protein kinase activity	SymbC1.scaffold1657.2	Protein kinase domain
T0_T3	T0	MF	GO:0004672 - protein kinase activity	SymbC1.scaffold166.13	Protein kinase domain
T0_T3	T0	MF	GO:0004672 - protein kinase activity	SymbC1.scaffold1753.3	Protein kinase domain
T0_T3	T0	MF	GO:0004672 - protein kinase activity	SymbC1.scaffold1847.1	Protein kinase domain;Oxidoreductase family, NAD-binding Rossmann fold
T0_T3	T0	MF	GO:0004672 - protein kinase activity	SymbC1.scaffold1921.7	Protein kinase domain
T0_T3	T0	MF	GO:0004672 - protein kinase activity	SymbC1.scaffold2141.3	Protein kinase domain;Aldo/keto reductase family
T0_T3	T0	MF	GO:0004672 - protein kinase activity	SymbC1.scaffold2243.1	Protein kinase domain
T0_T3	T0	MF	GO:0004672 - protein kinase activity	SymbC1.scaffold2301.8	Protein kinase domain
T0_T3	T0	MF	GO:0004672 - protein kinase activity	SymbC1.scaffold2342.5	Protein kinase domain
T0_T3	T0	MF	GO:0004672 - protein kinase activity	SymbC1.scaffold2375.1	Protein kinase domain
T0_T3	T0	MF	GO:0004672 - protein kinase activity	SymbC1.scaffold247.9	Protein kinase domain
T0_T3	T0	MF	GO:0004672 - protein kinase activity	SymbC1.scaffold248.5	Protein kinase domain;EF-hand domain pair
T0_T3	T0	MF	GO:0004672 - protein kinase activity	SymbC1.scaffold2490.3	Protein kinase domain
T0_T3	T3	MF	GO:0004672 - protein kinase activity	SymbC1.scaffold252.6	Protein kinase domain;HEAT repeats
T0_T3	T3	MF	GO:0004672 - protein kinase activity	SymbC1.scaffold2654.1	Protein kinase domain;MYND finger;SET domain
T0_T3	T0	MF	GO:0004672 - protein kinase activity	SymbC1.scaffold2876.4	Protein kinase domain
T0_T3	T0	MF	GO:0004672 - protein kinase activity	SymbC1.scaffold2876.5	Protein kinase domain
T0_T3	T0	MF	GO:0004672 - protein kinase activity	SymbC1.scaffold2879.1	Protein kinase domain
T0_T3	T0	MF	GO:0004672 - protein kinase activity	SymbC1.scaffold3037.3	Protein kinase domain
T0_T3	T0	MF	GO:0004672 - protein kinase activity	SymbC1.scaffold3072.5	EF-hand domain pair;Protein kinase domain
T0_T3	T0	MF	GO:0004672 - protein kinase activity	SymbC1.scaffold3161.6	Protein kinase domain
T0_T3	T3	MF	GO:0004672 - protein kinase activity	SymbC1.scaffold3168.4	Protein kinase domain
T0_T3	T0	MF	GO:0004672 - protein kinase activity	SymbC1.scaffold3172.3	Protein kinase domain
T0_T3	T0	MF	GO:0004672 - protein kinase activity	SymbC1.scaffold3342.2	Protein kinase domain
T0_T3	T0	MF	GO:0004672 - protein kinase activity	SymbC1.scaffold3380.2	Protein kinase domain
T0_T3	T0	MF	GO:0004672 - protein kinase activity	SymbC1.scaffold3407.4	Protein kinase domain
T0_T3	T0	MF	GO:0004672 - protein kinase activity	SymbC1.scaffold3474.7	Protein kinase domain
T0_T3	T0	MF	GO:0004672 - protein kinase activity	SymbC1.scaffold3583.1	Protein kinase domain
T0_T3	T0	MF	GO:0004672 - protein kinase activity	SymbC1.scaffold3613.3	Protein kinase domain

T0_T3	T0	MF	GO:0004672 - protein kinase activity	SymbC1.scaffold3691.1	Protein kinase domain;Zinc finger, C3HC4 type (RING finger)
T0_T3	T0	MF	GO:0004672 - protein kinase activity	SymbC1.scaffold3988.4	Protein kinase domain
T0_T3	T0	MF	GO:0004672 - protein kinase activity	SymbC1.scaffold4265.1	Protein tyrosine and serine/threonine kinase
T0_T3	T0	MF	GO:0004672 - protein kinase activity	SymbC1.scaffold4387.1	Protein tyrosine and serine/threonine kinase
T0_T3	T0	MF	GO:0004672 - protein kinase activity	SymbC1.scaffold4972.3	Protein kinase domain
T0_T3	T0	MF	GO:0004672 - protein kinase activity	SymbC1.scaffold517.5	Protein kinase domain
T0_T3	T3	MF	GO:0004672 - protein kinase activity	SymbC1.scaffold518.5	Protein kinase domain
T0_T3	T3	MF	GO:0004672 - protein kinase activity	SymbC1.scaffold5324.1	Protein kinase domain;Cyclic nucleotide-binding domain
T0_T3	T0	MF	GO:0004672 - protein kinase activity	SymbC1.scaffold5362.1	Protein kinase domain
T0_T3	T3	MF	GO:0004672 - protein kinase activity	SymbC1.scaffold5416.4	EF-hand domain pair;Protein kinase domain
T0_T3	T0	MF	GO:0004672 - protein kinase activity	SymbC1.scaffold5435.5	Protein kinase domain
T0_T3	T3	MF	GO:0004672 - protein kinase activity	SymbC1.scaffold569.4	Protein kinase domain
T0_T3	T3	MF	GO:0004672 - protein kinase activity	SymbC1.scaffold574.4	Protein kinase domain
T0_T3	T0	MF	GO:0004672 - protein kinase activity	SymbC1.scaffold5966.4	Protein kinase domain
T0_T3	T3	MF	GO:0004672 - protein kinase activity	SymbC1.scaffold6028.1	Cyclic nucleotide-binding domain;Protein kinase domain
T0_T3	T3	MF	GO:0004672 - protein kinase activity	SymbC1.scaffold6468.4	Protein kinase domain
T0_T3	T0	MF	GO:0004672 - protein kinase activity	SymbC1.scaffold697.3	KH domain;Protein kinase domain
T0_T3	T0	MF	GO:0004672 - protein kinase activity	SymbC1.scaffold702.5	Protein kinase domain
T0_T3	T3	MF	GO:0004672 - protein kinase activity	SymbC1.scaffold7066.2	Protein kinase domain
T0_T3	T0	MF	GO:0004672 - protein kinase activity	SymbC1.scaffold7123.1	Protein kinase domain
T0_T3	T0	MF	GO:0004672 - protein kinase activity	SymbC1.scaffold7333.1	Protein kinase domain
T0_T3	T3	MF	GO:0004672 - protein kinase activity	SymbC1.scaffold776.25	Protein kinase domain
T0_T3	T0	MF	GO:0004672 - protein kinase activity	SymbC1.scaffold7859.3	Protein kinase domain
T0_T3	T3	MF	GO:0004672 - protein kinase activity	SymbC1.scaffold798.3	Protein tyrosine and serine/threonine kinase
T0_T3	T0	MF	GO:0004672 - protein kinase activity	SymbC1.scaffold8156.4	Alpha-kinase family
T0_T3	T0	MF	GO:0004672 - protein kinase activity	SymbC1.scaffold8444.2	Protein kinase domain
T0_T3	T0	MF	GO:0004672 - protein kinase activity	SymbC1.scaffold8515.1	Protein kinase domain;Poly(ADP-ribose) polymerase catalytic domain;WWE domain
T0_T3	T0	MF	GO:0004672 - protein kinase activity	SymbC1.scaffold859.1	Protein kinase domain
T0_T3	T0	MF	GO:0004672 - protein kinase activity	SymbC1.scaffold9730.1	Alpha-kinase family
T0_T3	T0	BP	GO:0006468 - protein phosphorylation	SymbC1.scaffold1077.6	Protein kinase domain
T0_T3	T0	BP	GO:0006468 - protein phosphorylation	SymbC1.scaffold1129.8	Protein kinase domain
T0_T3	T3	BP	GO:0006468 - protein phosphorylation	SymbC1.scaffold1236.5	Protein kinase domain
T0_T3	T3	BP	GO:0006468 - protein phosphorylation	SymbC1.scaffold1244.8	EF-hand domain pair;Protein kinase domain
T0_T3	T0	BP	GO:0006468 - protein phosphorylation	SymbC1.scaffold12477.1	Protein kinase domain;EF hand
T0_T3	T0	BP	GO:0006468 - protein phosphorylation	SymbC1.scaffold1504.6	Protein kinase domain
T0_T3	T0	BP	GO:0006468 - protein phosphorylation	SymbC1.scaffold1522.6	Protein kinase domain
T0_T3	T0	BP	GO:0006468 - protein phosphorylation	SymbC1.scaffold1598.8	Protein kinase domain
T0_T3	T0	BP	GO:0006468 - protein phosphorylation	SymbC1.scaffold1657.2	Protein kinase domain
T0_T3	T0	BP	GO:0006468 - protein phosphorylation	SymbC1.scaffold166.13	Protein kinase domain
T0_T3	T0	BP	GO:0006468 - protein phosphorylation	SymbC1.scaffold1753.3	Protein kinase domain
T0_T3	T0	BP	GO:0006468 - protein phosphorylation	SymbC1.scaffold1847.1	Protein kinase domain;Oxidoreductase family, NAD-binding Rossmann fold
T0_T3	T0	BP	GO:0006468 - protein phosphorylation	SymbC1.scaffold1921.7	Protein kinase domain
T0_T3	T0	BP	GO:0006468 - protein phosphorylation	SymbC1.scaffold2141.3	Protein kinase domain;Aldo/keto reductase family
T0_T3	T0	BP	GO:0006468 - protein phosphorylation	SymbC1.scaffold2243.1	Protein kinase domain
T0_T3	T0	BP	GO:0006468 - protein phosphorylation	SymbC1.scaffold2301.8	Protein kinase domain
T0_T3	T0	BP	GO:0006468 - protein phosphorylation	SymbC1.scaffold2342.5	Protein kinase domain
T0_T3	T0	BP	GO:0006468 - protein phosphorylation	SymbC1.scaffold2375.1	Protein kinase domain

T0_T3	T0	BP	GO:0006468 - protein phosphorylation	SymbC1.scaffold247.9	Protein kinase domain
T0_T3	T0	BP	GO:0006468 - protein phosphorylation	SymbC1.scaffold248.5	Protein kinase domain;EF-hand domain pair
T0_T3	T0	BP	GO:0006468 - protein phosphorylation	SymbC1.scaffold2490.3	Protein kinase domain
T0_T3	T3	BP	GO:0006468 - protein phosphorylation	SymbC1.scaffold252.6	Protein kinase domain;HEAT repeats
T0_T3	T3	BP	GO:0006468 - protein phosphorylation	SymbC1.scaffold2654.1	Protein kinase domain;MYND finger;SET domain
T0_T3	T0	BP	GO:0006468 - protein phosphorylation	SymbC1.scaffold2876.4	Protein kinase domain
T0_T3	T0	BP	GO:0006468 - protein phosphorylation	SymbC1.scaffold2876.5	Protein kinase domain
T0_T3	T0	BP	GO:0006468 - protein phosphorylation	SymbC1.scaffold2879.1	Protein kinase domain
T0_T3	T0	BP	GO:0006468 - protein phosphorylation	SymbC1.scaffold2952.2	Cyclin
T0_T3	T0	BP	GO:0006468 - protein phosphorylation	SymbC1.scaffold3037.3	Protein kinase domain
T0_T3	T0	BP	GO:0006468 - protein phosphorylation	SymbC1.scaffold3072.5	EF-hand domain pair;Protein kinase domain
T0_T3	T0	BP	GO:0006468 - protein phosphorylation	SymbC1.scaffold3161.6	Protein kinase domain
T0_T3	T3	BP	GO:0006468 - protein phosphorylation	SymbC1.scaffold3168.4	Protein kinase domain
T0_T3	T0	BP	GO:0006468 - protein phosphorylation	SymbC1.scaffold3172.3	Protein kinase domain
T0_T3	T0	BP	GO:0006468 - protein phosphorylation	SymbC1.scaffold3342.2	Protein kinase domain
T0_T3	T0	BP	GO:0006468 - protein phosphorylation	SymbC1.scaffold3380.2	Protein kinase domain
T0_T3	T0	BP	GO:0006468 - protein phosphorylation	SymbC1.scaffold3407.4	Protein kinase domain
T0_T3	T0	BP	GO:0006468 - protein phosphorylation	SymbC1.scaffold3474.7	Protein kinase domain
T0_T3	T0	BP	GO:0006468 - protein phosphorylation	SymbC1.scaffold3583.1	Protein kinase domain
T0_T3	T0	BP	GO:0006468 - protein phosphorylation	SymbC1.scaffold3613.3	Protein kinase domain
T0_T3	T0	BP	GO:0006468 - protein phosphorylation	SymbC1.scaffold3691.1	Protein kinase domain;Zinc finger, C3HC4 type (RING finger)
T0_T3	T0	BP	GO:0006468 - protein phosphorylation	SymbC1.scaffold3988.4	Protein kinase domain
T0_T3	T0	BP	GO:0006468 - protein phosphorylation	SymbC1.scaffold4265.1	Protein tyrosine and serine/threonine kinase
T0_T3	T0	BP	GO:0006468 - protein phosphorylation	SymbC1.scaffold4387.1	Protein tyrosine and serine/threonine kinase
T0_T3	T0	BP	GO:0006468 - protein phosphorylation	SymbC1.scaffold4972.3	Protein kinase domain
T0_T3	T0	BP	GO:0006468 - protein phosphorylation	SymbC1.scaffold517.5	Protein kinase domain
T0_T3	T3	BP	GO:0006468 - protein phosphorylation	SymbC1.scaffold518.5	Protein kinase domain
T0_T3	T3	BP	GO:0006468 - protein phosphorylation	SymbC1.scaffold5324.1	Protein kinase domain;Cyclic nucleotide-binding domain
T0_T3	T0	BP	GO:0006468 - protein phosphorylation	SymbC1.scaffold5362.1	Protein kinase domain
T0_T3	T3	BP	GO:0006468 - protein phosphorylation	SymbC1.scaffold5416.4	EF-hand domain pair;Protein kinase domain
T0_T3	T0	BP	GO:0006468 - protein phosphorylation	SymbC1.scaffold5435.5	Protein kinase domain
T0_T3	T3	BP	GO:0006468 - protein phosphorylation	SymbC1.scaffold569.4	Protein kinase domain
T0_T3	T3	BP	GO:0006468 - protein phosphorylation	SymbC1.scaffold574.4	Protein kinase domain
T0_T3	T0	BP	GO:0006468 - protein phosphorylation	SymbC1.scaffold5966.4	Protein kinase domain
T0_T3	T3	BP	GO:0006468 - protein phosphorylation	SymbC1.scaffold6028.1	Cyclic nucleotide-binding domain;Protein kinase domain
T0_T3	T3	BP	GO:0006468 - protein phosphorylation	SymbC1.scaffold6468.4	Protein kinase domain
T0_T3	T0	BP	GO:0006468 - protein phosphorylation	SymbC1.scaffold697.3	KH domain;Protein kinase domain
T0_T3	T0	BP	GO:0006468 - protein phosphorylation	SymbC1.scaffold702.5	Protein kinase domain
T0_T3	T3	BP	GO:0006468 - protein phosphorylation	SymbC1.scaffold7066.2	Protein kinase domain
T0_T3	T0	BP	GO:0006468 - protein phosphorylation	SymbC1.scaffold7123.1	Protein kinase domain
T0_T3	T0	BP	GO:0006468 - protein phosphorylation	SymbC1.scaffold7333.1	Protein kinase domain
T0_T3	T3	BP	GO:0006468 - protein phosphorylation	SymbC1.scaffold776.25	Protein kinase domain
T0_T3	T0	BP	GO:0006468 - protein phosphorylation	SymbC1.scaffold7859.3	Protein kinase domain
T0_T3	T3	BP	GO:0006468 - protein phosphorylation	SymbC1.scaffold798.3	Protein tyrosine and serine/threonine kinase
T0_T3	T0	BP	GO:0006468 - protein phosphorylation	SymbC1.scaffold8156.4	Alpha-kinase family
T0_T3	T0	BP	GO:0006468 - protein phosphorylation	SymbC1.scaffold8444.2	Protein kinase domain
T0_T3	T0	BP	GO:0006468 - protein phosphorylation	SymbC1.scaffold8515.1	Protein kinase domain;Poly(ADP-ribose) polymerase catalytic domain;WWE domain

B1_B4	B4	MF	GO:0005515 - protein binding	SymbC1.scaffold2601.11	WD domain, G-beta repeat
B1_B4	B4	MF	GO:0005515 - protein binding	SymbC1.scaffold2708.3	Glycosyl transferase family 2;BTB/POZ domain
B1_B4	B1	MF	GO:0005515 - protein binding	SymbC1.scaffold273.1	Reverse transcriptase (RNA-dependent DNA polymerase)
B1_B4	B4	MF	GO:0005515 - protein binding	SymbC1.scaffold2768.1	SET domain
B1_B4	B4	MF	GO:0005515 - protein binding	SymbC1.scaffold2819.3	Ankyrin repeats (3 copies);Ankyrin repeat
B1_B4	B1	MF	GO:0005515 - protein binding	SymbC1.scaffold2905.5	Ankyrin repeats (3 copies)
B1_B4	B1	MF	GO:0005515 - protein binding	SymbC1.scaffold2920.5	EF-hand domain pair;SH3 domain;Calpain family cysteine protease
B1_B4	B4	MF	GO:0005515 - protein binding	SymbC1.scaffold2952.2	Cyclin
B1_B4	B4	MF	GO:0005515 - protein binding	SymbC1.scaffold3016.1	Glycogen recognition site of AMP-activated protein kinase
B1_B4	B1	MF	GO:0005515 - protein binding	SymbC1.scaffold3018.7	Ankyrin repeats (3 copies)
B1_B4	B4	MF	GO:0005515 - protein binding	SymbC1.scaffold3037.1	Activator of Hsp90 ATPase, N-terminal
B1_B4	B4	MF	GO:0005515 - protein binding	SymbC1.scaffold305.8	FHA domain
B1_B4	B4	MF	GO:0005515 - protein binding	SymbC1.scaffold3151.1	Ubiquitin family;XPC-binding domain;UBA/TS-N domain
B1_B4	B4	MF	GO:0005515 - protein binding	SymbC1.scaffold3187.1	C-terminal region of eIF3h;JAB1/Mov34/MPN/PAD-1 ubiquitin protease
B1_B4	B4	MF	GO:0005515 - protein binding	SymbC1.scaffold319.5	Cyclin
B1_B4	B1	MF	GO:0005515 - protein binding	SymbC1.scaffold3197.6	DnaJ C terminal domain;DnaJ domain;Ankyrin repeats (many copies)
B1_B4	B1	MF	GO:0005515 - protein binding	SymbC1.scaffold333.6	BTB/POZ domain
B1_B4	B1	MF	GO:0005515 - protein binding	SymbC1.scaffold3370.1	Ankyrin repeats (3 copies)
B1_B4	B4	MF	GO:0005515 - protein binding	SymbC1.scaffold3492.1	WD domain, G-beta repeat
B1_B4	B1	MF	GO:0005515 - protein binding	SymbC1.scaffold3548.4	KH domain;MMPL family;WW domain
B1_B4	B1	MF	GO:0005515 - protein binding	SymbC1.scaffold384.7	WD domain, G-beta repeat
B1_B4	B1	MF	GO:0005515 - protein binding	SymbC1.scaffold3852.1	SAM domain (Sterile alpha motif)
B1_B4	B1	MF	GO:0005515 - protein binding	SymbC1.scaffold3949.3	Kinesin motor domain
B1_B4	B4	MF	GO:0005515 - protein binding	SymbC1.scaffold4041.2	Ankyrin repeats (3 copies)
B1_B4	B1	MF	GO:0005515 - protein binding	SymbC1.scaffold4076.5	Kinesin motor domain
B1_B4	B1	MF	GO:0005515 - protein binding	SymbC1.scaffold4084.2	Ankyrin repeats (3 copies)
B1_B4	B4	MF	GO:0005515 - protein binding	SymbC1.scaffold4113.6	Aminotransferase class I and II
B1_B4	B4	MF	GO:0005515 - protein binding	SymbC1.scaffold4143.1	WD domain, G-beta repeat
B1_B4	B4	MF	GO:0005515 - protein binding	SymbC1.scaffold4163.3	FHA domain
B1_B4	B4	MF	GO:0005515 - protein binding	SymbC1.scaffold4166.4	Ankyrin repeat
B1_B4	B4	MF	GO:0005515 - protein binding	SymbC1.scaffold4200.3	Ankyrin repeats (3 copies)
B1_B4	B4	MF	GO:0005515 - protein binding	SymbC1.scaffold423.1	BTB/POZ domain
B1_B4	B4	MF	GO:0005515 - protein binding	SymbC1.scaffold4316.3	WW domain
B1_B4	B1	MF	GO:0005515 - protein binding	SymbC1.scaffold4346.2	BTB/POZ domain;Glutaredoxin
B1_B4	B1	MF	GO:0005515 - protein binding	SymbC1.scaffold436.14	Kinesin motor domain
B1_B4	B1	MF	GO:0005515 - protein binding	SymbC1.scaffold439.8	Ankyrin repeats (3 copies)
B1_B4	B4	MF	GO:0005515 - protein binding	SymbC1.scaffold4424.3	Fibronectin type III domain;Cyclophilin type peptidyl-prolyl cis-trans isomerase/CLD
B1_B4	B4	MF	GO:0005515 - protein binding	SymbC1.scaffold443.8	WD domain, G-beta repeat;Glyoxalase/Bleomycin resistance protein/Dioxygenase superfamily
B1_B4	B4	MF	GO:0005515 - protein binding	SymbC1.scaffold4568.2	GAF domain;Transmembrane protein 65
B1_B4	B4	MF	GO:0005515 - protein binding	SymbC1.scaffold4576.1	Kelch motif;Phenazine biosynthesis-like protein;Acetyltransferase (GNAT) family
B1_B4	B4	MF	GO:0005515 - protein binding	SymbC1.scaffold4792.2	Ankyrin repeats (3 copies)
B1_B4	B4	MF	GO:0005515 - protein binding	SymbC1.scaffold4906.1	Ankyrin repeat;Ankyrin repeats (3 copies)
B1_B4	B4	MF	GO:0005515 - protein binding	SymbC1.scaffold51.6	Ubiquitin family
B1_B4	B1	MF	GO:0005515 - protein binding	SymbC1.scaffold517.2	Ankyrin repeats (3 copies);FYVE zinc finger;Leucine rich repeat
B1_B4	B4	MF	GO:0005515 - protein binding	SymbC1.scaffold541.6	Ankyrin repeats (many copies);BD-FAE
B1_B4	B4	MF	GO:0005515 - protein binding	SymbC1.scaffold551.2	WW domain;'Cold-shock' DNA-binding domain
B1_B4	B4	MF	GO:0005515 - protein binding	SymbC1.scaffold555.11	Sec7 domain;Ankyrin repeats (3 copies)

T0_T3	T0	BP	GO:0006468 - protein phosphorylation	SymbC1.scaffold859.1	Protein kinase domain
T0_T3	T0	BP	GO:0006468 - protein phosphorylation	SymbC1.scaffold9730.1	Alpha-kinase family
T0_T3	T0	BP	GO:0006811 - ion transport	SymbC1.scaffold10041.3	Endoplasmic reticulum protein ERp29, C-terminal domain;ERp29, N-terminal domain
T0_T3	T3	BP	GO:0006811 - ion transport	SymbC1.scaffold1095.11	Ion transport protein
T0_T3	T0	BP	GO:0006811 - ion transport	SymbC1.scaffold1129.3	EF-hand domain pair;Ion transport protein
T0_T3	T0	BP	GO:0006811 - ion transport	SymbC1.scaffold11359.1	Ion transport protein
T0_T3	T0	BP	GO:0006811 - ion transport	SymbC1.scaffold1160.3	KH domain;Zinc knuckle;Na+/Pi-cotransporter
T0_T3	T3	BP	GO:0006811 - ion transport	SymbC1.scaffold11886.1	Ion transport protein
T0_T3	T0	BP	GO:0006811 - ion transport	SymbC1.scaffold1236.3	Inorganic H+ pyrophosphatase
T0_T3	T0	BP	GO:0006811 - ion transport	SymbC1.scaffold1247.6	Ion transport protein
T0_T3	T0	BP	GO:0006811 - ion transport	SymbC1.scaffold128.2	Plug domain of Sec61p;SecY
T0_T3	T0	BP	GO:0006811 - ion transport	SymbC1.scaffold130.11	Ion transport protein
T0_T3	T0	BP	GO:0006811 - ion transport	SymbC1.scaffold136.11	Ion transport protein
T0_T3	T0	BP	GO:0006811 - ion transport	SymbC1.scaffold151.5	EF-hand domain pair;Ion transport protein
T0_T3	T3	BP	GO:0006811 - ion transport	SymbC1.scaffold1537.6	Ion transport protein
T0_T3	T0	BP	GO:0006811 - ion transport	SymbC1.scaffold158.2	Ion transport protein
T0_T3	T3	BP	GO:0006811 - ion transport	SymbC1.scaffold1602.1	Signal recognition particle, alpha subunit, N-terminal
T0_T3	T0	BP	GO:0006811 - ion transport	SymbC1.scaffold1605.10	EF hand;Ion transport protein
T0_T3	T0	BP	GO:0006811 - ion transport	SymbC1.scaffold1609.4	Nucleotide-sugar transporter
T0_T3	T0	BP	GO:0006811 - ion transport	SymbC1.scaffold1618.4	Ion transport protein;EF hand
T0_T3	T0	BP	GO:0006811 - ion transport	SymbC1.scaffold1639.9	Cation efflux family
T0_T3	T3	BP	GO:0006811 - ion transport	SymbC1.scaffold1655.1	Adaptin C-terminal domain
T0_T3	T0	BP	GO:0006811 - ion transport	SymbC1.scaffold176.3	C-5 cytosine-specific DNA methylase;Ion transport protein
T0_T3	T3	BP	GO:0006811 - ion transport	SymbC1.scaffold245.6	Ion transport protein;EF hand
T0_T3	T0	BP	GO:0006811 - ion transport	SymbC1.scaffold2507.1	HCO3- transporter family
T0_T3	T3	BP	GO:0006811 - ion transport	SymbC1.scaffold2514.3	HCO3- transporter family
T0_T3	T3	BP	GO:0006811 - ion transport	SymbC1.scaffold2635.4	Neurotransmitter-gated ion-channel ligand binding domain
T0_T3	T0	BP	GO:0006811 - ion transport	SymbC1.scaffold2717.3	Nucleotide-sugar transporter
T0_T3	T0	BP	GO:0006811 - ion transport	SymbC1.scaffold2718.1	Ciliary BBSome complex subunit 2, N-terminal
T0_T3	T0	BP	GO:0006811 - ion transport	SymbC1.scaffold2758.5	Ion transport protein
T0_T3	T0	BP	GO:0006811 - ion transport	SymbC1.scaffold2884.7	Ion transport protein
T0_T3	T0	BP	GO:0006811 - ion transport	SymbC1.scaffold2911.1	Adaptin N terminal region
T0_T3	T3	BP	GO:0006811 - ion transport	SymbC1.scaffold3086.1	Adaptin N terminal region;Beta2-adaptin appendage, C-terminal sub-domain
T0_T3	T0	BP	GO:0006811 - ion transport	SymbC1.scaffold3110.5	Magnesium transporter NIPA
T0_T3	T0	BP	GO:0006811 - ion transport	SymbC1.scaffold3196.1	Ion transport protein
T0_T3	T0	BP	GO:0006811 - ion transport	SymbC1.scaffold3520.1	Inorganic H+ pyrophosphatase
T0_T3	T3	BP	GO:0006811 - ion transport	SymbC1.scaffold3552.4	Ion transport protein;EF-hand domain pair
T0_T3	T0	BP	GO:0006811 - ion transport	SymbC1.scaffold3589.4	Inorganic H+ pyrophosphatase
T0_T3	T0	BP	GO:0006811 - ion transport	SymbC1.scaffold3640.2	Sec23/Sec24 zinc finger
T0_T3	T0	BP	GO:0006811 - ion transport	SymbC1.scaffold3693.2	Ion transport protein
T0_T3	T0	BP	GO:0006811 - ion transport	SymbC1.scaffold380.3	Inorganic H+ pyrophosphatase
T0_T3	T0	BP	GO:0006811 - ion transport	SymbC1.scaffold3861.2	V-type ATPase 116kDa subunit family
T0_T3	T0	BP	GO:0006811 - ion transport	SymbC1.scaffold394.1	Sodium/hydrogen exchanger family
T0_T3	T3	BP	GO:0006811 - ion transport	SymbC1.scaffold397.1	Ion transport protein
T0_T3	T0	BP	GO:0006811 - ion transport	SymbC1.scaffold4148.8	Voltage gated chloride channel
T0_T3	T0	BP	GO:0006811 - ion transport	SymbC1.scaffold4318.3	Ion transport protein
T0_T3	T3	BP	GO:0006811 - ion transport	SymbC1.scaffold4486.1	Ion transport protein

T0_T3	T0	BP	GO:0006811 - ion transport	SymbC1.scaffold45.13	Ion transport protein
T0_T3	T0	BP	GO:0006811 - ion transport	SymbC1.scaffold4673.1	Ion transport protein;Glycosyl transferase family 8
T0_T3	T0	BP	GO:0006811 - ion transport	SymbC1.scaffold4753.3	Ion transport protein
T0_T3	T0	BP	GO:0006811 - ion transport	SymbC1.scaffold564.4	Ammonium Transporter Family
T0_T3	T0	BP	GO:0006811 - ion transport	SymbC1.scaffold5649.8	Ion transport protein
T0_T3	T0	BP	GO:0006811 - ion transport	SymbC1.scaffold59.5	Helicase conserved C-terminal domain
T0_T3	T0	BP	GO:0006811 - ion transport	SymbC1.scaffold5956.1	Sodium/hydrogen exchanger family
T0_T3	T0	BP	GO:0006811 - ion transport	SymbC1.scaffold60.7	Ion transport protein;B-box zinc finger;LUC7 N_terminus
T0_T3	T3	BP	GO:0006811 - ion transport	SymbC1.scaffold6085.2	EF hand;Ion transport protein;EF-hand domain
T0_T3	T0	BP	GO:0006811 - ion transport	SymbC1.scaffold61.8	ATP synthase alpha/beta family, beta-barrel domain
T0_T3	T0	BP	GO:0006811 - ion transport	SymbC1.scaffold648.6	Ion transport protein
T0_T3	T3	BP	GO:0006811 - ion transport	SymbC1.scaffold6501.2	Scramblase
T0_T3	T0	BP	GO:0006811 - ion transport	SymbC1.scaffold6770.2	Ion transport protein
T0_T3	T0	BP	GO:0006811 - ion transport	SymbC1.scaffold8171.4	Transmembrane amino acid transporter protein;Ion transport protein;WD domain, G-beta repeat
T0_T3	T0	BP	GO:0006811 - ion transport	SymbC1.scaffold826.1	Ion transport protein
T0_T3	T3	BP	GO:0006811 - ion transport	SymbC1.scaffold8325.1	Voltage gated chloride channel
T0_T3	T3	BP	GO:0006811 - ion transport	SymbC1.scaffold845.2	Protein of unknown function (DUF974);Ion transport protein
T0_T3	T3	BP	GO:0006811 - ion transport	SymbC1.scaffold8492.2	Sugar-tranasporters, 12 TM
T0_T3	T0	BP	GO:0006811 - ion transport	SymbC1.scaffold9202.1	Ammonium Transporter Family
T0_T3	T0	BP	GO:0006811 - ion transport	SymbC1.scaffold9293.1	Ammonium Transporter Family
T0_T3	T0	BP	GO:0006811 - ion transport	SymbC1.scaffold935.2	Ion transport protein
T0_T3	T0	BP	GO:0006811 - ion transport	SymbC1.scaffold9432.2	Signal peptide binding domain
T0_T3	T3	BP	GO:0006811 - ion transport	SymbC1.scaffold9526.1	Ion transport protein
T0_T3	T0	BP	GO:0006811 - ion transport	SymbC1.scaffold986.11	Nucleotide-sugar transporter
T0_T3	T0	MF	GO:0051082 - unfolded protein binding	SymbC1.scaffold10965.1	DnaJ central domain;DnaJ C terminal domain
T0_T3	T0	MF	GO:0051082 - unfolded protein binding	SymbC1.scaffold15268.1	Hsp90 protein
T0_T3	T0	MF	GO:0051082 - unfolded protein binding	SymbC1.scaffold1589.5	Hsp90 protein
T0_T3	T0	MF	GO:0051082 - unfolded protein binding	SymbC1.scaffold16094.1	Calreticulin family
T0_T3	T0	MF	GO:0051082 - unfolded protein binding	SymbC1.scaffold2700.1	Histidine kinase-, DNA gyrase B-, and HSP90-like ATPase;Hsp90 protein
T0_T3	T0	MF	GO:0051082 - unfolded protein binding	SymbC1.scaffold2700.6	Histidine kinase-, DNA gyrase B-, and HSP90-like ATPase;Hsp90 protein
T0_T3	T0	MF	GO:0051082 - unfolded protein binding	SymbC1.scaffold3183.5	Calreticulin family;MORN repeat
T0_T3	T0	MF	GO:0051082 - unfolded protein binding	SymbC1.scaffold351.7	Hsp90 protein;Histidine kinase-, DNA gyrase B-, and HSP90-like ATPase
T0_T3	T0	MF	GO:0051082 - unfolded protein binding	SymbC1.scaffold5158.2	Prefoldin subunit;Tetratricopeptide repeat;DTW domain
T0_T3	T0	MF	GO:0051082 - unfolded protein binding	SymbC1.scaffold6635.1	Hsp90 protein
B1_B4	B4	MF	GO:0003735 - structural constituent of ribosome	SymbC1.scaffold1015.3	Ribosomal protein L35Ae
B1_B4	B4	MF	GO:0003735 - structural constituent of ribosome	SymbC1.scaffold10803.1	KH domain;Ribosomal protein S3, C-terminal domain
B1_B4	B4	MF	GO:0003735 - structural constituent of ribosome	SymbC1.scaffold1092.5	Ribosomal protein L16p/L10e
B1_B4	B4	MF	GO:0003735 - structural constituent of ribosome	SymbC1.scaffold11574.1	Ribosomal protein L23, N-terminal domain;Ribosomal protein L23
B1_B4	B4	MF	GO:0003735 - structural constituent of ribosome	SymbC1.scaffold1291.12	Ribosomal protein L36e
B1_B4	B4	MF	GO:0003735 - structural constituent of ribosome	SymbC1.scaffold1291.13	Ribosomal protein L36e
B1_B4	B4	MF	GO:0003735 - structural constituent of ribosome	SymbC1.scaffold1337.4	Ribosomal L40e family;Ubiquitin family
B1_B4	B1	MF	GO:0003735 - structural constituent of ribosome	SymbC1.scaffold1367.7	Ribosomal protein S5, N-terminal domain
B1_B4	B4	MF	GO:0003735 - structural constituent of ribosome	SymbC1.scaffold154.11	Ribosomal protein S19e
B1_B4	B4	MF	GO:0003735 - structural constituent of ribosome	SymbC1.scaffold1593.4	Ribosomal protein L13
B1_B4	B4	MF	GO:0003735 - structural constituent of ribosome	SymbC1.scaffold163.7	Ribosomal protein S16
B1_B4	B1	MF	GO:0003735 - structural constituent of ribosome	SymbC1.scaffold170.4	Ribosomal Proteins L2, C-terminal domain;Ribosomal Proteins L2, RNA binding domain
B1_B4	B4	MF	GO:0003735 - structural constituent of ribosome	SymbC1.scaffold193.9	Ribosomal protein L34e

B1_B4	B4	MF	GO:0003735 - structural constituent of ribosome	SymbC1.scaffold1954.5	Ribosomal L22e protein family
B1_B4	B4	MF	GO:0003735 - structural constituent of ribosome	SymbC1.scaffold1979.3	Ribosomal protein L22p/L17e
B1_B4	B4	MF	GO:0003735 - structural constituent of ribosome	SymbC1.scaffold2154.5	Ribosomal protein L37e
B1_B4	B4	MF	GO:0003735 - structural constituent of ribosome	SymbC1.scaffold2216.1	Ribosomal protein S2
B1_B4	B4	MF	GO:0003735 - structural constituent of ribosome	SymbC1.scaffold2373.2	Ribosomal protein S19e
B1_B4	B4	MF	GO:0003735 - structural constituent of ribosome	SymbC1.scaffold249.14	Ubiquitin family;Ribosomal L40e family
B1_B4	B4	MF	GO:0003735 - structural constituent of ribosome	SymbC1.scaffold257.7	Ribosomal protein L14p/L23e
B1_B4	B4	MF	GO:0003735 - structural constituent of ribosome	SymbC1.scaffold27.16	Ribosomal proteins L26 eukaryotic, L24P archaeal;KOW motif
B1_B4	B4	MF	GO:0003735 - structural constituent of ribosome	SymbC1.scaffold2720.1	Ribosomal S13/S15 N-terminal domain
B1_B4	B4	MF	GO:0003735 - structural constituent of ribosome	SymbC1.scaffold2899.2	Ribosomal L22e protein family
B1_B4	B4	MF	GO:0003735 - structural constituent of ribosome	SymbC1.scaffold3021.4	Ribosomal protein S2
B1_B4	B4	MF	GO:0003735 - structural constituent of ribosome	SymbC1.scaffold356.4	Ribosomal L29 protein
B1_B4	B4	MF	GO:0003735 - structural constituent of ribosome	SymbC1.scaffold3580.6	Ribosomal S17
B1_B4	B4	MF	GO:0003735 - structural constituent of ribosome	SymbC1.scaffold3580.7	Ribosomal S17
B1_B4	B4	MF	GO:0003735 - structural constituent of ribosome	SymbC1.scaffold3713.7	Ribosomal protein L33
B1_B4	B4	MF	GO:0003735 - structural constituent of ribosome	SymbC1.scaffold3882.8	Ribosomal protein S8
B1_B4	B4	MF	GO:0003735 - structural constituent of ribosome	SymbC1.scaffold409.14	Ribosomal protein L3
B1_B4	B4	MF	GO:0003735 - structural constituent of ribosome	SymbC1.scaffold4442.3	Ribosomal protein L14
B1_B4	B1	MF	GO:0003735 - structural constituent of ribosome	SymbC1.scaffold520.2	Ribosomal protein S15
B1_B4	B4	MF	GO:0003735 - structural constituent of ribosome	SymbC1.scaffold5416.2	Ribosomal protein S19
B1_B4	B4	MF	GO:0003735 - structural constituent of ribosome	SymbC1.scaffold5627.3	Ribosomal protein L32
B1_B4	B4	MF	GO:0003735 - structural constituent of ribosome	SymbC1.scaffold582.3	Ribosomal protein L16p/L10e
B1_B4	B1	MF	GO:0003735 - structural constituent of ribosome	SymbC1.scaffold610.1	Ribosomal protein S2
B1_B4	B4	MF	GO:0003735 - structural constituent of ribosome	SymbC1.scaffold625.1	Ribosomal protein L37e
B1_B4	B4	MF	GO:0003735 - structural constituent of ribosome	SymbC1.scaffold6598.3	Ribosomal protein L11, N-terminal domain
B1_B4	B4	MF	GO:0003735 - structural constituent of ribosome	SymbC1.scaffold700.4	Ribosomal protein S12/S23
B1_B4	B4	MF	GO:0003735 - structural constituent of ribosome	SymbC1.scaffold7628.1	Ribosomal protein L11, N-terminal domain
B1_B4	B4	MF	GO:0003735 - structural constituent of ribosome	SymbC1.scaffold786.6	Ribosomal protein L3
B1_B4	B4	MF	GO:0003735 - structural constituent of ribosome	SymbC1.scaffold819.2	Ribosomal protein L6e
B1_B4	B4	MF	GO:0003735 - structural constituent of ribosome	SymbC1.scaffold8790.1	Ribosomal protein S9/S16
B1_B4	B4	MF	GO:0003735 - structural constituent of ribosome	SymbC1.scaffold883.5	Ribosomal protein L21e
B1_B4	B4	MF	GO:0003735 - structural constituent of ribosome	SymbC1.scaffold923.7	Ribosomal L15
B1_B4	B4	MF	GO:0003735 - structural constituent of ribosome	SymbC1.scaffold943.2	Ribosomal L22e protein family
B1_B4	B4	MF	GO:0003735 - structural constituent of ribosome	SymbC1.scaffold968.3	60S ribosomal protein L4 C-terminal domain
B1_B4	B4	MF	GO:0005216 - ion channel activity	SymbC1.scaffold117.6	Ion transport protein
B1_B4	B1	MF	GO:0005216 - ion channel activity	SymbC1.scaffold1520.5	EF-hand domain pair;Ion transport protein
B1_B4	B1	MF	GO:0005216 - ion channel activity	SymbC1.scaffold1537.1	Ion transport protein
B1_B4	B1	MF	GO:0005216 - ion channel activity	SymbC1.scaffold1537.6	Ion transport protein
B1_B4	B4	MF	GO:0005216 - ion channel activity	SymbC1.scaffold1545.3	PAN domain;Ion transport protein
B1_B4	B4	MF	GO:0005216 - ion channel activity	SymbC1.scaffold168.1	Glyceraldehyde 3-phosphate dehydrogenase, NAD binding domain
B1_B4	B1	MF	GO:0005216 - ion channel activity	SymbC1.scaffold176.3	C-5 cytosine-specific DNA methylase;Ion transport protein
B1_B4	B1	MF	GO:0005216 - ion channel activity	SymbC1.scaffold1764.11	Ion transport protein
B1_B4	B1	MF	GO:0005216 - ion channel activity	SymbC1.scaffold1982.3	Ion transport protein
B1_B4	B1	MF	GO:0005216 - ion channel activity	SymbC1.scaffold2108.2	Ion transport protein
B1_B4	B4	MF	GO:0005216 - ion channel activity	SymbC1.scaffold2113.3	ATP synthase
B1_B4	B1	MF	GO:0005216 - ion channel activity	SymbC1.scaffold220.13	Ion transport protein
B1_B4	B1	MF	GO:0005216 - ion channel activity	SymbC1.scaffold2218.11	Ion transport protein

B1_B4	B1	MF	GO:0005216 - ion channel activity	SymbC1.scaffold226.6	Ion transport protein
B1_B4	B1	MF	GO:0005216 - ion channel activity	SymbC1.scaffold2342.2	Ion transport protein
B1_B4	B1	MF	GO:0005216 - ion channel activity	SymbC1.scaffold2552.4	Ion transport protein
B1_B4	B1	MF	GO:0005216 - ion channel activity	SymbC1.scaffold2758.5	Ion transport protein
B1_B4	B1	MF	GO:0005216 - ion channel activity	SymbC1.scaffold2791.1	Ion transport protein
B1_B4	B1	MF	GO:0005216 - ion channel activity	SymbC1.scaffold2968.2	Ion transport protein
B1_B4	B1	MF	GO:0005216 - ion channel activity	SymbC1.scaffold3067.7	Ion transport protein
B1_B4	B1	MF	GO:0005216 - ion channel activity	SymbC1.scaffold3462.7	Ion transport protein
B1_B4	B1	MF	GO:0005216 - ion channel activity	SymbC1.scaffold3849.1	Ion transport protein
B1_B4	B1	MF	GO:0005216 - ion channel activity	SymbC1.scaffold388.1	Ion transport protein
B1_B4	B1	MF	GO:0005216 - ion channel activity	SymbC1.scaffold397.1	Ion transport protein
B1_B4	B1	MF	GO:0005216 - ion channel activity	SymbC1.scaffold4004.2	Ion transport protein
B1_B4	B1	MF	GO:0005216 - ion channel activity	SymbC1.scaffold412.10	Ion transport protein
B1_B4	B1	MF	GO:0005216 - ion channel activity	SymbC1.scaffold4295.3	S1 RNA binding domain;Ion transport protein
B1_B4	B4	MF	GO:0005216 - ion channel activity	SymbC1.scaffold4318.3	Ion transport protein
B1_B4	B1	MF	GO:0005216 - ion channel activity	SymbC1.scaffold4381.3	Ion transport protein
B1_B4	B1	MF	GO:0005216 - ion channel activity	SymbC1.scaffold4455.2	Ion transport protein
B1_B4	B1	MF	GO:0005216 - ion channel activity	SymbC1.scaffold45.13	Ion transport protein
B1_B4	B1	MF	GO:0005216 - ion channel activity	SymbC1.scaffold460.5	Ion transport protein
B1_B4	B1	MF	GO:0005216 - ion channel activity	SymbC1.scaffold460.8	Ion transport protein
B1_B4	B1	MF	GO:0005216 - ion channel activity	SymbC1.scaffold4701.2	Ion transport protein
B1_B4	B1	MF	GO:0005216 - ion channel activity	SymbC1.scaffold5088.3	Ligand-gated ion channel
B1_B4	B1	MF	GO:0005216 - ion channel activity	SymbC1.scaffold5190.4	Ion transport protein
B1_B4	B1	MF	GO:0005216 - ion channel activity	SymbC1.scaffold5363.2	EF hand;Ion transport protein
B1_B4	B4	MF	GO:0005216 - ion channel activity	SymbC1.scaffold5437.2	Bestrophin, RFP-TM, chloride channel
B1_B4	B1	MF	GO:0005216 - ion channel activity	SymbC1.scaffold5818.2	Ion transport protein
B1_B4	B1	MF	GO:0005216 - ion channel activity	SymbC1.scaffold5974.2	Ion transport protein
B1_B4	B1	MF	GO:0005216 - ion channel activity	SymbC1.scaffold6020.2	Ion transport protein
B1_B4	B1	MF	GO:0005216 - ion channel activity	SymbC1.scaffold6244.1	Ion transport protein
B1_B4	B1	MF	GO:0005216 - ion channel activity	SymbC1.scaffold64.5	Ion transport protein
B1_B4	B1	MF	GO:0005216 - ion channel activity	SymbC1.scaffold6444.6	Ion transport protein
B1_B4	B1	MF	GO:0005216 - ion channel activity	SymbC1.scaffold645.9	CBS domain;Voltage gated chloride channel
B1_B4	B1	MF	GO:0005216 - ion channel activity	SymbC1.scaffold6515.3	EF-hand domain pair;EF hand;Ion transport protein
B1_B4	B1	MF	GO:0005216 - ion channel activity	SymbC1.scaffold6636.1	Reverse transcriptase (RNA-dependent DNA polymerase);Ion transport protein
B1_B4	B1	MF	GO:0005216 - ion channel activity	SymbC1.scaffold6704.2	Ion transport protein
B1_B4	B1	MF	GO:0005216 - ion channel activity	SymbC1.scaffold6963.1	Ion transport protein
B1_B4	B1	MF	GO:0005216 - ion channel activity	SymbC1.scaffold731.3	Ion transport protein
B1_B4	B1	MF	GO:0005216 - ion channel activity	SymbC1.scaffold7358.3	EF hand;Ion transport protein
B1_B4	B1	MF	GO:0005216 - ion channel activity	SymbC1.scaffold7480.3	Ion transport protein
B1_B4	B1	MF	GO:0005216 - ion channel activity	SymbC1.scaffold776.14	Ion transport protein
B1_B4	B1	MF	GO:0005216 - ion channel activity	SymbC1.scaffold7921.1	Ion transport protein
B1_B4	B1	MF	GO:0005216 - ion channel activity	SymbC1.scaffold815.1	EF-hand domain pair;Ion transport protein
B1_B4	B1	MF	GO:0005216 - ion channel activity	SymbC1.scaffold930.9	Ion transport protein
B1_B4	B1	MF	GO:0005216 - ion channel activity	SymbC1.scaffold9309.1	Bestrophin, RFP-TM, chloride channel
B1_B4	B1	MF	GO:0005216 - ion channel activity	SymbC1.scaffold932.3	Ion transport protein
B1_B4	B1	MF	GO:0005216 - ion channel activity	SymbC1.scaffold945.1	Ion transport protein
B1_B4	B1	MF	GO:0005216 - ion channel activity	SymbC1.scaffold9526.1	Ion transport protein

B1_B4	B1	MF	GO:0005216 - ion channel activity	SymbC1.scaffold988.2	Ion transport protein
B1_B4	B1	MF	GO:0005509 - calcium ion binding	SymbC1.scaffold100.11	EF hand
B1_B4	B1	MF	GO:0005509 - calcium ion binding	SymbC1.scaffold1154.2	Calpain family cysteine protease;EF-hand domain pair
B1_B4	B1	MF	GO:0005509 - calcium ion binding	SymbC1.scaffold13529.1	EF-hand domain pair
B1_B4	B4	MF	GO:0005509 - calcium ion binding	SymbC1.scaffold1382.8	EF-hand domain pair
B1_B4	B1	MF	GO:0005509 - calcium ion binding	SymbC1.scaffold1416.6	Calpain family cysteine protease;EF-hand domain pair
B1_B4	B1	MF	GO:0005509 - calcium ion binding	SymbC1.scaffold1519.1	Ankyrin repeats (3 copies);EF-hand domain pair
B1_B4	B1	MF	GO:0005509 - calcium ion binding	SymbC1.scaffold1520.5	EF-hand domain pair;Ion transport protein
B1_B4	B4	MF	GO:0005509 - calcium ion binding	SymbC1.scaffold1573.2	EF hand;EF-hand domain pair
B1_B4	B1	MF	GO:0005509 - calcium ion binding	SymbC1.scaffold1819.3	EF hand;EF-hand domain pair;PPPDE putative peptidase domain
B1_B4	B1	MF	GO:0005509 - calcium ion binding	SymbC1.scaffold1880.2	EF-hand domain pair;EF hand
B1_B4	B4	MF	GO:0005509 - calcium ion binding	SymbC1.scaffold2037.3	EF-hand domain pair
B1_B4	B1	MF	GO:0005509 - calcium ion binding	SymbC1.scaffold2051.7	Inner membrane complex protein;EF hand
B1_B4	B4	MF	GO:0005509 - calcium ion binding	SymbC1.scaffold2133.2	EF-hand domain pair
B1_B4	B1	MF	GO:0005509 - calcium ion binding	SymbC1.scaffold2463.1	EF hand;EF-hand domain pair;Calcineurin-like phosphoesterase;ThiF family
B1_B4	B4	MF	GO:0005509 - calcium ion binding	SymbC1.scaffold248.4	EF-hand domain pair;Protein kinase domain
B1_B4	B1	MF	GO:0005509 - calcium ion binding	SymbC1.scaffold2632.4	EF-hand domain pair;Protein kinase domain
B1_B4	B1	MF	GO:0005509 - calcium ion binding	SymbC1.scaffold282.2	EF hand;EF-hand domain pair
B1_B4	B1	MF	GO:0005509 - calcium ion binding	SymbC1.scaffold2920.5	EF-hand domain pair;SH3 domain;Calpain family cysteine protease
B1_B4	B1	MF	GO:0005509 - calcium ion binding	SymbC1.scaffold310.5	EF-hand domain pair;EF hand
B1_B4	B1	MF	GO:0005509 - calcium ion binding	SymbC1.scaffold3768.1	EF-hand domain pair;Calpain family cysteine protease
B1_B4	B1	MF	GO:0005509 - calcium ion binding	SymbC1.scaffold3825.3	EF-hand domain pair
B1_B4	B1	MF	GO:0005509 - calcium ion binding	SymbC1.scaffold399.1	EF-hand domain pair
B1_B4	B1	MF	GO:0005509 - calcium ion binding	SymbC1.scaffold4270.2	Calcium-activated BK potassium channel alpha subunit;EF-hand domain
B1_B4	B1	MF	GO:0005509 - calcium ion binding	SymbC1.scaffold4357.3	EF hand;EXS family;SPX domain
B1_B4	B1	MF	GO:0005509 - calcium ion binding	SymbC1.scaffold449.4	EF-hand domain pair;CAP-Gly domain
B1_B4	B4	MF	GO:0005509 - calcium ion binding	SymbC1.scaffold5246.4	OmpA family;EF-hand domain pair;EF hand
B1_B4	B1	MF	GO:0005509 - calcium ion binding	SymbC1.scaffold5363.2	EF hand;Ion transport protein
B1_B4	B1	MF	GO:0005509 - calcium ion binding	SymbC1.scaffold5416.4	EF-hand domain pair;Protein kinase domain
B1_B4	B1	MF	GO:0005509 - calcium ion binding	SymbC1.scaffold5445.2	Plasma-membrane choline transporter;EF hand
B1_B4	B4	MF	GO:0005509 - calcium ion binding	SymbC1.scaffold5467.4	EF hand;EF-hand domain pair
B1_B4	B1	MF	GO:0005509 - calcium ion binding	SymbC1.scaffold5784.2	EF-hand domain pair;Glycosyl hydrolases family 31
B1_B4	B1	MF	GO:0005509 - calcium ion binding	SymbC1.scaffold6130.2	EF-hand domain pair
B1_B4	B1	MF	GO:0005509 - calcium ion binding	SymbC1.scaffold623.6	EF-hand domain pair
B1_B4	B4	MF	GO:0005509 - calcium ion binding	SymbC1.scaffold6405.5	EF-hand domain pair
B1_B4	B1	MF	GO:0005509 - calcium ion binding	SymbC1.scaffold6515.3	EF-hand domain pair;EF hand;Ion transport protein
B1_B4	B1	MF	GO:0005509 - calcium ion binding	SymbC1.scaffold6912.3	EF hand;EF-hand domain pair
B1_B4	B1	MF	GO:0005509 - calcium ion binding	SymbC1.scaffold7358.3	EF hand;Ion transport protein
B1_B4	B1	MF	GO:0005509 - calcium ion binding	SymbC1.scaffold753.1	EF hand;EF-hand domain pair
B1_B4	B1	MF	GO:0005509 - calcium ion binding	SymbC1.scaffold7664.2	Aldos-2-ulose dehydratase/isomerase (AUDH) Cupin domain;EF-hand domain pair
B1_B4	B1	MF	GO:0005509 - calcium ion binding	SymbC1.scaffold79.10	EF-hand domain pair
B1_B4	B4	MF	GO:0005509 - calcium ion binding	SymbC1.scaffold8102.2	Protein kinase domain;EF-hand domain pair
B1_B4	B4	MF	GO:0005509 - calcium ion binding	SymbC1.scaffold8102.3	EF-hand domain pair
B1_B4	B1	MF	GO:0005509 - calcium ion binding	SymbC1.scaffold815.1	EF-hand domain pair;Ion transport protein
B1_B4	B1	MF	GO:0005509 - calcium ion binding	SymbC1.scaffold8404.1	Ankyrin repeat;EF-hand domain pair;Ankyrin repeats (3 copies)
B1_B4	B1	MF	GO:0005509 - calcium ion binding	SymbC1.scaffold9352.1	EF hand;Protein kinase domain
B1_B4	B4	MF	GO:0005515 - protein binding	SymbC1.scaffold100.9	Tetratricopeptide repeat;FKBP-type peptidyl-prolyl cis-trans isomerase

B1_B4	B4	MF	GO:0005515 - protein binding	SymbC1.scaffold1003.6	Leucine Rich repeat
B1_B4	B4	MF	GO:0005515 - protein binding	SymbC1.scaffold10088.2	Ankyrin repeat
B1_B4	B1	MF	GO:0005515 - protein binding	SymbC1.scaffold1038.1	BTB/POZ domain
B1_B4	B4	MF	GO:0005515 - protein binding	SymbC1.scaffold1064.11	Leucine rich repeat
B1_B4	B1	MF	GO:0005515 - protein binding	SymbC1.scaffold1144.8	Phosphatidylinositol 3- and 4-kinase;Protein kinase domain;FATC domain
B1_B4	B1	MF	GO:0005515 - protein binding	SymbC1.scaffold11474.1	Kinesin motor domain
B1_B4	B4	MF	GO:0005515 - protein binding	SymbC1.scaffold1198.3	Domain of unknown function (DUF4116);Ubiquitin family
B1_B4	B1	MF	GO:0005515 - protein binding	SymbC1.scaffold122.2	WD domain, G-beta repeat
B1_B4	B1	MF	GO:0005515 - protein binding	SymbC1.scaffold1231.2	Vitamin K epoxide reductase family;Astacin (Peptidase family M12A);WD domain, G-beta repeat
B1_B4	B4	MF	GO:0005515 - protein binding	SymbC1.scaffold124.8	Fibronectin type III domain;C-5 cytosine-specific DNA methylase
B1_B4	B4	MF	GO:0005515 - protein binding	SymbC1.scaffold1244.12	FHA domain;Zinc finger C-x8-C-x5-C-x3-H type (and similar)
B1_B4	B4	MF	GO:0005515 - protein binding	SymbC1.scaffold1255.1	Ubiquitin family
B1_B4	B4	MF	GO:0005515 - protein binding	SymbC1.scaffold131.6	Cyclophilin type peptidyl-prolyl cis-trans isomerase/CLD
B1_B4	B4	MF	GO:0005515 - protein binding	SymbC1.scaffold13177.1	Ankyrin repeats (many copies);Ankyrin repeats (3 copies)
B1_B4	B4	MF	GO:0005515 - protein binding	SymbC1.scaffold1318.1	Cop9 signalosome subunit 5 C-terminal domain;JAB1/Mov34/MPN/PAD-1 ubiquitin protease
B1_B4	B4	MF	GO:0005515 - protein binding	SymbC1.scaffold1326.1	Domain of unknown function (DUF4116);Ubiquitin family
B1_B4	B4	MF	GO:0005515 - protein binding	SymbC1.scaffold1337.4	Ribosomal L40e family;Ubiquitin family
B1_B4	B4	MF	GO:0005515 - protein binding	SymbC1.scaffold1363.2	'Cold-shock' DNA-binding domain;WW domain
B1_B4	B1	MF	GO:0005515 - protein binding	SymbC1.scaffold1382.1	Armadillo/beta-catenin-like repeat;Protein kinase domain
B1_B4	B4	MF	GO:0005515 - protein binding	SymbC1.scaffold141.11	SPRY domain
B1_B4	B4	MF	GO:0005515 - protein binding	SymbC1.scaffold14146.1	WW domain
B1_B4	B1	MF	GO:0005515 - protein binding	SymbC1.scaffold1415.11	Ankyrin repeats (3 copies)
B1_B4	B4	MF	GO:0005515 - protein binding	SymbC1.scaffold1454.3	MIF4G domain;MA3 domain
B1_B4	B1	MF	GO:0005515 - protein binding	SymbC1.scaffold1519.1	Ankyrin repeats (3 copies);EF-hand domain pair
B1_B4	B4	MF	GO:0005515 - protein binding	SymbC1.scaffold1598.5	BTB/POZ domain
B1_B4	B4	MF	GO:0005515 - protein binding	SymbC1.scaffold166.6	Ctr copper transporter family;Leucine Rich repeat;Heavy-metal-associated domain
B1_B4	B1	MF	GO:0005515 - protein binding	SymbC1.scaffold1660.1	WD domain, G-beta repeat
B1_B4	B1	MF	GO:0005515 - protein binding	SymbC1.scaffold1751.4	Galactose oxidase, central domain;BTB/POZ domain;Kelch motif
B1_B4	B1	MF	GO:0005515 - protein binding	SymbC1.scaffold1772.3	SMC proteins Flexible Hinge Domain
B1_B4	B4	MF	GO:0005515 - protein binding	SymbC1.scaffold1862.3	NHL repeat;Reverse transcriptase (RNA-dependent DNA polymerase)
B1_B4	B4	MF	GO:0005515 - protein binding	SymbC1.scaffold1948.6	Leucine Rich repeat;Eukaryotic translation initiation factor 3 subunit 7 (eIF-3)
B1_B4	B1	MF	GO:0005515 - protein binding	SymbC1.scaffold2011.1	IQ calmodulin-binding motif
B1_B4	B1	MF	GO:0005515 - protein binding	SymbC1.scaffold2014.3	Fibronectin type III domain
B1_B4	B4	MF	GO:0005515 - protein binding	SymbC1.scaffold206.1	Ubiquitin family
B1_B4	B1	MF	GO:0005515 - protein binding	SymbC1.scaffold21211.1	Hsp90 protein
B1_B4	B4	MF	GO:0005515 - protein binding	SymbC1.scaffold2165.1	WD domain, G-beta repeat
B1_B4	B4	MF	GO:0005515 - protein binding	SymbC1.scaffold2167.2	NHL repeat
B1_B4	B1	MF	GO:0005515 - protein binding	SymbC1.scaffold2222.3	Leucine Rich repeat
B1_B4	B4	MF	GO:0005515 - protein binding	SymbC1.scaffold2291.6	Ankyrin repeats (many copies)
B1_B4	B1	MF	GO:0005515 - protein binding	SymbC1.scaffold23012.1	Ankyrin repeats (many copies)
B1_B4	B4	MF	GO:0005515 - protein binding	SymbC1.scaffold2317.7	Ankyrin repeats (many copies)
B1_B4	B1	MF	GO:0005515 - protein binding	SymbC1.scaffold235.1	Leucine Rich repeat
B1_B4	B4	MF	GO:0005515 - protein binding	SymbC1.scaffold2471.3	Kelch motif
B1_B4	B4	MF	GO:0005515 - protein binding	SymbC1.scaffold249.14	Ubiquitin family;Ribosomal L40e family
B1_B4	B4	MF	GO:0005515 - protein binding	SymbC1.scaffold2496.5	PDZ domain
B1_B4	B1	MF	GO:0005515 - protein binding	SymbC1.scaffold2502.4	FAD binding domain;Hsp33 protein
B1_B4	B4	MF	GO:0005515 - protein binding	SymbC1.scaffold2507.3	Prefoldin subunit

B1_B4	B4	MF	GO:0005515 - protein binding	SymbC1.scaffold5588.1	Ankyrin repeats (3 copies);Ankyrin repeat
B1_B4	B1	MF	GO:0005515 - protein binding	SymbC1.scaffold575.3	Ankyrin repeats (many copies)
B1_B4	B4	MF	GO:0005515 - protein binding	SymbC1.scaffold578.13	DnaJ domain;DnaJ central domain;DnaJ C terminal domain
B1_B4	B4	MF	GO:0005515 - protein binding	SymbC1.scaffold581.3	Ankyrin repeats (3 copies)
B1_B4	B1	MF	GO:0005515 - protein binding	SymbC1.scaffold591.2	Kinesin motor domain
B1_B4	B1	MF	GO:0005515 - protein binding	SymbC1.scaffold592.5	BTB/POZ domain
B1_B4	B4	MF	GO:0005515 - protein binding	SymbC1.scaffold6080.1	Ankyrin repeats (3 copies)
B1_B4	B1	MF	GO:0005515 - protein binding	SymbC1.scaffold614.6	Ankyrin repeats (3 copies);3'5'-cyclic nucleotide phosphodiesterase
B1_B4	B4	MF	GO:0005515 - protein binding	SymbC1.scaffold635.3	Mitochondrial carrier protein;Transcription factor TFIIB repeat
B1_B4	B4	MF	GO:0005515 - protein binding	SymbC1.scaffold6357.3	Ankyrin repeats (3 copies)
B1_B4	B1	MF	GO:0005515 - protein binding	SymbC1.scaffold6431.3	Ankyrin repeats (3 copies);Ankyrin repeat
B1_B4	B1	MF	GO:0005515 - protein binding	SymbC1.scaffold6530.1	Armadillo/beta-catenin-like repeat
B1_B4	B1	MF	GO:0005515 - protein binding	SymbC1.scaffold6580.4	C-terminal duplication domain of Friend of PRMT1;Ankyrin repeats (3 copies)
B1_B4	B1	MF	GO:0005515 - protein binding	SymbC1.scaffold6734.3	Calpain large subunit, domain III;Kinesin motor domain
B1_B4	B4	MF	GO:0005515 - protein binding	SymbC1.scaffold6813.5	WW domain;Pentatricopeptide repeat domain
B1_B4	B4	MF	GO:0005515 - protein binding	SymbC1.scaffold688.11	Ubiquitin family;Domain of unknown function (DUF4116)
B1_B4	B1	MF	GO:0005515 - protein binding	SymbC1.scaffold6912.1	Leucine Rich repeat;RNA pseudouridylate synthase
B1_B4	B4	MF	GO:0005515 - protein binding	SymbC1.scaffold7109.3	WW domain
B1_B4	B4	MF	GO:0005515 - protein binding	SymbC1.scaffold7128.1	SET domain;PlH1 CS-like domain
B1_B4	B4	MF	GO:0005515 - protein binding	SymbC1.scaffold7230.2	SET domain
B1_B4	B1	MF	GO:0005515 - protein binding	SymbC1.scaffold7290.1	BTB And C-terminal Kelch;BTB/POZ domain
B1_B4	B1	MF	GO:0005515 - protein binding	SymbC1.scaffold742.14	Kinesin motor domain
B1_B4	B1	MF	GO:0005515 - protein binding	SymbC1.scaffold757.10	WD domain, G-beta repeat
B1_B4	B4	MF	GO:0005515 - protein binding	SymbC1.scaffold763.1	JAB1/Mov34/MPN/PAD-1 ubiquitin protease
B1_B4	B4	MF	GO:0005515 - protein binding	SymbC1.scaffold764.3	Semialdehyde dehydrogenase, NAD binding domain
B1_B4	B4	MF	GO:0005515 - protein binding	SymbC1.scaffold784.2	Kelch motif;UTP--glucose-1-phosphate uridylyltransferase
B1_B4	B1	MF	GO:0005515 - protein binding	SymbC1.scaffold8089.2	Ankyrin repeat
B1_B4	B4	MF	GO:0005515 - protein binding	SymbC1.scaffold8186.1	BTB/POZ domain
B1_B4	B1	MF	GO:0005515 - protein binding	SymbC1.scaffold8404.1	Ankyrin repeat;EF-hand domain pair;Ankyrin repeats (3 copies)
B1_B4	B4	MF	GO:0005515 - protein binding	SymbC1.scaffold8494.5	Globin;SAM domain (Sterile alpha motif)
B1_B4	B4	MF	GO:0005515 - protein binding	SymbC1.scaffold869.13	Glycosyl hydrolase catalytic core;Kelch motif
B1_B4	B4	MF	GO:0005515 - protein binding	SymbC1.scaffold877.4	Ankyrin repeats (3 copies)
B1_B4	B1	MF	GO:0005515 - protein binding	SymbC1.scaffold8781.1	SET domain
B1_B4	B4	MF	GO:0005515 - protein binding	SymbC1.scaffold8967.1	'Cold-shock' DNA-binding domain;WW domain
B1_B4	B1	MF	GO:0005515 - protein binding	SymbC1.scaffold911.17	Kinesin motor domain
B1_B4	B1	MF	GO:0005515 - protein binding	SymbC1.scaffold914.7	Fibronectin type III domain;GDP-mannose 4,6 dehydratase
B1_B4	B4	MF	GO:0005515 - protein binding	SymbC1.scaffold9152.1	Anaphase-promoting complex subunit 11 RING-H2 finger
B1_B4	B1	MF	GO:0005515 - protein binding	SymbC1.scaffold923.6	Ankyrin repeats (many copies)
B1_B4	B4	MF	GO:0005515 - protein binding	SymbC1.scaffold9516.1	Armadillo/beta-catenin-like repeat
B1_B4	B1	MF	GO:0005515 - protein binding	SymbC1.scaffold9599.1	Leucine Rich repeat
B1_B4	B4	MF	GO:0005515 - protein binding	SymbC1.scaffold960.8	WD domain, G-beta repeat
B1_B4	B1	MF	GO:0005515 - protein binding	SymbC1.scaffold968.9	Zinc finger, C3HC4 type (RING finger)
B1_B4	B1	MF	GO:0005515 - protein binding	SymbC1.scaffold9981.1	Leucine Rich repeat
B1_B4	B4	CC	GO:0005839 - proteasome core complex	SymbC1.scaffold10043.1	Proteasome subunit
B1_B4	B4	CC	GO:0005839 - proteasome core complex	SymbC1.scaffold11237.1	Proteasome subunit
B1_B4	B4	CC	GO:0005839 - proteasome core complex	SymbC1.scaffold1157.2	Proteasome subunit
B1_B4	B4	CC	GO:0005839 - proteasome core complex	SymbC1.scaffold12258.1	Proteasome subunit;Proteasome subunit A N-terminal signature

B1_B4	B4	CC	GO:0005839 - proteasome core complex	SymbC1.scaffold147.12	Proteasome subunit
B1_B4	B4	CC	GO:0005839 - proteasome core complex	SymbC1.scaffold1935.6	Proteasome subunit A N-terminal signature;Proteasome subunit
B1_B4	B4	CC	GO:0005839 - proteasome core complex	SymbC1.scaffold2918.1	Proteasome subunit
B1_B4	B4	CC	GO:0005839 - proteasome core complex	SymbC1.scaffold4308.2	Proteasome subunit;Proteasome subunit A N-terminal signature
B1_B4	B4	CC	GO:0005840 - ribosome	SymbC1.scaffold1015.3	Ribosomal protein L35Ae
B1_B4	B4	CC	GO:0005840 - ribosome	SymbC1.scaffold1092.5	Ribosomal protein L16p/L10e
B1_B4	B4	CC	GO:0005840 - ribosome	SymbC1.scaffold11574.1	Ribosomal protein L23, N-terminal domain;Ribosomal protein L23
B1_B4	B4	CC	GO:0005840 - ribosome	SymbC1.scaffold1291.12	Ribosomal protein L36e
B1_B4	B4	CC	GO:0005840 - ribosome	SymbC1.scaffold1291.13	Ribosomal protein L36e
B1_B4	B4	CC	GO:0005840 - ribosome	SymbC1.scaffold1337.4	Ribosomal L40e family;Ubiquitin family
B1_B4	B1	CC	GO:0005840 - ribosome	SymbC1.scaffold1367.7	Ribosomal protein S5, N-terminal domain
B1_B4	B4	CC	GO:0005840 - ribosome	SymbC1.scaffold154.11	Ribosomal protein S19e
B1_B4	B4	CC	GO:0005840 - ribosome	SymbC1.scaffold1593.4	Ribosomal protein L13
B1_B4	B4	CC	GO:0005840 - ribosome	SymbC1.scaffold163.7	Ribosomal protein S16
B1_B4	B1	CC	GO:0005840 - ribosome	SymbC1.scaffold170.4	Ribosomal Proteins L2, C-terminal domain
B1_B4	B4	CC	GO:0005840 - ribosome	SymbC1.scaffold193.9	Ribosomal protein L34e
B1_B4	B4	CC	GO:0005840 - ribosome	SymbC1.scaffold1954.5	Ribosomal L22e protein family
B1_B4	B4	CC	GO:0005840 - ribosome	SymbC1.scaffold1979.3	Ribosomal protein L22p/L17e
B1_B4	B4	CC	GO:0005840 - ribosome	SymbC1.scaffold2154.5	Ribosomal protein L37e
B1_B4	B4	CC	GO:0005840 - ribosome	SymbC1.scaffold2216.1	Ribosomal protein S2
B1_B4	B4	CC	GO:0005840 - ribosome	SymbC1.scaffold2373.2	Ribosomal protein S19e
B1_B4	B4	CC	GO:0005840 - ribosome	SymbC1.scaffold249.14	Ubiquitin family;Ribosomal L40e family
B1_B4	B4	CC	GO:0005840 - ribosome	SymbC1.scaffold257.7	Ribosomal protein L14p/L23e
B1_B4	B4	CC	GO:0005840 - ribosome	SymbC1.scaffold27.16	Ribosomal proteins L26 eukaryotic, L24P archaeal;KOW motif
B1_B4	B4	CC	GO:0005840 - ribosome	SymbC1.scaffold2720.1	Ribosomal S13/S15 N-terminal domain
B1_B4	B4	CC	GO:0005840 - ribosome	SymbC1.scaffold2899.2	Ribosomal L22e protein family
B1_B4	B4	CC	GO:0005840 - ribosome	SymbC1.scaffold3021.4	Ribosomal protein S2
B1_B4	B4	CC	GO:0005840 - ribosome	SymbC1.scaffold356.4	Ribosomal L29 protein
B1_B4	B4	CC	GO:0005840 - ribosome	SymbC1.scaffold3580.6	Ribosomal S17
B1_B4	B4	CC	GO:0005840 - ribosome	SymbC1.scaffold3580.7	Ribosomal S17
B1_B4	B4	CC	GO:0005840 - ribosome	SymbC1.scaffold3713.7	Ribosomal protein L33
B1_B4	B4	CC	GO:0005840 - ribosome	SymbC1.scaffold3882.8	Ribosomal protein S8
B1_B4	B4	CC	GO:0005840 - ribosome	SymbC1.scaffold409.14	Ribosomal protein L3
B1_B4	B4	CC	GO:0005840 - ribosome	SymbC1.scaffold4442.3	Ribosomal protein L14
B1_B4	B1	CC	GO:0005840 - ribosome	SymbC1.scaffold520.2	Ribosomal protein S15
B1_B4	B4	CC	GO:0005840 - ribosome	SymbC1.scaffold5416.2	Ribosomal protein S19;Sugar (and other) transporter
B1_B4	B4	CC	GO:0005840 - ribosome	SymbC1.scaffold5627.3	Ribosomal protein L32
B1_B4	B4	CC	GO:0005840 - ribosome	SymbC1.scaffold582.3	Ribosomal protein L16p/L10e
B1_B4	B1	CC	GO:0005840 - ribosome	SymbC1.scaffold610.1	Ribosomal protein S2
B1_B4	B4	CC	GO:0005840 - ribosome	SymbC1.scaffold625.1	Ribosomal protein L37e
B1_B4	B4	CC	GO:0005840 - ribosome	SymbC1.scaffold6598.3	Ribosomal protein L11, N-terminal domain;Ribosomal protein L11, RNA binding domain
B1_B4	B4	CC	GO:0005840 - ribosome	SymbC1.scaffold700.4	Ribosomal protein S12/S23
B1_B4	B4	CC	GO:0005840 - ribosome	SymbC1.scaffold7628.1	Ribosomal protein L11, N-terminal domain;Ribosomal protein L11, RNA binding domain
B1_B4	B4	CC	GO:0005840 - ribosome	SymbC1.scaffold786.6	Ribosomal protein L3
B1_B4	B4	CC	GO:0005840 - ribosome	SymbC1.scaffold819.2	Ribosomal protein L6e
B1_B4	B4	CC	GO:0005840 - ribosome	SymbC1.scaffold8790.1	Ribosomal protein S9/S16
B1_B4	B4	CC	GO:0005840 - ribosome	SymbC1.scaffold883.5	Ribosomal protein L21e

B1_B4	B4	CC	GO:0005840 - ribosome	SymbC1.scaffold923.7	Ribosomal L15
B1_B4	B4	CC	GO:0005840 - ribosome	SymbC1.scaffold943.2	Ribosomal L22e protein family
B1_B4	B4	CC	GO:0005840 - ribosome	SymbC1.scaffold968.3	60S ribosomal protein L4 C-terminal domain;Ribosomal protein L4/L1 family
B1_B4	B4	BP	GO:0006412 - translation	SymbC1.scaffold1015.3	Ribosomal protein L35Ae
B1_B4	B4	BP	GO:0006412 - translation	SymbC1.scaffold10803.1	KH domain;Ribosomal protein S3, C-terminal domain
B1_B4	B4	BP	GO:0006412 - translation	SymbC1.scaffold1092.5	Ribosomal protein L16p/L10e
B1_B4	B1	BP	GO:0006412 - translation	SymbC1.scaffold1096.3	tRNA synthetases class I (E and Q), catalytic domain
B1_B4	B4	BP	GO:0006412 - translation	SymbC1.scaffold11574.1	Ribosomal protein L23, N-terminal domain;Ribosomal protein L23
B1_B4	B4	BP	GO:0006412 - translation	SymbC1.scaffold1291.12	Ribosomal protein L36e
B1_B4	B4	BP	GO:0006412 - translation	SymbC1.scaffold1291.13	Ribosomal protein L36e
B1_B4	B4	BP	GO:0006412 - translation	SymbC1.scaffold1337.4	Ribosomal L40e family;Ubiquitin family
B1_B4	B1	BP	GO:0006412 - translation	SymbC1.scaffold1367.7	Ribosomal protein S5, N-terminal domain
B1_B4	B4	BP	GO:0006412 - translation	SymbC1.scaffold154.11	Ribosomal protein S19e
B1_B4	B4	BP	GO:0006412 - translation	SymbC1.scaffold1593.4	Ribosomal protein L13
B1_B4	B1	BP	GO:0006412 - translation	SymbC1.scaffold1622.11	tRNA synthetases class I (W and Y)
B1_B4	B4	BP	GO:0006412 - translation	SymbC1.scaffold163.7	Ribosomal protein S16
B1_B4	B4	BP	GO:0006412 - translation	SymbC1.scaffold165.7	Eukaryotic elongation factor 5A hypusine, DNA-binding OB fold
B1_B4	B1	BP	GO:0006412 - translation	SymbC1.scaffold170.4	Ribosomal Proteins L2, C-terminal domain;Ribosomal Proteins L2, RNA binding domain
B1_B4	B4	BP	GO:0006412 - translation	SymbC1.scaffold193.9	Ribosomal protein L34e
B1_B4	B4	BP	GO:0006412 - translation	SymbC1.scaffold1954.5	Ribosomal L22e protein family
B1_B4	B4	BP	GO:0006412 - translation	SymbC1.scaffold1979.3	Ribosomal protein L22p/L17e
B1_B4	B1	BP	GO:0006412 - translation	SymbC1.scaffold2092.2	tRNA synthetase class II core domain (G, H, P, S and T);Anticodon binding domain
B1_B4	B4	BP	GO:0006412 - translation	SymbC1.scaffold2154.5	Ribosomal protein L37e
B1_B4	B4	BP	GO:0006412 - translation	SymbC1.scaffold2216.1	Ribosomal protein S2
B1_B4	B4	BP	GO:0006412 - translation	SymbC1.scaffold2373.2	Ribosomal protein S19e
B1_B4	B4	BP	GO:0006412 - translation	SymbC1.scaffold2377.2	Eukaryotic initiation factor 4E
B1_B4	B4	BP	GO:0006412 - translation	SymbC1.scaffold249.14	Ubiquitin family;Ribosomal L40e family
B1_B4	B4	BP	GO:0006412 - translation	SymbC1.scaffold257.7	Ribosomal protein L14p/L23e
B1_B4	B4	BP	GO:0006412 - translation	SymbC1.scaffold27.16	Ribosomal proteins L26 eukaryotic, L24P archaeal;KOW motif
B1_B4	B4	BP	GO:0006412 - translation	SymbC1.scaffold2720.1	Ribosomal S13/S15 N-terminal domain
B1_B4	B1	BP	GO:0006412 - translation	SymbC1.scaffold2776.7	Domain of unknown function (DUF5915);Anticodon-binding domain of tRNA ligase
B1_B4	B4	BP	GO:0006412 - translation	SymbC1.scaffold2899.2	Ribosomal L22e protein family
B1_B4	B4	BP	GO:0006412 - translation	SymbC1.scaffold3021.4	Ribosomal protein S2
B1_B4	B4	BP	GO:0006412 - translation	SymbC1.scaffold3107.3	Translation initiation factor SUI1
B1_B4	B4	BP	GO:0006412 - translation	SymbC1.scaffold356.4	Ribosomal L29 protein
B1_B4	B4	BP	GO:0006412 - translation	SymbC1.scaffold3580.6	Ribosomal S17
B1_B4	B4	BP	GO:0006412 - translation	SymbC1.scaffold3580.7	Ribosomal S17
B1_B4	B4	BP	GO:0006412 - translation	SymbC1.scaffold3656.5	Domain found in IF2B/IF5
B1_B4	B4	BP	GO:0006412 - translation	SymbC1.scaffold3713.7	Ribosomal protein L33
B1_B4	B4	BP	GO:0006412 - translation	SymbC1.scaffold3882.8	Ribosomal protein S8
B1_B4	B4	BP	GO:0006412 - translation	SymbC1.scaffold409.14	Ribosomal protein L3
B1_B4	B4	BP	GO:0006412 - translation	SymbC1.scaffold4442.3	Ribosomal protein L14
B1_B4	B1	BP	GO:0006412 - translation	SymbC1.scaffold520.2	Ribosomal protein S15
B1_B4	B4	BP	GO:0006412 - translation	SymbC1.scaffold5416.2	Ribosomal protein S19;Sugar (and other) transporter
B1_B4	B4	BP	GO:0006412 - translation	SymbC1.scaffold5627.3	Ribosomal protein L32
B1_B4	B4	BP	GO:0006412 - translation	SymbC1.scaffold582.3	Ribosomal protein L16p/L10e
B1_B4	B1	BP	GO:0006412 - translation	SymbC1.scaffold610.1	Ribosomal protein S2

B1_B4	B4	BP	GO:0006412 - translation	SymbC1.scaffold625.1	Ribosomal protein L37e
B1_B4	B4	BP	GO:0006412 - translation	SymbC1.scaffold6598.3	Ribosomal protein L11, N-terminal domain
B1_B4	B4	BP	GO:0006412 - translation	SymbC1.scaffold670.6	tRNA synthetase B5 domain
B1_B4	B4	BP	GO:0006412 - translation	SymbC1.scaffold671.5	Translation initiation factor 1A / IF-1
B1_B4	B4	BP	GO:0006412 - translation	SymbC1.scaffold700.4	Ribosomal protein S12/S23
B1_B4	B4	BP	GO:0006412 - translation	SymbC1.scaffold7628.1	Ribosomal protein L11, N-terminal domain
B1_B4	B4	BP	GO:0006412 - translation	SymbC1.scaffold786.6	Ribosomal protein L3
B1_B4	B4	BP	GO:0006412 - translation	SymbC1.scaffold819.2	Ribosomal protein L6e
B1_B4	B4	BP	GO:0006412 - translation	SymbC1.scaffold8790.1	Ribosomal protein S9/S16
B1_B4	B4	BP	GO:0006412 - translation	SymbC1.scaffold883.5	Ribosomal protein L21e
B1_B4	B1	BP	GO:0006412 - translation	SymbC1.scaffold91.18	Elongation factor TS
B1_B4	B4	BP	GO:0006412 - translation	SymbC1.scaffold923.7	Ribosomal L15
B1_B4	B4	BP	GO:0006412 - translation	SymbC1.scaffold943.2	Ribosomal L22e protein family
B1_B4	B4	BP	GO:0006412 - translation	SymbC1.scaffold968.3	60S ribosomal protein L4 C-terminal domain
B1_B4	B1	BP	GO:0006468 - protein phosphorylation	SymbC1.scaffold1066.7	Protein kinase domain
B1_B4	B1	BP	GO:0006468 - protein phosphorylation	SymbC1.scaffold1144.8	Phosphatidylinositol 3- and 4-kinase;Protein kinase domain;FATC domain
B1_B4	B4	BP	GO:0006468 - protein phosphorylation	SymbC1.scaffold1251.1	Mitochondrial carrier protein;Protein kinase domain
B1_B4	B1	BP	GO:0006468 - protein phosphorylation	SymbC1.scaffold12518.1	Protein kinase domain
B1_B4	B1	BP	GO:0006468 - protein phosphorylation	SymbC1.scaffold1346.7	Protein kinase domain
B1_B4	B1	BP	GO:0006468 - protein phosphorylation	SymbC1.scaffold1382.1	Armadillo/beta-catenin-like repeat;Protein kinase domain
B1_B4	B4	BP	GO:0006468 - protein phosphorylation	SymbC1.scaffold1398.5	Protein kinase domain
B1_B4	B4	BP	GO:0006468 - protein phosphorylation	SymbC1.scaffold1404.3	Reverse transcriptase (RNA-dependent DNA polymerase);Protein kinase domain
B1_B4	B4	BP	GO:0006468 - protein phosphorylation	SymbC1.scaffold1461.5	Protein kinase domain
B1_B4	B1	BP	GO:0006468 - protein phosphorylation	SymbC1.scaffold1527.6	Protein kinase domain;Protein phosphatase 2C
B1_B4	B1	BP	GO:0006468 - protein phosphorylation	SymbC1.scaffold1699.6	Protein kinase domain
B1_B4	B4	BP	GO:0006468 - protein phosphorylation	SymbC1.scaffold18358.1	Protein kinase domain
B1_B4	B1	BP	GO:0006468 - protein phosphorylation	SymbC1.scaffold1855.3	Protein kinase domain
B1_B4	B4	BP	GO:0006468 - protein phosphorylation	SymbC1.scaffold194.5	Protein kinase domain
B1_B4	B1	BP	GO:0006468 - protein phosphorylation	SymbC1.scaffold2072.3	Protein kinase domain
B1_B4	B4	BP	GO:0006468 - protein phosphorylation	SymbC1.scaffold2141.3	Protein kinase domain;Aldo/keto reductase family
B1_B4	B4	BP	GO:0006468 - protein phosphorylation	SymbC1.scaffold2200.6	Protein kinase domain
B1_B4	B1	BP	GO:0006468 - protein phosphorylation	SymbC1.scaffold2209.8	Protein kinase domain
B1_B4	B4	BP	GO:0006468 - protein phosphorylation	SymbC1.scaffold2368.2	Protein kinase domain
B1_B4	B1	BP	GO:0006468 - protein phosphorylation	SymbC1.scaffold2421.2	Protein kinase domain
B1_B4	B4	BP	GO:0006468 - protein phosphorylation	SymbC1.scaffold248.4	EF-hand domain pair;Protein kinase domain
B1_B4	B1	BP	GO:0006468 - protein phosphorylation	SymbC1.scaffold252.6	Protein kinase domain;HEAT repeats
B1_B4	B1	BP	GO:0006468 - protein phosphorylation	SymbC1.scaffold2632.4	EF-hand domain pair;Protein kinase domain
B1_B4	B1	BP	GO:0006468 - protein phosphorylation	SymbC1.scaffold2635.3	Alpha-kinase family;von Willebrand factor type A domain
B1_B4	B1	BP	GO:0006468 - protein phosphorylation	SymbC1.scaffold2684.1	Protein kinase domain
B1_B4	B1	BP	GO:0006468 - protein phosphorylation	SymbC1.scaffold2723.2	Protein kinase domain
B1_B4	B4	BP	GO:0006468 - protein phosphorylation	SymbC1.scaffold2876.5	Protein kinase domain
B1_B4	B4	BP	GO:0006468 - protein phosphorylation	SymbC1.scaffold2952.2	Cyclin
B1_B4	B4	BP	GO:0006468 - protein phosphorylation	SymbC1.scaffold31.10	Protein kinase domain
B1_B4	B4	BP	GO:0006468 - protein phosphorylation	SymbC1.scaffold319.5	Cyclin
B1_B4	B4	BP	GO:0006468 - protein phosphorylation	SymbC1.scaffold3192.2	Fumarylacetoacetate (FAA) hydrolase family;Protein kinase domain
B1_B4	B1	BP	GO:0006468 - protein phosphorylation	SymbC1.scaffold3206.2	Protein kinase domain
B1_B4	B1	BP	GO:0006468 - protein phosphorylation	SymbC1.scaffold3220.2	Protein kinase domain

B1_B4	B4	BP	GO:0006468 - protein phosphorylation	SymbC1.scaffold3273.4	Protein kinase domain
B1_B4	B1	BP	GO:0006468 - protein phosphorylation	SymbC1.scaffold3342.2	Protein kinase domain
B1_B4	B4	BP	GO:0006468 - protein phosphorylation	SymbC1.scaffold3474.7	Protein kinase domain
B1_B4	B4	BP	GO:0006468 - protein phosphorylation	SymbC1.scaffold3664.7	Protein kinase domain
B1_B4	B4	BP	GO:0006468 - protein phosphorylation	SymbC1.scaffold3691.1	Protein kinase domain;Zinc finger, C3HC4 type (RING finger)
B1_B4	B1	BP	GO:0006468 - protein phosphorylation	SymbC1.scaffold373.7	Protein kinase domain;C2 domain
B1_B4	B4	BP	GO:0006468 - protein phosphorylation	SymbC1.scaffold3771.2	FMN-dependent dehydrogenase
B1_B4	B4	BP	GO:0006468 - protein phosphorylation	SymbC1.scaffold3885.5	Protein kinase domain
B1_B4	B1	BP	GO:0006468 - protein phosphorylation	SymbC1.scaffold409.1	Cyclic nucleotide-binding domain;Protein kinase domain
B1_B4	B1	BP	GO:0006468 - protein phosphorylation	SymbC1.scaffold4270.2	Calcium-activated BK potassium channel alpha subunit
B1_B4	B1	BP	GO:0006468 - protein phosphorylation	SymbC1.scaffold4523.6	Kinase associated domain 1;Protein kinase domain
B1_B4	B4	BP	GO:0006468 - protein phosphorylation	SymbC1.scaffold5042.2	Protein kinase domain
B1_B4	B1	BP	GO:0006468 - protein phosphorylation	SymbC1.scaffold5206.6	Protein kinase domain
B1_B4	B4	BP	GO:0006468 - protein phosphorylation	SymbC1.scaffold541.8	FKBP-type peptidyl-prolyl cis-trans isomerase;Protein kinase domain
B1_B4	B1	BP	GO:0006468 - protein phosphorylation	SymbC1.scaffold5416.4	EF-hand domain pair;Protein kinase domain
B1_B4	B4	BP	GO:0006468 - protein phosphorylation	SymbC1.scaffold5680.1	Protein tyrosine and serine/threonine kinase
B1_B4	B1	BP	GO:0006468 - protein phosphorylation	SymbC1.scaffold589.5	Protein kinase domain
B1_B4	B1	BP	GO:0006468 - protein phosphorylation	SymbC1.scaffold619.3	Protein kinase domain
B1_B4	B1	BP	GO:0006468 - protein phosphorylation	SymbC1.scaffold645.7	Phospholipase/Carboxylesterase;DnaJ domain
B1_B4	B1	BP	GO:0006468 - protein phosphorylation	SymbC1.scaffold6872.1	Protein kinase domain
B1_B4	B1	BP	GO:0006468 - protein phosphorylation	SymbC1.scaffold7066.2	Protein kinase domain
B1_B4	B1	BP	GO:0006468 - protein phosphorylation	SymbC1.scaffold7147.2	Protein kinase domain
B1_B4	B4	BP	GO:0006468 - protein phosphorylation	SymbC1.scaffold7859.3	Protein kinase domain
B1_B4	B4	BP	GO:0006468 - protein phosphorylation	SymbC1.scaffold806.10	Protein kinase domain;DnaJ domain
B1_B4	B4	BP	GO:0006468 - protein phosphorylation	SymbC1.scaffold8102.2	Protein kinase domain;EF-hand domain pair
B1_B4	B4	BP	GO:0006468 - protein phosphorylation	SymbC1.scaffold840.2	Protein kinase domain
B1_B4	B1	BP	GO:0006468 - protein phosphorylation	SymbC1.scaffold895.8	Protein kinase domain
B1_B4	B4	BP	GO:0006468 - protein phosphorylation	SymbC1.scaffold9123.2	Protein kinase domain
B1_B4	B1	BP	GO:0006468 - protein phosphorylation	SymbC1.scaffold9352.1	EF hand;Protein kinase domain
B1_B4	B4	BP	GO:0006468 - protein phosphorylation	SymbC1.scaffold9730.1	Alpha-kinase family
B1_B4	B4	BP	GO:0006511 - ubiquitin-dependent protein catabolic pr…	SymbC1.scaffold12258.1	Proteasome subunit;Proteasome subunit A N-terminal signature
B1_B4	B4	BP	GO:0006511 - ubiquitin-dependent protein catabolic pr…	SymbC1.scaffold1935.6	Proteasome subunit A N-terminal signature;Proteasome subunit
B1_B4	B4	BP	GO:0006511 - ubiquitin-dependent protein catabolic pr…	SymbC1.scaffold2144.5	Ubiquitin carboxyl-terminal hydrolase, family 1
B1_B4	B4	BP	GO:0006511 - ubiquitin-dependent protein catabolic pr…	SymbC1.scaffold2633.4	Skp1 family, tetramerisation domain;Skp1 family, dimerisation domain
B1_B4	B4	BP	GO:0006511 - ubiquitin-dependent protein catabolic pr…	SymbC1.scaffold3151.1	Ubiquitin family;XPC-binding domain;UBA/TS-N domain
B1_B4	B4	BP	GO:0006511 - ubiquitin-dependent protein catabolic pr…	SymbC1.scaffold4308.2	Proteasome subunit;Proteasome subunit A N-terminal signature
B1_B4	B4	BP	GO:0006511 - ubiquitin-dependent protein catabolic pr…	SymbC1.scaffold9152.1	Anaphase-promoting complex subunit 11 RING-H2 finger
B1_B4	B1	BP	GO:0006511 - ubiquitin-dependent protein catabolic pr…	SymbC1.scaffold968.9	Zinc finger, C3HC4 type (RING finger)
B1_B4	B4	BP	GO:0006811 - ion transport	SymbC1.scaffold10041.3	Endoplasmic reticulum protein ERp29, C-terminal domain
B1_B4	B4	BP	GO:0006811 - ion transport	SymbC1.scaffold11121.1	ATP synthase, Delta/Epsilon chain, beta-sandwich domain
B1_B4	B4	BP	GO:0006811 - ion transport	SymbC1.scaffold117.6	Ion transport protein
B1_B4	B4	BP	GO:0006811 - ion transport	SymbC1.scaffold12201.1	ATP synthase subunit C
B1_B4	B4	BP	GO:0006811 - ion transport	SymbC1.scaffold130.7	CorA-like Mg2+ transporter protein
B1_B4	B4	BP	GO:0006811 - ion transport	SymbC1.scaffold1353.4	Na+/Pi-cotransporter
B1_B4	B1	BP	GO:0006811 - ion transport	SymbC1.scaffold1520.5	EF-hand domain pair;Ion transport protein
B1_B4	B4	BP	GO:0006811 - ion transport	SymbC1.scaffold1530.7	Ammonium Transporter Family
B1_B4	B1	BP	GO:0006811 - ion transport	SymbC1.scaffold1537.1	Ion transport protein

B1_B4	B1	BP	GO:0006811 - ion transport	SymbC1.scaffold1537.6	Ion transport protein
B1_B4	B4	BP	GO:0006811 - ion transport	SymbC1.scaffold1545.3	PAN domain;Ion transport protein
B1_B4	B4	BP	GO:0006811 - ion transport	SymbC1.scaffold1548.5	Nucleotide-sugar transporter
B1_B4	B1	BP	GO:0006811 - ion transport	SymbC1.scaffold1602.1	Signal recognition particle, alpha subunit, N-terminal
B1_B4	B4	BP	GO:0006811 - ion transport	SymbC1.scaffold166.6	Heavy-metal-associated domain
B1_B4	B4	BP	GO:0006811 - ion transport	SymbC1.scaffold168.1	Glyceraldehyde 3-phosphate dehydrogenase, NAD binding domain
B1_B4	B1	BP	GO:0006811 - ion transport	SymbC1.scaffold176.3	C-5 cytosine-specific DNA methylase;Ion transport protein
B1_B4	B1	BP	GO:0006811 - ion transport	SymbC1.scaffold1764.11	Ion transport protein
B1_B4	B4	BP	GO:0006811 - ion transport	SymbC1.scaffold1816.3	Ammonium Transporter Family
B1_B4	B1	BP	GO:0006811 - ion transport	SymbC1.scaffold1982.3	Ion transport protein
B1_B4	B1	BP	GO:0006811 - ion transport	SymbC1.scaffold2108.2	Ion transport protein
B1_B4	B4	BP	GO:0006811 - ion transport	SymbC1.scaffold2113.3	ATP synthase
B1_B4	B1	BP	GO:0006811 - ion transport	SymbC1.scaffold220.13	Ion transport protein
B1_B4	B1	BP	GO:0006811 - ion transport	SymbC1.scaffold2218.11	Ion transport protein
B1_B4	B1	BP	GO:0006811 - ion transport	SymbC1.scaffold226.6	Ion transport protein
B1_B4	B1	BP	GO:0006811 - ion transport	SymbC1.scaffold2342.2	Ion transport protein
B1_B4	B1	BP	GO:0006811 - ion transport	SymbC1.scaffold2378.2	Sec23/Sec24 beta-sandwich domain
B1_B4	B4	BP	GO:0006811 - ion transport	SymbC1.scaffold2514.3	HCO3- transporter family
B1_B4	B1	BP	GO:0006811 - ion transport	SymbC1.scaffold2552.4	Ion transport protein
B1_B4	B4	BP	GO:0006811 - ion transport	SymbC1.scaffold2557.2	MatE;Magnesium transporter NIPA
B1_B4	B4	BP	GO:0006811 - ion transport	SymbC1.scaffold2607.3	Natural resistance-associated macrophage protein
B1_B4	B1	BP	GO:0006811 - ion transport	SymbC1.scaffold2758.5	Ion transport protein
B1_B4	B1	BP	GO:0006811 - ion transport	SymbC1.scaffold2791.1	Ion transport protein
B1_B4	B1	BP	GO:0006811 - ion transport	SymbC1.scaffold2968.2	Ion transport protein
B1_B4	B1	BP	GO:0006811 - ion transport	SymbC1.scaffold3067.7	Ion transport protein
B1_B4	B4	BP	GO:0006811 - ion transport	SymbC1.scaffold3419.8	Nucleotide-sugar transporter
B1_B4	B1	BP	GO:0006811 - ion transport	SymbC1.scaffold3462.7	Ion transport protein
B1_B4	B4	BP	GO:0006811 - ion transport	SymbC1.scaffold37.17	Nucleoside transporter
B1_B4	B1	BP	GO:0006811 - ion transport	SymbC1.scaffold3849.1	Ion transport protein
B1_B4	B1	BP	GO:0006811 - ion transport	SymbC1.scaffold3861.2	V-type ATPase 116kDa subunit family
B1_B4	B1	BP	GO:0006811 - ion transport	SymbC1.scaffold388.1	Ion transport protein
B1_B4	B1	BP	GO:0006811 - ion transport	SymbC1.scaffold397.1	Ion transport protein
B1_B4	B4	BP	GO:0006811 - ion transport	SymbC1.scaffold3992.3	Urea transporter
B1_B4	B1	BP	GO:0006811 - ion transport	SymbC1.scaffold4004.2	Ion transport protein
B1_B4	B1	BP	GO:0006811 - ion transport	SymbC1.scaffold412.10	Ion transport protein
B1_B4	B1	BP	GO:0006811 - ion transport	SymbC1.scaffold4270.2	Calcium-activated BK potassium channel alpha subunit
B1_B4	B1	BP	GO:0006811 - ion transport	SymbC1.scaffold4295.3	S1 RNA binding domain;Ion transport protein
B1_B4	B4	BP	GO:0006811 - ion transport	SymbC1.scaffold4318.3	Ion transport protein
B1_B4	B1	BP	GO:0006811 - ion transport	SymbC1.scaffold4381.3	Ion transport protein
B1_B4	B1	BP	GO:0006811 - ion transport	SymbC1.scaffold4455.2	Ion transport protein
B1_B4	B1	BP	GO:0006811 - ion transport	SymbC1.scaffold45.13	Ion transport protein
B1_B4	B1	BP	GO:0006811 - ion transport	SymbC1.scaffold460.5	Ion transport protein
B1_B4	B1	BP	GO:0006811 - ion transport	SymbC1.scaffold460.8	Ion transport protein
B1_B4	B1	BP	GO:0006811 - ion transport	SymbC1.scaffold4701.2	Ion transport protein
B1_B4	B1	BP	GO:0006811 - ion transport	SymbC1.scaffold5190.4	Ion transport protein
B1_B4	B1	BP	GO:0006811 - ion transport	SymbC1.scaffold5363.2	EF hand;Ion transport protein
B1_B4	B4	BP	GO:0006811 - ion transport	SymbC1.scaffold552.9	Sideroflexins

B1_B4	B4	BP	GO:0006811 - ion transport	SymbC1.scaffold581.2	Mitochondrial pyruvate carriers
B1_B4	B1	BP	GO:0006811 - ion transport	SymbC1.scaffold5818.2	Ion transport protein
B1_B4	B4	BP	GO:0006811 - ion transport	SymbC1.scaffold5956.1	Sodium/hydrogen exchanger family
B1_B4	B1	BP	GO:0006811 - ion transport	SymbC1.scaffold5974.2	Ion transport protein
B1_B4	B1	BP	GO:0006811 - ion transport	SymbC1.scaffold6020.2	Ion transport protein
B1_B4	B4	BP	GO:0006811 - ion transport	SymbC1.scaffold623.5	mttA/Hcf106 family
B1_B4	B1	BP	GO:0006811 - ion transport	SymbC1.scaffold6244.1	Ion transport protein
B1_B4	B4	BP	GO:0006811 - ion transport	SymbC1.scaffold6396.1	Ammonium Transporter Family
B1_B4	B1	BP	GO:0006811 - ion transport	SymbC1.scaffold64.5	Ion transport protein
B1_B4	B1	BP	GO:0006811 - ion transport	SymbC1.scaffold6444.6	Ion transport protein
B1_B4	B1	BP	GO:0006811 - ion transport	SymbC1.scaffold645.9	CBS domain;Voltage gated chloride channel
B1_B4	B1	BP	GO:0006811 - ion transport	SymbC1.scaffold6515.3	EF-hand domain pair;EF hand;Ion transport protein
B1_B4	B1	BP	GO:0006811 - ion transport	SymbC1.scaffold6636.1	Reverse transcriptase (RNA-dependent DNA polymerase);Ion transport protein
B1_B4	B1	BP	GO:0006811 - ion transport	SymbC1.scaffold6704.2	Ion transport protein
B1_B4	B4	BP	GO:0006811 - ion transport	SymbC1.scaffold6735.1	ATP synthase, Delta/Epsilon chain, beta-sandwich domain
B1_B4	B1	BP	GO:0006811 - ion transport	SymbC1.scaffold6963.1	Ion transport protein
B1_B4	B4	BP	GO:0006811 - ion transport	SymbC1.scaffold7121.4	Ammonium Transporter Family
B1_B4	B1	BP	GO:0006811 - ion transport	SymbC1.scaffold731.3	Ion transport protein
B1_B4	B1	BP	GO:0006811 - ion transport	SymbC1.scaffold7358.3	EF hand;Ion transport protein
B1_B4	B1	BP	GO:0006811 - ion transport	SymbC1.scaffold7480.3	Ion transport protein
B1_B4	B1	BP	GO:0006811 - ion transport	SymbC1.scaffold7684.3	Ammonium Transporter Family
B1_B4	B1	BP	GO:0006811 - ion transport	SymbC1.scaffold7720.1	SecA preprotein cross-linking domain
B1_B4	B1	BP	GO:0006811 - ion transport	SymbC1.scaffold776.14	Ion transport protein
B1_B4	B1	BP	GO:0006811 - ion transport	SymbC1.scaffold7921.1	Ion transport protein
B1_B4	B1	BP	GO:0006811 - ion transport	SymbC1.scaffold815.1	EF-hand domain pair;Ion transport protein
B1_B4	B4	BP	GO:0006811 - ion transport	SymbC1.scaffold8353.2	ATP synthase alpha/beta family, beta-barrel domain
B1_B4	B1	BP	GO:0006811 - ion transport	SymbC1.scaffold8382.2	Sodium/hydrogen exchanger family
B1_B4	B4	BP	GO:0006811 - ion transport	SymbC1.scaffold8747.1	Ammonium Transporter Family
B1_B4	B4	BP	GO:0006811 - ion transport	SymbC1.scaffold8860.1	Ammonium Transporter Family
B1_B4	B1	BP	GO:0006811 - ion transport	SymbC1.scaffold930.9	Ion transport protein
B1_B4	B1	BP	GO:0006811 - ion transport	SymbC1.scaffold932.3	Ion transport protein
B1_B4	B1	BP	GO:0006811 - ion transport	SymbC1.scaffold9432.2	Signal peptide binding domain
B1_B4	B1	BP	GO:0006811 - ion transport	SymbC1.scaffold945.1	Ion transport protein
B1_B4	B1	BP	GO:0006811 - ion transport	SymbC1.scaffold9526.1	Ion transport protein
B1_B4	B1	BP	GO:0006811 - ion transport	SymbC1.scaffold988.2	Ion transport protein
B1_B4	B4	BP	GO:0051603 - proteolysis involved in cellular protein…	SymbC1.scaffold10043.1	Proteasome subunit
B1_B4	B4	BP	GO:0051603 - proteolysis involved in cellular protein…	SymbC1.scaffold11237.1	Proteasome subunit
B1_B4	B4	BP	GO:0051603 - proteolysis involved in cellular protein…	SymbC1.scaffold1157.2	Proteasome subunit
B1_B4	B4	BP	GO:0051603 - proteolysis involved in cellular protein…	SymbC1.scaffold12258.1	Proteasome subunit;Proteasome subunit A N-terminal signature
B1_B4	B4	BP	GO:0051603 - proteolysis involved in cellular protein…	SymbC1.scaffold147.12	Proteasome subunit
B1_B4	B4	BP	GO:0051603 - proteolysis involved in cellular protein…	SymbC1.scaffold1935.6	Proteasome subunit A N-terminal signature;Proteasome subunit
B1_B4	B4	BP	GO:0051603 - proteolysis involved in cellular protein…	SymbC1.scaffold2144.5	Ubiquitin carboxyl-terminal hydrolase, family 1
B1_B4	B4	BP	GO:0051603 - proteolysis involved in cellular protein…	SymbC1.scaffold2633.4	Skp1 family, tetramerisation domain;Skp1 family, dimerisation domain
B1_B4	B4	BP	GO:0051603 - proteolysis involved in cellular protein…	SymbC1.scaffold2918.1	Proteasome subunit
B1_B4	B4	BP	GO:0051603 - proteolysis involved in cellular protein…	SymbC1.scaffold3151.1	Ubiquitin family;XPC-binding domain;UBA/TS-N domain
B1_B4	B4	BP	GO:0051603 - proteolysis involved in cellular protein…	SymbC1.scaffold4308.2	Proteasome subunit;Proteasome subunit A N-terminal signature
B1_B4	B4	BP	GO:0051603 - proteolysis involved in cellular protein…	SymbC1.scaffold9152.1	Anaphase-promoting complex subunit 11 RING-H2 finger